

การพัฒนาระบบตัวทำละลายที่มีเทอร์เซียร์เอมีนสำหรับการดูดซับคาร์บอนไดออกไซด์



นางสาวสุคคณิง สิงห์โต

จุฬาลงกรณ์มหาวิทยาลัย

CHULALONGKORN UNIVERSITY

บทคัดย่อและแฟ้มข้อมูลฉบับเต็มของวิทยานิพนธ์ตั้งแต่ปีการศึกษา 2554 ที่ให้บริการในคลังปัญญาจุฬาฯ (CUIR)  
เป็นแฟ้มข้อมูลของนิสิตเจ้าของวิทยานิพนธ์ ที่ส่งผ่านทางบัณฑิตวิทยาลัย

The abstract and full text of theses from the academic year 2011 in Chulalongkorn University Intellectual Repository (CUIR)  
are the thesis authors' files submitted through the University Graduate School.

วิทยานิพนธ์นี้เป็นส่วนหนึ่งของการศึกษาตามหลักสูตรปริญญาวิทยาศาสตรดุษฎีบัณฑิต

สาขาวิชาปิโตรเคมี

คณะวิทยาศาสตร์ จุฬาลงกรณ์มหาวิทยาลัย

ปีการศึกษา 2558

ลิขสิทธิ์ของจุฬาลงกรณ์มหาวิทยาลัย

DEVELOPMENT OF SOLVENT SYSTEMS CONTAINING TERTIARYAMINES  
FOR CO<sub>2</sub> ABSORPTION

Miss Sudkanueng Singto



A Dissertation Submitted in Partial Fulfillment of the Requirements  
for the Degree of Doctor of Philosophy Program in Petrochemistry  
Faculty of Science  
Chulalongkorn University  
Academic Year 2015  
Copyright of Chulalongkorn University



สุดคณิง สิงห์โต : การพัฒนาระบบตัวทำละลายที่มีเทอร์เชียรีแอมีนสำหรับการดูดซึมคาร์บอนไดออกไซด์ (DEVELOPMENT OF SOLVENT SYSTEMS CONTAINING TERTIARYAMINES FOR CO<sub>2</sub> ABSORPTION) อ. ที่ปรึกษาวิทยานิพนธ์หลัก: ศ. ดร. ศุภวรรณ ต้นตยานนท์, อ.ที่ปรึกษาวิทยานิพนธ์ร่วม: ศ. ดร. ไพฑูรย์ ต้นติเวชวุฒิกุล, ดร. วีระเดช สุภาพ, 190 หน้า.

ได้สังเคราะห์เทอร์เชียรีแอมีนชนิดใหม่โดยแปรความยาวสายโซ่แอลคิลที่มีและไม่มีหมู่ไฮดรอกซิลในโครงสร้าง ได้ประเมินผลของโครงสร้างทางเคมีของเทอร์เชียรีแอมีนชนิดใหม่ที่สังเคราะห์ได้ ได้แก่ 4-(ไดเมทิลเอมิโน)-2-บิวทานอล (ดีเอ็มเอบี) 4-(ไดโพรพิลเอมิโน)-2-บิวทานอล (ดีพีเอบี) 4-(ไดบิวทิลเอมิโน)-2-บิวทานอล (ดีบีเอบี) 4-((2-ไฮดรอกซีเอทิล)(เมทิล)เอมิโน)-2-บิวทานอล (เอชอีเอ็มเอบี) และ 4-((2-ไฮดรอกซีเอทิล)(เอทิล)เอมิโน)-2-บิวทานอล (เอชอีอีเอบี) จากการละลายที่สมดุล และความจุต่อรอบของคาร์บอนไดออกไซด์ อัตราและความร้อนของการดูดซับและการคายคาร์บอนไดออกไซด์ อัตราและความร้อนการคายคาร์บอนไดออกไซด์ จลนศาสตร์ของการดูดซึมคาร์บอนไดออกไซด์ และสมบัติทางกายภาพ เช่น ความหนาแน่น ความหนืด และดัชนีการกระเจิงแสง พบว่าแอมีน 3 ชนิด (ได้แก่ ดีเอ็มเอบี เอชอีเอ็มเอบี เอชอีอีเอบี) มีความสามารถการดูดซึมคาร์บอนไดออกไซด์ (0.88, 0.44 และ 0.68 โมลคาร์บอนไดออกไซด์/โมลแอมีน ตามลำดับ ที่อุณหภูมิ 313 เคลวิน และความดันส่วนคาร์บอนไดออกไซด์ 15 กิโลปาสกาล) และความจุต่อรอบสูงมาก (0.52, 0.26 และ 0.40 ตามลำดับ ที่อุณหภูมิ 313-353 เคลวิน และความดันส่วนคาร์บอนไดออกไซด์ 15 กิโลปาสกาล) แอมีนเหล่านี้มีอัตราการดูดซึมคาร์บอนไดออกไซด์ (0.082, 0.111 และ 0.142 โมลคาร์บอนไดออกไซด์/นาที่ ตามลำดับ) และอัตราการคายคาร์บอนไดออกไซด์เร็ว (0.512, 0.452 และ 0.295 โมลคาร์บอนไดออกไซด์/นาที่ ตามลำดับ) ขณะที่ใช้ความร้อนต่ำในการดูดซึมคาร์บอนไดออกไซด์ (-34.17, -56.21 และ -69.79 กิโลจูล/โมลคาร์บอนไดออกไซด์ ตามลำดับ) และใช้พลังงานต่ำในการคายคาร์บอนไดออกไซด์ (39.73, 60.48 และ 72.44 กิโลจูล/โมลคาร์บอนไดออกไซด์ ตามลำดับ)

สารละลายแอมีนผสม 3 ชนิด (เอ็มอีเอ-ดีเอ็มเอบี เอ็มอีเอ-เอชอีเอ็มเอบี และ เอ็มอีเอ-เอชอีอีเอบี) ที่อัตราส่วน 5:1.25 โมลาร์ ทั้งหมดมีความจุการดูดซึมคาร์บอนไดออกไซด์ (0.50, 0.48 และ 0.50 โมลคาร์บอนไดออกไซด์/โมลแอมีน ตามลำดับ ที่อุณหภูมิ 313 เคลวิน และความดันส่วนคาร์บอนไดออกไซด์ 15 กิโลปาสกาล) และความจุต่อรอบสูง (0.12, 0.13 และ 0.13 ตามลำดับ ที่อุณหภูมิ 313-353 เคลวิน และความดันส่วนคาร์บอนไดออกไซด์ 15 กิโลปาสกาล) แอมีนผสมเหล่านี้มีอัตราการดูดซึมคาร์บอนไดออกไซด์ (0.094, 0.108 และ 0.129 โมลคาร์บอนไดออกไซด์/นาที่ ตามลำดับ) อัตราการคายคาร์บอนไดออกไซด์สูง (0.070, 0.072 และ 0.064 โมลคาร์บอนไดออกไซด์/นาที่ ตามลำดับ) และใช้พลังงานต่ำเพื่อคายคาร์บอนไดออกไซด์ (130.27, 171.85 และ 188.78 กิโลจูล/โมลคาร์บอนไดออกไซด์ ตามลำดับ)

จลนพลศาสตร์ของปฏิกิริยาของการดูดซึมคาร์บอนไดออกไซด์ของ ดีเอ็มเอบี เอชอีเอ็มเอบี และ เอชอีอีเอบี ในเทอมของค่าคงที่การเกิดปฏิกิริยาอันดับ 2 ( $k_2$ ) โดยใช้เทคนิคสโตปโพลที่ช่วงอุณหภูมิ 298-313 เคลวิน และช่วงความเข้มข้นแอมีน 0.1-1.0 โมลต่อลิตร ค่า  $k_2$  ของคาร์บอนไดออกไซด์ในสารละลายแอมีน (เอชอีอีเอบี และ เอชอีเอ็มเอบี) สูงที่สุดเป็นอันดับหนึ่งและสอง (1096.9 และ 1043.6 เมตร<sup>3</sup>/กิโลโมล.วินาที) เปรียบเทียบกับ ดีอีเอบี ดีเอ็มเอบี และ เอ็มดีอีเอ (47.25, 19.94 และ 11.15 เมตร<sup>3</sup>/กิโลโมล.วินาที) ตามลำดับ ได้ประเมินความสัมพันธ์อาร์เรเนียสของค่า  $k_2$  ที่อุณหภูมิต่างๆ ของแอมีนทั้งหมด ซึ่งสัมพันธ์กับพลังงานกระตุ้น ( $E_a$ ) และปัจจัยความถี่ ( $A$ ) เอชอีเอ็มเอบี และ เอชอีอีเอบี มีค่าพลังงานกระตุ้น (26.78 และ 24.45 กิโลจูล/โมล) ต่ำกว่าค่าของ ดีเอ็มเอบี และ ดีอีเอบี (54.34, 52.65 กิโลจูล/โมล) สมบัติทางกายภาพ เช่น ความหนาแน่น ความหนืด และดัชนีการกระเจิงแสงของแอมีนชนิดใหม่ที่สังเคราะห์ได้มีค่าต่ำกว่าค่าของเอ็มดีอีเอ จากผลการศึกษา ดีเอ็มเอบี เอชอีเอ็มเอบี และ เอชอีอีเอบี เป็นแอมีนที่น่าสนใจสำหรับกระบวนการดักจับคาร์บอนไดออกไซด์หลังการเผาไหม้

สาขาวิชา ปีโดครเคมี

ปีการศึกษา 2558

ลายมือชื่อนิสิท .....

ลายมือชื่อ อ.ที่ปรึกษาหลัก .....

ลายมือชื่อ อ.ที่ปรึกษาร่วม .....

ลายมือชื่อ อ.ที่ปรึกษาร่วม .....



# # 5472887023 : MAJOR PETROCHEMISTRY

KEYWORDS: CARBON DIOXIDE ABSORPTION, TERTIARY AMINES, EQUILIBRIUM SOLUBILITY, CARBON DIOXIDE KINETICS, STOPPED-FLOW APPARATUS

SUDKANUENG SINGTO: DEVELOPMENT OF SOLVENT SYSTEMS CONTAINING TERTIARYAMINES FOR CO<sub>2</sub> ABSORPTION. ADVISOR: PROF. SUPAWAN TANTAYANON, Ph.D., CO-ADVISOR: PROF. PAITON TONTIWACHWUTHIKUL, Ph.D., TEERADET SUPAP, Ph.D., 190 pp.

The new tertiary amines were synthesized by varying the alkyl chain length with and without (-OH) hydroxyl groups in the structure. The effect of chemical structure of newly synthesized tertiary amines; 4-(dimethylamino)-2-butanol (DMAB), 4-(dipropylamino)-2-butanol (DPAB), 4-(dibutylamino)-2-butanol (DBAB), 4-((2-hydroxyethyl)(methyl)amino)-2-butanol (HEMAB) and 4-((2-hydroxyethyl)(ethyl)amino)-2-butanol (HEEAB) were evaluated based on CO<sub>2</sub> equilibrium solubility and cyclic capacity, rates and heats of CO<sub>2</sub> absorption and regeneration, the kinetics of CO<sub>2</sub> absorption, as well as physical properties such as density, viscosity and refractive indices. The results showed that three amines (i.e. DMAB, HEMAB and HEEAB) had substantially high CO<sub>2</sub> absorption capacity (0.88, 0.44 and 0.68 mol CO<sub>2</sub>/mol amine at 313 K temperature and 15 kPa CO<sub>2</sub> partial pressure, respectively), and cyclic capacity (0.52, 0.26 and 0.40, respectively, at 313-353 K temperature range, 15 kPa CO<sub>2</sub> partial pressure). These amines also had fast CO<sub>2</sub> absorption rates (0.082, 0.111 and 0.142 mol CO<sub>2</sub>/min, respectively) and CO<sub>2</sub> regeneration rates (0.512, 0.452 and 0.295 mol CO<sub>2</sub>/min, respectively) while maintaining a low heat of CO<sub>2</sub> absorption (-34.17, -56.21 and -69.79 kJ/mol CO<sub>2</sub>, respectively) and heat input of CO<sub>2</sub> regeneration (39.73, 60.48 and 72.44 kJ/mol CO<sub>2</sub>, respectively).

The three blended amine solutions (MEA-DMAB, MEA-HEMAB and MEA-HEEAB) at the ratio 5:1.25 M all had high CO<sub>2</sub> absorption capacity (0.50 and 0.48 and 0.50 mol CO<sub>2</sub>/mol amine, respectively, at 313 K temperature and 15 kPa CO<sub>2</sub> partial pressure), and cyclic capacity (0.12, 0.13 and 0.13, respectively, at 313-353 K temperature range, 15 kPa CO<sub>2</sub> partial pressure). These blended amines also had fast CO<sub>2</sub> absorption rates (0.094, 0.108 and 0.129 mol CO<sub>2</sub>/min, respectively) and CO<sub>2</sub> regeneration rates (0.070, 0.072 and 0.064 mol CO<sub>2</sub>/min, respectively) and low heat input of CO<sub>2</sub> regeneration (130.27, 171.85 and 188.78 kJ/mol CO<sub>2</sub>, respectively).

The kinetics of the reactions of CO<sub>2</sub> absorption of DMAB, HEMAB and HEEAB in terms of the second-order reaction rate constant ( $k_2$ ) using the stopped-flow technique at the temperature range of 298-313 K and amine concentration range of 0.1-1.0 mol/L. The second-order reaction rate constant ( $k_2$ ) of CO<sub>2</sub> in amine solutions (HEEAB and HEMAB) were the first and second highest (1096.9 and 1043.6 m<sup>3</sup>/kmol.s) comparing to DEAB, DMAB and MDEA (47.25, 19.94 and 11.15 m<sup>3</sup>/kmol.s), respectively. The Arrhenius relationship of the second-order reaction rate constant ( $k_2$ ) at different temperatures of all amines related to their respective activation energy ( $E_a$ ) and frequency factor ( $A$ ) were then evaluated. HEMAB and HEEAB showed lower  $E_a$  values (26.78 and 24.45 kJ/mol) than those of DMAB and DEAB (54.34, 52.65 kJ/mol). Physical properties such as density, viscosity and refractive indices of these newly synthesized amines were lower than that of MDEA. Based on these results, HEMAB, HEEAB and DMAB, can be considered to be promising amine components for a post-combustion CO<sub>2</sub> capture process.

Field of Study: Petrochemistry

Academic Year: 2015

Student's Signature .....

Advisor's Signature .....

Co-Advisor's Signature .....

Co-Advisor's Signature .....

## ACKNOWLEDGEMENTS

I take this opportunity to place on record my deep sense of gratitude to my advisor, Professor Dr. Supawan Tantayanon for her continuous support and encouragement during my education at Chulalongkorn University. I am deeply indebted for her guidance through my thesis and her valuable advice at all times. I am sincerely grateful to my co-adviser, Professor Dr. Paitoon Tontiwachwuthikul and Dr. Teeradet Supap for suggestions, guidance, encouragement and financial support during my research at Clean Energy Technologies Research Institute (CETRI), Faculty of Engineering and Applied Science, University of Regina, Regina, Saskatchewan, Canada. I would also like to express my deepest gratitude to Professor Dr. Raphael Idem for his support, and very helpful suggestions for this study.

I am grateful to a research funding from Overseas Research Experience Scholarship for Graduate Students, Graduate School at Chulalongkorn University. I am also gratefully acknowledged from Clean Energy Technologies Research Institute - CETRI (previously known as International Test Center for CO<sub>2</sub> Capture - ITC) at the University of Regina for providing research facilities throughout this work and giving me a responsibility as a Research Assistant. In addition, I would also like to acknowledge the financial support in parts of this work provided by an NPRP Grant # 7-1154-2-433 from the Qatar National Research Fund (a member of Qatar Foundation). Appreciation is also extended to National Center of Excellence for Petroleum, Petrochemicals, and Advanced Materials, NCE-PPAM, the 90th Anniversary of Chulalongkorn University Fund (Ratchadaphiseksomphot Endowment Fund and the program of Petrochemistry and Polymer Science, Chulalongkorn University, Thailand.

I would also like to give special thanks to Dr. Christopher Zoto, a Ph.D. in Chemistry Department from Worcester Polytechnic Institute (WPI), Massachusetts, USA for his assistance with the thesis revision. I would like also to express my sincere appreciation to Jirayu Cunningham, Dr. Fatemeh Pouryousefi Dargah, Wayuta Srisang, Helei Liu and my friends in CETRI for advice and good friendship over the year and making me feel comfortable, even during the most difficult times.

Finally, I am at a total loss of words in expressing the depth of my emotion for my parents and brothers for their constant support and inspiration.

## CONTENTS

	Page
THAI ABSTRACT .....	iv
ENGLISH ABSTRACT.....	v
ACKNOWLEDGEMENTS.....	vi
CONTENTS.....	vii
LIST OF TABLES .....	xi
LIST OF FIGURES .....	xiv
LIST OF SCHEMES.....	xix
ABBREVIATION.....	xx
CHAPTER I.....	1
INTRODUCTION .....	1
1.1 Introduction.....	1
1.2 Objective of this research .....	4
1.3 Scope of investigation.....	4
CHAPTER II.....	7
THEORETICAL STUDIES AND LITERATURE REVIEW.....	7
2.1 Technology for reducing CO <sub>2</sub> emissions.....	8
2.1.1 Pre-combustion process.....	8
2.1.2 Oxy-combustion process .....	8
2.1.3 Post-combustion process .....	9
2.2 Technology for separation of CO <sub>2</sub> from post-combustion flue gas.....	10
2.2.1 Absorption technology .....	10
2.2.1.1 Physical absorption.....	10
2.2.1.2 Chemical absorption.....	10
2.2.2 Adsorption technology .....	11
2.2.3 Membrane.....	11
2.2.4 Cryogenics.....	11
2.3 General description of CO <sub>2</sub> absorption using aqueous amines.....	12
2.4 Chemical solvents for CO <sub>2</sub> absorption .....	14

	Page
2.5 The synthesis of tertiary amines .....	18
2.6 Absorption and desorption.....	19
2.7 Kinetics of CO <sub>2</sub> absorption into aqueous amine solutions .....	21
2.7.1 Zwitterion mechanism.....	21
2.7.2 Base-catalyzed hydration mechanism .....	22
2.8 Physical properties.....	23
2.9 Related literatures .....	24
CHAPTER III .....	28
EXPERIMENTAL.....	28
3.1 Chemicals and equipment.....	28
3.1.1 Materials .....	28
3.1.2 Equipment .....	29
3.2 Instrumentation .....	30
3.3 Experimental procedure .....	31
3.3.1 Amine synthesis .....	32
3.3.1.1 Synthesis of 4-(dimethylamino)-2-butanol (DMAB).....	32
3.3.1.2 Synthesis of 4-(diethylamino)-2-butanol (DEAB).....	34
3.3.1.3 Synthesis of 4-(dipropylamino)-2-butanol (DPAB).....	35
3.3.1.4 Synthesis of 4-(dibutylamino)-2-butanol (DBAB).....	35
3.3.1.5 Synthesis of 4-((2-hydroxyethyl)(methyl)amino)-2-butanol (HEMAB) .....	36
3.3.1.6 Synthesis of 4-((2-hydroxyethyl)(ethyl)amino)-2-butanol (HEEAB) .....	37
3.4 Equilibrium solubility of CO <sub>2</sub> and cyclic capacity in aqueous amine solution .	38
3.4.1 CO <sub>2</sub> loading using the Chittick apparatus .....	39
3.5 Heat of CO <sub>2</sub> absorption in aqueous amine solutions .....	41
3.6 CO <sub>2</sub> absorption and regeneration kinetic rates at actual concentration .....	42
3.7 Amine dissociation constant analysis using a pH meter.....	44
3.8 Heat input of CO <sub>2</sub> regeneration in aqueous amine solutions.....	46

	Page
3.9 Measurement of kinetic data from stopped-flow apparatus.....	47
3.10 Physical properties.....	49
3.10.1 Density and Viscosity.....	49
3.10.2 Refractive index.....	49
CHAPTER IV.....	50
RESULTS AND DISCUSSION.....	50
4.1 Amine synthesis.....	50
4.1.1 Synthesis of 4-(dimethylamino)-2-butanol (DMAB).....	50
4.1.2 Synthesis of 4-(diethylamino)-2-butanol (DEAB).....	59
4.1.3 Synthesis of 4-(dipropylamino)-2-butanol (DPAB).....	64
4.1.4 Synthesis of 4-(dibutylamino)-2-butanol (DBAB).....	69
4.1.5 Synthesis of 4-((2-hydroxyethyl)(methyl)amino)-2-butanol (HEMAB).....	75
4.1.6 Synthesis of 4-((2-hydroxyethyl)(ethyl)amino)-2-butanol (HEEAB).....	81
4.2 Preparation of aqueous amine solution.....	86
4.3 CO <sub>2</sub> equilibrium solubility and cyclic capacity in aqueous amine solutions.....	87
4.4 Heat of CO <sub>2</sub> absorption in aqueous amine solutions.....	97
4.5 CO <sub>2</sub> absorption rate in aqueous amine solutions.....	101
4.6 CO <sub>2</sub> regeneration rate and heat input of CO <sub>2</sub> regeneration in aqueous amine solutions.....	104
4.7 CO <sub>2</sub> equilibrium solubility and cyclic capacity in blended amine solutions.....	106
4.8 CO <sub>2</sub> absorption rate in blended amine solutions.....	113
4.9 CO <sub>2</sub> regeneration rate and heat input of CO <sub>2</sub> regeneration in blended amine solutions.....	115
4.10 CO <sub>2</sub> absorption kinetics of tertiary amines using the stopped-flow apparatus.....	117
4.11 pK <sub>a</sub> values of aqueous tertiary amine solutions.....	129
4.12 The physical properties.....	134
CHAPTER V.....	137
CONCLUSION.....	137

	Page
REFERENCES .....	140
APPENDIX.....	152
Appendix A: Determination of CO <sub>2</sub> concentration in amine samples.....	153
Appendix B: Kinetic reaction from stopped-flow apparatus determination.....	154
Appendix C: The pH and p <i>K</i> <sub>a</sub> values of tertiary amines.....	170
Appendix D: Density, viscosity and refractive index .....	187
VITA.....	190



## LIST OF TABLES

<b>Table 2.1</b> Chemical structures of amines used for CO <sub>2</sub> capture.....	15
<b>Table 4.1</b> <sup>1</sup> H-NMR data of 4-(dimethylamino)-2-butanone.....	51
<b>Table 4.2</b> <sup>13</sup> C-NMR data of 4-(dimethylamino)-2-butanone. ....	52
<b>Table 4.3</b> <sup>1</sup> H-NMR data of 4-(dimethylamino)-2-butanol (DMAB).....	56
<b>Table 4.4</b> <sup>13</sup> C-NMR data of 4-(dimethylamino)-2-butanol (DMAB).....	57
<b>Table 4.5</b> <sup>1</sup> H-NMR data of 4-(diethylamino)-2-butanol (DEAB).....	61
<b>Table 4.6</b> <sup>13</sup> C-NMR data of 4-(diethylamino)-2-butanol (DEAB).....	62
<b>Table 4.7</b> <sup>1</sup> H-NMR data of 4-(dipropylamino)-2-butanone (DPAB).....	66
<b>Table 4.8</b> <sup>13</sup> C-NMR data of 4-(dipropylamino)-2-butanone (DPAB).....	67
<b>Table 4.9</b> <sup>1</sup> H-NMR data of 4-(dibutylamino)-2-butanone (DBAB).....	71
<b>Table 4.10</b> <sup>13</sup> C-NMR data of 4-(dibutylamino)-2-butanone (DBAB).....	72
<b>Table 4.11</b> <sup>1</sup> H-NMR data of 4-((2-hydroxyethyl)(methyl)amino)-2-butanol (HEMAB). ....	77
<b>Table 4.12</b> <sup>13</sup> C-NMR data of 4-((2-hydroxyethyl)(methyl)amino)-2-butanol (HEMAB). ....	78
<b>Table 4.13</b> <sup>1</sup> H-NMR data of 4-((2 hydroxyethyl)(ethyl)amino)-2-butanol (HEEAB).....	83
<b>Table 4.14</b> <sup>13</sup> C-NMR data of 4-((2 hydroxyethyl)(ethyl)amino)-2-butanol (HEEAB).....	84
<b>Table 4.15</b> Molecular weight and solubility of amines at 2 M in deionized water at different temperatures. ....	86
<b>Table 4.16</b> Equilibrium solubility and cyclic capacity of CO <sub>2</sub> in 2 M aqueous DMAB solution.....	88
<b>Table 4.17</b> Equilibrium solubility and cyclic capacity of CO <sub>2</sub> in 2 M aqueous DPAB solution. ....	88
<b>Table 4.18</b> Equilibrium solubility and cyclic capacity of CO <sub>2</sub> in 2 M aqueous DBAB solution.....	89

<b>Table 4.19</b> Equilibrium solubility and cyclic capacity of CO <sub>2</sub> in 2 M aqueous HEMAB solution. ....	89
<b>Table 4.20</b> Equilibrium solubility and cyclic capacity of CO <sub>2</sub> in 2 M aqueous HEEAB solution. ....	90
<b>Table 4.21</b> Equilibrium solubility and cyclic capacity of CO <sub>2</sub> in 2 M aqueous MDEA solution. ....	90
<b>Table 4.22</b> Equilibrium solubility and cyclic capacity of CO <sub>2</sub> in 2 M aqueous DEAB solution. ....	91
<b>Table 4.23</b> Heat of CO <sub>2</sub> absorption, CO <sub>2</sub> absorption rate, pK <sub>a</sub> , CO <sub>2</sub> regeneration rate and heat input for regeneration in aqueous solutions of DMAB, HEMAB and HEEAB compared with MDEA and DEAB. ....	100
<b>Table 4.24</b> Equilibrium solubility and cyclic capacity of CO <sub>2</sub> in blended amine solutions (MEA-DMAB at ratio 5:1.25 M in water). ....	107
<b>Table 4.25</b> Equilibrium solubility and cyclic capacity of CO <sub>2</sub> in blended amine solutions (MEA-HEMAB at ratio 5:1.25 M in water). ....	107
<b>Table 4.26</b> Equilibrium solubility and cyclic capacity of CO <sub>2</sub> in blended amine solutions (MEA-HEEAB at ratio 5:1.25 M in water). ....	108
<b>Table 4.27</b> Equilibrium solubility and cyclic capacity of CO <sub>2</sub> in blended amine solutions (MEA-DEAB at ratio 5:1.25 M in water). ....	108
<b>Table 4.28</b> Equilibrium solubility and cyclic capacity of CO <sub>2</sub> in blended amine solutions (MEA-MDEA at ratio 5:1.25 M in water). ....	109
<b>Table 4.29</b> Equilibrium solubility and cyclic capacity of CO <sub>2</sub> in 5 M aqueous MEA solution. ....	109
<b>Table 4.30</b> CO <sub>2</sub> absorption rate, CO <sub>2</sub> regeneration rate and heat input for regeneration of blended amine solution (i.e. MEA-DMAB, MEA-HEMAB, MEA-HEEAB, MEA-DEAB and MEA-MDEA at concentration ratio of 5:1.25 M) compare with single 5 M MEA in water. ....	114
<b>Table 4.31</b> Experimental kinetics data for HEMAB over ranges of concentration and temperature of 0.1-0.5 M and 293-313 K. ....	119
<b>Table 4.32</b> Experimental kinetics data for HEEAB over ranges of concentration and temperature of 0.1-0.5 M and 293-313 K. ....	119
<b>Table 4.33</b> Experimental kinetics data for DMAB over ranges of concentration and temperature of 0.10-1.0 M and 293-313 K. ....	119



<b>Table 4.34</b> Experimental kinetics data for DEAB over ranges of concentration and temperature of 0.10-1.0 M and 293-313 K. ....	120
<b>Table 4.35</b> Experimental kinetics data for MDEA over ranges of concentration and temperature of 0.10-1.0 M and 293-313 K. ....	120
<b>Table 4.36</b> The second-order reaction rate constants ( $k_2$ ) of CO <sub>2</sub> absorption at 298 K, activation energy ( $E_a$ ) and frequency factor (A) at 298-313 K in aqueous solutions of HEEAB, HEMAB and DMAB compared with DEAB and MDEA.....	128
<b>Table 4.37</b> $pK_a$ values of HEMAB, HEEAB, and DMAB compared with DEAB and MDEA at 296.5-333.0 K.....	130



## LIST OF FIGURES

<b>Figure 2.1</b> Shares of greenhouse gas emission. ....	7
<b>Figure 2.2</b> Pre-combustion process. ....	8
<b>Figure 2.3</b> Oxy-combustion process. ....	9
<b>Figure 2.4</b> Post-combustion process. ....	9
<b>Figure 2.5</b> Schematic flow diagram of the amine absorption unit for CO <sub>2</sub> recovery from flue gas stream. ....	13
<b>Figure 2.6</b> Chemical structures of primary, secondary and tertiary amine. ....	14
<b>Figure 3.1</b> The chemical structures of synthesized amines, DEAB, and MDEA used in this study. ....	32
<b>Figure 3.2</b> Schematic diagram of the experimental setup for CO <sub>2</sub> equilibrium loading measurement. ....	38
<b>Figure 3.3</b> CO <sub>2</sub> loading measurement equipment. ....	40
<b>Figure 3.4</b> The simplified apparatus of CO <sub>2</sub> absorption and regeneration kinetic rates. ....	42
<b>Figure 3.5</b> Schematic diagram of stopped-flow equipment. ....	48
<b>Figure 4.1</b> <sup>1</sup> H-NMR (500 MHz, CDCl <sub>3</sub> ) spectrum of 4-(dimethylamino)-2-butanone. ....	51
<b>Figure 4.2</b> <sup>13</sup> C-NMR (125 MHz, CDCl <sub>3</sub> ) spectrum of 4-(dimethylamino)-2-butanone. ....	52
<b>Figure 4.3</b> GC-MS chromatogram of 4-(dimethylamino)-2-butanone. ....	53
<b>Figure 4.4</b> Mass spectrum of 4-(dimethylamino)-2-butanone. ....	53
<b>Figure 4.5</b> FT-IR spectrum of 4-(dimethylamino)-2-butanol (DMAB). ....	55
<b>Figure 4.6</b> <sup>1</sup> H-NMR (500 MHz, D <sub>2</sub> O) spectrum of 4-(dimethylamino)-2-butanol (DMAB). ....	56
<b>Figure 4.7</b> <sup>13</sup> C-NMR (125 MHz, D <sub>2</sub> O) spectrum of 4-(dimethylamino)-2-butanol (DMAB). ....	57
<b>Figure 4.8</b> GC-MS chromatogram of 4-(dimethylamino)-2-butanol (DMAB). ....	58
<b>Figure 4.9</b> Mass spectrum of 4-(dimethylamino)-2-butanol (DMAB). ....	58

<b>Figure 4.10</b> FT-IR spectrum of 4-(diethylamino)-2-butanol (DEAB).....	60
<b>Figure 4.11</b> $^1\text{H-NMR}$ (500 MHz, $\text{CDCl}_3$ ) spectrum of 4-(diethylamino)-2-butanol (DEAB).....	61
<b>Figure 4.12</b> $^{13}\text{C-NMR}$ (125 MHz, $\text{CDCl}_3$ ) spectrum of 4-(diethylamino)-2-butanol (DEAB).....	62
<b>Figure 4.13</b> GC-MS chromatogram of 4-(diethylamino)-2-butanol (DEAB).....	63
<b>Figure 4.14</b> Mass spectrum of 4-(diethylamino)-2-butanol (DEAB). ....	63
<b>Figure 4.15</b> FT-IR spectrum of 4-(dipropylamino)-2-butanol (DPAB).....	65
<b>Figure 4.16</b> $^1\text{H-NMR}$ (500 MHz, $\text{CDCl}_3$ ) spectrum of 4-(dipropylamino)-2-butanone (DPAB).....	66
<b>Figure 4.17</b> $^{13}\text{C-NMR}$ (125 MHz, $\text{CDCl}_3$ ) spectrum of 4-(dipropylamino)-2-butanone (DPAB).....	67
<b>Figure 4.18</b> GC-MS chromatogram of 4-(dipropylamino)-2-butanone (DPAB). ....	68
<b>Figure 4.19</b> Mass spectrum of 4-(dipropylamino)-2-butanone (DPAB).....	68
<b>Figure 4.20</b> FT-IR spectrum of 4-(dibutylamino)-2-butanol (DBAB). ....	70
<b>Figure 4.21</b> $^1\text{H-NMR}$ (500 MHz, $\text{CDCl}_3$ ) spectrum of 4-(dibutylamino)-2-butanone (DBAB). ....	71
<b>Figure 4.22</b> $^{13}\text{C-NMR}$ (125 MHz, $\text{CDCl}_3$ ) spectrum of 4-(dibutylamino)-2-butanone (DBAB). ....	72
<b>Figure 4.23</b> GC-MS chromatogram of 4-(dibutylamino)-2-butanone (DBAB).....	73
<b>Figure 4.24</b> Mass spectrum of 4-(dibutylamino)-2-butanone (DBAB). ....	74
<b>Figure 4.25</b> FT-IR spectrum of 4-((2-hydroxyethyl) (methyl)amino)-2-butanol (HEMAB). ....	76
<b>Figure 4.26</b> $^1\text{H-NMR}$ (500 MHz, $\text{CDCl}_3$ ) spectrum of 4-((2-hydroxyethyl)(methyl) amino)-2-butanol (HEMAB). ....	77
<b>Figure 4.27</b> $^{13}\text{C-NMR}$ (125 MHz, $\text{CDCl}_3$ ) spectrum of 4-((2-hydroxyethyl)(methyl) amino)-2-butanol (HEMAB). ....	78
<b>Figure 4.28</b> GC-MS chromatogram of 4-((2-hydroxyethyl)(methyl)amino)-2-butanol (HEMAB). ....	79
<b>Figure 4.29</b> Mass spectrum of 4-((2-hydroxyethyl)(methyl)amino)-2-butanol (HEMAB). ....	80

<b>Figure 4.30</b> FT-IR spectrum of 4-((2-hydroxyethyl)(ethyl)amino)-2-butanol (HEEAB).....	82
<b>Figure 4.31</b> <sup>1</sup> H-NMR (500 MHz, CDCl <sub>3</sub> ) spectrum of 4-((2 hydroxyethyl)(ethyl)amino)-2-butanol (HEEAB).....	83
<b>Figure 4.32</b> <sup>13</sup> C-NMR (125 MHz, CDCl <sub>3</sub> ) spectrum of 4-((2-hydroxyethyl)(ethyl)amino)-2-butanol (HEEAB).....	84
<b>Figure 4.33</b> GC-MS chromatogram of 4-((2-hydroxyethyl)(ethyl)amino)-2-butanol (HEEAB).....	85
<b>Figure 4.34</b> Mass spectrum of 4-((2-hydroxyethyl)(ethyl)amino)-2-butanol (HEEAB).....	85
<b>Figure 4.35</b> Validation of CO <sub>2</sub> equilibrium solubility in the aqueous solutions of 2 M MDEA and 2 M DEAB solutions at 313 K.....	87
<b>Figure 4.36</b> Equilibrium solubility of CO <sub>2</sub> in 2 M DMAB, DPAB, DBAB, HEMAB, HEEAB, DEAB and MDEA solution at 298 K.....	92
<b>Figure 4.37</b> Equilibrium solubility of CO <sub>2</sub> in 2 M DMAB, DPAB, DBAB, HEMAB, HEEAB, DEAB and MDEA solution at 313 K.....	92
<b>Figure 4.38</b> Equilibrium solubility of CO <sub>2</sub> in 2 M DMAB, DPAB, DBAB, HEMAB, HEEAB, DEAB and MDEA solution at 333 K.....	93
<b>Figure 4.39</b> Equilibrium solubility of CO <sub>2</sub> in 2 M DMAB, DPAB, DBAB, HEMAB, HEEAB, DEAB and MDEA solution at 353 K.....	93
<b>Figure 4.40</b> The relationship between CO <sub>2</sub> solubility at temperature at 313 K, 15 kPa CO <sub>2</sub> partial pressure and cyclic capacity at different temperatures (313-353 K) of seven amines (DMAB, DPAB, DBAB, HEMAB, HEEAB, MDEA and DEAB). .	96
<b>Figure 4.41</b> Plot of ln <i>P</i> <sub>CO<sub>2</sub></sub> and 1/ <i>T</i> of 2 M DMAB. ....	98
<b>Figure 4.42</b> Plot of ln <i>P</i> <sub>CO<sub>2</sub></sub> and 1/ <i>T</i> of 2 M HEMAB. ....	98
<b>Figure 4.43</b> Plot of ln <i>P</i> <sub>CO<sub>2</sub></sub> and 1/ <i>T</i> of 2 M HEEAB. ....	99
<b>Figure 4.44</b> Plot of ln <i>P</i> <sub>CO<sub>2</sub></sub> and 1/ <i>T</i> of 2 M MDEA .....	99
<b>Figure 4.45</b> The plot of ln <i>P</i> <sub>CO<sub>2</sub></sub> and 1/ <i>T</i> of 2 M DEAB. ....	100
<b>Figure 4.46</b> CO <sub>2</sub> loading as a function of time for five amines (DMAB, HEMAB, HEEAB, MDEA and DEAB) at temperature of 313 K. ....	101
<b>Figure 4.47</b> The relationship between heat of CO <sub>2</sub> absorption and CO <sub>2</sub> absorption rate of five amines (DMAB, HEMAB, HEEAB, MDEA and DEAB).....	103

<b>Figure 4.48</b> CO <sub>2</sub> loading as a function of time for five amines (DMAB, HEMAB, HEEAB, MDEA and DEAB) at temperature of 363 K. ....	104
<b>Figure 4.49</b> The relationship between heat input and regeneration rate of five amines (DMAB, HEMAB, HEEAB, MDEA and DEAB). ....	105
<b>Figure 4.50</b> Equilibrium solubility of CO <sub>2</sub> in blended amine solutions (MEA-DMAB, MEA-HEMAB, MEA-HEEAB, MEA-DEAB and MEA-MDEA at ratio 5:1.25 M) compare with 5 M MEA in water at 298 K. ....	110
<b>Figure 4.51</b> Equilibrium solubility of CO <sub>2</sub> in blended amine solutions (MEA-DMAB, MEA-HEMAB, MEA-HEEAB, MEA-DEAB and MEA-MDEA at ratio 5:1.25 M) compare with 5 M MEA in water at 313 K. ....	110
<b>Figure 4.52</b> Equilibrium solubility of CO <sub>2</sub> in blended amine solutions (MEA-DMAB, MEA-HEMAB, MEA-HEEAB, MEA-DEAB and MEA-MDEA at ratio 5:1.25 M) compare with 5 M MEA in water at 353 K. ....	111
<b>Figure 4.53</b> CO <sub>2</sub> loading as a function of time for blended amine solvents (i.e. MEA-DMAB, MEA-HEMAB, MEA-HEEAB, MEA-DEAB and MEA-MDEA at concentration ratio of 5:1.25 M) compare with single 5 M MEA in water at temperature of 313 K. ....	114
<b>Figure 4.54</b> CO <sub>2</sub> loading as a function of time for blended amine solvents (i.e. MEA-DMAB, MEA-HEMAB, MEA-HEEAB, MEA-DEAB and MEA-MDEA at concentration ratio of 5 : 1.25 M) compare with single 5 M MEA in water at temperature of 363 K. ....	115
<b>Figure 4.55</b> Validation of $k_0$ values of MEA solution at 298 K. ....	118
<b>Figure 4.56</b> Effect of HEMAB concentration range 0.1-0.5 M and temperature range of 298-313 K on kinetics data in terms of $k_0$ . ....	121
<b>Figure 4.57</b> Effect of HEEAB concentration range 0.1-0.5 M and temperature range of 298-313 K on kinetics data in terms of $k_0$ . ....	121
<b>Figure 4.58</b> Effect of DMAB concentration range 0.1-1.0 M and temperature range of 298-313 K on kinetics data in terms of $k_0$ . ....	122
<b>Figure 4.59</b> Effect of DEAB concentration range 0.1-1.0 M and temperature range of 298-313 K on kinetics data in terms of $k_0$ . ....	122
<b>Figure 4.60</b> Effect of MDEA concentration range 0.2-1.0 M and temperature range of 298-313 K on kinetics data in terms of $k_0$ . ....	123
<b>Figure 4.61</b> Arrhenius plot of the second-order reaction rate constant ( $k_2$ ) of all amines. ....	125
<b>Figure 4.62</b> $pK_a$ values of tertiary amines over a temperature range of 298-313 K. ....	129

- Figure 4.63** Brønsted plots of HEMAB, HEEAB, DMAB compared with DEAB and MDEA. .... 132
- Figure 4.64** The density changes of pure DMAB, DPAB, DBAB, HEMAB, HEEAB, DEAB, MDEA, MEA, and water at temperatures from 293 to 333 K. .... 134
- Figure 4.65** The viscosity of pure DMAB, DPAB, DBAB, HEMAB, HEEAB, DEAB, MDEA, MEA, and water at temperatures from 293 to 333 K. .... 135
- Figure 4.66** The refractive indices of pure DMAB, DPAB, DBAB, HEMAB, HEEAB, DEAB, MDEA, MEA, and water at temperatures ranging from 293 to 323 K. .... 136



**LIST OF SCHEMES**

<b>Scheme 2.1</b> Mechanism of 1,4-Michael addition reaction. ....	18
<b>Scheme 2.2</b> Mechanism of Mannich reaction. ....	19
<b>Scheme 4.1</b> Synthesis route of 4-(dimethylamino)-2-butanone. ....	50
<b>Scheme 4.2</b> Synthesis route of 4-(dimethylamino)-2-butanol (DMAB). ....	54
<b>Scheme 4.3</b> Synthesis route of 4-(diethylamino)-2-butanol (DEAB). ....	59
<b>Scheme 4.4</b> Synthesis route of 4-(dipropylamino)-2-butanol (DPAB). ....	64
<b>Scheme 4.5</b> Synthesis route of 4-(dibutylamino)-2-butanol (DBAB). ....	69
<b>Scheme 4.6</b> Synthesis route of 4-((2-hydroxyethyl)(methyl)amino)-2-butanol (HEMAB). ....	75
<b>Scheme 4.7</b> Synthesis route of 4-((2-hydroxyethyl)(ethyl)amino)-2-butanol (HEEAB). ....	81

## ABBREVIATION

DMAB	4-(dimethylamino)-2-butanol
DPAB	4-(dipropylamino)-2-butanol
DBAB	4-(dibutylamino)-2-butanol
HEMAB	4-((2-hydroxyethyl)(methyl)amino)-2-butanol
HEEAB	4-((2-hydroxyethyl)(ethyl)amino)-2-butanol
DEAB	4-(diethylamino)-2-butanol
MDEA	methyldiethanolamine
$\Delta H_{\text{abs}}$	heat of CO <sub>2</sub> absorption (J/mol)
$P_{\text{CO}_2}$	CO <sub>2</sub> partial pressure (kPa)
$T$	temperature (K)
$R$	universal gas constant (8.315 J/mol K)
$K_a$	amine dissociation constant (mol/L)
pH	potential hydrogen
$pK_a$	acid dissociation constant
$n_{0,\text{Amine}}$	initial number of mole of amine (mol)
$n_{\text{HCl}}$	number of moles of HCl added during the titration (mol)
$V_{\text{total}}$	total liquid volume after titration (L)
$q$	rate of heat transfer (J/s)
$Q$	heat input of CO <sub>2</sub> regeneration (kJ/mol)
$k$	thermal conductivity of glass (W/m. °C)
$A$	surface area of flask's spherical section with 100 mL amine volume (m)
$R$	flask's spherical radius (m)



$h$	height of the spherical sector (m)
$dT$	temperature difference between oil bath and amine solution (°C)
$dr$	glass wall thickness (m)
$k_0$	the observed pseudo-first order reaction rate constant
$k_2$	the second-order rate constant (m <sup>3</sup> /kmol.s)
$n$	average reaction order
$A$	pre-exponential factor or frequency factor (s <sup>-1</sup> )
$E_a$	the activation energy (kJ/mol)
$R$	the universal gas constant (0.008315 kJ/mol.K)
$A$	the amplitude of signal
$Y$	conductance (S)
$Y_\infty$	conductance at the end of observed reaction (S)

### Greek letter

$\beta$	beta
$\delta$	chemical shift (ppm)
$\alpha$	CO <sub>2</sub> loading (mol CO <sub>2</sub> /mol amine)
$\Delta\alpha$ , at 0-80 min	CO <sub>2</sub> loading difference between 0 and 80 min

# CHAPTER I

## INTRODUCTION

### 1.1 Introduction

Carbon dioxide (CO<sub>2</sub>) is one of the major greenhouse gases known to contribute to climate change and give rise to environmental problems. There are several technologies currently employed for the separation and capture of CO<sub>2</sub> from flue gases such as absorption, adsorption, cryogenics distillation, and membrane separation [1-6]. Based on the literature [1, 7-11] one of the most mature technologies for reducing CO<sub>2</sub> emissions, especially from large point sources including fossil fuel based power stations is the post-combustion capture process using amine reactive solvents. However, the use of a highly reactive amine is one of the key factors to the success of the capture technology in industrial process, which can satisfy several essential requirements, such as, high absorption capacity, cyclic capacity, solvent stability and mass transfer coefficient, fast reaction kinetics, low corrosion, degradation and heat duty requirement for the solvent regeneration [12-15].

Although extensively used conventional amines such as primary amines (such as monoethanolamine (MEA), 2-amino-2-methyl-1-propanol (AMP)), secondary amine (such as diethanolamine (DEA)), tertiary amine (such as methyldiethanolamine (MDEA)), and polyamines (such as piperazine (PZ), 2-(2-aminoethylamino)ethanol (AEEA), diethylenetriamine (DETA)) are effective for capturing CO<sub>2</sub> from various industrial processes (e.g. natural gas sweetening, petroleum refining, reformat gas stream and carbon dioxide capture from fossil fuel-fired power plant flue gas), there are still some drawbacks in their use such as low absorption rate, amine loss by degradation and volatilization, high energy consumption for CO<sub>2</sub> regeneration and severe corrosion of equipments. For example, primary amines form a very stable carbamate with CO<sub>2</sub> which requires a high regeneration energy in its break-down process. Secondary amines such as DEA can directly react with NO<sub>x</sub>, a common impurity in fossil fuel fired flue gas, emitting potentially hazardous nitrosamines with the off-gas. Also, although tertiary amines need less heat of regeneration compared to

the other amines, they suffer from having a slow rate of reaction with CO<sub>2</sub>, thus affecting the kinetics of capture process.

The kinetics of the reaction of CO<sub>2</sub> with many amine systems, including primary amines (such as MEA, AMP), secondary amines (such as DEA), tertiary amines (such as MDEA), also, mixed-amines (such as AMP mixed with MEA or DEA) have been successfully studied for many years [16-21]. Currently, tertiary amines, which are considered to be reasonable solvents because they need less heat of regeneration compared to other amines, although its disadvantage is that it has a slow reaction rate with CO<sub>2</sub> [22-25]. The technique for evaluating the potential of the new amine solvent that can be used for removing CO<sub>2</sub> from flue gas in terms of the kinetics of CO<sub>2</sub> absorption into aqueous amine solution is the stopped-flow technique, which is considered to be a direct method because CO<sub>2</sub> is saturated in the liquid phase, directly reacting with the amine solvent. This frequently used technique offers several intrinsic advantages, such as no limitation of a gas-liquid mass transfer, no effect on reversibility of the reaction, small amount of solvent is consumed ( $\sim 0.1$  mL for every experiment), easy operation, and short experiment runtime [18, 19].

To cope with such inefficiency of these amines, efforts are constantly being made in developing new amines that can have better CO<sub>2</sub> capture properties of high absorption and cyclic capacity, fast reaction kinetics, low corrosion, degradation, and heat duty requirement for solvent regeneration [14, 15]. Recently, new amino alcohols have been developed based on an approach of rational molecular design and synthesis. The synthesis approach involved a systematic modification of the amino alcohol structure by appropriately placing, specifically hydroxyl (-OH) or alkyl (-R) groups, relative to the position of the amino group (-NH<sub>2</sub>) [9-12].

The previously developed tertiary amines, specifically, 4-(diethylamino)-2-butanol (DEAB) and 4-(ethyl-methylamino)-2-butanol (EMAB) have shown quite an improvement from the conventional MDEA solvent. Compared to MDEA, DEAB and EMAB have a higher absorption and cyclic capacity for CO<sub>2</sub> removal and lower energy consumption [26-28]. To improve the properties of these amines even further, a proper molecular structure modification can be done as to help the amines to better absorb and desorb CO<sub>2</sub> during the regeneration process while maintaining a low heat

of reaction and heat duty requirement and high CO<sub>2</sub> absorption rate, and cyclic capacity.

In this work, new tertiary amines (i.e. DMAB, DPAB, DBAB, HEMAB and HEEAB) were synthesized by varying the alkyl chain length with and without a hydroxyl (-OH) group, attached to the amino nitrogen atom based on our DEAB structure. The development was based on the concept of increasing amine reactivity of the amines via the use of an effective electron donating alkyl group and proper placement of hydroxyl (-OH) group within the amine structure [29]. The newly synthesized amines using 2 M concentration and blended new amines with MEA at ratio 5:1.25 M were evaluated based on their equilibrium CO<sub>2</sub> absorption capacity and cyclic capacity measured in the temperature range of 298-353 K and partial CO<sub>2</sub> pressure range of 3-100 kPa. The kinetic absorption and regeneration rates at actual concentrations were also measured respectively at 313 K and 363 K. The amines were also measured for heats of absorption and regeneration.

This work also investigated the kinetics of the reaction of CO<sub>2</sub> absorption of the newly synthesized tertiary amines (i.e. HEMAB, HEEAB and DMAB) as compared with DEAB and MDEA using the stopped-flow apparatus in temperature range of 298-313 K and amine concentration range of 0.1-1.0 mol/L. Furthermore, the physical properties of these new amine solvents in terms of density, viscosity and refractive index are also considered in this research.

## 1.2 Objective of this research

1. To synthesize novel new tertiary amine solvents (i.e. DMAB, DPAB, DBAB, HEMAB and HEEAB) that can be used for the capture of CO<sub>2</sub> from industrial flue gas.
2. To obtain the CO<sub>2</sub> solubility data into aqueous solutions of the single newly synthesized tertiary amines and blended newly synthesized tertiary amines with MEA.
3. To obtain the kinetic reaction rates of absorption and regeneration at actual concentrations, and heats of absorption and regeneration into the single newly synthesized tertiary amines and heat input of CO<sub>2</sub> regeneration of blended amines.
4. To obtain the reaction kinetics of CO<sub>2</sub> absorption of the newly synthesized tertiary amines (i.e. HEMAB, HEEAB and DMAB) compared with DEAB and MDEA using the stopped-flow apparatus.
5. To obtain the physical properties of the single newly synthesized tertiary amines such as density, viscosity and refractive index.

## 1.3 Scope of investigation

The stepwise investigation was carried out as follows:

1. Literature survey of related research work
2. Part I: Synthesis and characterization of the newly synthesized tertiary amines
  - 2.1 Synthesize tertiary amines; 4-(dimethylamino)-2-butanol (DMAB) and 4-(diethylamino)-2-butanol (DEAB) *via* Mannish reaction
  - 2.2 Synthesize tertiary amines; 4-(dipropylamino)-2-butanol (DPAB), 4-(dibutylamino)-2-butanol (DBAB), 4-((2-hydroxyethyl)(methyl)amino)-2-butanol (HEMAB) and 4-((2-hydroxyethyl)(ethyl)amino)-2-butanol (HEEAB) *via* Michael addition reaction
  - 2.3 Characterization of the newly synthesized tertiary amines by spectroscopic techniques, namely Fourier Transform infrared spectroscopy (FT-IR), <sup>1</sup>H and <sup>13</sup>C-NMR and Gas Chromatography-Mass Spectroscopy (GC-MS)

- 2.4 Investigate the solubility properties of amines in H<sub>2</sub>O and blended solvents (H<sub>2</sub>O : MeOH at ratio 2:1) at room temperature
3. Part II: Investigation of CO<sub>2</sub> absorption performance of the newly synthesized tertiary amines in terms of absorption capacity, cyclic capacity, and heat of CO<sub>2</sub> absorption at various conditions
  - 3.1 The types and amounts of amines
    - Single newly synthesized tertiary amines at 2 M concentration in water
    - Blended newly synthesized tertiary amines with MEA at ratio 5:1.25 M in water
  - 3.2 Partial pressure for CO<sub>2</sub> at 3, 8, 15, 30 and 100 kPa
  - 3.3 Temperature at 298, 313, 333 and 353 K
  - 3.4 Total gas flow rate of 200-250 mL/min
  - 3.5 Duration of experiment 20-22 hours
4. Part III: To study the CO<sub>2</sub> absorption and regeneration rates at actual concentration, and heat input of CO<sub>2</sub> regeneration
  - 4.1 The type and amount of amines
    - Single newly synthesized tertiary amines at 2 M concentration in water
    - Blended newly synthesized tertiary amines with MEA at ratio 5:1.25 M in water
  - 4.2 Partial pressure for CO<sub>2</sub> at 3, 8, 15, 30 and 100 kPa
  - 4.3 Temperature at 313 and 363 K
  - 4.4 Total gas flow rate of 200 mL/min ( $\pm 2$  mL/min accuracy)
5. Part IV: To study the amine dissociation constant analysis using a pH meter at various temperatures
  - 5.1 Temperature at 296.5, 298, 303, 308, 313, 318, 323, 328 and 333 K
6. Part V: To study the kinetics of the reaction of CO<sub>2</sub> absorption using the stopped-flow apparatus
  - 6.1 The type and amount of amines
    - Single newly synthesized tertiary amines at 2 M concentration in water
  - 6.2 Amine concentrations
    - High amine concentration range of 0.1-1 M of DMAB, DEAB and MDEA

- Low amine concentration range of 0.1-0.5 M of HEMAB and HEEAB

6.3 Temperature at 298, 303, 308 and 313 K

7. Part VI: To study the physical properties of single newly synthesized tertiary amines such as density, viscosity and refractive index in pure solvent

7.1 Temperature at 293, 298, 303, 308, 313, 318, 323, 328 and 333 K



## CHAPTER II

### THEORETICAL STUDIES AND LITERATURE REVIEW

The global warming and climate change from increased levels of greenhouse gases (GHGs) have become critical environmental issues. Among GHGs, carbon dioxide (CO<sub>2</sub>) is considered to be the largest fraction of greenhouse gas emissions to the atmosphere. According to the Emissions Database for Global Atmospheric Research (EDGAR, 2015) based in the International Energy Agency (IEA), about 64 % of CO<sub>2</sub> emissions from fossil-fuel combustion and industrial processes represents two-thirds of global total greenhouse gas emissions, with the other sources of greenhouse gas emissions contributing to the remaining third as shown in Figure 2.1. Thus, carbon capture and storage (CCS) from industrial flue gases has become an essential in order to make any mitigation impact on critical CO<sub>2</sub> emission. The capture CO<sub>2</sub> can then be used in many ways such as beverage grade CO<sub>2</sub> in carbonated drink industry, catalytic converted to methanol or diethyl ether, used as a flooding medium in the enhanced oil recovery process as widely known as CO<sub>2</sub>-EOR [30, 31].

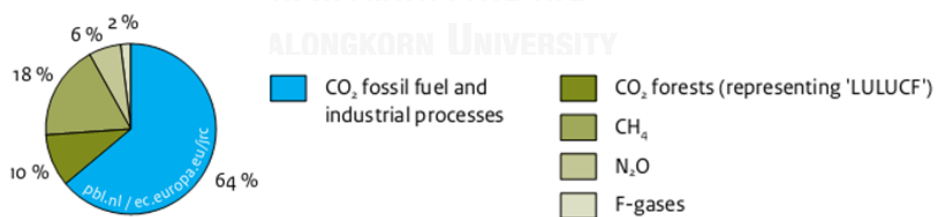


**Figure 2.1** Shares of greenhouse gas emission.



## 2.1 Technology for reducing CO<sub>2</sub> emissions

The technology for reducing CO<sub>2</sub> emissions into the atmosphere from industrial gas streams from coal-fired power plants can generally be divided into three major categories such as pre-combustion, oxy-combustion and post-combustion processes.

### 2.1.1 Pre-combustion process

This process is accomplished by reacting coal with steam and oxygen (O<sub>2</sub>) at high temperature and pressure, a process call partial oxidation or gasification. The result is a gaseous fuel consisting mainly of carbon monoxide (CO) and hydrogen (H<sub>2</sub>) (synthesis gas), which is then reacted with steam to form a mixture of H<sub>2</sub> and CO<sub>2</sub>. The pre-combustion process as shown in Figure 2.2.

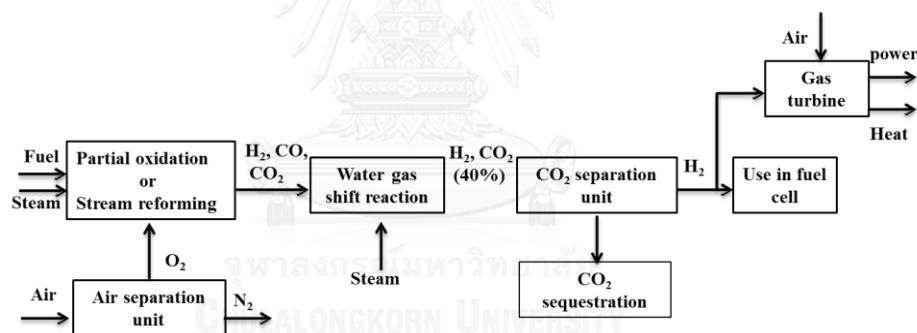


**Figure 2.2** Pre-combustion process.

### 2.1.2 Oxy-combustion process

This process burns fossil fuel in almost pure O<sub>2</sub> instead of air. The exhaust gas is made up mostly of pure CO<sub>2</sub> and water, which is easily separated and it does not require a CO<sub>2</sub> capture device. However, producing pure O<sub>2</sub> is an expensive and energy-intensive process. This concept is still under development and is not yet commercial in power plant operations. The oxy-combustion process as shown in Figure 2.3.

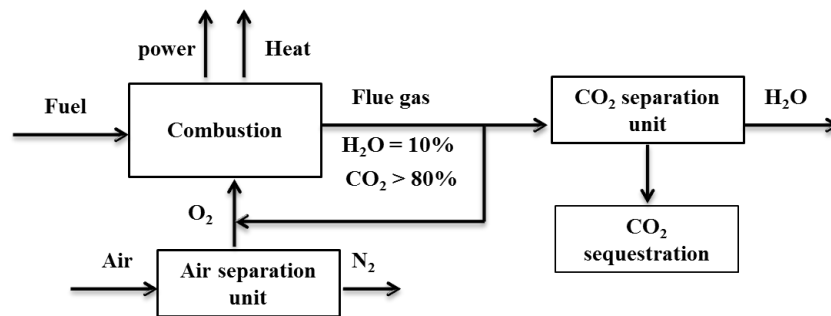


**Figure 2.3** Oxy-combustion process.

### 2.1.3 Post-combustion process

Post-combustion process for capture of CO<sub>2</sub> from the exhaust gas, which are amines solvent that selectively react with CO<sub>2</sub>. Heating this solvent releases concentrated CO<sub>2</sub>, allowing the solvent to be recycled. This technology can be properly retrofitted to existing power plants and widely used processes [7-9]. The post-combustion process as shown in Figure 2.4.

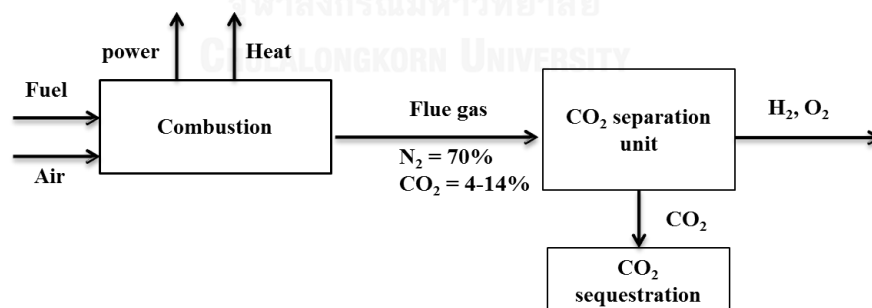


**Figure 2.4** Post-combustion process.

## **2.2 Technology for separation of CO<sub>2</sub> from post-combustion flue gas**

Currently, there are several technologies for the capture and separation of CO<sub>2</sub> from post-combustion flue gas streams including absorption, adsorption, membrane and cryogenics. Choosing the suitable techniques are dependent on many factors, such as the purity of the treated gases, partial pressure of CO<sub>2</sub> in gas streams, extent of CO<sub>2</sub> recovery required, operating costs of the process, etc. [11, 26, 32-36].

### **2.2.1 Absorption technology**

Absorption technology, which is at present the most viable technique for CO<sub>2</sub> capture due to the CO<sub>2</sub> can be absorbed chemically, physically, or both chemically and physically by the solvent at low temperatures (25-40 °C) and desorbed from the amine solvent by applying heat or reducing the pressure. Hence, the use of a highly reactive amine solvent is one of the key importance to the success of the capture technology in industrial processes. The absorption of CO<sub>2</sub> is normally carried out in a counter current flow process using a contact tower. The gas is introduced near the bottom of the absorber and the amine solvent is introduced at the top of the absorber as shown in Figure 2.5. Absorption can be divided into chemical absorption and physical absorption.

#### **2.2.1.1 Physical absorption**

The physical process is based on dissolving CO<sub>2</sub> molecules into a solvent in the absence of a chemical reaction. This process is generally suitable for natural gas processing plants that have a high partial pressure of CO<sub>2</sub>.

#### **2.2.1.2 Chemical absorption**

Chemical absorption involves a chemical reaction between the gaseous component being absorbed and a component of the liquid phase to form reaction products. This process is suitable for coal fire power generation plants that have low partial pressure of CO<sub>2</sub> and low temperature.

### **2.2.2 Adsorption technology**

The adsorption process relies on the attraction between CO<sub>2</sub> and the solid absorbent. In this process, the fluid is passed through the bed (solid absorbent) and the bed is regenerated from the amine solvent by applying heat or other methods. This technology is simple and easy to operate but it has a high operation cost and low efficiency.

### **2.2.3 Membrane**

Membrane technology is a semi-permeable barrier that allows the passage of selected components. There are two approaches applied in the literature for this technology, and those are a membrane that can be used for the separation of CO<sub>2</sub> from the stream and a membrane that is used to increase the CO<sub>2</sub> amine interface.

### **2.2.4 Cryogenics**

Cryogenic separation has been used commercially for the purification of CO<sub>2</sub> from streams that already have high CO<sub>2</sub> concentrations of least 70 %. In this process, CO<sub>2</sub> from combustion gas streams can be liquefied by compression and cooling, and the liquefied CO<sub>2</sub> is separated directly from the process. However, cryogenic methods are expensive and require high energy refrigeration consumption.

### 2.3 General description of CO<sub>2</sub> absorption using aqueous amines

The process flow diagram for an acid-gas absorption process system is shown in Figure 2.5 [37]. It consists of the absorber and regenerator (desorber) columns, lean-rich heat exchanger, and reboiler. The absorber and desorber columns contain the materials packing. The CO<sub>2</sub> in the gas stream enters from the bottom of the absorber, passing upwards through the absorber, countercurrent to a stream of amine entering at the top of the absorber. The CO<sub>2</sub> in the gas stream reacts reversibly with the amine (referred to as the rich amine solution) flowing to the bottom of the absorber. The treated CO<sub>2</sub> lean gas exits at the top of the absorber. The rich amine from the bottom of the absorber is pumped to the lean-rich heat exchanger before it is introduced to the top of the regenerator. In the regenerator column, the rich amine reacts reversibly with a stream of water, resulting in CO<sub>2</sub> desorption from the solution and amine evaporation. The top of the regenerator is also connected to a condenser to help recover water and amine carry over back into the system. The amine solution containing a low concentration of CO<sub>2</sub> referred to as the lean amine solution. The lean amine solution coming out from the bottom of the regenerator after CO<sub>2</sub> stripping was cooled down by a water cooling system and directly flowed back to the top of the absorber to complete the cycle.

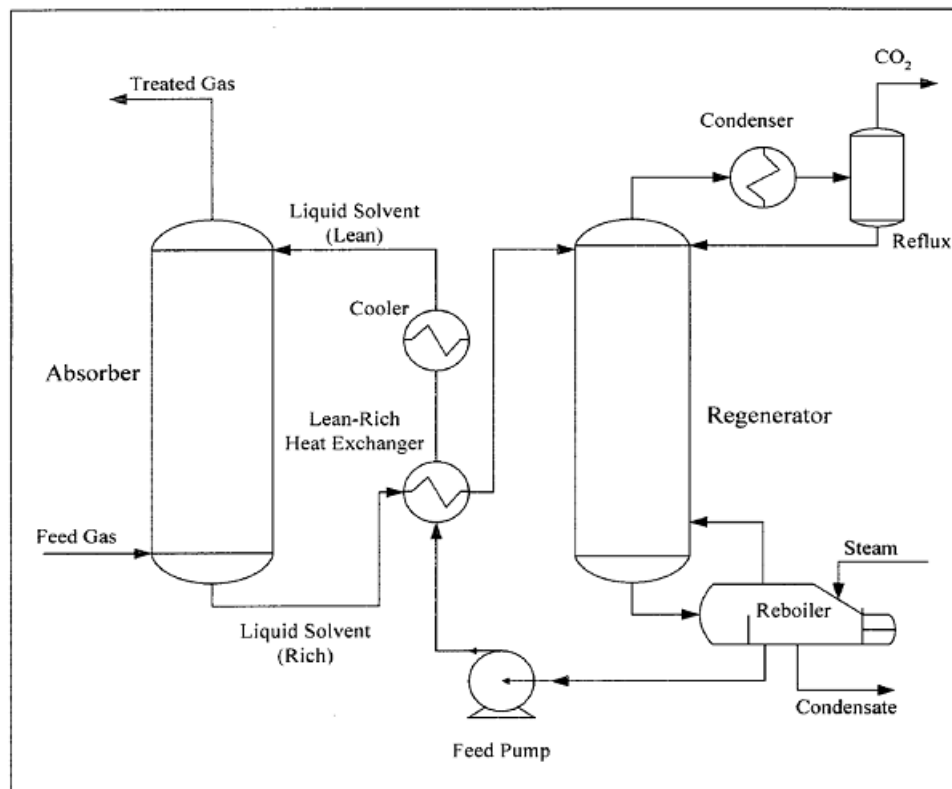
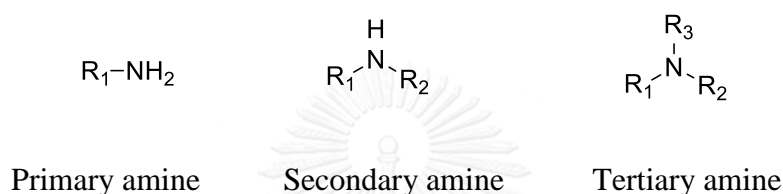


**Figure 2.5** Schematic flow diagram of the amine absorption unit for CO<sub>2</sub> recovery from flue gas stream.

## 2.4 Chemical solvents for CO<sub>2</sub> absorption

Currently, amines are particularly important for CO<sub>2</sub> capture because of their wide use in various industrial processes (e.g. natural gas sweetening, petroleum refining, reformat gas stream and carbon dioxide capture from fossil fuel-fired power plant flue gas). Amines for CO<sub>2</sub> capture can be classified into different groups depending on the number of carbon atoms directly bonded to the nitrogen atom. There are primary, secondary, and tertiary amines as shown in Figure 2.6.

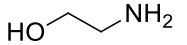
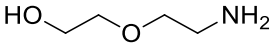
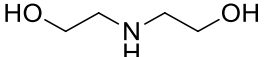
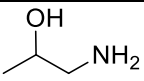
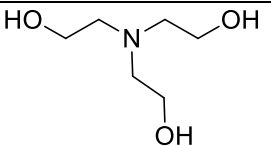
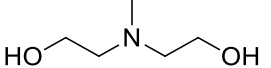
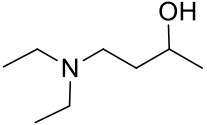
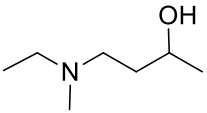
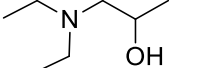
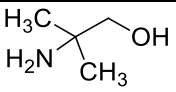
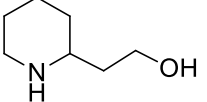
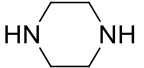
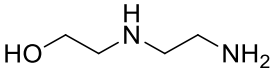
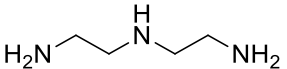


Where, R<sub>1</sub>, R<sub>2</sub> and R<sub>3</sub> are alkyl chain with/without hydroxyl (OH)

**Figure 2.6** Chemical structures of primary, secondary and tertiary amine.

Conventional amines that have been extensively used for the capture of CO<sub>2</sub> from various industrial processes include primary amines (such as monoethanolamine (MEA), 2-amino-2-methyl-1-propanol (AMP), and diglycolamine (DGA)), secondary amines (such as diethanolamine (DEA) and diisopropanolamine (DIPA)), tertiary amines (such as Triethanolamine (TEA) and methyldiethanolamine (MDEA)), and polyamines (such as piperazine (PZ), 2-(2-aminoethylamino)ethanol (AEEA) and diethylenetriamine (DETA)). Table 2.1 shows the chemical structures of different amines that have been used for the capture of CO<sub>2</sub>.

**Table 2.1** Chemical structures of amines used for CO<sub>2</sub> capture.

Group	Name	Structure formula
Primary amine	Monoethanolamine (MEA)	
	Diglycolamine (DGA)	
Secondary amines	Diethanolamine (DEA)	
	Diisopropanolamine (DIPA)	
Tertiary amines	Triethanolamine (TEA)	
	Methyldiethanolamine (MDEA)	
	4-(Diethylamino)-2-butanol (DEAB)	
	4-(Dimethylamino)-2-butanol (DMAB)	
	1-Diethylamino-2-propanol (1DEA2P)	
Sterically hindered amines	2-Amino-2-methyl-propanol (AMP)	
	2-Piperidine ethanol (PE)	
Polyamines	Piperazine (PZ)	
	2-((2-Aminoethyl)amino) ethanol (AEEA)	
	Diethylenetriamine (EDTA)	



Primary and secondary amine such as MEA and DEA, respectively were used almost exclusively for many years for the removal of CO<sub>2</sub> from natural and certain synthesis gases. The low molecular weights of MEA and DEA results in high reactivity with CO<sub>2</sub> at moderate concentrations and its high alkalinity [38, 39]. However, several disadvantages of these amines are highly corrosive, have low CO<sub>2</sub> absorption capacity, high solvent degradation rates and high heats of regeneration. Especially, MEA constituted 80 % of the total energy consumption for absorption processes during solvent regeneration [33, 40].

Tertiary amines such as MDEA are also rapidly increasing in importance as a solvent for the removal of high concentrations of CO<sub>2</sub>, because of their low energy requirements, high absorption capacity, excellent stability, high resistance to thermal, chemical degradation, and low heats of regeneration but are substantially limited by their slow kinetics [22-25].

Sterically hindered amines such as AMP and PE contain a bulky alkyl group attached to the amino group and have been introduced as commercially attractive amines for the capture of CO<sub>2</sub>. AMP and PE each have an excellent absorption capacity and require less energy for regeneration in comparison with MEA. These amines are useful as promoters and they are becoming strong competitors on conventional amine solvents, MEA and MDEA [27, 32, 41]. In addition, solvents containing polyamines, such as PZ, AEEA and EDTA have gained considerable attraction due to their high absorption capacity and exceptionally fast reaction kinetics [39]. A synthetic amine which can be broadly defined as an amine that has been specifically designed to perform specific tasks; for example, selective separation of H<sub>2</sub>S from light hydrocarbons in the presence of CO<sub>2</sub>, shows the development of bulk separation of CO<sub>2</sub>.

Recently, tertiary amines DEAB and EMAB were developed by Tontiwachwuthikul et al. [27]. These amines are found to be very attractive for capturing CO<sub>2</sub> due to their significantly high absorption capacity. Thermal energy consumption for regenerating these solvents is expected to be significantly less than that of conventional MEA process. In addition, the solvent circulation rates (which is one of the most important factors in the economics of gas treatment with chemical

solvents) of these solvents are much lower than that of MEA, resulting in an operation cost saving [26, 28]. With these properties, DEAB can be considered as a promising solvent in the CO<sub>2</sub> capture process. Both DEAB and EMAB were designed and involved a systematic modification of the structure of amino alcohols by an appropriate placement of substituent functional groups, especially the hydroxyl function, relative to the position of the amino group on the performance for CO<sub>2</sub> capture. The research observed that the hydroxyl group increased the solubility of amines in aqueous solutions, thereby allowing the use of highly concentrated absorbing solutions and the presence of the amino group provides the necessary alkalinity to absorb CO<sub>2</sub> [27, 29]. Another tertiary amine, 1-diethylamino-2-propanol (1DEA2P), whose structure is similar to that of DEAB. 1DEA2P shows excellent performance in absorption capacity, energy requirement for solvent regeneration, reaction kinetics, and mass transfer. This amine is considered a promising alternative solvent for CO<sub>2</sub> capture [23].

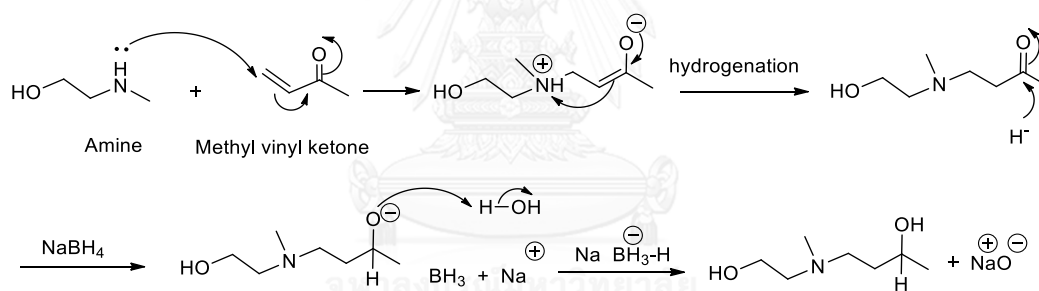
Although amine solvents have been used abundantly in the capture process of CO<sub>2</sub>, recently, the researchers are more interested in formulating new solvents composed of blended amines and chemical additives [42]. Blended amines, structurally composed of a variety of amines, have become popular in the gas treatment industry because blended amine can be maintain the regeneration cost, and enhance the CO<sub>2</sub> absorption rate. These solutions provide a higher absorption performance when compared to the aqueous solutions of a single amine. For example, the combination of primary or secondary amines with tertiary amines, such as MEA or DEA in MDEA, has been implemented to increase the rate of CO<sub>2</sub> absorption and eliminate the regeneration cost significantly, since about 80 % of the total energy consumption in an amine absorption process happens during regeneration [32, 40, 43-46]. However, MEA has been selected to be blended with MDEA rather than DEA due to the higher reactivity of MEA over DEA.

Regarding as DEAB is a good candidate for CO<sub>2</sub> capture [27], DEAB is now being considered to be mixed with a primary amine such as MEA. Mixing MEA with DEAB was proposed in order to enhance the CO<sub>2</sub> absorption rate of DEAB, counter the high energy requirement of MEA, and compensate for the low CO<sub>2</sub> absorption

capacity of MEA [47]. These mixed amines take advantage of each amine's high-performing components. This means the disadvantage of one amine are compensated by another amines [40].

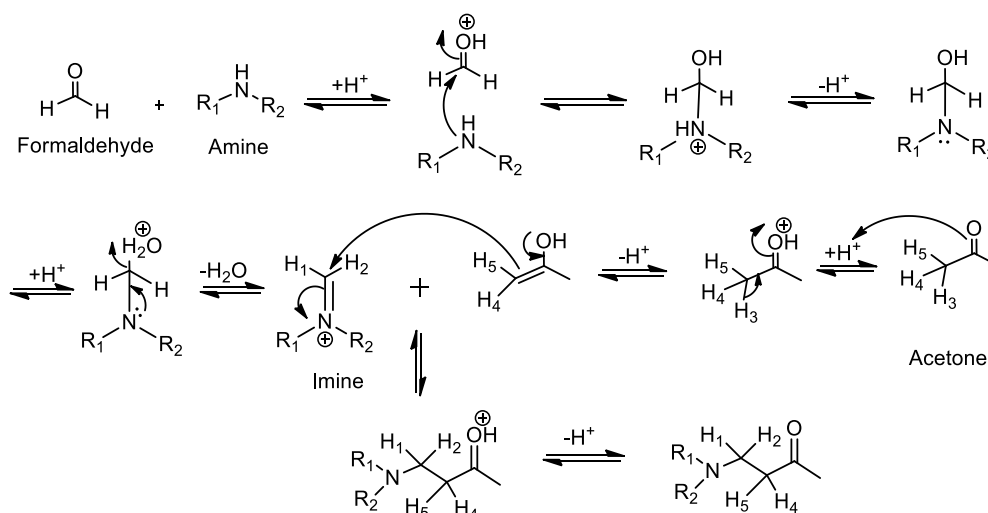
## 2.5 The synthesis of tertiary amines

The synthesis method of developed tertiary amines, specially, DMAB and DEAB were adopted as described in the literature [27]. The 1,4-Michael addition reaction method is the nucleophilic addition of an enolate of ketone to an  $\alpha,\beta$ -unsaturated carbonyl compound at the  $\beta$  carbon. Finally, the intermediate was reduced to amine by using sodium borohydride as a reducing agent. This method is suitable for synthesizing tertiary amines that can be used in the CO<sub>2</sub> capture process. The mechanism is illustrated in the Scheme 2.1.



**Scheme 2.1** Mechanism of 1,4-Michael addition reaction.

In this study, the method for making other new tertiary amines is the Mannich reaction method. This method is suitable for synthesizing  $\beta$ -amino carbonyl compound that can be used in pharmaceutical product. Formaldehydes and amines are reacted at elevated temperature to form the imine occurs without isolation of the imine intermediate. Acetone can be successfully accepted the proton due to the high temperature used and formed to amino-ketone. The mechanism is illustrated in the Scheme 2.2.

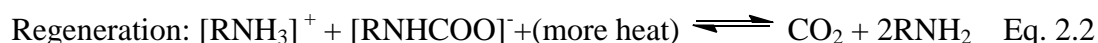


**Scheme 2.2** Mechanism of Mannich reaction.

## 2.6 Absorption and desorption

The chemical absorption of  $\text{CO}_2$  with amines typically occurs through the formation of two products, a carbamate and/or bicarbonate species. The mechanism of reactions between  $\text{CO}_2$  and primary and secondary amines are shown in Route 1, equations 2.1 and 2.2 [4, 39, 48, 49].

Route 1: Carbamate formation

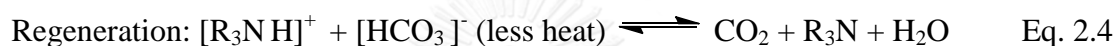


According to this mechanism, carbamate is formed via the reaction of one  $\text{CO}_2$  molecule and two amine molecules as shown in Equation 2.1. The maximum capacity of the solution for  $\text{CO}_2$  is limited to approximately 0.5 mole of  $\text{CO}_2$ /mole of amine. This pathway is favored to form highly stable primary and secondary amines. By applying heat, the carbamate intermediate dissociates to reproduce  $\text{CO}_2$  and amine, as

shown in Equation 2.2. Since the carbamate formed during absorption is quite stable, a large amount of heat energy is required to break the bonds and to regenerate the amine.

The reaction mechanisms between CO<sub>2</sub> and tertiary amines are shown in Route 2, equations 2.3 and 2.4.

Route 2: Bicarbonate formation



The bicarbonate pathway is commonly associated with tertiary amines, which are unable to form carbamate. Bicarbonate formation occurs by the reaction of one CO<sub>2</sub> molecule with one water molecule, it does not react directly with CO<sub>2</sub> but rather acts as a base that catalyzes the hydration of CO<sub>2</sub> as shown in Equations 2.3 and 2.4. The regeneration of the tertiary amines requires lesser amount of heat energy as compared with those of primary and secondary amines.

## 2.7 Kinetics of CO<sub>2</sub> absorption into aqueous amine solutions

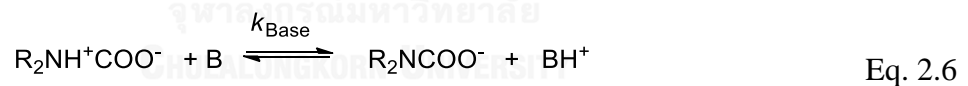
The reaction of CO<sub>2</sub> with primary and secondary amines is generally explained with the zwitterion mechanism, whereas the reaction with tertiary amines is interpreted using the base-catalyzed hydration of CO<sub>2</sub>.

### 2.7.1 Zwitterion mechanism

Caplow [50] proposed the zwitterion mechanism for the reaction of CO<sub>2</sub> with primary and secondary amines. The reaction follows a two-step mechanism. Initially, CO<sub>2</sub> reacts with the amine to form an intermediate zwitterion as shown in Equation 2.5.



The zwitterion can be deprotonated by base present in the solution producing a carbamate ion and protonated base as shown in Equation 2.6.



Where, B can be an amine, a hydroxyl ion (OH<sup>-</sup>) and water can contribute to the deprotonation step. However, for aqueous solution, the deprotonation proceeds mainly *via* water and the amine according to [51].

By applying the steady-state principle to the intermediate zwitterion, the reaction rate of CO<sub>2</sub> in aqueous solution can be shown in Equation 2.7.

$$-r_{\text{CO}_2} = k_{\text{ov}}[\text{CO}_2] = \frac{[\text{CO}_2][\text{RNH}_2]}{(1/k_2) + (k_{-1}/k_2) \sum k_{\text{Base}}[\text{B}]} = \frac{[\text{CO}_2][\text{RNH}_2]}{(1/k_2) + (1/\sum k_{\text{Base}}[\text{B}])} \quad \text{Eq. 2.7}$$

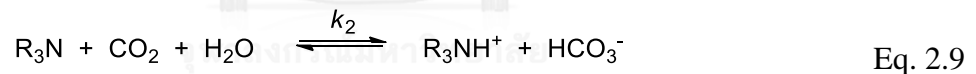
$$\text{Where, } k_B = \frac{k_2 k_{\text{Base}}}{k_{-1}}$$

The reaction in this mechanism can display a fractional order between one and two with respect to the amine concentration. When the zwitterion formation is considered the rate determining step, i.e., the deprotonation of zwitterion is instantaneous when compared to the reverse reaction, equation 2.7 becomes as shown in Equation 2.8 [22].

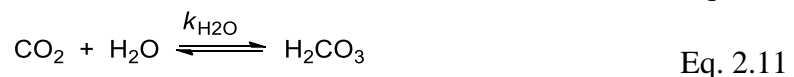
$$-r_{\text{CO}_2} = k_{ov}[\text{CO}_2] = k_2[\text{CO}_2][\text{RNH}_2] \quad \text{Eq. 2.8}$$

### 2.7.2 Base-catalyzed hydration mechanism

Donaldson and Nguyen [52] proposed the base-catalyzed hydration mechanism for the reaction of  $\text{CO}_2$  with tertiary amine. Tertiary amines do not react directly with  $\text{CO}_2$ , but act as a base that catalyzes the hydration of  $\text{CO}_2$  as can be shown as in Equation. 2.9.



In aqueous solution, the following reactions can occur shown in Equation 2.10 and 2.11.



Based on reactions 2.9-2.11, the overall reaction rate of  $\text{CO}_2$  absorption ( $r_{\text{CO}_2}$ ;  $\text{kmol/m}^3 \text{ s}$ ) can be expressed in Equation 2.12.

$$r_{\text{CO}_2} = k_0[\text{CO}_2] = \{k_2[\text{R}_3\text{N}] + k_{\text{OH}^-}[\text{OH}^-] + k_{\text{H}_2\text{O}}[\text{H}_2\text{O}]\} [\text{CO}_2] \quad \text{Eq. 2.12}$$

Where,  $k_0$  is the overall reaction rate constant or observed pseudo first-order reaction rate constant ( $\text{s}^{-1}$ ),  $k_2$  is the second-order reaction rate constant of Equation 2.9 ( $\text{m}^3/\text{kmol s}$ ),  $k_{\text{OH}^-}$  is the reaction rate constant of Equation 2.10 ( $\text{m}^3/\text{kmol s}$ ),  $k_{\text{H}_2\text{O}}$  is the reaction rate constant of Equation 2.11 ( $\text{m}^3/\text{kmol s}$ ), and [ ] is the concentration ( $\text{kmol}/\text{m}^3$ ).

In aqueous amine solution, the contribution of uncatalyzed reaction shown in Equation 2.11 (slow reaction rate) to the overall reaction rate is usually negligible. As same as the contribution of  $\text{OH}^-$  to overall reaction could also be neglected [51]. Thus, the main contributor is amine itself. The overall reaction rate expression of  $\text{CO}_2$  absorption into aqueous solution of tertiary amines based on base-catalyzed hydration mechanism can be written in Equations 2.13 and 2.14.

$$r_{\text{CO}_2} = k_0[\text{CO}_2] = k_2[\text{R}_3\text{N}][\text{CO}_2] \quad \text{Eq. 2.13}$$

Therefore

$$k_0 = k_2[\text{R}_3\text{N}] \quad \text{Eq. 2.14}$$

## 2.8 Physical properties

Physical properties of aqueous amine solutions are very important, since these properties can play a significant role in efficient design of gas treating process plants [32, 42]. Density and viscosity of the solutions are significant in modeling the absorber and regenerator because these properties affect the hydrodynamics and mass transfer coefficients [53, 54]. Moreover, these properties are required to estimate other properties such as diffusivity and reaction rate constant [55]. The data can be used for dimensioning velocities, column diameters, pipes, pumps, and other parameters in the process plant. Refractive index is a fundamental physical property, and can be applied to a component's identification, concentration determination, and purity confirmation.



## 2.9 Related literatures

Recently, new amino alcohols have been developed based on an approach of rational molecular design and synthesis. The synthesis approach involved a systematic modification of the amino alcohol structure by appropriately placing, specifically hydroxyl (-OH) or alkyl (-R) groups, relative to the position of the amino group (-NH<sub>2</sub>). Puxty et al. [15] studied the equilibrium measurements of the CO<sub>2</sub> capture of aqueous amine solutions for 76 different amines moieties. Seven amines, consisting of one primary, three secondary and three tertiary amines, were identified as exhibiting outstanding absorption capacities. Most have a number of structural features in common including steric hindrance and hydroxyl functionality at 2 or 3 carbon atoms away from the nitrogen atom. They suggested that the relationship between reaction energy for the bicarbonate and carbamate pathway is more complicated than the simple framework of amine base strength, local geometry, and interaction ratios previously used to characterize amine-CO<sub>2</sub> reactions. Chowdhury et al. [12, 49] focused on synthesizing new amine absorbents (e.g. 2-(isopropylamino)ethanol (IPAE), 2-(isobutylamino)ethanol (IBAE), 1-methyl-2-piperidineethanol (1M-2PPE) and 2-(isopropyl)diethanolamine (IPDEA)) to evaluate the effect of functional group placement (e.g. methyl, ethyl, and propyl) on the CO<sub>2</sub> absorption rate, cyclic capacity and heat of reaction. Their work has also shown that an increase of the carbon chain length and hydroxyl (-OH) group decreased the absorption rate and CO<sub>2</sub> loading capacity. The results showed that the placement of functional groups within the amino alcohols affects the performance of the amino alcohols in CO<sub>2</sub> capture performance. Singh et al. [56, 57] investigated the effect of carbon chain length and types of different functional groups such as hydroxyl (-OH) group, alkylamine, and diamine within the primary amine structure. For most amines, an increase of chain length was found to decrease the initial absorption rate but increase the absorption capacity expressed by equilibrium CO<sub>2</sub> solubility in mols CO<sub>2</sub> per mol amine unit. Rayer et al. [41] focused on the solubility of CO<sub>2</sub> in solvents for screening solvent to design CO<sub>2</sub> capture processes. They found that the increase in sterically hindered structure of the amino groups increased the loading capacity in the following order: primary amines < hindered amines < secondary amines < tertiary amines. Mixed solvents with sterically

hindered amines have the advantages of maximum CO<sub>2</sub> loading capacity at lower temperatures but low loading at higher temperatures.

The previous developed tertiary amines were synthesized by Maneeintr et al. [28]. This work reported the success of synthesizing a new kind of amino alcohol compounds such as 4-diethylamino-2-butanol (DEAB), 4-isopropylamino-2-butanol (IPAB), 4-(piperidino)-2-butanol (PRNB), 4-propylamino-2-butanol (PPAB) and 4-(ethylmethyl-amino)-2-butanol (EMAB). The superior performance of these amino alcohols in terms of higher CO<sub>2</sub> absorption capacities at all temperatures (40, 60 and 80 °C) and at CO<sub>2</sub> partial pressures of 15 and 100 kPa and cyclic capacities should lead to a reduction in the circulation rate and energy efficiency for solvent regeneration, such as in CO<sub>2</sub> stripping, compared to that of MEA. Maneeintr et al. [58] have also shown that 4-diethylamino-2-butanol (DEAB) and methyldiethanolamine (MDEA) have much higher CO<sub>2</sub> absorption and cyclic capacities compared to that of MEA. This led to reduction of the circulation rate and energy for solvent regeneration. The DEAB system provided an excellent overall mass transfer coefficient that is higher than that of the MDEA system for the capture of CO<sub>2</sub> from industrial flue gas in a packed-bed absorption column. Tontiwachawuthikul et al. [27] reported the method for removing CO<sub>2</sub> from gas stream by liquid absorbent having an amino alcohol. In comparison to conventional amines such as MEA, the synthetic amino alcohols of the present invention as 4-(diethylamino)-2-butanol (DEAB), 4-(isopropylamino)-2-butanol (IPAB), 4-(piperidino)-2-butanol (PRNB), 4-propylamino-2-butanol (PPAB) and 4-ethylmethyl-amino-2-butanol (EMAB) have been found to provide a higher CO<sub>2</sub> absorption capacity and a higher cyclic capacity for CO<sub>2</sub> removal. It has been demonstrated that certain amino 2-butanol compounds are highly effective reagents for CO<sub>2</sub> absorption capacity and higher cyclic capacity than that of MEA from gas streams. Sema et al. [26] investigated that 4-diethylamino-2-butanol (DEAB) was found to be a very attractive for capturing CO<sub>2</sub> due to its significantly higher absorption capacity and cyclic capacity for CO<sub>2</sub> removal, lower energy consumption and lower solvent regeneration better than the conventional amines (i.e. AMP, MDEA, DEA and MEA). Charkravarty et al. [40] first focused on a mixing of primary or secondary amines with tertiary amines to take advantage of each amine's

high-performing components. This means the disadvantages of one amine are compensated by another amine. Aroonwilas et al. [59] studied the performance of different mixed amines such as MEA-MDEA, DEA-MDEA, MEA-AMP, and DEA-AMP for CO<sub>2</sub> capture. The results showed that the AMP-based solvents, especially MEA-AMP, are more effective in CO<sub>2</sub> absorption than MDEA-based solvents. Sema et al. [47] investigated the equilibrium solubility of CO<sub>2</sub> in aqueous solutions of blended MEA-DEAB solvent over a temperature range of 298-333 K, CO<sub>2</sub> partial pressure range of 10-100 kPa. It was found that 5 M MEA + 1.5 M DEAB is the best MEA-DEAB formulation over a concentration range of 5 M MEA + 0.25 M DEAB to 5 M MEA + 2 M DEAB and prediction equilibrium solubility of CO<sub>2</sub> in aqueous solution of blended MEA-DEAB obtained from the mathematical modeling fit moderately well with the experimental results with an ADD of 6.3 %.

Currently, the technique for evaluating the potential of the new amine solvent that can be used for removing CO<sub>2</sub> from flue gas in terms of kinetic of CO<sub>2</sub> absorption is laminar jet absorber which was presented in the work of Sema et al. [39]. It was shown that DEAB's reaction kinetics of CO<sub>2</sub> absorption is faster than those in diethylmonoethanolamine (DEMEA), dimethylmonoethanolamine (DMMEA), and MDEA but comparable with those of AMP and DEA and slower than those of piperazine (PZ) and MEA using a laminar jet absorber. Another technique that can be used for studying the kinetics of CO<sub>2</sub> absorption into aqueous amine solution is the stopped-flow technique. According to the work of Liu et al. [24], the kinetics of DEAB was investigated at 298-313 K by the stopped-flow apparatus. It was found that DEAB exhibited faster reaction kinetics than those of DEMEA, DMMEA and MDEA, respectively. It was also shown that the activation energy ( $E_a$ ) of DEAB was close to those obtained from using a laminar jet absorber. Kaliwala et al. [22] focused on the kinetics for CO<sub>2</sub> absorption with tertiary amines, 3-dimethylamino-1-propanol (3DM1P) and 1-dimethylamino-2-propanol (1DMA2P) using the stopped-flow apparatus and found that the kinetic reaction of these amines was faster than MDEA. Liu et al. [23] investigated the kinetics of CO<sub>2</sub> absorption into aqueous solution of 1-diethylamino-2-propanol (1DEA2P) using the stopped-flow technique. Their work has shown that the CO<sub>2</sub> absorption kinetics increased as the concentration of 1DEA2P and/or the temperature increased. Compared to MDEA, DEMEA and DMMEA,

1DEA2P has a higher equilibrium solubility and faster reaction kinetics. Li et al. [25] investigated the kinetics of CO<sub>2</sub> absorption into tertiary amines using the stopped-flow technique. The results demonstrated that 3-diethylamino-1,2-propane-diol (DEA-1,2-PD) exhibited faster reaction kinetics than those of 3-dimethylamino-1-propanol (3DMA1P), 1-dimethylamino-2-propanol (1DMA2P), DMMEA, and MDEA, but slower than those of DEAB, 1DEA2P, and DEMEA. This can be explained by the steric hindrance of the hydroxyl group in the DEA-1,2-PD molecule that is predominant compared to the supply electronic effect (i.e. DEAB, 1DEA2P and DEMEA).

Li et al. [60] reported the data of density and viscosities of water and 2-((2-aminoethyl)amino)ethanol (AEEA) solution from 25-70 °C and also measured refractive indices of water and AEEA from 25-70 °C. Chowdhury et al. [61] measured densities of different aqueous solutions of MDEA, DEA, EDEA, and BDEA at 303 K to 323 K in the range of 0 to 1 for the mole fraction of amine. Mandal et al. [55] measured the density and viscosity of aqueous solutions of MDEA+MEA, MDEA+DEA, AMP+MEA, and MDEA+AMP at temperatures from 25 °C to 50 °C. Maneeintr et al. [42] measured the densities, viscosities, and refractive indices of 4-diethylamino-2-butanol (DEAB) + water mixtures over the concentration ranging from 0 to 1 mole fraction and temperatures from 25-70 °C for density and viscosity and from 25-60 °C for refractive index. It was found that the Redlich-Kister equation gave low % AAD and provided a suitable correlation to represent the experimental data of density, viscosity, and refractive index for DEAB + water mixtures. Fatemeh et al. [32] investigated the density, viscosity, and refractive index of pure solvents such as DEAB, MDEA, aqueous loaded and unloaded DEAB solution at different temperatures, concentrations, and CO<sub>2</sub> loading. From the results, DEAB showed the least density among MEA, water, MDEA and also showed the least viscosity among MEA and MDEA.

## CHAPTER III

### EXPERIMENTAL

#### 3.1 Chemicals and equipment

##### 3.1.1 Materials

- 1) Methyl vinyl ketone (MVK) ( $C_4H_6O$ ) (Sigma-Aldrich Co., Canada) with purity of  $\geq 95\%$  was simple distilled before used.
- 2) 2-(Methylamino)ethanol ( $C_3H_9NO$ ) (Sigma-Aldrich Co., Canada) with purity of  $\geq 98\%$  was used as received.
- 3) 2-(Ethylamino)ethanol ( $C_4H_{11}NO$ ) (Sigma-Aldrich Co., Canada) with purity of  $\geq 98\%$  was used as received.
- 4) Dibutylamine ( $C_8H_{19}N$ ) (Sigma-Aldrich Co., Canada) with purity of  $\geq 98\%$  was used as received.
- 5) Sodium borohydride ( $NaBH_4$ ) (Sigma-Aldrich Co., Canada) with purity of  $\geq 98\%$  was used as received.
- 6) Dipropylamine ( $C_6H_{15}N$ ) (Sigma-Aldrich Co., Canada) with purity of  $\geq 99\%$  was used as received.
- 7) Paraformaldehyde power ( $OH(CH_2O)_nH$  ( $n = 8-100$ )) (Sigma-Aldrich Co., Canada) with purity of  $95\%$  was used as received.
- 8) Dimethylamine hydrochloride ( $(CH_3)_2NH.HCl$ ) (Sigma-Aldrich Co., Canada) with purity of  $\geq 99\%$  was used as received.
- 9) Methyldiethanolamine (MDEA) ( $C_5H_{13}NO_2$ ) (Sigma-Aldrich Co., Canada) with purity of  $99.9\%$  was used as received.
- 10) Ethanolamine (MEA) ( $C_2H_7NO$ ) (Sigma-Aldrich Co., Canada) with purity of  $\geq 98\%$  was used as received.
- 11) Standard 1 N hydrochloric acid (HCl) (Sigma-Aldrich Co., Canada) was used as received.

- 12) Hydrochloric acid (HCl) (Sigma-Aldrich Co., Canada) with purity of 37 % was used as received.
- 13) Sodium hydroxide (NaOH) (Sigma-Aldrich Co., Canada) was used as received.
- 14) Celite 545 (Fisher Scientific Co., Canada) was used as received.
- 15) Sodium sulfate anhydrous (Na<sub>2</sub>SO<sub>4</sub>) (Fisher Scientific Co., Canada) was used as received.
- 16) Acetone (C<sub>3</sub>H<sub>6</sub>O) (Sigma-Aldrich Co., Canada) was used as received.
- 17) Absolute ethanol (C<sub>2</sub>H<sub>5</sub>OH) (Sigma-Aldrich Co., Canada) was used as received.
- 18) Methanol (CH<sub>3</sub>OH) (Sigma-Aldrich Co., Canada) was used as received.
- 19) Ethyl acetate (C<sub>4</sub>H<sub>8</sub>O<sub>2</sub>) (Sigma-Aldrich Co., Canada) was used as received.
- 20) Sodium chloride (NaCl) (Sigma-Aldrich Co., Canada) with purity of 99% was used as received.
- 21) Sodium bicarbonate (NaHCO<sub>3</sub>) (Sigma-Aldrich Co., Canada) with purity of 99.9 % was used as received.
- 22) Methyl orange indicator, 0.1 % was dissolved in water before used.
- 23) Deuterium oxide (D<sub>2</sub>O) (Sigma-Aldrich Co., Canada) was used as received.
- 24) Deuterated Chloroform (CDCl<sub>3</sub>) (Sigma-Aldrich Co., Canada) was used as received.
- 25) Carbon dioxide (CO<sub>2</sub>) 3, 8, 15, 30 and 100 % with N<sub>2</sub> balance (Praxair Inc., Regina, Canada) were used as received.
- 26) Air Zero (Praxair Inc., Regina, Canada) was used as received.

### 3.1.2 Equipment

- 1) Rotary evaporator, Buchi, Canada
- 2) Digital flow meter, Aalborg GFM-17 gas flow meters with  $\pm 0.15$  %/ $^{\circ}$ C, Canada

- 3) Temperature controller within a temperature range of -20 to 200 °C capacity with  $\pm 0.01$  °C accuracy, Cole-Parmer, Canada

### 3.2 Instrumentation

- 1) Nuclear Magnetic Resonance (NMR) Spectrometer

Carbon and proton nuclear magnetic resonance ( $^1\text{H}$  and  $^{13}\text{C}$ -NMR) spectra of amines were obtained in deuterium oxide ( $\text{D}_2\text{O}$ ) or deuterated chloroform ( $\text{CDCl}_3$ ) using a Varian Mercury 500 MHz, Varian, USA. Chemical shifts ( $\delta$ ) are reported in parts per million (ppm) relative to the residual protonated solvent signal as a reference.

- 2) Fourier Transform infrared spectroscopy (FT-IR)

Fourier Transform infrared spectra were performed on a Perkin Elmer<sup>®</sup> Spectrum One. FTIR spectroscopy technique is used to measure an infrared spectrum of absorption of a solid or liquid.

- 3) Gas Chromatography-Mass Spectrometry (GC-MS)

GC-MS are provides a powerful technique to separate and identify the various organic compounds. The purity and identification of all amines were analyzed using the GC-MS, Restek RTX-5Amines Capillary Column, model 6890/5073, Hewlett-Packard Ltd., Canada.

- 4) pH meter

The pH value of amine concentrations were recorded using a pH meter (Accumet AB 15 m) standardize with pH 4, 7, and 10 buffer solutions.

- 5) Chittick apparatus

The Chittick apparatus was used for measuring the  $\text{CO}_2$  loading according to Association of Official Analytical Chemists (AOAC) methods reported by Horwitz [62] (see in section 3.4.1).

- 6) Stopped-flow apparatus

The stopped flow apparatus is used to investigate the kinetics of the reaction of  $\text{CO}_2$  absorption into aqueous amine solution (see in section 3.9).

#### 7) Density meter

The density of solutions is important in the mass transfer rate modeling and the experimental data analysis [32]. Densities of amines were measured with an Anton Paar DMA-4500 density meter with an accuracy of  $0.00001 \text{ g/cm}^3$ .

#### 8) Viscometer

Solution viscosity is also essential in the modeling of mass transfer rate and experimental data analysis [32]. The viscosities were measured using Lovis 2000 M/ME from Anton Paar with an accuracy of 0.5 % for viscosity and  $0.02 \text{ }^\circ\text{C}$  for temperature.

#### 9) Refractometer

Refractive index is an elemental physical property that explains how light propagates through that medium, and can be applied to a component's identification, concentration determination, and purity confirmation [32]. The refractive indices were measured using Abbemat 550, and automatic refractometer with an accuracy of 0.00002 %.

### 3.3 Experimental procedure

The experiment was divided into 6 main parts

- 1) Synthesis and characterization of the newly synthesized tertiary amines
- 2)  $\text{CO}_2$  absorption performance of the newly synthesized tertiary amines and blended amine solvents in terms of absorption capacity, cyclic capacity at various conditions and heat of  $\text{CO}_2$  absorption in aqueous amine solutions
- 3)  $\text{CO}_2$  absorption and regeneration kinetic rates at actual concentration and heat input of  $\text{CO}_2$  regeneration in aqueous amine solutions
- 4) Amine dissociation constant analysis using a pH meter at various temperatures
- 5) Measurement for the kinetics of the reaction of  $\text{CO}_2$  absorption using the stopped-flow apparatus
- 6) Physical properties of the newly synthesized tertiary amines in pure solvent such as density, viscosity, and refractive index



### 3.3.1 Amine synthesis

The structures of the tertiary amines developed in this study are shown in Figure 3.1.

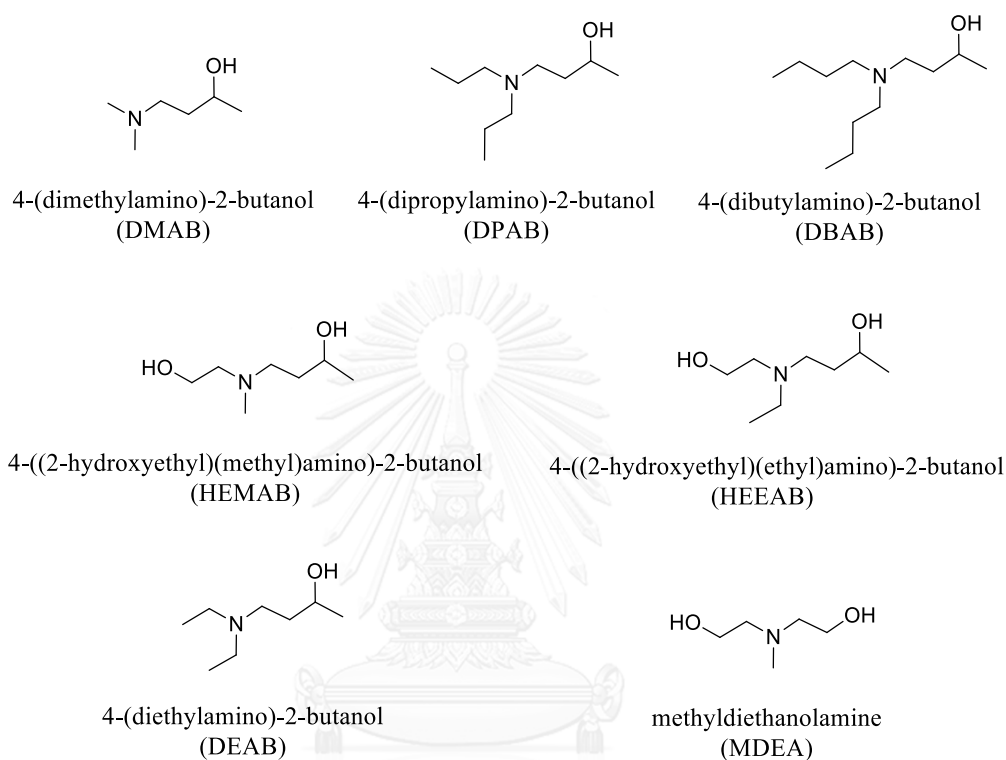


**Figure 3.1** The chemical structures of synthesized amines, DEAB, and MDEA used in this study.

#### 3.3.1.1 Synthesis of 4-(dimethylamino)-2-butanol (DMAB)

Step I. Synthesis of 4-(dimethylamino)-2-butanone, the starting reagent for DMAB's synthesis

The Mannich reaction method commonly used in pharmaceutical production [63, 64] for synthesis of  $\beta$ -amino carbonyl compound was used to produce 4-(dimethylamino)-2-butanone. Acetone (58.1 g, 1.0 mol), dimethylamine hydrochloride (93.8 g, 1.15 mol), paraformaldehyde (33 g, 1.1 mol), 37 % HCl (1 mL) and anhydrous ethanol (90 mL) were loaded and mixed in 1 L of a three-necked

round-bottom flask. The mixture was continuously refluxed for 24 hours. Agitation was then introduced while cooling the solution down to room temperature. The solvent was removed from the reaction mixture using a rotary evaporator before being cooled in an ice water bath. The mixture was adjusted to a pH of 11-12 by adding 50 mL of 40 % sodium hydroxide and 30 g of solid sodium hydroxide. The mixture was stirred further for an hour before being filtered through a short pad of celite. 4-(Dimethylamino)-2-butanone was separated from the filtrate by extracting twice using ethyl acetate. The butanone was purified further by removing solvent with anhydrous sodium sulfate followed by vacuum distillation set at 70-72 °C and 20-22 in Hg. About 50 g of 4-(dimethylamino)-2-butanone corresponding to 43 % yield was finally obtained with purity of 76 % confirmed by the GC-MS. The compound was used further to produce DMAB in step II. The structural information confirmed by  $^1\text{H}$  and  $^{13}\text{C}$ -NMR was  $^1\text{H}$ -NMR ( $\text{CDCl}_3$ , 500 MHz)  $\delta_{\text{H}}$ : 2.05 (3H, s), 2.10 (6H, s), 2.47 (4H, m);  $^{13}\text{C}$ -NMR ( $\text{CDCl}_3$ , 125 MHz)  $\delta_{\text{C}}$ : 30.1 ( $\text{CH}_3$ , q), 41.9 ( $\text{CH}_2$ , t), 45.3 ( $\text{CH}_3 \times 2$ , q), 53.9 ( $\text{CH}_2$ , t), 207.81 (CH, s). The GC-MS also confirmed the compound's chemical formula ( $\text{C}_6\text{H}_{13}\text{NO}$ ) and 115 molecular weight.

#### Step II. Synthesis of 4-(dimethylamino)-2-butanol (DMAB)

To make DMAB, 4-(dimethylamino)-2-butanone obtained earlier (73 g, 0.63 mol) was diluted with 30 mL methanol in an ice water bath. Subsequently, sodium borohydride (29 g, 0.76 mol) was slowly added into the solution with continuous stirring for 1 hour. To maximize the reaction yield, the mixture was stirred for another 3 hours at room temperature before slowly adding 30 mL of water and mixing further for 1 hour in a cooled water bath. 4-(Dimethylamino)-2-butanol (DMAB) of 35 g (47.0 % yield) was finally separated from the mixture by removing sodium borohydride salt using suction filtration and vacuum distillation set at 71-73 °C and 20-22 in Hg. The DMAB purity determined by GC-MS was found to be 78.7 %. The NMR data of the amine is given as;  $^1\text{H}$ -NMR ( $\text{D}_2\text{O}$ , 500 MHz)  $\delta_{\text{H}}$ : 0.91 (3H, d,  $J = 6$  Hz), 1.35 (2H, m), 1.95 (6H, s), 2.08 (1H, m), 2.16 (1H, m), 3.07 (1H, s), 3.55 (1H, m);  $^{13}\text{C}$ -NMR ( $\text{D}_2\text{O}$ , 125 MHz)  $\delta_{\text{C}}$ : 22.3 ( $\text{CH}_3$ , q), 35.41 ( $\text{CH}_2$ , t), 44.1 ( $\text{CH}_3 \times 2$ , q),

55.4 (CH<sub>2</sub>, t), 66.5 (CH, d). DMAB chemical formula (C<sub>6</sub>H<sub>15</sub>NO) and 117 molecular weight were also confirmed by the GC-MS.

### 3.3.1.2 Synthesis of 4-(diethylamino)-2-butanol (DEAB)

The synthesis of DEAB was similar to synthesis of DMAB. Acetone (133.58 g, 2.3 mol), diethylamine hydrochloride (219.2 g, 2 mol), paraformaldehyde (60.06 g, 2 mol), 37 % HCl (2 mL) and anhydrous ethanol (180 mL) were loaded and mixed in 1 L of three-necked round-bottom flask. The mixture was continuously refluxed for 24 hours. Agitation was then introduced while cooling the solution down to room temperature. The solvent was removed from the reaction mixture using a rotary evaporator before being cooled in an ice water bath. The mixture was adjusted to a pH of 11-12 by adding 100 mL 40 % sodium hydroxide and 60 g solid sodium hydroxide. The mixture was stirred further for an hour before being filtered through a short pad of celite. 4-(Diethylamino)-2-butanone was separated from the filtrate by extracting twice using ethyl acetate. The butanone was purified further by removing solvent with anhydrous sodium sulfate followed by vacuum distillation set at 85-90 °C and 20-23 in Hg. About 50 g of 4-(diethylamino)-2-butanone corresponding to (153 g, 53.5 % yield) was finally obtained with purity of 68.2 % confirmed by the GC-MS. 4-(diethylamino)-2-butanone obtained earlier (153 g, 1.069 mol) was diluted with 30 mL methanol in an ice water bath. Subsequently, sodium borohydride (40.4 g, 1.069 mol) was slowly added into the solution with a continuous stirring for 1 hour. To maximize the reaction yield, the mixture was stirred for another 3 hours at room temperature before slowly adding 30 mL of water and mixing further for 1 hour in cooled water bath. 4-(Diethylamino)-2-butanol (DEAB) of 74 g (47.7 % yield) was finally separated from the mixture by removing sodium borohydride salt using suction filtration and vacuum distillation set at 125-130 °C and 24-25 in Hg. The DEAB purity determined by GC-MS was found to be 82 %. The NMR data of the amine is given as; <sup>1</sup>H-NMR (CDCl<sub>3</sub>, 500 MHz) δ<sub>H</sub>: 1.05 (6H, t, *J* = 7 Hz), 1.15 (3H, d, *J* = 6 Hz), 1.46 (1H, m), 1.57 (1H, m), 2.37 (2H, sex, *J* = 6 Hz), 2.58 (1H, dt, *J* = 5 Hz), 2.68 (3H, m, *J* = 7.5 Hz), 3.35 (1H, s, OH), 3.94 (1H, m); <sup>13</sup>C-NMR (CDCl<sub>3</sub>, 125 MHz) δ<sub>C</sub>: 11.6 (CH<sub>3</sub>, q), 23.5 (CH<sub>3</sub>, q), 34.0 (CH<sub>2</sub>, t), 46.7 (CH<sub>2</sub>x2, t), 52.8 (CH<sub>2</sub>, t), 69.7 (CH,

d). DEAB chemical formula ( $C_8H_{19}NO$ ) and 145 molecular weight were also confirmed by the GC-MS.

### 3.3.1.3 Synthesis of 4-(dipropylamino)-2-butanol (DPAB)

The synthesis method of DPAB was adopted as described in the literature [27]. Dipropylamine (101.19, 1 mol) was added dropwise into MVK (70 g, 1 mol) chilled in an ice water bath. The mixture was stirred continuously for 1 hour, after which was removed to stir for another 6 hours at room temperature. The mixture was then put back in an ice water bath and added with 30 mL of methanol followed by sodium borohydride (37.9 g, 1 mol). The solution was continuously stirred in an ice water bath for 1 hour before removing to room temperature to be stirred further for 6 hours. In cooled water bath, 30 mL of water was slowly added to the mixture which was then stirred for another 2 hours. 4-(Dipropylamino)-2-butanol (DPAB) of 72.74 g (42 % yield) was finally separated from the mixture by removing sodium borohydride salt using suction filtration and vacuum distillation set at 139-143 °C and 20-22 in Hg. The DPAB purity determined by GC-MS was found to be 82 %. The NMR data of the amine is given as;  $^1H$ -NMR ( $CDCl_3$ , 500 MHz)  $\delta_H$ : 0.74 (6H, t,  $J = 7.5$  Hz), 0.99 (3H, d,  $J = 6.5$  Hz), 1.37 (6H, m), 2.07 (2H, m), 2.38 (3H, m), 2.54 (1H, dt,  $J = 3$  and 12.5 Hz), 3.77 (1H, m), 6.17 (1H, s);  $^{13}C$ -NMR ( $CDCl_3$ , 125 MHz)  $\delta_c$ : 11.5 ( $CH_3 \times 2$ , q), 19.7 ( $CH_2 \times 2$ , t), 23.2 ( $CH_3$ , q), 33.9 ( $CH_2$ , t), 54.4 ( $CH_2$ , t), 55.8 ( $CH_2 \times 2$ , t), 69.4 (CH, d). DPAB chemical formula ( $C_{10}H_{23}NO$ ) and 173 molecular weight were also confirmed by the GC-MS.

### 3.3.1.4 Synthesis of 4-(dibutylamino)-2-butanol (DBAB)

The synthesis method of DBAB was adopted as described in the literature [27]. Dibutylamine (129.24, 1 mol) was added dropwise into MVK (70 g, 1 mol) chilled in an ice water bath. The mixture was stirred continuously for 1 hour, after which was removed to stir for another 6 hours at room temperature. The mixture was then put back in an ice water bath and added with 30 mL of methanol followed by sodium borohydride (37.9 g, 1 mol). The solution was continuously stirred in an ice water bath for 1 hour before removing to room temperature to be stirred further for 6

hours. In cooled water bath, 30 mL of water was slowly added to the mixture which was then stirred for another 2 hours. 4-(Dibutylamino)-2-butanol (DBAB) of 81.4 g (40.05 % yield) was finally separated from the mixture by removing sodium borohydride salt using suction filtration and vacuum distillation set at 166-170 °C and 20-22 in Hg. The DBAB purity determined by GC-MS was found to be 80.5 %. The NMR data of the amine is given as;  $^1\text{H-NMR}$  ( $\text{CDCl}_3$ , 500 MHz)  $\delta_{\text{H}}$ : 0.78 (6H, t,  $J = 7.5$  Hz), 1.01 (3H, d,  $J = 6.5$  Hz), 1.16 (4H, m), 1.31 (5H, m), 1.44 (1H, m), 2.09 (2H, m), 2.42 (3H, m), 2.57 (1H, dt,  $J = 3$  and 12 Hz), 3.79 (1H, dsex,  $J = 2$  and 6 Hz), 6.28 (1H, brs);  $^{13}\text{C-NMR}$  ( $\text{CDCl}_3$ , 125 MHz)  $\delta_{\text{C}}$ : 14.1 ( $\text{CH}_3 \times 2$ , q), 20.4 ( $\text{CH}_2 \times 2$ , t), 23.25 ( $\text{CH}_3$ , q), 28.7 ( $\text{CH}_2 \times 2$ , t), 33.9 ( $\text{CH}_2$ , t), 53.5 ( $\text{CH}_2 \times 2$ , t), 54.0 ( $\text{CH}_2$ , t), 69.5 (CH, d). DBAB chemical formula ( $\text{C}_{12}\text{H}_{27}\text{NO}$ ) and 201 molecular weight were also confirmed by the GC-MS.

### 3.3.1.5 Synthesis of 4-((2-hydroxyethyl)(methyl)amino)-2-butanol (HEMAB)

The synthesis method of HEMAB was adopted as described in the literature [27]. 2-(methylamino)ethanol (75.11 g, 1 mol) was added dropwise into MVK (70 g, 1 mol) chilled in an ice water bath. The mixture was stirred continuously for 1 hour, after which was removed to stir for another 6 hours at room temperature. In a cooled water bath, 30 mL of methanol followed by sodium borohydride (37.9 g, 1 mol). The solution was continuously stirred in an ice water bath for 1 hour before removing to room temperature to be stirred further for 6 hours. In cooled water bath, 30 mL of water was slowly added to the mixture which was then stirred for another 2 hours. 2-(methylamino)ethanol (HEMAB) of 84.55 g (57.48 % yield) was finally separated from the mixture by removing sodium borohydride salt using suction filtration and vacuum distillation set at 133-135 °C and 20-22 in Hg. The HEMAB purity determined by GC-MS was found to be 80.5 %. The NMR data of the amine is given as;  $^1\text{H-NMR}$  ( $\text{CDCl}_3$ , 500 MHz)  $\delta_{\text{H}}$ : 0.93 (3H, d,  $J = 6$  Hz), 1.29 (1H, m), 1.36 (1H, m), 2.05 (3H, s), 2.25 (1H, m), 2.37 (3H, m), 3.43 (2H, t,  $J = 6$  Hz), 3.69 (1H, m);  $^{13}\text{C-NMR}$  ( $\text{CDCl}_3$ , 125 MHz)  $\delta_{\text{C}}$ : 22.9 ( $\text{CH}_3$ , q), 34.0 ( $\text{CH}_2$ , t), 41.6 ( $\text{CH}_3$ , t), 55.9 ( $\text{CH}_2$ , t), 58.6 ( $\text{CH}_2$ , t), 59.0 ( $\text{CH}_2$ , t), 67.7 (CH, d). HEMAB

chemical formula ( $C_7H_{17}NO_2$ ) and 147 molecular weight were also confirmed by the GC-MS.

### 3.3.1.6 Synthesis of 4-((2-hydroxyethyl)(ethyl)amino)-2-butanol (HEEAB)

The synthesis method of HEEAB was adopted as described in the literature [27]. 2-(Ethylamino)ethanol (89.14 g, 1 mol) was added dropwise into MVK (70 g, 1 mol) chilled in an ice water bath. The mixture was stirred continuously for 1 hour, after which was removed to stir for another 6 hours at room temperature. The mixture was then put back in an ice water bath and added with 30 mL of methanol followed by sodium borohydride (37.9 g, 1 mol). The solution was continuously stirred in an ice water bath for 1 hour before removing to room temperature to be stirred further for 6 hours. In a cooled water bath, 30 mL of water was slowly added to the mixture which was then stirred for another 2 hours. 2-(ethylamino)ethanol (HEEAB) of 87.56 g (54.35 % yield) was finally separated from the mixture by removing sodium borohydride salt using suction filtration and vacuum distillation set at 155-157 °C and 22-24 in Hg. The HEEAB purity determined by GC-MS was found to be 94 %. The NMR data of the amine is given as;  $^1H$ -NMR ( $CDCl_3$ , 500 MHz)  $\delta_H$ : 0.94 (3H, t,  $J = 7.5$  Hz), 1.05 (3H, d,  $J = 6$  Hz), 1.39 (1H, m), 1.47 (1H, m), 2.36-2.58 (6H, m), 3.55 (2H, q,  $J = 6$  Hz), 3.82 (1H, m);  $^{13}C$ -NMR ( $CDCl_3$ , 125 MHz)  $\delta_c$ : 11.3 ( $CH_3$ , q), 23.3 ( $CH_3$ , q), 34.2 ( $CH_2$ , t), 47.8 ( $CH_2$ , t), 52.7 ( $CH_2$ , t), 55.5 ( $CH_2$ , t), 59.4 ( $CH_2$ , t), 68.8 (CH, d). HEEAB chemical formula ( $C_8H_{19}NO_2$ ) and 161 molecular weight were also confirmed by the GC-MS.

### 3.4 Equilibrium solubility of CO<sub>2</sub> and cyclic capacity in aqueous amine solution

The experiment set-up shown in Figure 3.2 previously used by Maneeintr et al. [28, 42] was also used in this work to determine CO<sub>2</sub> solubility.

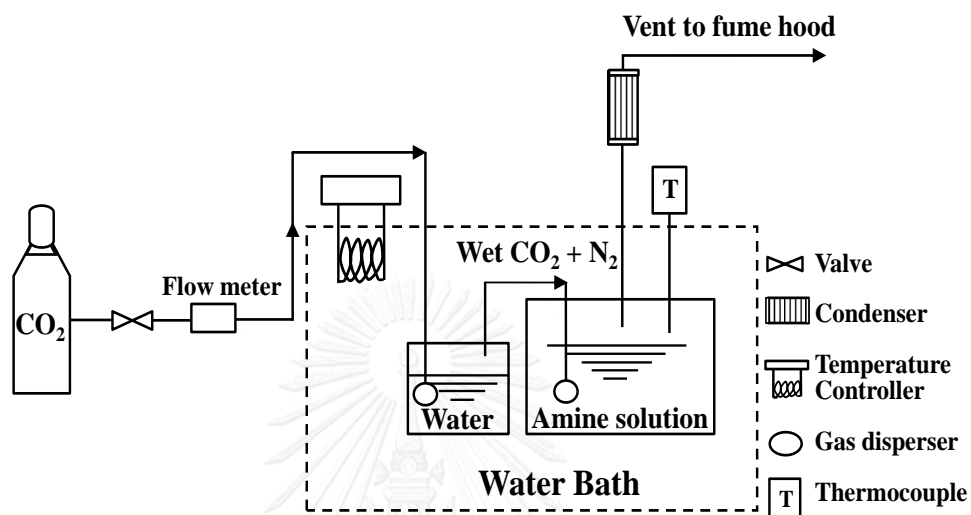


**Figure 3.2** Schematic diagram of the experimental setup for CO<sub>2</sub> equilibrium loading measurement.

For CO<sub>2</sub> equilibrium solubility measurements, 25 mL of 2 M single amine solution or blended amine solutions (MEA-MDEA, MEA-DMAB, MEA-DEAB, MEA-HEMAB, and MEA-HEEAB at concentration ratio of 5: 1.25 M in water) was loaded into an absorption reactor of which its inlet was also connected to the outlet of the water saturation cell. A water bath equipped with a temperature controller (-20 to 200 °C capacity with  $\pm 0.01$  °C accuracy, Cole-Parmer, Canada) was used to control the amine to the desired temperature (i.e. 298, 313, 333 and 353 K) prior to the test. After the set temperature was reached, a premixed gas stream containing the desired CO<sub>2</sub> partial pressure (i.e. 3, 8, 15, 30 and 100 kPa) was introduced, first into the water saturation cell and then into the amine in the absorption reactor through a gas dispersion tube. The CO<sub>2</sub> feed was regulated at a flow rate of 200 mL/min throughout the run. The outlet of the absorption reactor was also connected to a condenser to help

recover water and amine carry over back to the system. At time intervals, 1 mL of amine sample was taken for analysis of CO<sub>2</sub> loading expressed in terms of mol per mol amine by the chittick apparatus as described by Horwitz [62]. The averaged loading was used and reported for each sample based on three repeated measurements. The accuracy of the loading shown in terms of the standard deviation was found to be in the range of 2-5 %. Generally, time taken for each test to be finished was up to 20-22 hours when CO<sub>2</sub> was fully saturated in the amine solution. This could also be observed when the amine loading became unchanged. The cyclic capacity of each amine was also calculated using the difference of the maximum CO<sub>2</sub> loadings at 313 K and 353 K.

The experimental set-up and procedure used in this study were also used to measure the equilibrium CO<sub>2</sub> loading of 2 M MDEA and DEAB at 313 K and 3 to 100 kPa CO<sub>2</sub> partial pressure. MDEA and DEAB data were then used to validate this experiment by comparing with literature values of Sema et al., and Benamor and Aroua [26, 65].

### **3.4.1 CO<sub>2</sub> loading using the Chittick apparatus**

The CO<sub>2</sub> loading for each amine was determined by using the procedure of the Association of Official Analytical Chemists (AOAC) [62].

For preparation of the displacement solution, 100 g of NaCl was dissolved in 350 mL of distilled water. 1 g of NaHCO<sub>3</sub> and 2 mL of methyl orange indicator was added to the solution which was then stirred until all CO<sub>2</sub> is removed. The solution should be a sharp pink color. This solution was loaded in a graduated gas-measuring tube (E).

For CO<sub>2</sub> loading measurements, 1 or 2 mL of rich amine solution was pipetted and transferred into a 250 mL Erlenmeyer flask (A). The solution was added 2-3 drops of 0.1 % methyl orange indicator and rinsed with some distilled water. The flask (A) was fitted with a 2-hold rubber stopper and also connected to the Chittick apparatus as shown in Figure 3.3 [36]. A glass stopcock (D) was opened to adjust the pressure inside the system. The leveling bulb (F) containing the displacement solution



was used to adjust the liquid level to the zero mark at graduated gas-measuring tube (E). After the displacement solution level was kept constant at zero mark, a glass stopcock (D) was closed and then lowered the leveling bulb (F) down to reduce pressure within apparatus prior to the test. The amine was also continuously stirred constantly at 300 rpm using a magnetic stir bar during the test.

The rich amine solution was titrated carefully of 1.0 N HCl standard solution until the methyl orange end point was observed. Then, excess 1.0 N HCl was added to 2-3 mL sample to be certain that all of the released CO<sub>2</sub> was removed from the solution and collected in the glass T-tube (C) and graduated gas-measuring tube (E). The solution was stirred for 10-15 min to secure equilibrium and turned off the magnetic stirrer. Equalize pressure in graduated gas-measuring tube (E) by adjusting the leveling bulb (F) and read volume of the released CO<sub>2</sub> on the scale of graduated gas-measuring tube (E). The concentration of amines and CO<sub>2</sub> was determined using this equipment. The CO<sub>2</sub> loading calculations are given in Appendix A.

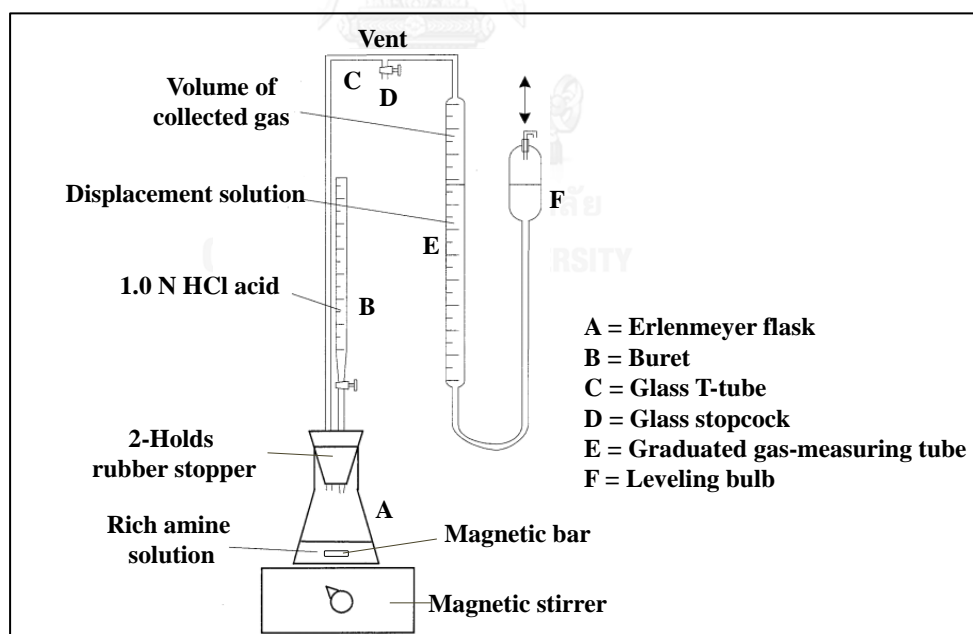


**Figure 3.3** CO<sub>2</sub> loading measurement equipment.

### 3.5 Heat of CO<sub>2</sub> absorption in aqueous amine solutions

The heat of CO<sub>2</sub> absorption ( $\Delta H_{\text{abs}}$ ) for all amines were calculated using the Gibbs-Helmholtz equation, as shown in Equation 3.1 [66-71].

$$\left[ \frac{d(\ln P_{\text{CO}_2})}{d(1/T)} \right]_{\alpha} = \frac{\Delta H_{\text{abs}}}{R} \quad \text{Eq. 3.1}$$

Where,  $\Delta H_{\text{abs}}$  is the heat of CO<sub>2</sub> absorption (J/mol),  $P_{\text{CO}_2}$  is CO<sub>2</sub> partial pressure,  $T$  is temperature (K), and  $R$  is the universal gas constant (J/mol K).

To determine  $\Delta H_{\text{abs}}$ , equilibrium CO<sub>2</sub> data similar to those obtained in section 3.4 was used. For each amine, a set of  $P_{\text{CO}_2}$  and  $T$  data of a similar equilibrium CO<sub>2</sub> loading was determined. A semi-logarithmic plot of  $P_{\text{CO}_2}$  and  $1/T$  was generated which then,  $\Delta H_{\text{abs}}$  was determined from the slope of the plot. The accuracy of  $\Delta H_{\text{abs}}$  measured from this study was calculated by comparing MDEA and DEAB data with the literature values [47, 69].

### 3.6 CO<sub>2</sub> absorption and regeneration kinetic rates at actual concentration

The experimental set-up for measurement of CO<sub>2</sub> absorption and regeneration kinetics rates are shown in Figure 3.4.

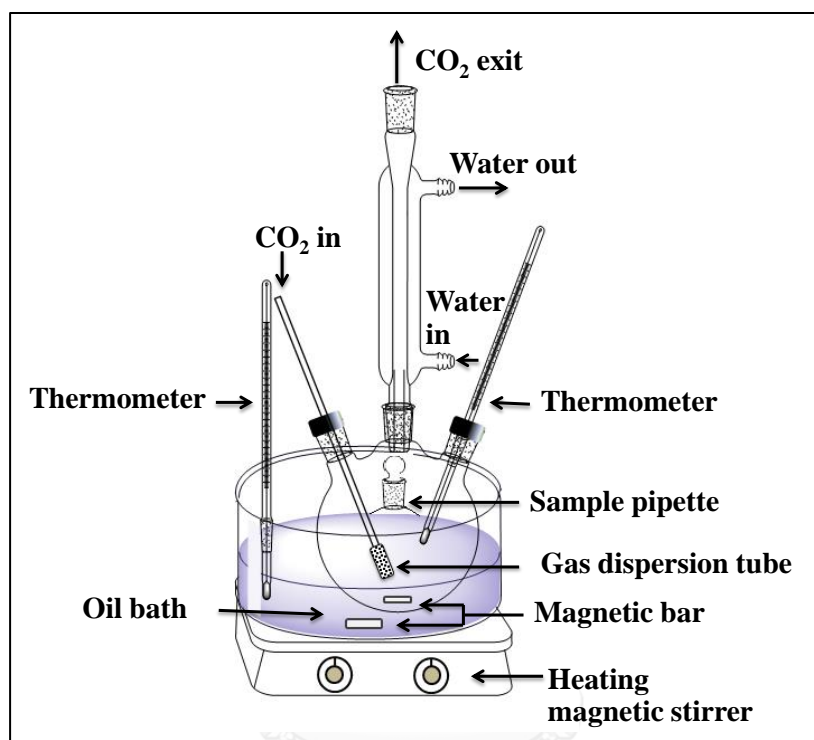


**Figure 3.4** The simplified apparatus of CO<sub>2</sub> absorption and regeneration kinetic rates.

The set-up is made of a 500 mL four-necked round-bottom flask which was used as the reaction cell. To minimize vapor loss, a condenser was used and connected to the flask at its mid-opening. One of the angled necks was hooked up to a gas dispersion tube by ensuring its disperser tip was always immersed in the amine solution throughout the run. The other end of the tube was hooked up to a premixed cylinder containing 15 % CO<sub>2</sub> for feed gas delivery. The other neck was fitted with a thermometer for amine temperature measurement. The remaining neck was served as the amine sampling port. The reaction cell assembly was immersed in a hot oil bath to maintain a constant amine temperature at 313 K ( $\pm 2$  °C accuracy).

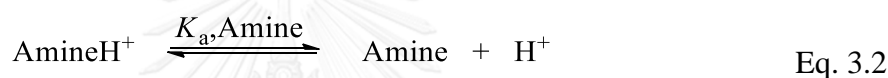
For an absorption run, 100 mL of a desired amine solution was transferred into the flask and placed in the hot oil bath. Concentration of all amines tested in this study were kept constant at 2 mol/L. The amine was also continuously agitated constantly at 300 rpm using a magnetic stir bar during the test. After the amine temperature had reached 313 K, 15 kPa CO<sub>2</sub> feed regulated at 200 mL/min ( $\pm 2$  mL/min accuracy) was introduced into the amine solution through the gas dispersion tube. Reaction time at zero was marked when the first bubble emerged into the solution from the disperser tip. First sample was taken by pipetting 1 mL of amine after 15 min had passed. The next samples were taken at 15, 30, and 45 min intervals, respectively during the first, second and third hour and onwards. CO<sub>2</sub> loading was determined using the same procedures described previously in section 3.4.1. The test was terminated when the loading became constant with time, implying that the CO<sub>2</sub> equilibrium in amine had been reached. CO<sub>2</sub> loading and time were plotted and used to determine the absorption kinetic rate based on its slope. The loaded amine after the test was used later for the regeneration rate measurement.

For regeneration runs, the same set-up shown in Figure 3.4 used for the absorption rate measurement was used. However, the gas dispersion tube was removed and replaced by a lid. In this test, 90 mL of the rich amine obtained earlier from the absorption test was transferred into the flask. The loaded amine was heated to the test temperature set at 363 K. Once the desired temperature was reached and become stabilized, the sample was taken by carefully pipetting 1 mL of the amine to quickly determine its CO<sub>2</sub> loading and used as the loading at time zero. Sampling was continued every 8 min to determine the amine's loading. The test was finished when there was no further change in CO<sub>2</sub> loading with time. Similar to the absorption rate measurement, a plot of CO<sub>2</sub> loading ( $\alpha$ ) versus time (min) was generated and then used to calculate the regeneration rate of amines based on its slope.

### 3.7 Amine dissociation constant analysis using a pH meter

Amine reactivity can be generally indicated by its dissociation constant often expressed using the  $pK_a$  value. Typically, a higher  $pK_a$  amine is more basic, thus able to provide a faster reaction kinetics with  $CO_2$  [24, 29, 72]. Previous studies have also reported this relationship between the rate constant of the reaction of amine with  $CO_2$  and the amine basicity (e.g.  $pK_a$ ) [51, 52, 73]. Thus, it was worth the effort to measure the  $pK_a$  of the newly synthesized amines in this study.

Amine dissociation constant ( $K_a$ ) was determined by the titration technique with standard 1 N HCl. For an aqueous amine solution, the deprotonation reaction of conjugate acid of amine ( $AmineH^+$ ) is shown in Equation 3.2.



Based on the assumption that the solution is ideal (when the concentration is very low, the activity coefficient equals to 1) [23, 72, 74], the  $K_a$  can be calculated using Equations 3.3 and 3.4.

$$K_{a, Amine} = ([Amine][H^+]) / [AmineH^+] \quad \text{Eq. 3.3}$$

or

$$pK_a = -\log(K_{a, Amine}) = -\log([Amine][H^+] / [AmineH^+]) \quad \text{Eq. 3.4}$$

The concentration of  $H^+$  in the solution can be measured by a pH meter. The disappearance of  $H^+$  during titration is a result of its reaction with amine to form  $AmineH^+$  as shown in Equation 3.5. The concentration of  $AmineH^+$  can be calculated using the mass balance of protons as in the Equation 3.6.

$$n_{HCl} - [H^+]V_{total} = [AmineH^+]V_{total} \quad \text{Eq. 3.5}$$

Finally, the concentration of free amine can be calculated using the amine balance equation as in the Equation 3.6.

$$([\text{Amine}] + [\text{AmineH}^+])V_{\text{total}} = n_{0, \text{Amine}} \quad \text{Eq. 3.6}$$

Where,  $n_{\text{HCl}}$  is the number of moles of HCl added during the titration,  $V_{\text{total}}$  is the total liquid volume after titration, and  $n_{0, \text{Amine}}$  is the initial number of moles of amine, which can be determined by titration with 1.0 N HCl until the methyl orange end point.

For the experiment, the amine's  $K_a$  was determined according to the procedure described by Shi et al. [74]. Briefly, 100 mL of 0.05 mol/L amine solution was prepared and titrated carefully with 5 mL of 1.0 N HCl standard solution at 23.5 °C until the methyl orange end point was observed. During titration, the pH of the solution was recorded after the addition of HCl every 0.5 mL. A plot of pH and HCl was then generated and used to determine the  $\text{AmineH}^+$ , amine concentration and dissociation constant ( $K_a$ ) together with Equations 3.3-3.6.



### 3.8 Heat input of CO<sub>2</sub> regeneration in aqueous amine solutions

The heat input is directly related to the steam requirements needed to strip CO<sub>2</sub> from the amine solution [75]. In this work, the total heat input of CO<sub>2</sub> regeneration was determined using the data obtained previously from the measurement of regeneration kinetic rate in section 3.6. To calculate the heat input of each amine, the amount of heat given to the loaded amine solution from the oil bath during the regeneration test must first be calculated. The calculation can be done using the rate of heat transfer equation of a spherical flask as used in the test. This equation based on Fourier's law is shown in Equation 3.7 [76].

$$q = k(2\pi Rh) \frac{dT}{dr} = kA \frac{dT}{dr} \quad \text{Eq. 3.7}$$

Where,  $q$  is the rate of heat transfer (J/s);  $k$  is the thermal conductivity of glass (1.14 W/m.<sup>0</sup>C);  $A$  is the surface area of flask's spherical section with 100 mL amine volume ( $2.51 \times 10^{-3}$  m);  $R$  is the flask's spherical radius ( $51 \times 10^{-3}$  m);  $h$  is the height of the spherical sector ( $28.87 \times 10^{-3}$  m);  $dT$  is temperature difference between oil bath and amine solution (<sup>0</sup>C); and  $dr$  is glass wall thickness ( $4 \times 10^{-3}$  m).

Once, the  $q$  has been determined. The heat input ( $Q$ ) can be calculated using Equation 3.8.

$$q = k(2\pi Rh) \frac{dT}{dr} = kA \frac{dT}{dr} \quad \text{Eq. 3.8}$$

Where, CO<sub>2</sub> produced was obtained from CO<sub>2</sub> loading difference between 0 and 80 min ( $\Delta\alpha$ , at 0-80 min).

### 3.9 Measurement of kinetic data from stopped-flow apparatus

Prior to kinetics testing, 10 mL of amine solution concentration range of 0.1, 0.2, 0.3, 0.4 and 0.5 mol/L for HEMAB and HEEAB, and 0.1, 0.2, 0.4, 0.6, 0.8 and 1 mol/L for DMAB, DEAB and MDEA in deionized water was loaded into individual plastic syringes. For fresh CO<sub>2</sub> solutions, 100 mL of deionized water was loaded into a 250 mL Erlenmeyer flask which on top was placed with a rubber stopper inserts the inlet and outlet stainless tube. The pure gases containing 100 % CO<sub>2</sub> with gentle bubbling into the deionized water for 30 min through the inlet stainless tube. The concentration of CO<sub>2</sub> was determined by gas chromatography (GC, model 6890, Agilent Ltd., Canada) [22]. It was then diluted with deionized water to keep the CO<sub>2</sub> solution at least 10 times lower than the amine solution in order to achieve the pseudo first-order conditions.

The experimental set-up for measurement of the kinetics for CO<sub>2</sub> absorption is a standard SF-51 stopped flow system supplied by Hi-Tech Scientific Ltd., UK as shown in Figure 3.5 previously used by Li et al. [18]. It consists of four major parts: a sample handling unit, a conductivity detection cell, A/D converter, and microprocessor. A fresh CO<sub>2</sub> solution and amine solution at desired concentration were loaded into individual plastic syringes about 5 mL. The solutions were placed on the top of the sample handling unit that is comprised of a stainless steel which provides support and the enclosure of the sample flow circuit. The sample flow circuit is enclosed in a constant temperature water bath that is used to maintain a constant temperature at (i.e. 298, 303, 308 and 313 K  $\pm$  0.1 °C accuracy) prior to the test. A pneumatic air supply is used to control the movement of drive plate located at the bottom of the internal syringes. The “Kinetasyst” software is used to actuate the pneumatically controlled drive plate which pushes the amine and CO<sub>2</sub> solution accurately into the conductivity detection cell through a mixing loop. The conductivity change is measured as a function of time by a circuit as described by Knipe et al. [77], which gives an output voltage directly proportional to solution conductivity. The observed pseudo-first order reaction rate constant ( $k_0$ ) can be automatically generated based on the typical graph of the change of conductivity in solution versus time and expressed as an exponential equation shown in Equation 3.9.



$$Y = -A \exp(-k_0 t) + Y_\infty$$

Eq. 3.9

Where,  $k_0$  is the pseudo-first order reaction rate constant ( $s^{-1}$ ),  $A$  is the amplitude of signal,  $Y$  is conductance (S) and  $Y_\infty$  is conductance at the end of observed reaction (S).

The experimental set-up and procedure used in this study were also used to measure the pseudo first-order reaction rate constant ( $k_0$ ) of 0.1-0.5 M for HEMAB and HEEAB and 0.1-1.0 M for DMAB, DEAB and MDEA at temperatures (i.e. 298, 303, 308 and 313 K) [18]. MEA data were then used to validate this experiment by comparing with literature values of Ali et al. [20].

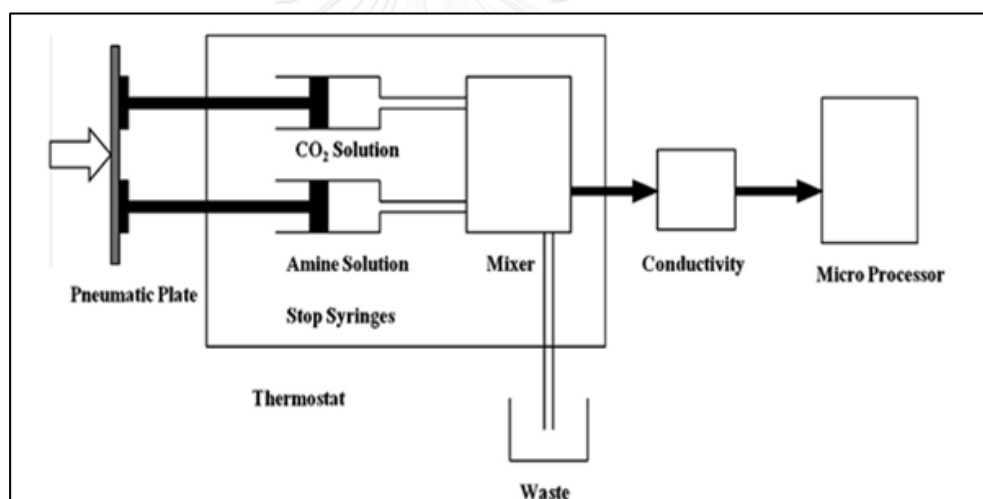


**Figure 3.5** Schematic diagram of stopped-flow equipment.

### **3.10 Physical properties**

#### **3.10.1 Density and Viscosity**

For measuring density and viscosity of pure amine solutions, about 15 mL of pure amine samples (i.e. DMAB, DPAB, DBAB, HEMAB, HEEAB, DEAB and MDEA with the purity range of 76-99.9 %) were loaded into the individual test tubes and the temperature condition were set at 20, 25, 30, 40, 50 and 60 °C with 5°C intervals. Amine samples were placed into the sample holder to be introduced to both the density meter and viscometer at the same time. The final results were obtained as an average of two measurements [32].

#### **3.10.2 Refractive index**

About 2-3 drops of pure amine samples (i.e. DMAB, DPAB, DBAB, HEMAB, HEEAB, DEAB and MDEA with the purity range of 76-99.9 %) were dropped on the sample window of the refractometer. The temperature conditions were set at 20, 25, 30, 40 and 50 °C with 5°C intervals. The final results were obtained as an average of two measurements [32].

## CHAPTER IV

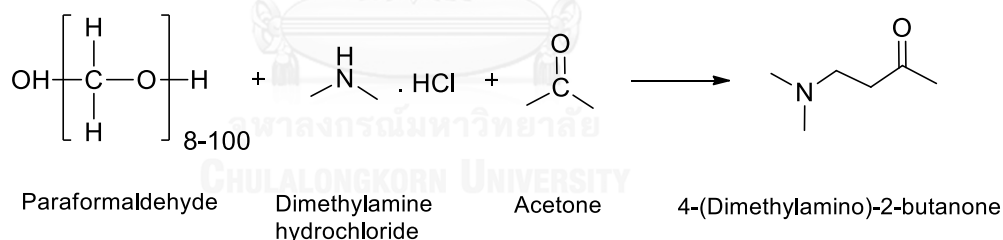
### RESULTS AND DISCUSSION

#### 4.1 Amine synthesis

##### 4.1.1 Synthesis of 4-(dimethylamino)-2-butanone (DMAB)

Step I. Synthesis of 4-(dimethylamino)-2-butanone, the starting reagent for DMAB's synthesis.

The synthesis of 4-(dimethylamino)-2-butanone was attempted by starting of paraformaldehyde, dimethylamine hydrochloride and acetone according to the Mannich reaction method [63, 64]. After a workup, the compound was obtained as a yellowish liquid in 43 % yield as shown in Scheme 4.1.



**Scheme 4.1** Synthesis route of 4-(dimethylamino)-2-butanone.

The compound was then characterized by  $^1\text{H}$  and  $^{13}\text{C}$ -NMR and GC-MS. Figure 4.1 shows the  $^1\text{H}$ -NMR spectrum of 4-(dimethylamino)-2-butanone, along with interpreted data presented in Table 4.1.

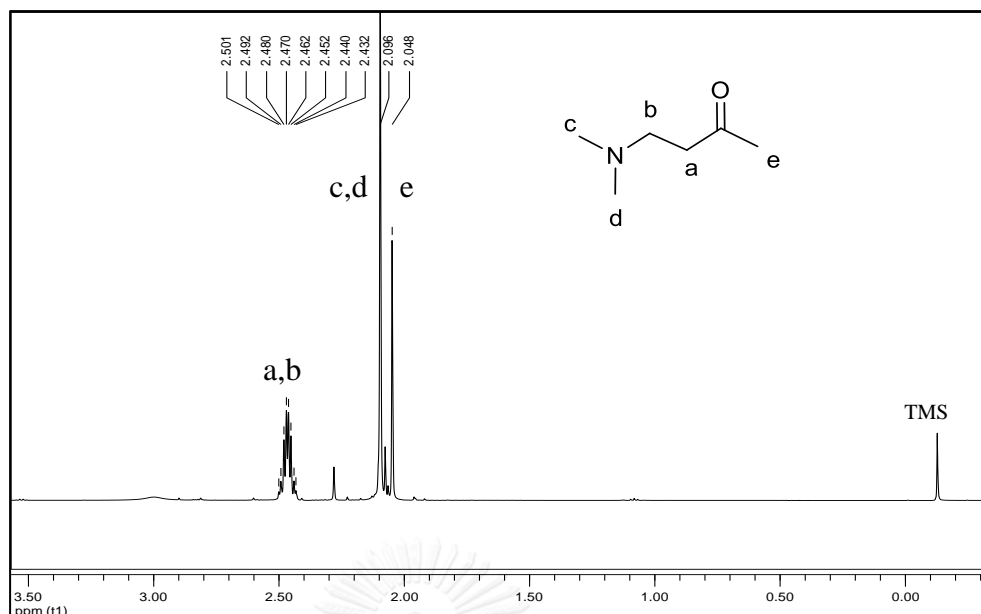


**Figure 4.1**  $^1\text{H-NMR}$  (500 MHz,  $\text{CDCl}_3$ ) spectrum of 4-(dimethylamino)-2-butanone.

**Table 4.1**  $^1\text{H-NMR}$  data of 4-(dimethylamino)-2-butanone.

$\delta$ (ppm)	type of proton, number of proton, position
2.50-2.43	m, 4H, (a,b)
2.1	s, 6H, (c,d)
2.05	s, 3H, (e)

Figure 4.2 shows the  $^{13}\text{C-NMR}$  spectrum of 4-(dimethylamino)-2-butanone. The downfield singlet signal at 207.75 ppm corresponds to  $\text{C=O}$ .  $^{13}\text{C-NMR}$  signals appearing at other chemical shifts were assigned for the corresponding carbons presented in Table 4.2.

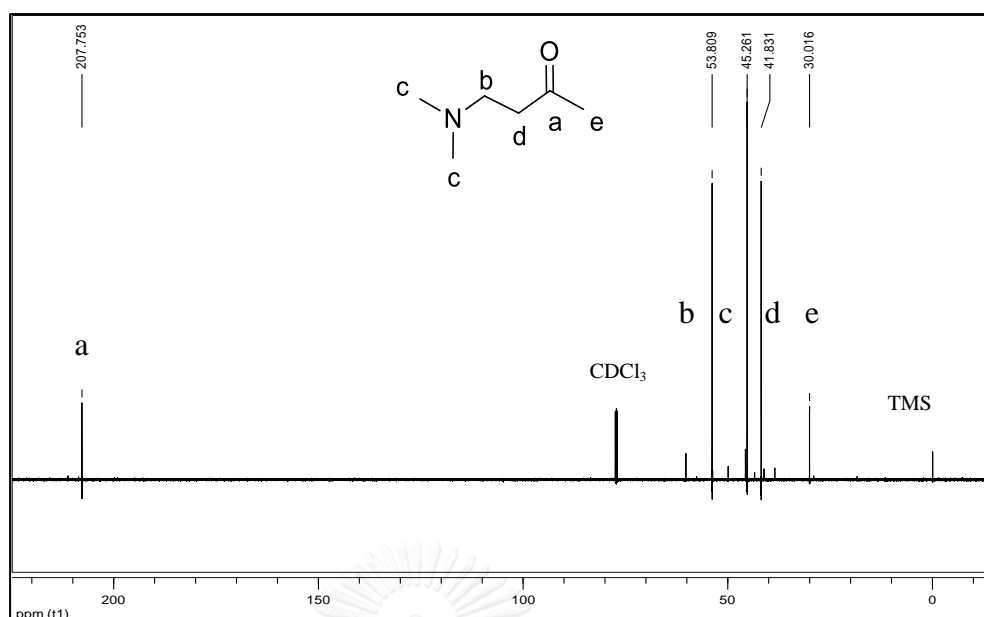


**Figure 4.2**  $^{13}\text{C}$ -NMR (125 MHz,  $\text{CDCl}_3$ ) spectrum of 4-(dimethylamino)-2-butanone.

**Table 4.2**  $^{13}\text{C}$ -NMR data of 4-(dimethylamino)-2-butanone.

$\delta$ (ppm)	type of carbon, position
207.75	s, (a)
53.81	t, (b)
45.26	q, (c)
41.83	t, (d)
30.01	q, (e)

Figures 4.3 and 4.4 illustrate the GC-MS chromatogram and mass spectra of 4-(dimethylamino)-2-butanone, respectively. The GC retention time of the compound was found at 4.02 min with the purity of 76 %. The mass spectrum pattern of the compound was found to be in excellent agreement with the GC-MS chromatograms, thus confirming the compound's chemical formula ( $\text{C}_6\text{H}_{13}\text{NO}$ ) and 115 molecular weight.

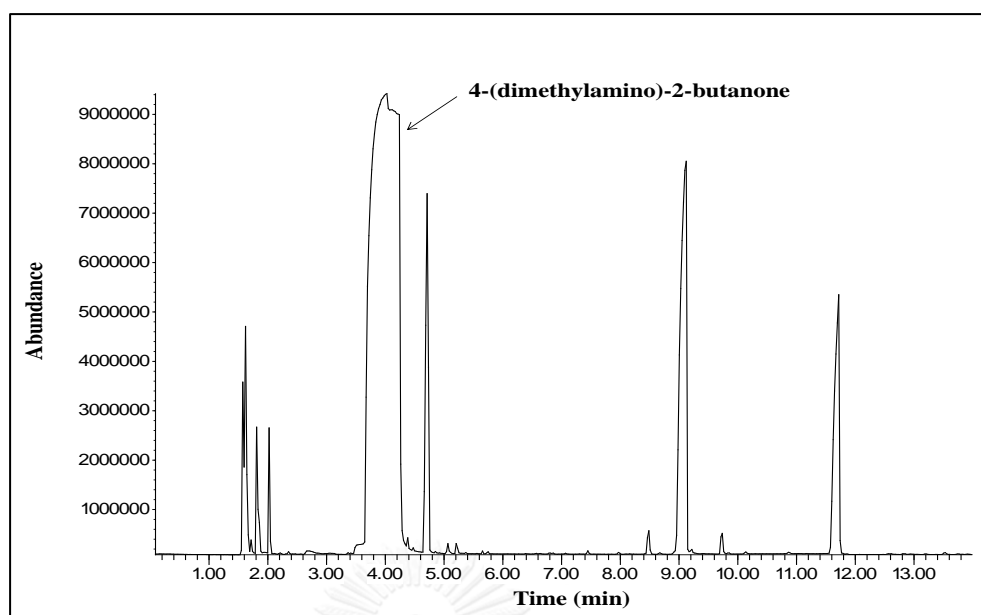


**Figure 4.3** GC-MS chromatogram of 4-(dimethylamino)-2-butanone.

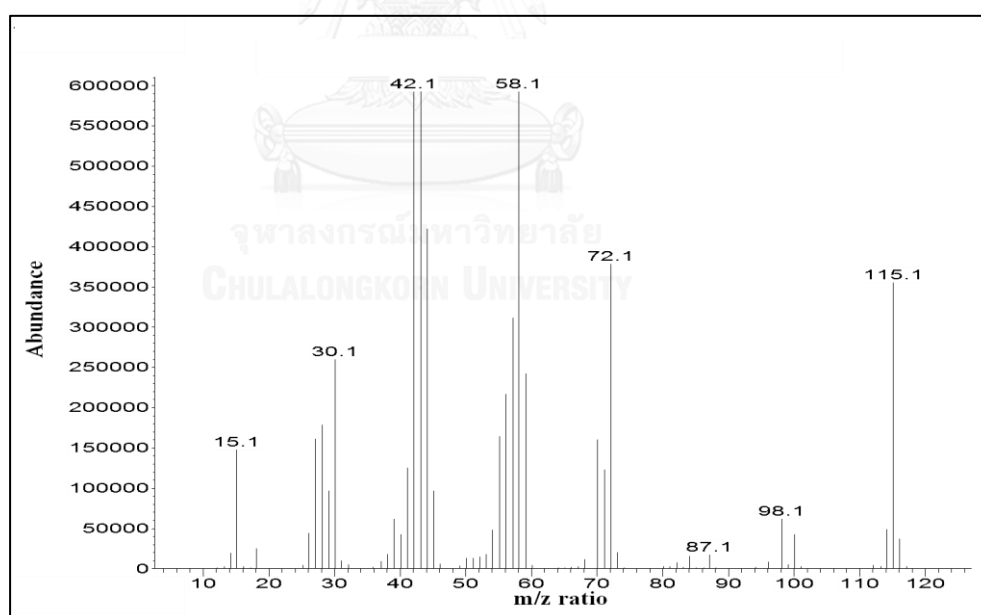
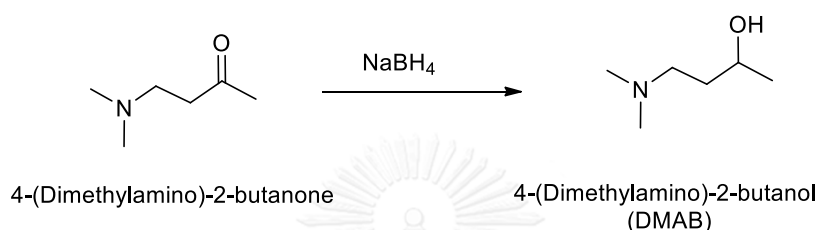


**Figure 4.4** Mass spectrum of 4-(dimethylamino)-2-butanone.

### Step II. Synthesis of 4-(dimethylamino)-2-butanol (DMAB)

To make DMAB, 4-(dimethylamino)-2-butanone obtained earlier was reacted with sodium borohydride as a reducing agent. The amino carbonyl compound was reduced into amino alcohol as indicated by a change in the color of the solution from yellowish to colorless. After workup and vacuum distillation, the compound was obtained in 47 % yield as shown in Scheme 4.2.



**Scheme 4.2** Synthesis route of 4-(dimethylamino)-2-butanol (DMAB).

The compound was then characterized by FT-IR, <sup>1</sup>H and <sup>13</sup>C-NMR and GC-MS. According to the infrared (IR) spectrum, tertiary amine usually has no absorption band at 3300 cm<sup>-1</sup>, which was due to the disappearance of the hydrogen atom (H) attached to the nitrogen atom (N) of the tertiary amine molecule. The broad absorption band at 3353 cm<sup>-1</sup> was found, which indicated the presence of the hydroxyl group (OH) in the structure. The absorption bands at 2963 (CH<sub>2</sub>), and 2935 (CH<sub>3</sub>) cm<sup>-1</sup> were shown as asymmetric stretching. For the symmetric stretching, the absorption bands were shown at 2818 (CH<sub>3</sub>), and 2778 (CH<sub>2</sub>) cm<sup>-1</sup>. DMAB structure also showed the absorption band at 1461 cm<sup>-1</sup> (CH<sub>2</sub> bending), 1375 cm<sup>-1</sup> (CH<sub>3</sub> bending), and 1067 cm<sup>-1</sup> (CN stretching). The infrared spectrum of DMAB is shown in Figure 4.5.

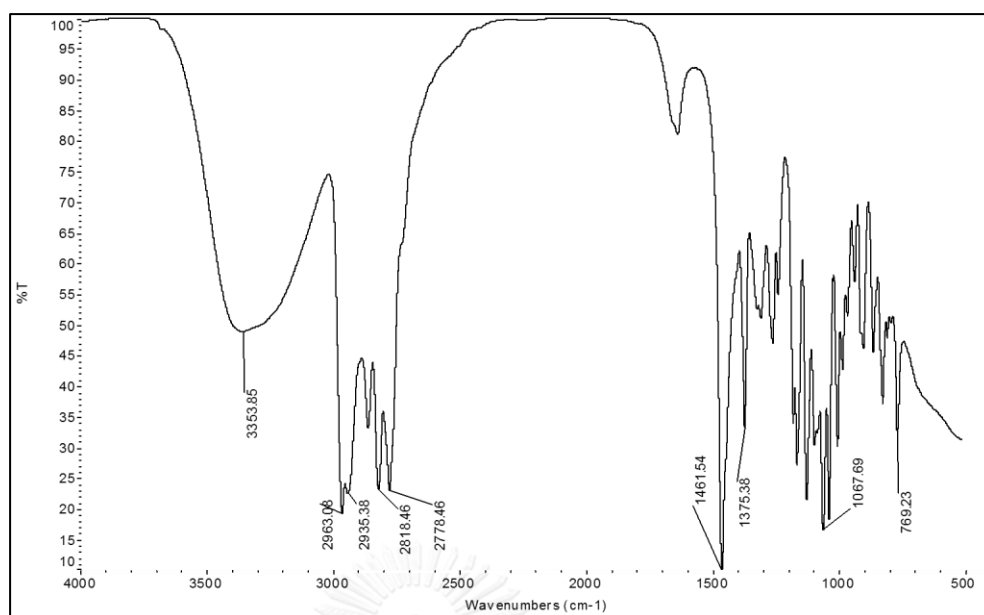


**Figure 4.5** FT-IR spectrum of 4-(dimethylamino)-2-butanol (DMAB).

The chemical structure of DMAB was also identified by <sup>1</sup>H and <sup>13</sup>C-NMR as shown in Figures 4.6 and 4.7, respectively. Tables 4.3 and 4.4 list the chemical shifts for the corresponding hydrogen and carbon atoms, respectively.



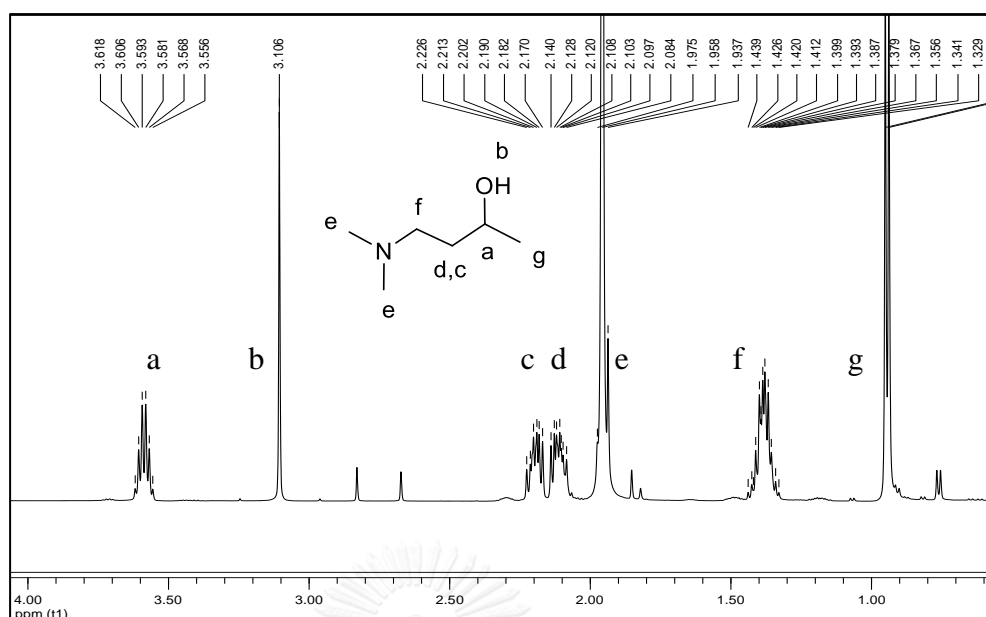


**Figure 4.6**  $^1\text{H-NMR}$  (500 MHz,  $\text{D}_2\text{O}$ ) spectrum of 4-(dimethylamino)-2-butanol (DMAB).

**Table 4.3**  $^1\text{H-NMR}$  data of 4-(dimethylamino)-2-butanol (DMAB).

$\delta$ (ppm)	type of proton, number of proton, position
3.62-3.56	m, 1H, (a)
3.01	s, 1H, (b)
2.23-2.17	m, 1H, (c)
2.14-2.08	m, 1H, (d)
1.96	s, 6H, (e)
1.44-1.33	m, 2H, (f)
0.95-0.94	d, 3H, $J = 6\text{Hz}$ , (g)

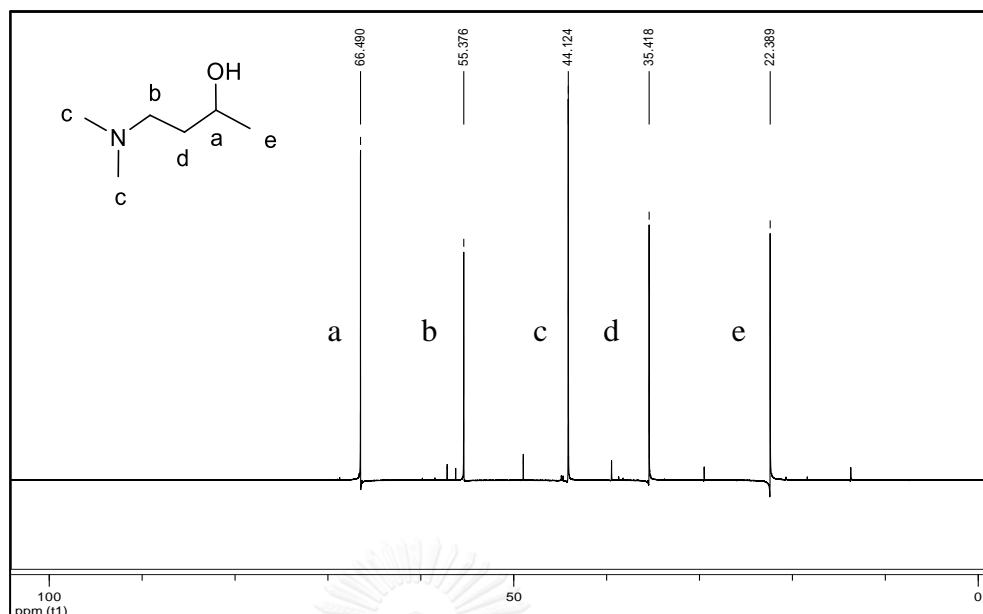


**Figure 4.7**  $^{13}\text{C}$ -NMR (125 MHz,  $\text{D}_2\text{O}$ ) spectrum of 4-(dimethylamino)-2-butanol (DMAB).

**Table 4.4**  $^{13}\text{C}$ -NMR data of 4-(dimethylamino)-2-butanol (DMAB).

$\delta$ (ppm)	type of carbon, position
66.49	d, (a)
55.37	t, (b)
44.12	q, (c)
35.42	t, (d)
22.39	q, (e)

Figures 4.8 and 4.9 illustrate the GC-MS chromatogram and mass spectra of DMAB, respectively. The GC retention time of the compound was found at 4.02 min with the purity of 76 %. The mass spectrum pattern of the compound was found to be in excellent agreement with the GC-MS chromatogram, thus confirming the compound's chemical formula ( $\text{C}_6\text{H}_{13}\text{NO}$ ) and 117 molecular weight.

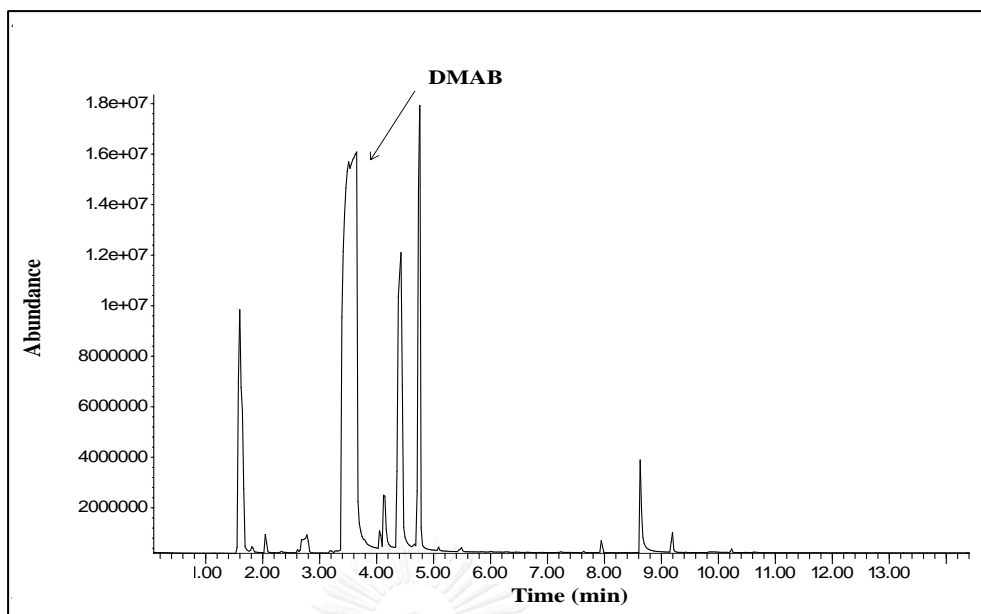


**Figure 4.8** GC-MS chromatogram of 4-(dimethylamino)-2-butanol (DMAB).

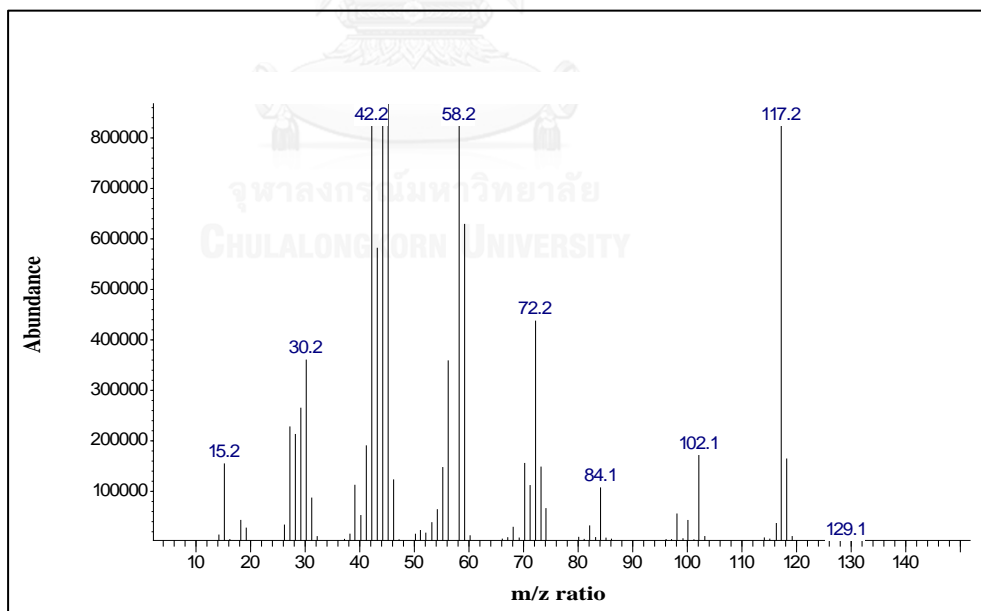
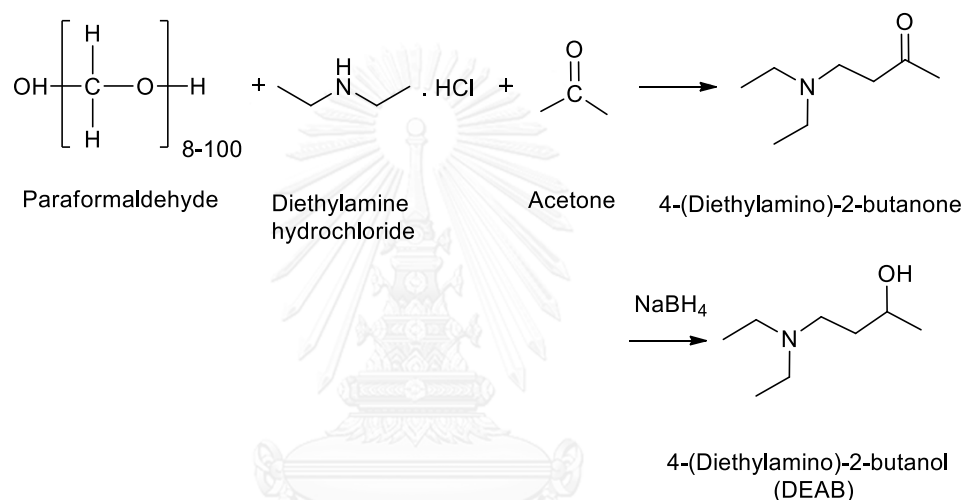


**Figure 4.9** Mass spectrum of 4-(dimethylamino)-2-butanol (DMAB).

#### 4.1.2 Synthesis of 4-(diethylamino)-2-butanol (DEAB)

Normally, DEAB can be synthesized by the Michael addition reaction method as described in the literature [27]. In this work, the synthesis of DEAB was similar to the synthesis of DMAB. It can be synthesized in two steps, which involve the formation and the subsequent reduction of 4-(diethylamino)-2-butanone. After a workup and vacuum distillation, the compound was obtained as a yellowish liquid in 53.5 % yield as shown in Scheme 4.3.



**Scheme 4.3** Synthesis route of 4-(diethylamino)-2-butanol (DEAB).

The chemical structure and purity of compound DEAB was identified by FT-IR,  $^1\text{H}$  and  $^{13}\text{C}$ -NMR, and GC-MS, respectively. According to the infrared spectrum, the absorption bands were shown at  $3347\text{ cm}^{-1}$  (OH stretching),  $2963\text{ cm}^{-1}$  ( $\text{CH}_2$  asymmetric stretching),  $2929\text{ cm}^{-1}$  ( $\text{CH}_3$  asymmetric stretching),  $2873\text{ cm}^{-1}$  ( $\text{CH}_3$  symmetric stretching),  $2818\text{ cm}^{-1}$  ( $\text{CH}_2$  symmetric stretching),  $1455\text{ cm}^{-1}$  ( $\text{CH}_2$  bending),  $1369\text{ cm}^{-1}$  ( $\text{CH}_3$  bending), and  $1070\text{ cm}^{-1}$  (CN stretching). The infrared spectrum of DEAB is shown in Figure 4.10.

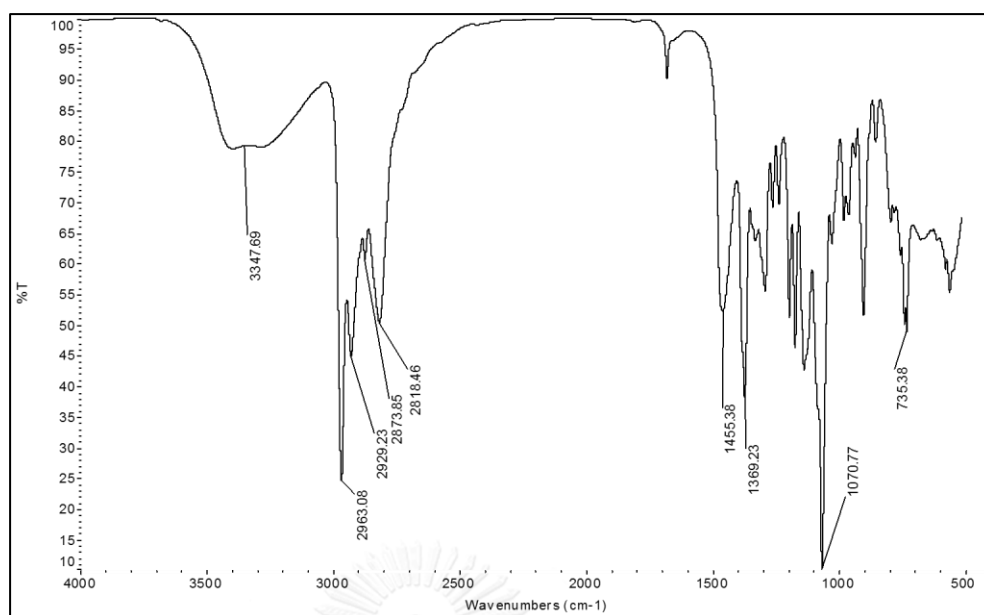


**Figure 4.10** FT-IR spectrum of 4-(diethylamino)-2-butanol (DEAB).

The chemical structure of DEAB was also identified by <sup>1</sup>H and <sup>13</sup>C-NMR as shown in Figures 4.11 and 4.12, respectively. Tables 4.5 and 4.6 list the chemical shifts for the corresponding of hydrogen and carbon atoms, respectively.

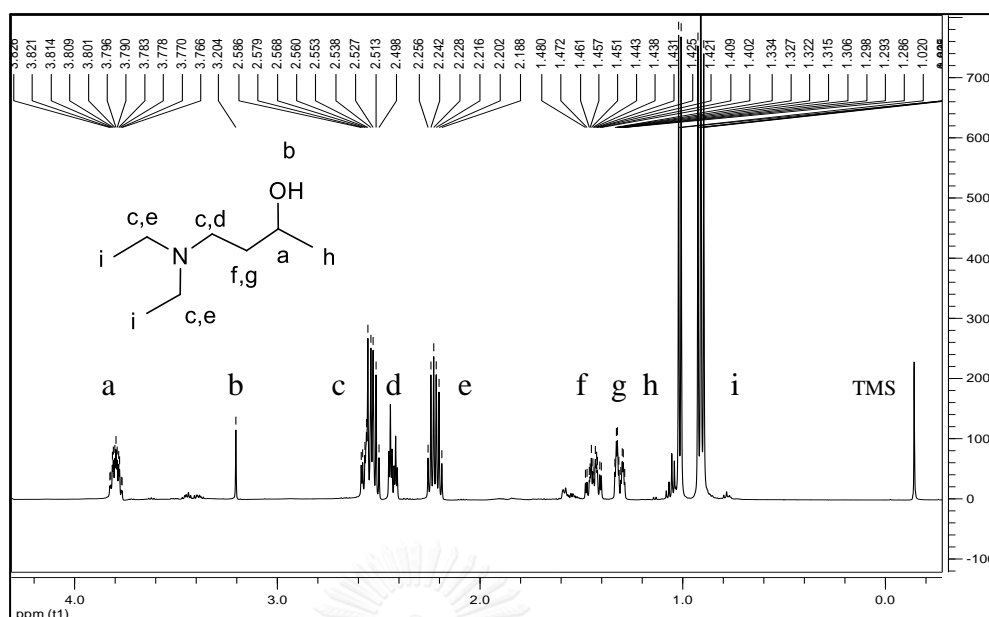


**Figure 4.11**  $^1\text{H-NMR}$  (500 MHz,  $\text{CDCl}_3$ ) spectrum of 4-(diethylamino)-2-butanol (DEAB).

**Table 4.5**  $^1\text{H-NMR}$  data of 4-(diethylamino)-2-butanol (DEAB).

$\delta$ (ppm)	type of proton, number of proton, position
3.84-3.77	m, 1H, (a)
3.30	s, 1H, -OH (b)
2.59-2.50	m, 3H, $J = 7.5$ Hz, (c)
2.45-2.41	dt, 1H, $J = 5$ Hz, (d)
2.26-2.19	sex, 2H, $J = 6$ Hz, (e)
1.48-1.40	m, 1H, (f)
1.33-1.29	m, 1H, (g)
1.02-1.01	d, 3H, $J = 6$ Hz, (h)
0.93-0.90	t, 6H, $J = 7$ Hz, (i)

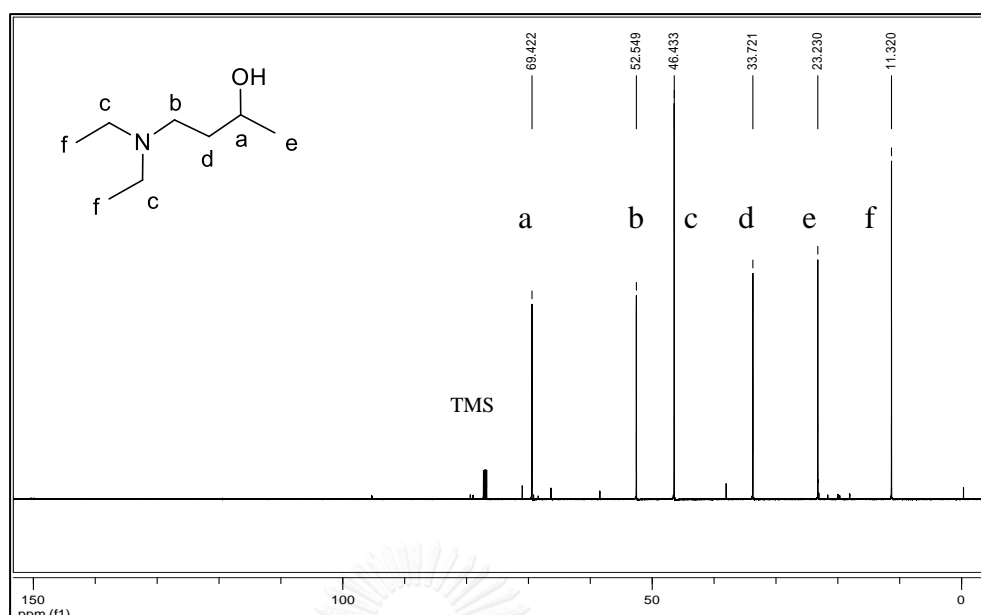


**Figure 4.12**  $^{13}\text{C}$ -NMR (125 MHz,  $\text{CDCl}_3$ ) spectrum of 4-(diethylamino)-2-butanol (DEAB).

**Table 4.6**  $^{13}\text{C}$ -NMR data of 4-(diethylamino)-2-butanol (DEAB).

$\delta$ (ppm)	type of carbon, position
69.42	d, (a)
52.55	t, (b)
46.43	t, (c)
33.72	t, (d)
23.23	q, (e)
11.32	q, (f)

Figures 4.13 and 4.14 illustrate the GC-MS chromatogram and mass spectrum of DEAB, respectively. The GC retention time of the compound was found at 5.79 min with the purity of 82 %. The mass spectrum pattern of the compound was found to be in excellent agreement with the GC-MS chromatogram, thus confirming the compound's chemical formula ( $\text{C}_8\text{H}_{19}\text{NO}$ ) and 145 molecular weight.

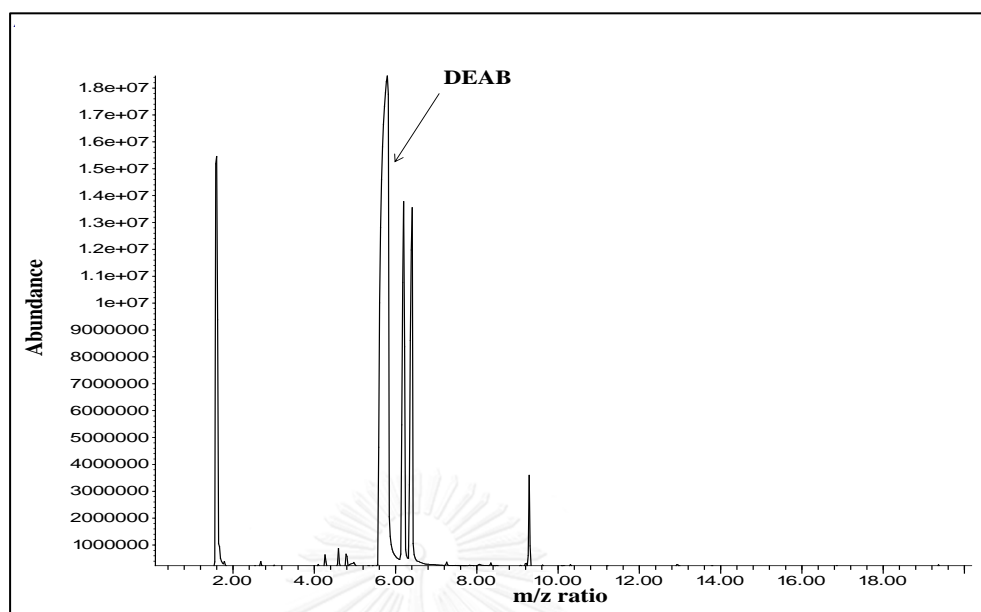


**Figure 4.13** GC-MS chromatogram of 4-(diethylamino)-2-butanol (DEAB).

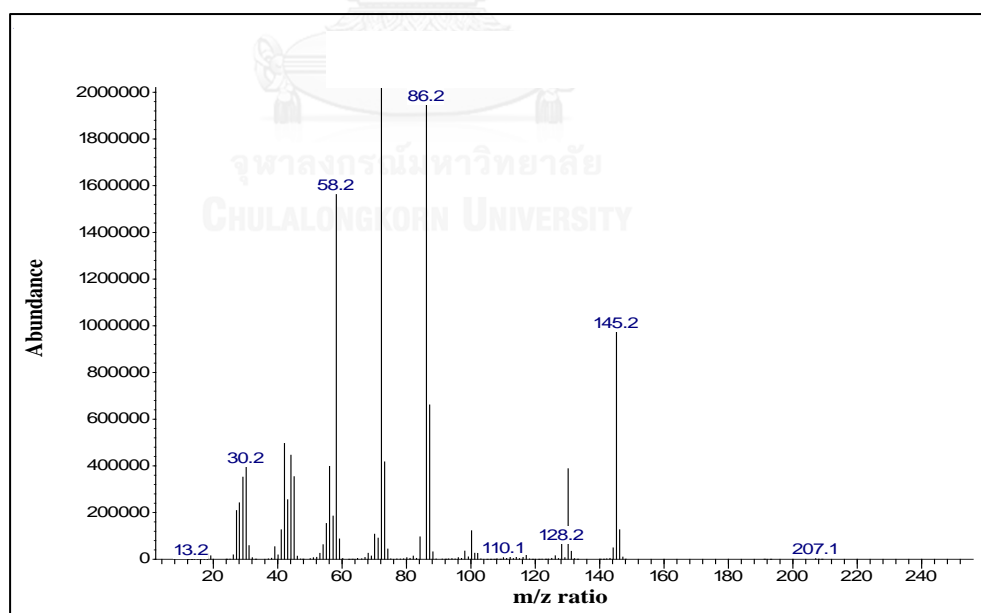
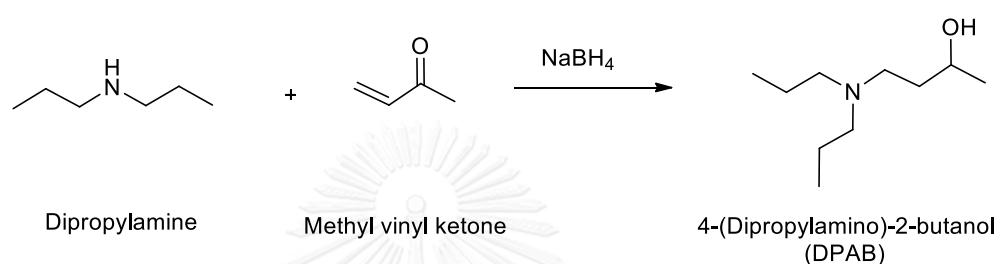


**Figure 4.14** Mass spectrum of 4-(diethylamino)-2-butanol (DEAB).



### 4.1.3 Synthesis of 4-(dipropylamino)-2-butanol (DPAB)

The synthesis method of DPAB was synthesized by the Michael addition reaction and procedure given in the literature [27]. The synthesis of DPAB was attempted by starting with dipropylamine and methyl vinyl ketone (MVK). After workup and distillation, the compound was obtained as a yellowish liquid in 42 % yield as shown in Scheme 4.4.



**Scheme 4.4** Synthesis route of 4-(dipropylamino)-2-butanol (DPAB)

The chemical structure and purity of compound DPAB was identified by FT-IR, <sup>1</sup>H and <sup>13</sup>C-NMR, and GC-MS, respectively. According to the infrared spectrum, the absorption bands were shown at 3353 cm<sup>-1</sup> (OH stretching), 2956 cm<sup>-1</sup> (CH<sub>2</sub> asymmetric stretching), 2929 cm<sup>-1</sup> (CH<sub>3</sub> asymmetric stretching), 2873 cm<sup>-1</sup> (CH<sub>3</sub> symmetric stretching), 2806 cm<sup>-1</sup> (CH<sub>2</sub> symmetric stretching), 1461 cm<sup>-1</sup> (CH<sub>2</sub> bending), 1369 cm<sup>-1</sup> (CH<sub>3</sub> bending), and 1073 cm<sup>-1</sup> (CN stretching). The infrared spectrum of DPAB is shown in Figure 4.15.

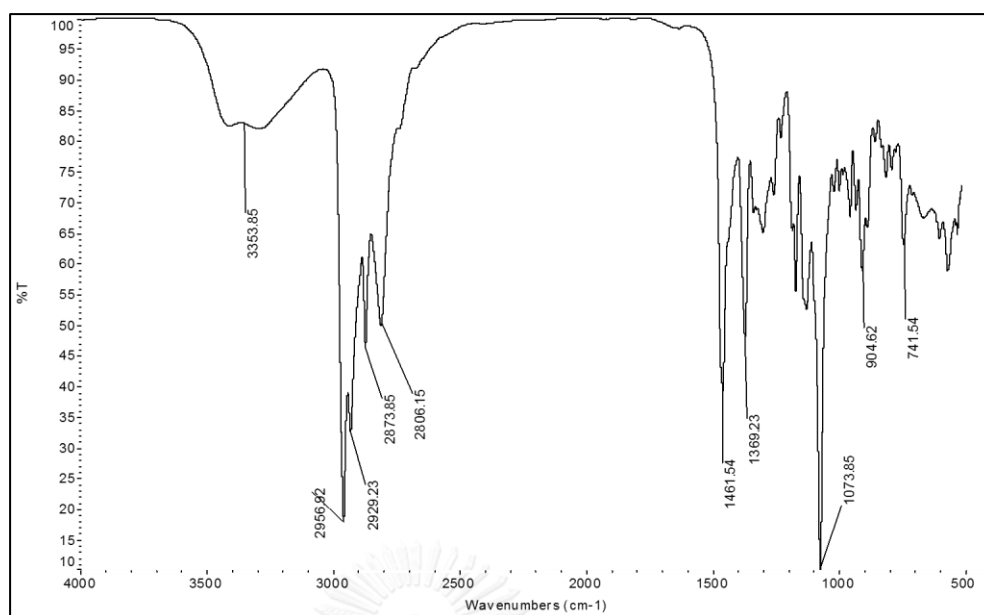


**Figure 4.15** FT-IR spectrum of 4-(dipropylamino)-2-butanol (DPAB).

The chemical structure of DPAB was also identified by  $^1\text{H}$  and  $^{13}\text{C}$ -NMR as shown in Figures 4.16 and 4.17, respectively. Tables 4.7 and 4.8 list the chemical shifts for the corresponding hydrogen and carbon atoms, respectively.

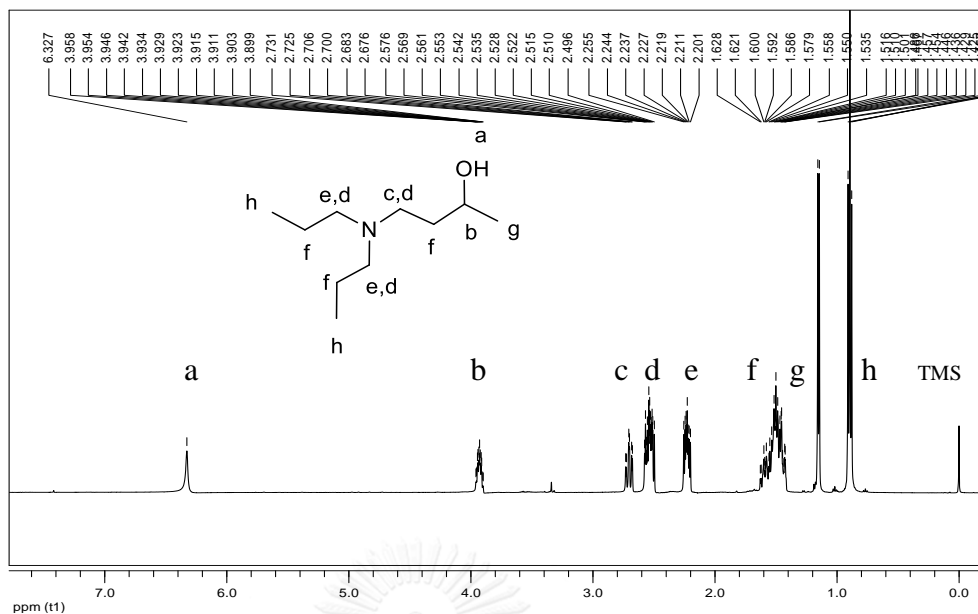


**Figure 4.16**  $^1\text{H-NMR}$  (500 MHz,  $\text{CDCl}_3$ ) spectrum of 4-(dipropylamino)-2-butanone (DPAB).

**Table 4.7**  $^1\text{H-NMR}$  data of 4-(dipropylamino)-2-butanone (DPAB).

$\delta$ (ppm)	type of proton, number of proton, position
6.33	s, 1H, (a)
3.96-3.9	m, 1H, (b)
2.73-2.68	dt, 1H, $J = 3$ and 12.5 Hz, (c)
2.58-2.2	m, 3H, (d)
2.25-2.2	m, 2H, (e)
1.63-1.42	m, 6H, (f)
1.16-1.15	d, 3H, $J = 6.5$ Hz (g)
0.91-0.88	t, 6H, $J = 7.5$ Hz, (h)

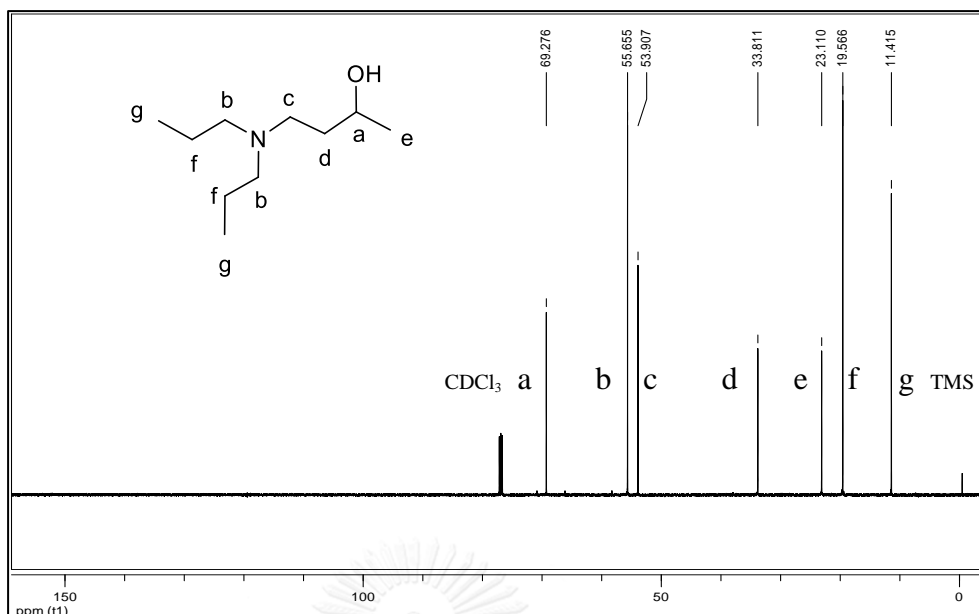


**Figure 4.17**  $^{13}\text{C}$ -NMR (125 MHz,  $\text{CDCl}_3$ ) spectrum of 4-(dipropylamino)-2-butanone (DPAB).

**Table 4.8**  $^{13}\text{C}$ -NMR data of 4-(dipropylamino)-2-butanone (DPAB).

$\delta$ (ppm)	type of carbon, position
69.28	d, (a)
55.65	t, (b)
53.91	t, (c)
33.81	t, (d)
23.11	q, (e)
19.57	t, (f)
11.42	q, (g)

Figures 4.18 and 4.19 illustrate the GC-MS chromatogram and mass spectra of DPAB, respectively. The GC retention time of compound was found at 8.77 min with the purity of 82 %. The mass spectrum pattern of the compound was found to be in

excellent agreement with the GC-MS chromatogram, thus confirming the compound's chemical formula ( $C_{10}H_{23}NO$ ) and 173 molecular weight.

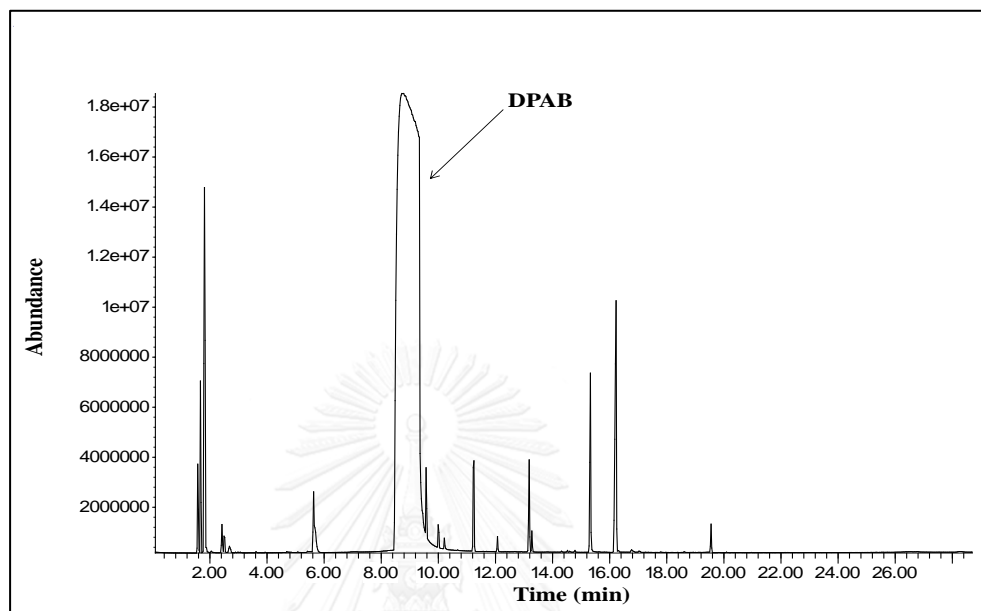


**Figure 4.18** GC-MS chromatogram of 4-(dipropylamino)-2-butanone (DPAB).

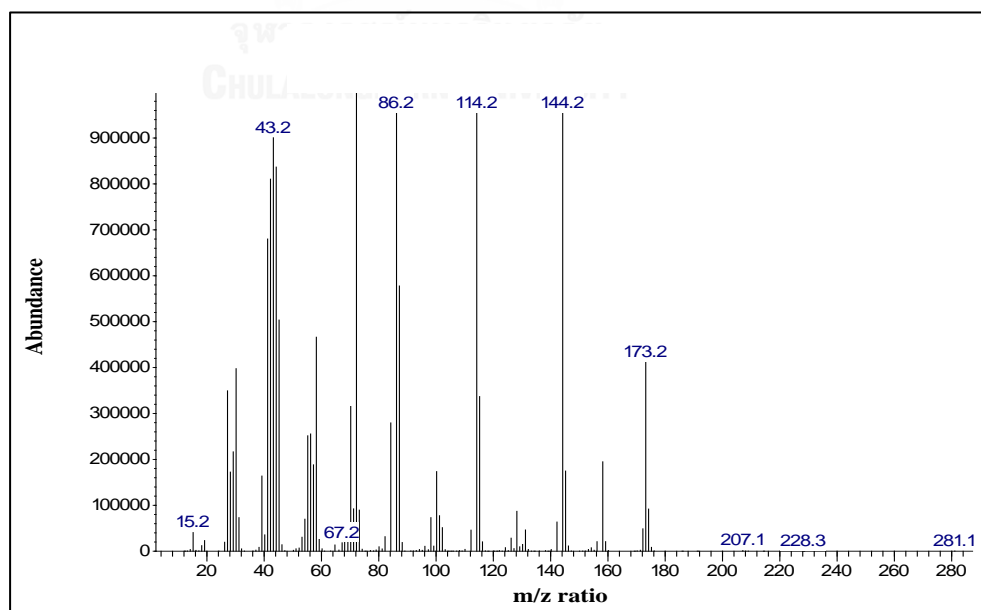
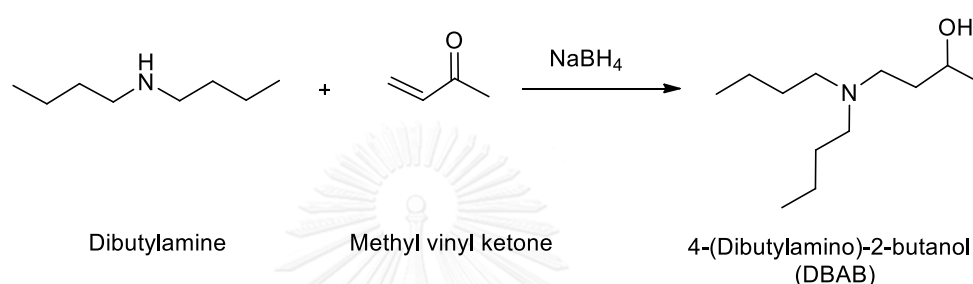


**Figure 4.19** Mass spectrum of 4-(dipropylamino)-2-butanone (DPAB).

#### 4.1.4 Synthesis of 4-(dibutylamino)-2-butanol (DBAB)

The synthesis method of DBAB was synthesized by the Michael addition reaction and procedure given in the literature [27]. The synthesis of DBAB was attempted by starting with dibutylamine and methyl vinyl ketone (MVK). After workup and distillation, the compound was obtained as a yellowish liquid in 40.05 % yield as shown in Scheme 4.5.



**Scheme 4.5** Synthesis route of 4-(dibutylamino)-2-butanol (DBAB).

The chemical structure and purity of compound DBAB was identified by FT-IR,  $^1\text{H}$  and  $^{13}\text{C}$ -NMR, and GC-MS, respectively. According to the infrared spectrum, the absorption bands were shown at  $3353\text{ cm}^{-1}$  (OH stretching),  $2956\text{ cm}^{-1}$  ( $\text{CH}_2$  asymmetric stretching),  $2926\text{ cm}^{-1}$  ( $\text{CH}_3$  asymmetric stretching),  $2861\text{ cm}^{-1}$  ( $\text{CH}_3$  symmetric stretching),  $2812\text{ cm}^{-1}$  ( $\text{CH}_2$  symmetric stretching),  $1461\text{ cm}^{-1}$  ( $\text{CH}_2$  bending),  $1369\text{ cm}^{-1}$  ( $\text{CH}_3$  bending), and  $1073\text{ cm}^{-1}$  (CN stretching). The infrared spectrum of DBAB is shown in Figure 4.20.

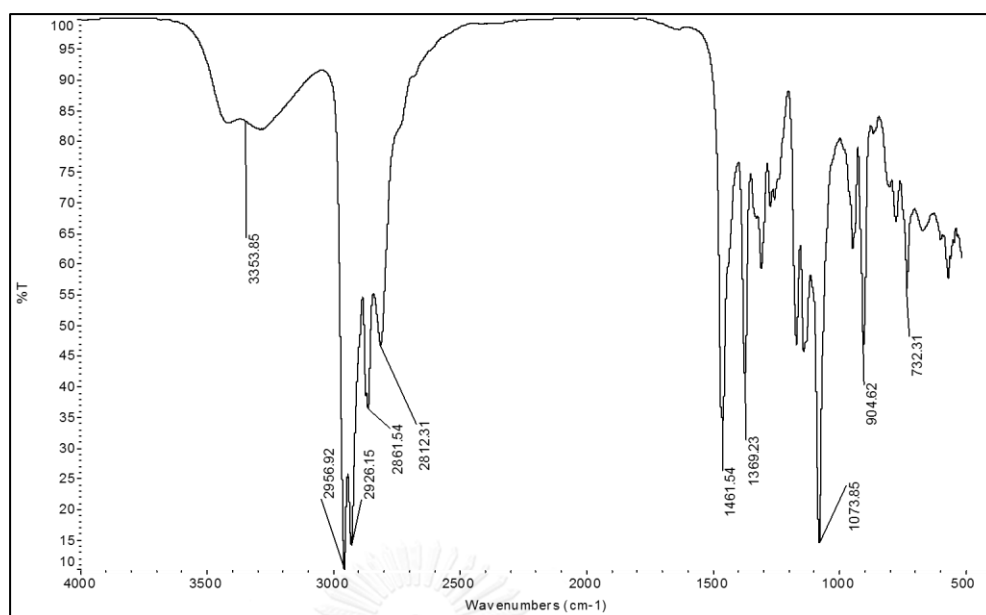


**Figure 4.20** FT-IR spectrum of 4-(dibutylamino)-2-butanol (DBAB).

The chemical structure of DBAB was also identified by  $^1\text{H}$  and  $^{13}\text{C}$ -NMR as shown in Figures 4.21 and 4.22, respectively. Tables 4.9 and 4.10 list the chemical shifts for the corresponding hydrogen and carbon atoms, respectively.

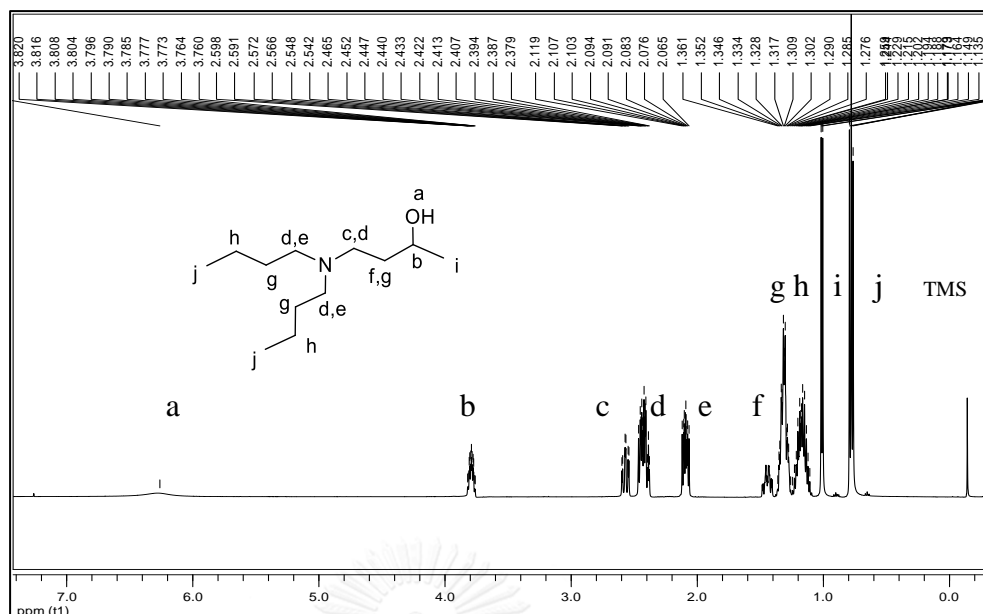


**Figure 4.21**  $^1\text{H-NMR}$  (500 MHz,  $\text{CDCl}_3$ ) spectrum of 4-(dibutylamino)-2-butanone (DBAB).

**Table 4.9**  $^1\text{H-NMR}$  data of 4-(dibutylamino)-2-butanone (DBAB).

$\delta$ (ppm)	type of proton, number of proton, position
6.26	brs, 1H, (a)
3.82-3.76	dsex, 1H, $J = 2$ and 6 Hz (b)
2.60-2.54	dt, 1H, $J = 3$ and 12 Hz, (c)
2.47-2.38	m, 3H, (d)
2.12-2.06	m, 2H, (e)
1.63-1.42	m, 1H, (f)
1.36-1.26	m, 5H, (g)
1.24-1.11	m, 4H, (h)
1.02-1.00	d, 3H, $J = 6$ Hz (i)
0.79-0.76	t, 6H, $J = 7.5$ Hz (j)



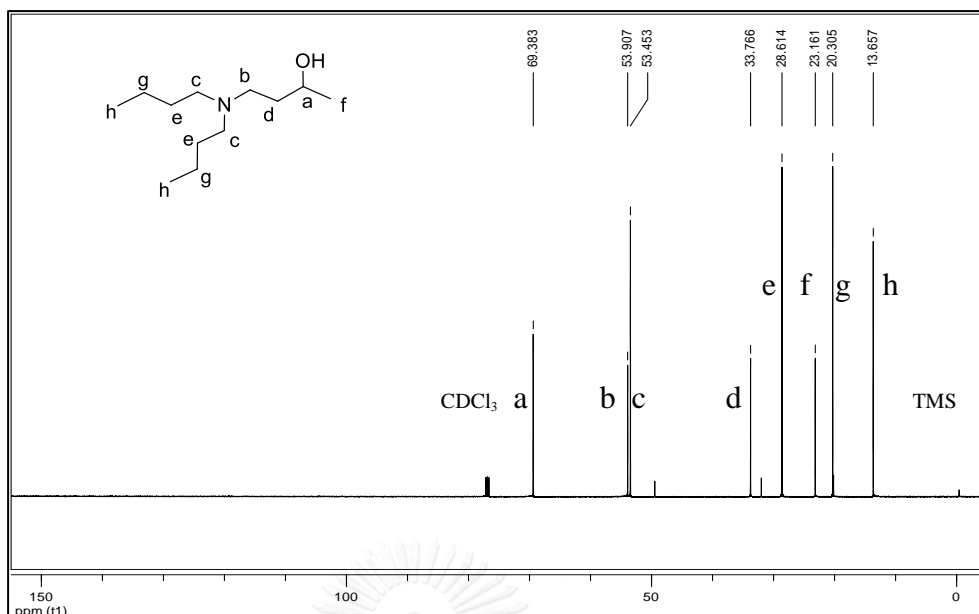


**Figure 4.22**  $^{13}\text{C}$ -NMR (125 MHz,  $\text{CDCl}_3$ ) spectrum of 4-(dibutylamino)-2-butanone (DBAB).

**Table 4.10**  $^{13}\text{C}$ -NMR data of 4-(dibutylamino)-2-butanone (DBAB).

$\delta$ (ppm)	type of carbon, position
69.38	d, (a)
53.91	t, (b)
53.45	t, (c)
33.77	t, (d)
28.61	t, (e)
23.16	q, (f)
20.31	t, (g)
13.66	q, (h)

Figures 4.23 and 4.24 illustrate the GC-MS chromatogram and mass spectrum of DBAB, respectively. The GC retention time of compound was found at 12 min with the purity of 80.5 %. The mass spectrum pattern of the compound was found to be in excellent agreement with the GC-MS chromatogram, thus confirming the compound's chemical formula ( $C_{12}H_{27}NO$ ) and 201 molecular weight.

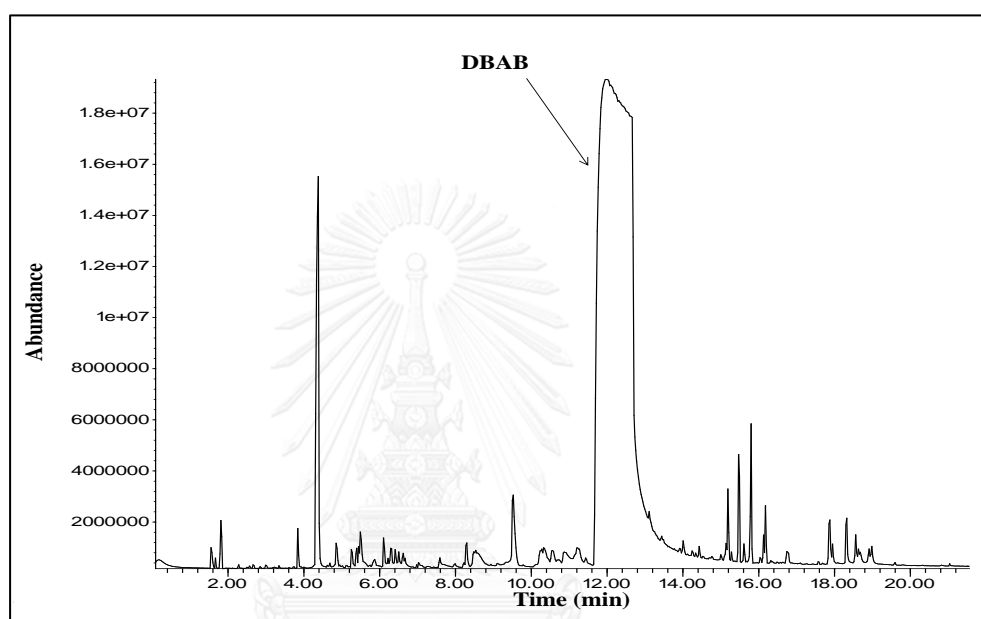


**Figure 4.23** GC-MS chromatogram of 4-(dibutylamino)-2-butanone (DBAB).

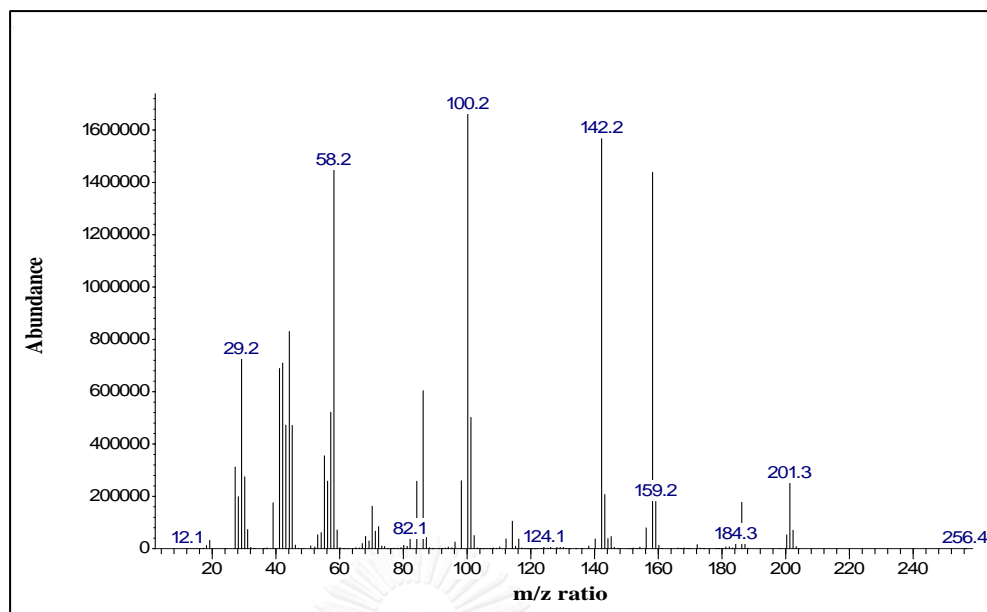
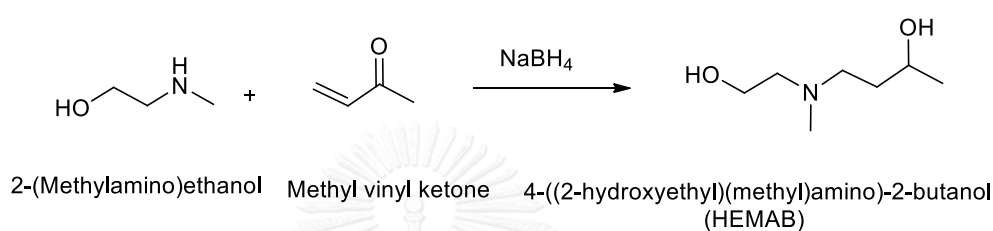


**Figure 4.24** Mass spectrum of 4-(dibutylamino)-2-butanone (DBAB).

#### 4.1.5 Synthesis of 4-((2-hydroxyethyl)(methyl)amino)-2-butanol (HEMAB)

Compound HEMAB was synthesized by the Michael addition reaction, following procedures given in the literature [27]. The synthesis of HEMAB was attempted by starting with 2-(methylamino)ethanol and methyl vinyl ketone (MVK). After workup and distillation, the compound was obtained as a yellowish liquid in 57.48 % yield as shown in Scheme 4.6.



**Scheme 4.6** Synthesis route of 4-((2-hydroxyethyl)(methyl)amino)-2-butanol (HEMAB).

The chemical structure and purity of compound HEMAB was identified by FT-IR,  $^1\text{H}$  and  $^{13}\text{C}$ -NMR, and GC-MS, respectively. According to the infrared spectrum, the absorption bands were shown at  $3329\text{ cm}^{-1}$  (OH stretching),  $2960\text{ cm}^{-1}$  ( $\text{CH}_2$  asymmetric stretching),  $2932\text{ cm}^{-1}$  ( $\text{CH}_3$  asymmetric stretching),  $2843\text{ cm}^{-1}$  ( $\text{CH}_3$  symmetric stretching),  $2800\text{ cm}^{-1}$  ( $\text{CH}_2$  symmetric stretching),  $1458\text{ cm}^{-1}$  ( $\text{CH}_2$  bending),  $1375\text{ cm}^{-1}$  ( $\text{CH}_3$  bending), and  $1033\text{ cm}^{-1}$  (CN stretching). The infrared spectrum of HEMAB is shown in Figure 4.25.

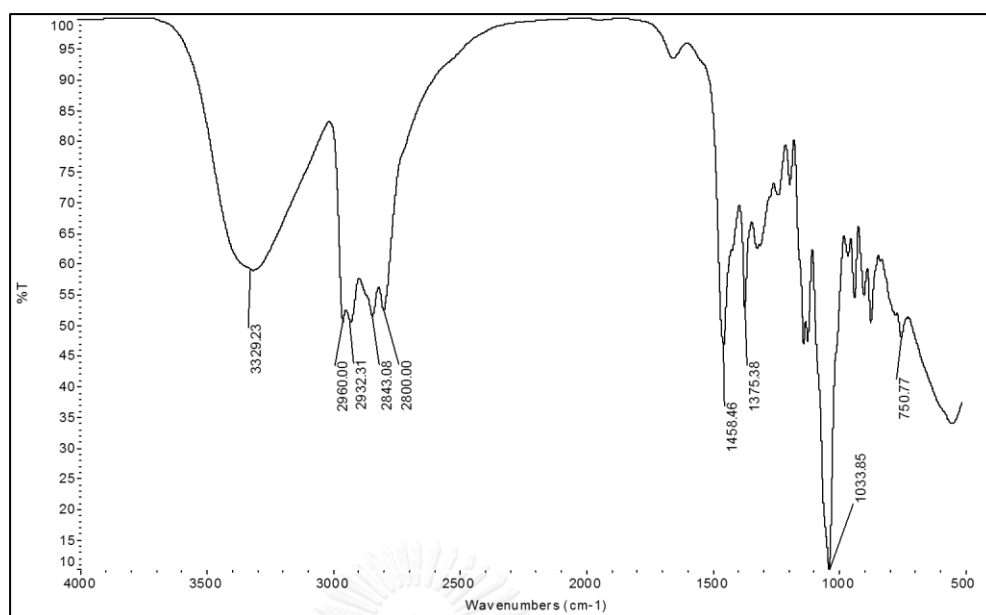


**Figure 4.25** FT-IR spectrum of 4-((2-hydroxyethyl) (methyl)amino)-2-butanol (HEMAB).

The chemical structure of HEMAB was also identified by  $^1\text{H}$  and  $^{13}\text{C}$ -NMR as shown in Figures 4.26 and 4.27, respectively. Tables 4.11 and 4.12 list the chemical shifts for the corresponding hydrogen and carbon atoms, respectively.

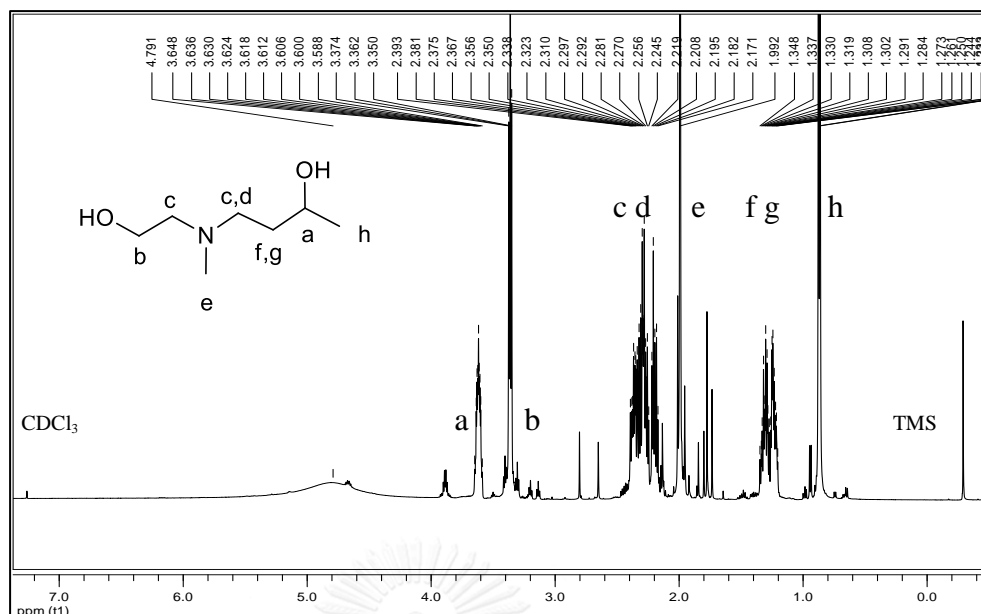


**Figure 4.26** <sup>1</sup>H-NMR (500 MHz, CDCl<sub>3</sub>) spectrum of 4-((2-hydroxyethyl)(methyl)amino)-2-butanol (HEMAB).

**Table 4.11** <sup>1</sup>H-NMR data of 4-((2-hydroxyethyl)(methyl)amino)-2-butanol (HEMAB).

$\delta$ (ppm)	type of proton, number of proton, position
3.65-3.59	m, 1H, (a)
3.37-3.35	t, 2H, $J = 6$ Hz, (b)
2.39-2.24	m, 3H, (c)
2.22-2.17	m, 1H, (d)
1.99	s, 3H, (e)
1.35-1.27	m, 1H, (f)
1.26-1.20	m, 1H, (g)
0.88-0.86	d, 3H, $J = 6$ Hz (h)

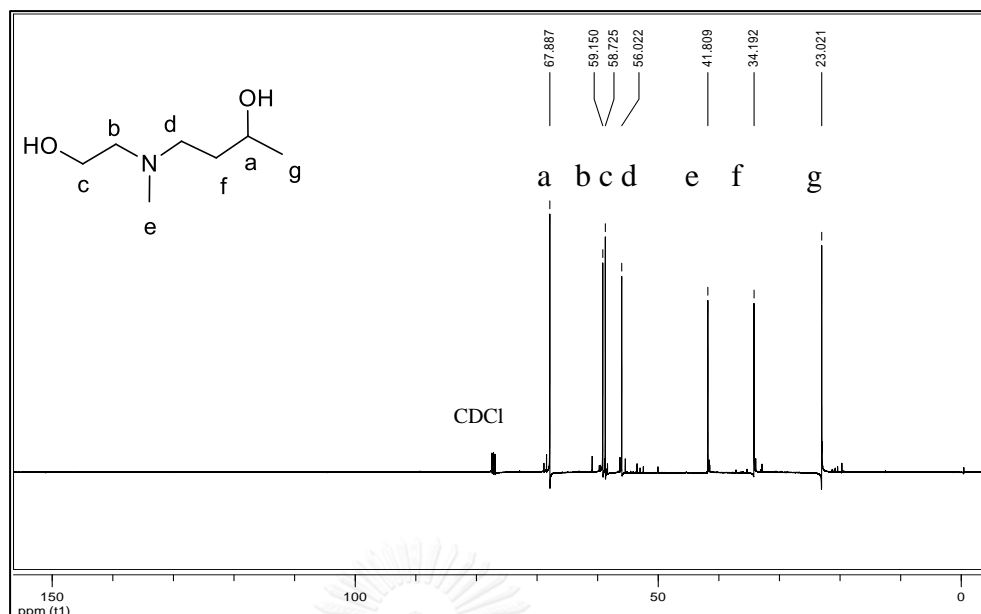


**Figure 4.27** <sup>13</sup>C-NMR (125 MHz, CDCl<sub>3</sub>) spectrum of 4-((2-hydroxyethyl)(methyl)amino)-2-butanol (HEMAB).

**Table 4.12** <sup>13</sup>C-NMR data of 4-((2-hydroxyethyl)(methyl)amino)-2-butanol (HEMAB).

δ (ppm)	type of carbon, position
67.89	d, (a)
59.15	t, (b)
58.72	t, (c)
56.02	t, (d)
41.81	t, (e)
34.19	t, (f)
23.02	q, (g)

Figures 4.28 and 4.29 show the GC-MS chromatogram and mass spectrum of HEMAB, respectively. The GC retention time of the compound was found at 9.1 min with the purity of 80.5 %. The mass spectrum pattern of the compound was found to be in excellent agreement with the GC-MS chromatogram, thus confirming the compound's chemical formula ( $C_7H_{17}NO_2$ ) and 147 molecular weight.

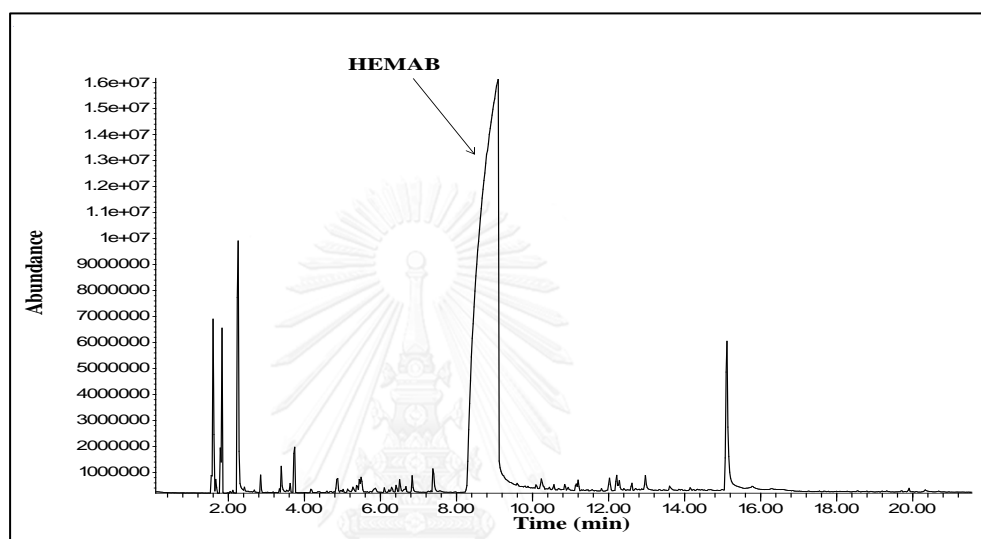


**Figure 4.28** GC-MS chromatogram of 4-((2-hydroxyethyl)(methyl)amino)-2-butanol (HEMAB).



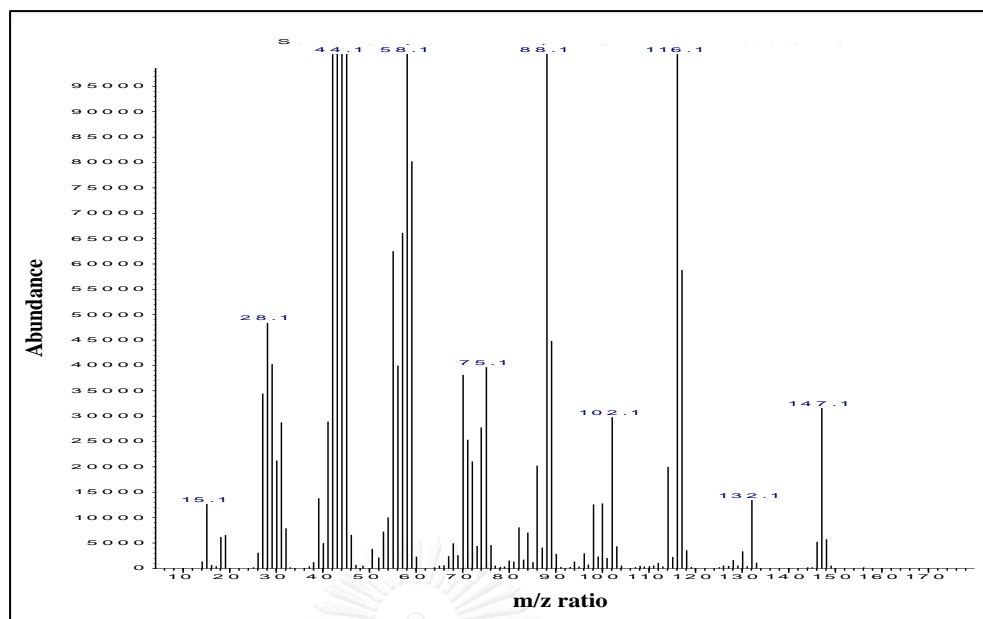
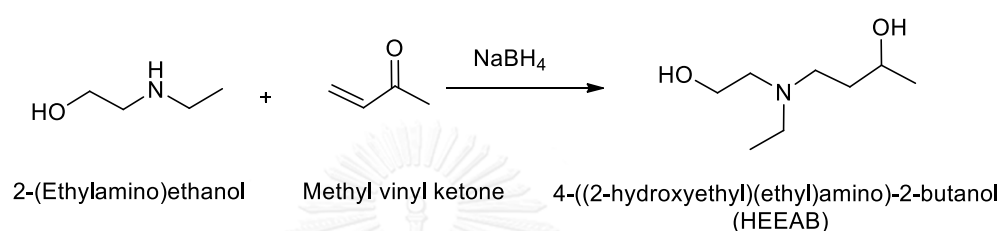


**Figure 4.29** Mass spectrum of 4-((2-hydroxyethyl)(methyl)amino)-2-butanol (HEMAB).

#### 4.1.6 Synthesis of 4-((2-hydroxyethyl)(ethyl)amino)-2-butanol (HEEAB)

Compound HEEAB was synthesized by the Michael addition reaction, following procedures given in the literature [27]. The synthesis of HEEAB was attempted by starting with 2-(ethylamino)ethanol and methyl vinyl ketone (MVK). After workup and distillation, the compound was obtained as a yellowish liquid in 54.35 % yield as shown in Scheme 4.7.



**Scheme 4.7** Synthesis route of 4-((2-hydroxyethyl)(ethyl)amino)-2-butanol (HEEAB).

The chemical structure and purity of compound HEEAB was identified by ATR-IR, <sup>1</sup>H and <sup>13</sup>C-NMR, and GC-MS, respectively. According to the infrared spectrum, the absorption bands were shown at 3320 cm<sup>-1</sup> (OH stretching), 2963 cm<sup>-1</sup> (CH<sub>2</sub> asymmetric stretching), 2923 cm<sup>-1</sup> (CH<sub>3</sub> asymmetric stretching), 2870 cm<sup>-1</sup> (CH<sub>3</sub> symmetric stretching), 2827 cm<sup>-1</sup> (CH<sub>2</sub> symmetric stretching), 1458 cm<sup>-1</sup> (CH<sub>2</sub> bending), 1369 cm<sup>-1</sup> (CH<sub>3</sub> bending), and 1046 cm<sup>-1</sup> (CN stretching). The infrared spectrum of DPAB is shown in Figure 4.30.

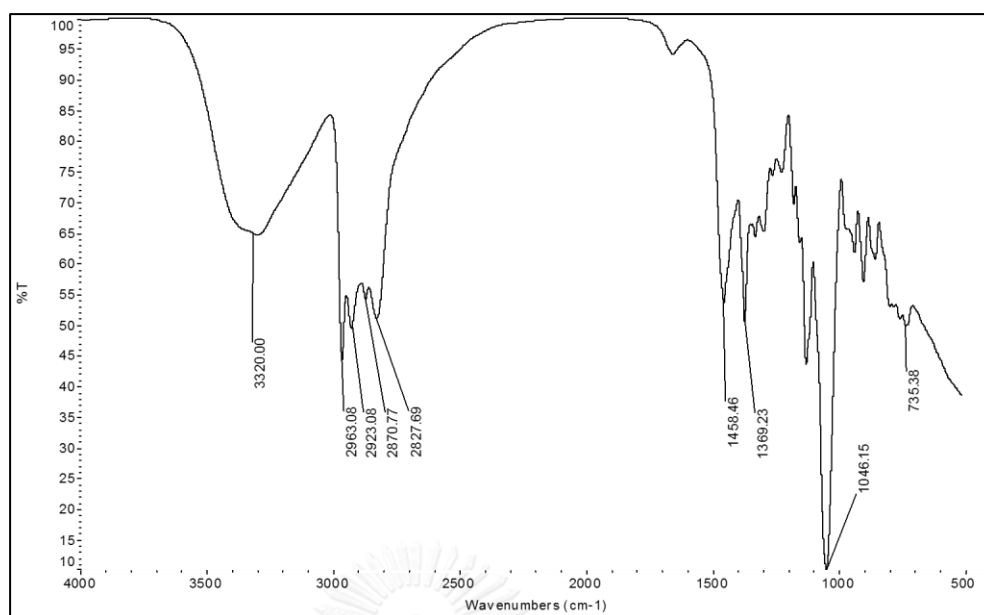


**Figure 4.30** FT-IR spectrum of 4-((2-hydroxyethyl)(ethyl)amino)-2-butanol (HEEAB).

The chemical structure of HEEAB was also identified by <sup>1</sup>H and <sup>13</sup>C-NMR as shown in Figures 4.31 and 4.32, respectively. Tables 4.13 and 4.14 list the chemical shifts for the corresponding hydrogen and carbon atoms, respectively.

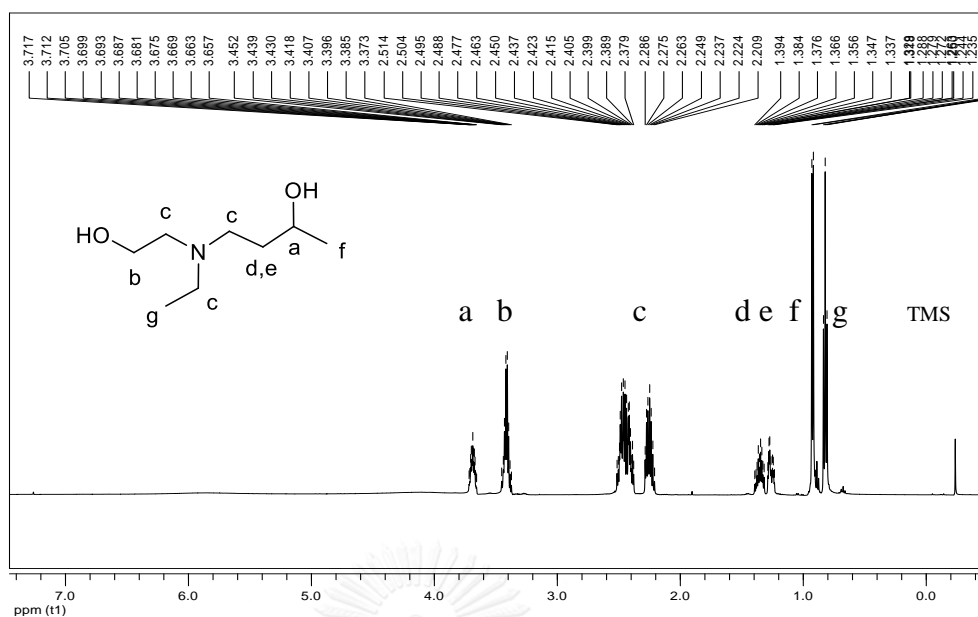


**Figure 4.31** <sup>1</sup>H-NMR (500 MHz, CDCl<sub>3</sub>) spectrum of 4-((2 hydroxyethyl)(ethyl)amino)-2-butanol (HEEAB).

**Table 4.13** <sup>1</sup>H-NMR data of 4-((2 hydroxyethyl)(ethyl)amino)-2-butanol (HEEAB).

δ (ppm)	type of proton, number of proton, position
3.72-3.66	m, 1H, (a)
3.45-3.37	q, 2H, $J = 6$ Hz, (b)
2.51-2.21	m, 6H, (c)
1.39-1.32	m, 1H, (d)
1.29-1.23	m, 1H, (e)
0.93-0.92	d, 3H, $J = 6$ Hz, (f)
0.84-0.81	t, 3H, $J = 7.5$ Hz, (g)

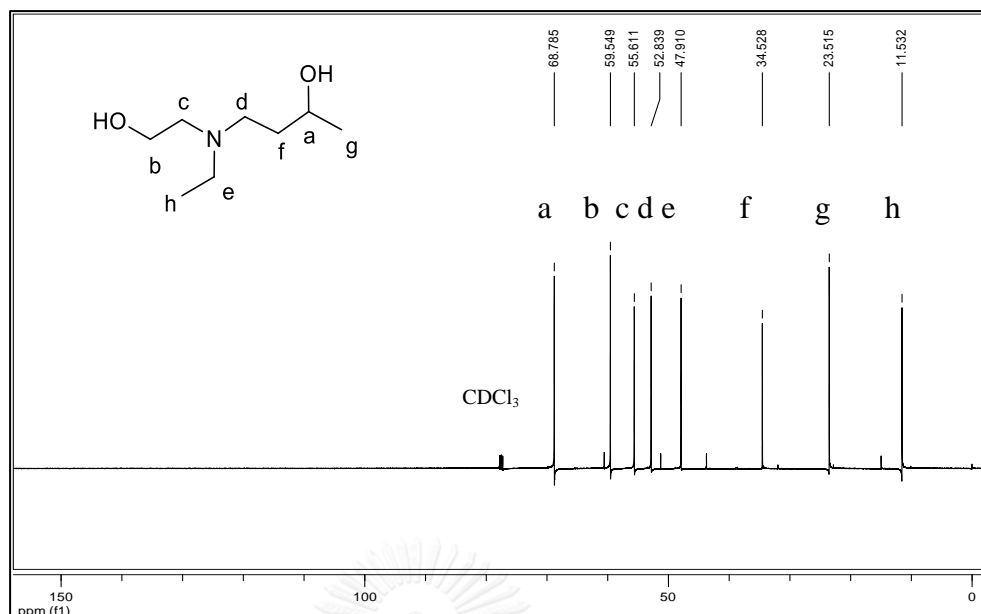


**Figure 4.32**  $^{13}\text{C}$ -NMR (125 MHz,  $\text{CDCl}_3$ ) spectrum of 4-((2-hydroxyethyl)(ethyl)amino)-2-butanol (HEEAB).

**Table 4.14**  $^{13}\text{C}$ -NMR data of 4-((2 hydroxyethyl)(ethyl)amino)-2-butanol (HEEAB).

$\delta$ (ppm)	type of carbon, position
68.79	d, (a)
59.55	t, (b)
55.61	t, (c)
52.84	t, (d)
47.91	t, (e)
34.53	t, (f)
23.51	q, (g)
11.53	q, (h)

Figures 4.33 and 4.34 illustrate the GC-MS chromatogram and mass spectrum of HEMAB, respectively. The GC retention time of the compound was found at 9.8 min with the purity of 94 %. The mass spectrum pattern of the compound was found

to be in excellent agreement with the GC-MS chromatogram, thus confirming the compound's chemical formula ( $C_8H_{19}NO_2$ ) and 161 molecular weight.

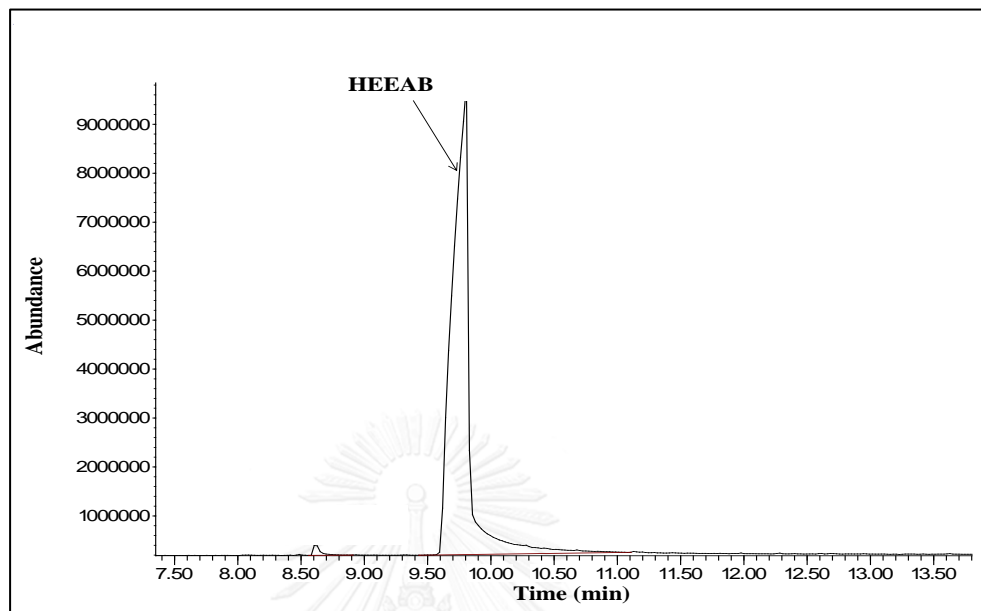


**Figure 4.33** GC-MS chromatogram of 4-((2-hydroxyethyl)(ethyl)amino)-2-butanol (HEEAB).

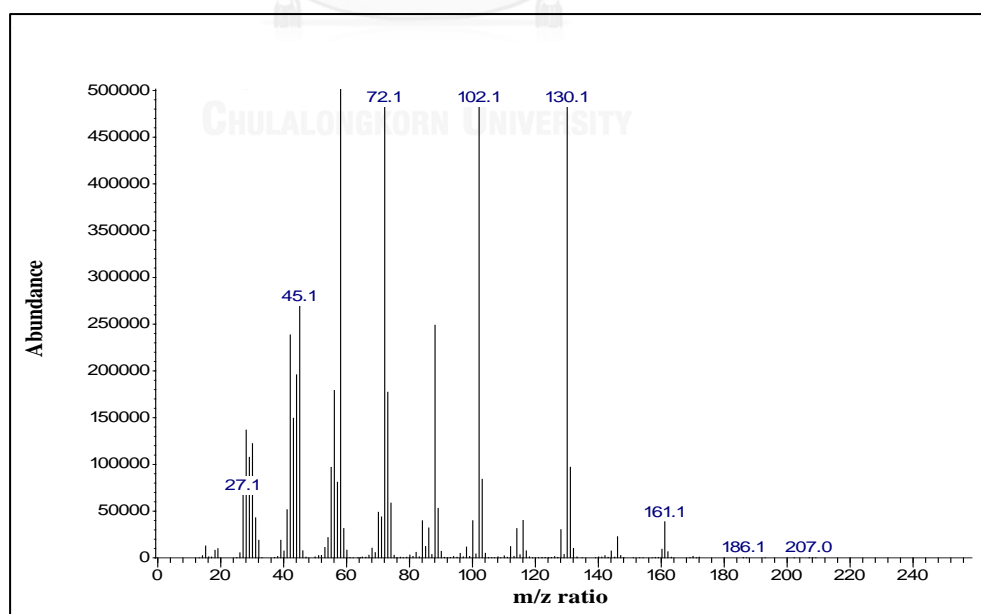


**Figure 4.34** Mass spectrum of 4-((2-hydroxyethyl)(ethyl)amino)-2-butanol (HEEAB).

## 4.2 Preparation of aqueous amine solution

Prior to all tests, the solubility of the newly synthesized amines in deionized water were also observed under 298-353 K which was the temperature range used in all tests in this study. This was done to ensure that the 2 M concentration solution needed for all experiments was dissolved completely in deionized water, thus preventing phase separation problem at a high temperature operation. Table 4.15 summarizes the solubility of DMAB, DPAB, DBAB, HEMAB, and HEEAB at various temperatures based on visual observation. DEAB and MDEA were also included for comparison. DMAB, HEMAB, HEEAB, DEAB, and MDEA were completely soluble in water. Thus, water was sufficient and used only to prepare aqueous solution of these amines for all subsequent tests. On the other hand, the separation of two phases (i.e. organic and aqueous layers) triggered by reduced solubility occurred for DPAB and DBAB containing longer di-alkyl chain being propyl (-CH<sub>2</sub>CH<sub>2</sub>CH<sub>3</sub>) and butyl (-CH<sub>2</sub>CH<sub>2</sub>CH<sub>2</sub>CH<sub>3</sub>), respectively. Therefore, to effectively measure CO<sub>2</sub> solubility of DPAB and DBAB, water and methanol mixture (of 1 to 2 ratio) was used to completely mix the amines to the desired 2 M concentration for the tests.

**Table 4.15** Molecular weight and solubility of amines at 2 M in deionized water at different temperatures.

Amines	Molecular weight (g/mol)	Deionized water			
		298 K	313 K	333 K	353 K
DMAB	117	+++	+++	+++	+++
DPAB	173	-	+	++	++
DBAB	201	-	-	+	+
HEMAB	147	++	+++	+++	+++
HEEAB	161	++	+++	+++	+++
MDEA	119	+++	+++	+++	+++
DEAB	145	+++	+++	+++	+++

+++ : completely soluble

++ : nearly soluble

+ : partially soluble

- : separate into two layers

### 4.3 CO<sub>2</sub> equilibrium solubility and cyclic capacity in aqueous amine solutions

Before measuring CO<sub>2</sub> equilibrium solubility of amines, the experiments were validated with 2 M MDEA and DEAB at 313 K and 3 to 100 kPa CO<sub>2</sub> partial pressure by comparing with literature values as shown in Figure 4.35. The results were in good agreement with previously reported data of Sema et al., and Benamor and Aroua [26, 65] with an absolute average deviation (% AAD) of 5.47 % and 4.23 %, respectively for MDEA and DEAB. The repeatability in terms of standard deviation based on three repeated runs was found to be less than 0.5 %. Therefore, the equipment and procedures for this study are considered to be properly applicable for measuring the equilibrium solubility of CO<sub>2</sub>.

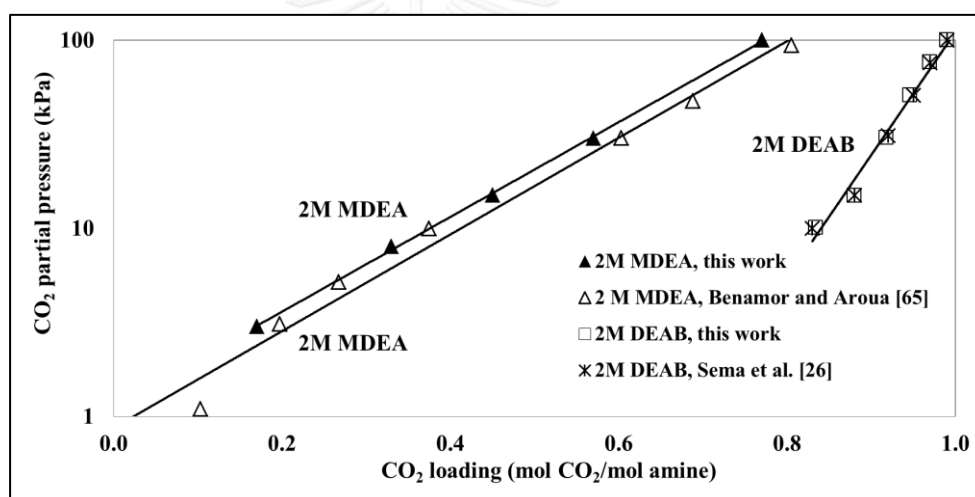


**Figure 4.35** Validation of CO<sub>2</sub> equilibrium solubility in the aqueous solutions of 2 M MDEA and 2 M DEAB solutions at 313 K by comparing with Sema et al., and Benamor and Aroua.

The equilibrium loading at 298, 313, 333, and 353 K, and cyclic capacity of DMAB, DPAB, DBAB, HEMAB, HEEAB, MDEA, and DEAB are summarized respectively in Tables 4.16-4.22. The amines' plots of CO<sub>2</sub> partial pressures and the equilibrium loadings at 298, 313, 333 and 353 K corresponding to the data in Tables 4.16-4.22 are also given in Figures 4.36-4.39, respectively.



**Table 4.16** Equilibrium solubility and cyclic capacity of CO<sub>2</sub> in 2 M aqueous DMAB solution.

CO <sub>2</sub> partial pressure (kPa)	298 K	313 K	333 K	353 K	Cyclic capacity 313-353 K
	CO <sub>2</sub> loading [mol CO <sub>2</sub> /mol amine]				
3	0.82	0.67	0.32	0.20	0.47
8	0.88	0.79	0.42	0.32	0.47
15	0.90	0.88	0.53	0.36	0.52
30	0.92	0.90	0.60	0.49	0.41
100	0.98	0.93	0.71	0.65	0.28

**Table 4.17** Equilibrium solubility and cyclic capacity of CO<sub>2</sub> in 2 M aqueous DPAB solution.

CO <sub>2</sub> partial pressure (kPa)	298 K	313 K	333 K	353 K	Cyclic capacity 313-353 K
	CO <sub>2</sub> loading [mol CO <sub>2</sub> /mol amine]				
3	0.11	0.05	0.03	0.02	0.03
8	0.27	0.07	0.05	0.02	0.05
15	0.41	0.12	0.08	0.02	0.10
30	0.50	0.18	0.12	0.03	0.15
100	0.56	0.25	0.18	0.04	0.21

**Table 4.18** Equilibrium solubility and cyclic capacity of CO<sub>2</sub> in 2 M aqueous DBAB solution.

CO <sub>2</sub> partial pressure (kPa)	298 K	313 K	333 K	353 K	Cyclic capacity 313-353 K
	CO <sub>2</sub> loading [mol CO <sub>2</sub> /mol amine]				
3	0.13	0.01	0.01	0.01	0.00
8	0.20	0.01	0.01	0.01	0.00
15	0.24	0.02	0.02	0.02	0.00
30	0.31	0.03	0.02	0.02	0.01
100	0.35	0.04	0.04	0.03	0.01

**Table 4.19** Equilibrium solubility and cyclic capacity of CO<sub>2</sub> in 2 M aqueous HEMAB solution.

CO <sub>2</sub> partial pressure (kPa)	298 K	313 K	333 K	353 K	Cyclic capacity 313-353 K
	CO <sub>2</sub> loading [mol CO <sub>2</sub> /mol amine]				
3	0.43	0.29	0.18	0.05	0.24
8	0.62	0.40	0.21	0.14	0.26
15	0.70	0.44	0.26	0.18	0.26
30	0.76	0.55	0.37	0.29	0.26
100	0.91	0.66	0.62	0.46	0.20

**Table 4.20** Equilibrium solubility and cyclic capacity of CO<sub>2</sub> in 2 M aqueous HEEAB solution.

CO <sub>2</sub> partial pressure (kPa)	298 K	313 K	333 K	353 K	Cyclic capacity 313-353 K
	CO <sub>2</sub> loading [mol CO <sub>2</sub> /mol amine]				
3	0.61	0.52	0.22	0.10	0.42
8	0.79	0.65	0.33	0.24	0.41
15	0.84	0.68	0.39	0.28	0.40
30	0.91	0.79	0.53	0.38	0.41
100	0.95	0.88	0.68	0.53	0.35

**Table 4.21** Equilibrium solubility and cyclic capacity of CO<sub>2</sub> in 2 M aqueous MDEA solution.

CO <sub>2</sub> partial pressure (kPa)	298 K	313 K	333 K	353 K	Cyclic capacity 313-353 K
	CO <sub>2</sub> loading [mol CO <sub>2</sub> /mol amine]				
3	0.39	0.17	0.08	0.02	0.15
8	0.51	0.33	0.14	0.05	0.28
15	0.57	0.45	0.18	0.09	0.36
30	0.71	0.57	0.25	0.17	0.40
100	0.83	0.77	0.50	0.25	0.52

**Table 4.22** Equilibrium solubility and cyclic capacity of CO<sub>2</sub> in 2 M aqueous DEAB solution.

CO <sub>2</sub> partial pressure (kPa)	298 K	313 K	333 K	353 K	Cyclic capacity 313-353 K
	CO <sub>2</sub> loading [mol CO <sub>2</sub> /mol amine]				
3	0.83	0.68	0.35	0.32	0.36
8	0.88	0.77	0.43	0.37	0.40
15	0.91	0.85	0.58	0.44	0.41
30	0.94	0.89	0.77	0.55	0.34
100	0.97	0.94	0.85	0.71	0.23



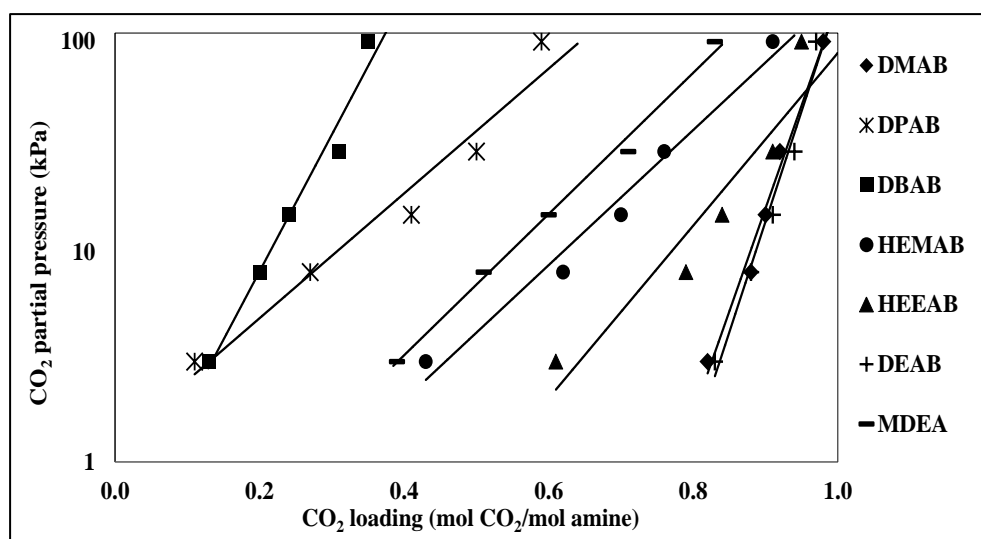


**Figure 4.36** Equilibrium solubility of CO<sub>2</sub> in 2 M DMAB, DPAB, DBAB, HEMAB, HEEAB, DEAB and MDEA solution at 298 K (solid lines are trend lines).

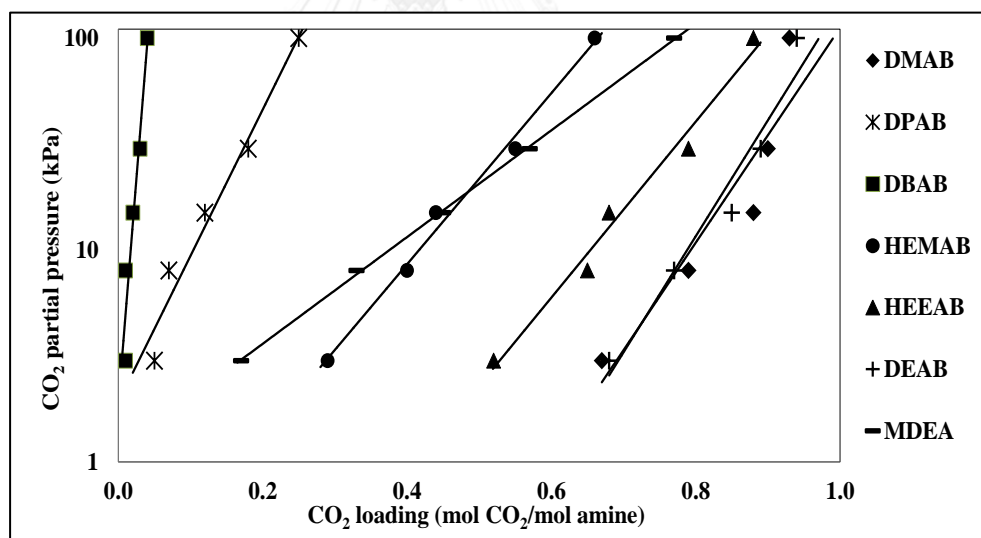


**Figure 4.37** Equilibrium solubility of CO<sub>2</sub> in 2 M DMAB, DPAB, DBAB, HEMAB, HEEAB, DEAB and MDEA solution at 313 K (solid lines are trend lines).

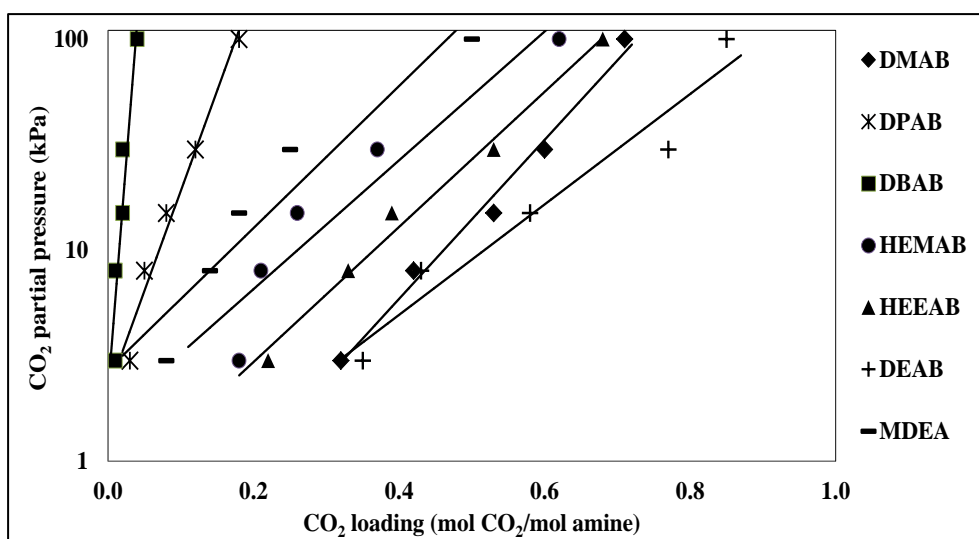


**Figure 4.38** Equilibrium solubility of CO<sub>2</sub> in 2 M DMAB, DPAB, DBAB, HEMAB, HEEAB, DEAB and MDEA solution at 333 K (solid lines are trend lines).

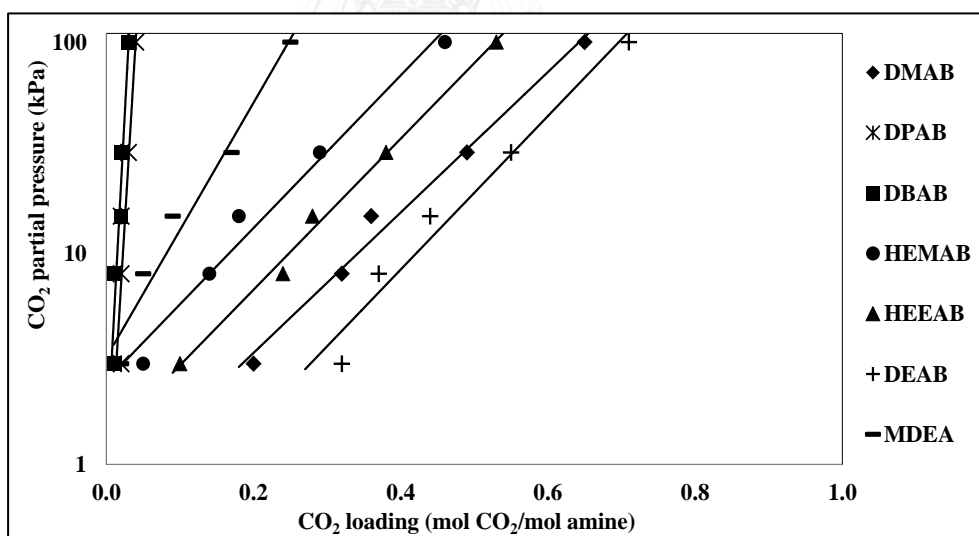


**Figure 4.39** Equilibrium solubility of CO<sub>2</sub> in 2 M DMAB, DPAB, DBAB, HEMAB, HEEAB, DEAB and MDEA solution at 353 K (solid lines are trend lines).

In Figure 4.36, DMAB showed the highest equilibrium absorption of CO<sub>2</sub> among the new amines synthesized in this study. The amine's loading between 0.11-0.98 mol/mol amine obtained from 3-100 kPa range was even comparable to our previously developed DEAB. For all partial pressures, HEEAB and HEMAB showed the second and third highest equilibrium loading in ranges of 0.61-0.95 and 0.43-0.91 mol/mol amine, respectively. In addition, DMAB, HEMAB and HEEAB were all superior to MDEA for CO<sub>2</sub> loading absorption capacity. Based on structural analysis, the new amines were categorized into two groups consisting of di-alkyl (i.e. DMAB, DPAB and DBAB) and hydroxy-alkyl-alkyl-amino-2-butanols (i.e. HEMAB and HEEAB). Specifically, the least sterically hindered DMAB, which contained the shortest alkyl chain length, provided the least electron donating effect. The amine could still allow the CO<sub>2</sub> absorption to occur more easily as shown by its high CO<sub>2</sub> loading capacity. Though, DEAB structure can potentially induce electron density around its nitrogen atom better based its longer di-ethyl group structure. This effect was not significant and probably overcome by its own steric effect, thus preventing DEAB's CO<sub>2</sub> absorption ability to surpass that of DMAB.

In the case of the hydroxy-alkyl-alkyl substituted amines, HEMAB and HEEAB could benefit from both hydroxy-alkyl (-ROH) and methyl/ethyl groups in the molecule. Firstly, the presence of more hydroxyl (-OH) groups increased the amine solubility in water. In addition, the electron-donating ability of the amines could be enhanced by their alkyl groups. By comparing the equilibrium solubility of CO<sub>2</sub>, HEEAB benefited fully from these properties that allowed more CO<sub>2</sub> to be taken compared to HEMAB. This was due to the presence of a better electron-donating ethyl group that increased the electron density of the amine structure. Thus, this likely made HEEAB more basic and absorb CO<sub>2</sub> better than HEMAB without suffering from the steric hindrance effect as shown earlier in the di-alkyl substituted amines.

For DPAB and DBAB, these amines contained even longer alkyl chains of di-propyl and di-butyl groups, respectively in the structure. As a result, steric effect induced by such a long alkyl length probably dominated and prevented the amines from performing as well as the baseline DEAB solvent. The bulkier structure also prevented the amines from reaching a higher CO<sub>2</sub> loading as seen in the hydroxy-

alkyl-alkyl substituted amines. This is evident from Figures 4.36-4.39 where the DPAB and DBAB's equilibrium CO<sub>2</sub> loading trend lines were placed at the most left of the graph. Also, DPAB and DBAB's poor solubility in deionized water showed a problematic phase separation even at low concentrations. To allow their CO<sub>2</sub> loading property to be evaluated, methanol mixed with water at a ratio of 2:1 M even had to be used. Due to these shortcomings, DPAB and DBAB were dropped out from further tests. It is also worth mentioning that the equilibrium solubility of CO<sub>2</sub> of di-alkyl substituted amines (i.e. DMAB and DEAB) was superior to that of the hydroxy-alkyl-alkyl substituted amines (i.e. HEMAB and HEEAB). This implied that having a proper di-alkyl group in the amine structure could promote the CO<sub>2</sub> equilibrium solubility more effectively than the hydroxy-alkyl-alkyl group *via* its electron donating ability.

Similar trends were still observed for all amines when the equilibrium loading was measured at 313, 333 and 353 K shown in Figures 4.37, 4.38 and 4.39, respectively. Equilibrium CO<sub>2</sub> loading of DMAB was still the highest between the new amines at both temperatures. Its loading was still comparable to DEAB at 313 K. However, the loading was reduced but insignificantly, to become less than that of DEAB at 333 and 353 K. HEEAB still remained the second highest amine in terms of the CO<sub>2</sub> equilibrium solubility followed by HEMAB, DPAB, and DBAB. DMAB, HEEAB, and HEMAB still gave a higher CO<sub>2</sub> loading at equilibrium condition than that of MDEA. Similar explanation given at 298 K for relationship of structure of the amines and their corresponding equilibrium CO<sub>2</sub> loadings could be used for 313, 333 and 353 K data.

In terms of cyclic capacity calculated as a difference between loadings at 353 and 313 K, the results suggested that a shorter chained DMAB possessed the highest cyclic capacity (i.e. 0.47-0.52 mol/mol amine between 3-15 kPa CO<sub>2</sub>) among the newly synthesized di-alkyl substituted amines (i.e. DPAB and DBAB). The capacity was also within the same range as that of DEAB. For HEMAB and HEEAB, though these amines showed moderate equilibrium CO<sub>2</sub> loadings as discussed previously. Their cyclic capacity, specifically that of HEEAB was high and also close to that of DEAB ranging between 0.40 and 0.42 mol/mol amine. Having a high cyclic capacity



implied that CO<sub>2</sub> was also easy to be removed from DMAB, HEEAB and DEAB at a higher temperature. Therefore, use of these amines in a real capture process could potentially lead to an operational cost saving during the regeneration process which have been also confirmed with the measurement of regeneration kinetic rate and heat input detailed later in Section 4.6. The relationship between equilibrium solubility of CO<sub>2</sub> and the cyclic capacities for all amines is also shown in Figure 4.40. Considering these 2 parameters, DMAB, HEMAB, and HEEAB showed a greater potential than the rest of amines in terms of high absorption capacity and high cyclic capacity. Thus, only these amines were selected for further evaluation.

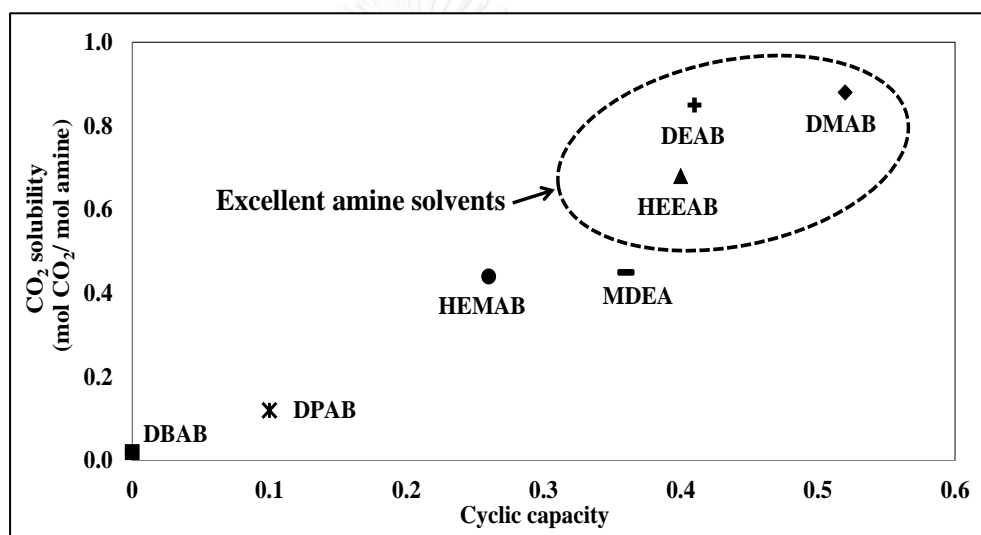
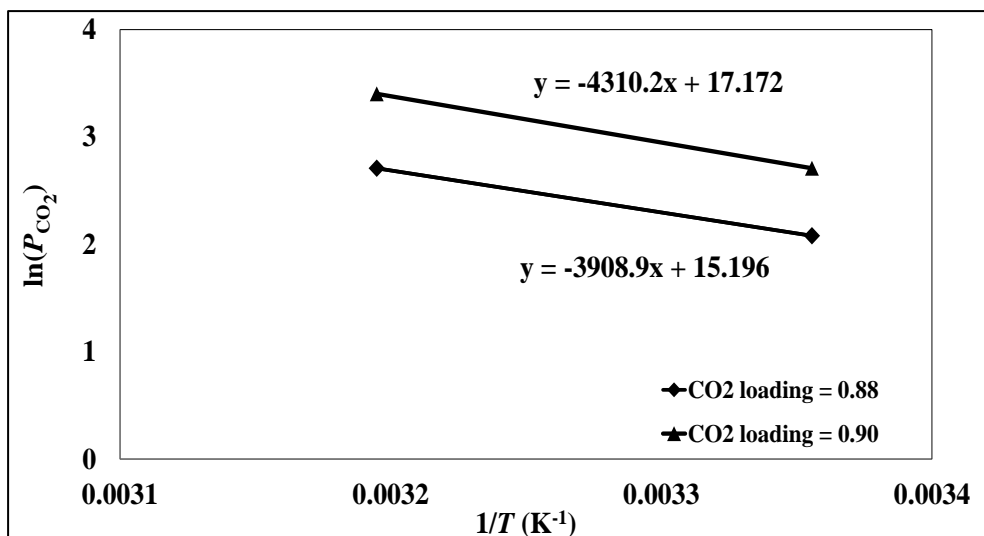


**Figure 4.40** The relationship between CO<sub>2</sub> solubility at temperature at 313 K, 15 kPa CO<sub>2</sub> partial pressure and cyclic capacity at different temperatures (313-353 K) of seven amines (DMAB, DPAB, DBAB, HEMAB, HEEAB, MDEA and DEAB).

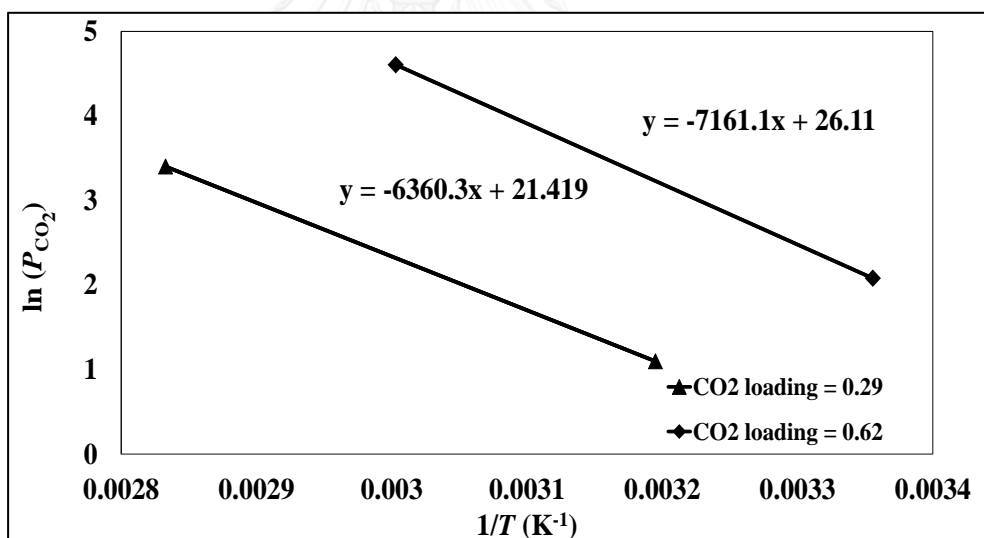
#### 4.4 Heat of CO<sub>2</sub> absorption in aqueous amine solutions

Table 4.23 summarizes the heat of CO<sub>2</sub> absorption of DMAB, HEMAB, and HEEAB estimated based on the Gibbs-Helmholtz equation. MDEA and DEAB were also measured and included in the table as base solvents for comparison. For DMAB, plots of  $\ln P_{\text{CO}_2}$  and  $1/T$  using 3, 8, 15, 30 and 100 kPa CO<sub>2</sub> partial pressure and 298-353 K data at 2 or 3 equilibrium CO<sub>2</sub> loadings between 0.88 and 0.90 are shown in Figure 4.41. The average slope found from the 2 plots was -4109.6 K which was correspondent to -34.17 kJ/mol heat of CO<sub>2</sub> absorption, with a 6.9 % error in terms of standard deviation (SD). Similar plots shown in Figure 4.41 for DMAB were generated to determine the heat of CO<sub>2</sub> absorption of HEMAB, HEEAB, MDEA, and DEAB, respectively given in Figures 4.42-4.45. Calculations of the heat of CO<sub>2</sub> absorption based on averaged slopes gave -69.79 (13.7 % SD), -59.76 (5.9 % SD), -56.21 (8.4 % SD), and -55.86 (7.5 % SD) kJ/mol for HEEAB, DEAB, HEMAB, and MDEA respectively. DMAB had the lowest absorption heat among the new amines. Its heat of CO<sub>2</sub> absorption was also comparable to that of MDEA and DEAB possibly due to the short chained structure. This was also consistent with the work of Chowdhury et al. [78] confirming the existence of the methyl and ethyl groups in the amine structure helping to decrease the heat of reaction but enhance the initial absorption rate and absorption capacity.

The same explanation used for DMAB holds true for hydroxy-alkyl-alkyl substituted amines. Though not to the extent of DMAB (with di-methyl), HEMAB could probably benefit still from its single methyl substituent, thus giving 20 % less heat of CO<sub>2</sub> absorption that of HEEAB with one ethyl chain in the structure.



**Figure 4.41** Plot of  $\ln P_{\text{CO}_2}$  and  $1/T$  of 2 M DMAB (solid lines are trend lines).



**Figure 4.42** Plot of  $\ln P_{\text{CO}_2}$  and  $1/T$  of 2 M HEMAB (solid lines are trend lines).

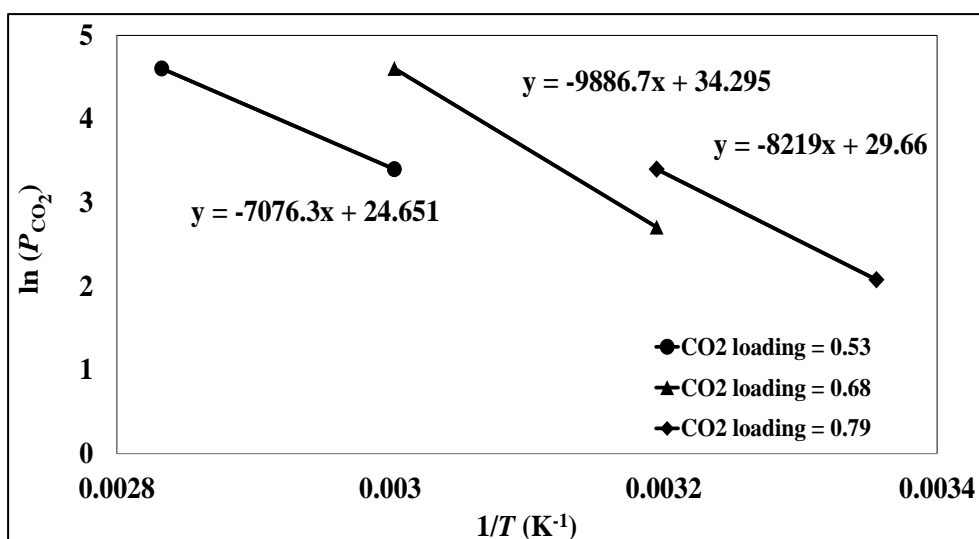


**Figure 4.43** Plot of  $\ln P_{\text{CO}_2}$  and  $1/T$  of 2 M HEEAB (solid lines are trend lines).

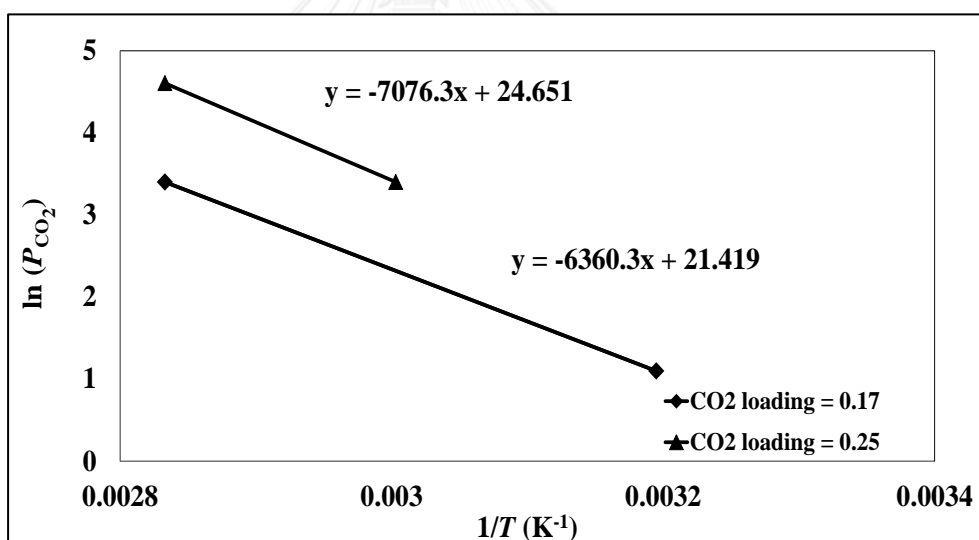


**Figure 4.44** Plot of  $\ln P_{\text{CO}_2}$  and  $1/T$  of 2 M MDEA (solid lines are trend lines)

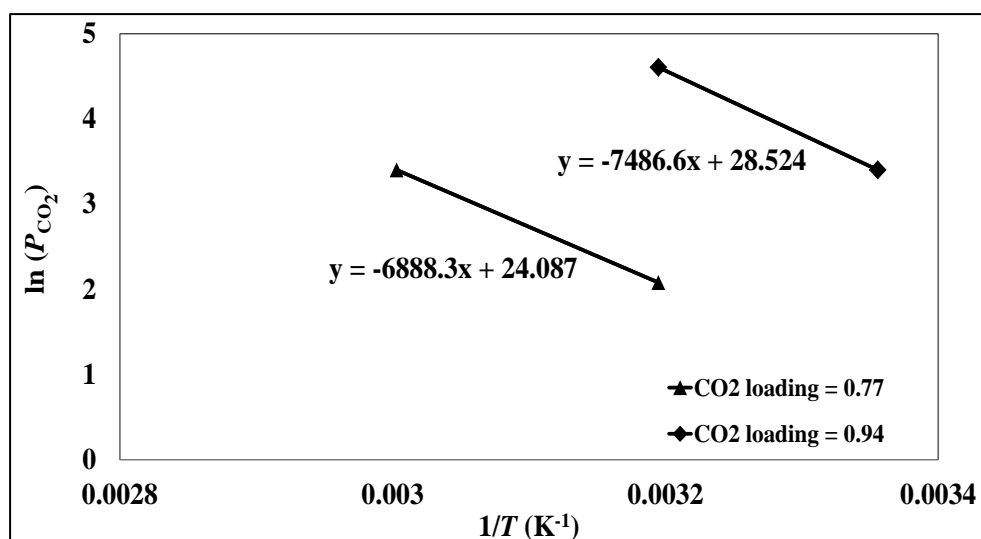


**Figure 4.45** The plot of  $\ln P_{\text{CO}_2}$  and  $1/T$  of 2 M DEAB (solid lines are trend lines).

**Table 4.23** Heat of  $\text{CO}_2$  absorption,  $\text{CO}_2$  absorption rate,  $\text{pK}_a$ ,  $\text{CO}_2$  regeneration rate and heat input for regeneration in aqueous solutions of DMAB, HEMAB and HEEAB compared with MDEA and DEAB.

Amine	Heat of $\text{CO}_2$ absorption, $\Delta H_{\text{abs}}$ (kJ/mol $\text{CO}_2$ )		$\text{CO}_2$ absorption rate at 313 K (mol $\text{CO}_2$ /min)	$\text{pK}_a$		$\text{CO}_2$ regeneration rate at 363 K (mol $\text{CO}_2$ /min)	Heat input for regeneration (kJ/mol $\text{CO}_2$ )
	estimated	experimental		experimental	literature		
MEA	-84.3 <sup>a</sup>	-82 <sup>d</sup>	N/A	N/A	11.12 <sup>f</sup>	N/A	N/A
DEA	-66.9 <sup>b</sup>	-69 <sup>d</sup>	N/A	N/A	8.89 <sup>g</sup>	N/A	N/A
MDEA	-54.6 <sup>c</sup>	-49 <sup>d</sup>	N/A	N/A	8.65 <sup>h</sup>	N/A	N/A
DEAB	-63.4 <sup>e</sup>	N/A	N/A	N/A	10.4 <sup>f</sup>	N/A	N/A
MDEA (this work)	-55.86	N/A	0.063	8.62	N/A	0.220	56.59
DEAB (this work)	-59.76	N/A	0.088	10.16	N/A	0.243	54.37
DMAB (this work)	-34.17	N/A	0.082	9.38	N/A	0.512	39.73
HEMAB (this work)	-56.21	N/A	0.111	9.15	N/A	0.452	60.48
HEEAB (this work)	-69.79	N/A	0.142	9.81	N/A	0.295	72.44

<sup>a</sup> Estimated values are obtained from Kim and Svendsen [68]

<sup>b</sup> Estimated values are obtained from Lee et al. [70]

<sup>c</sup> Estimated values are obtained from Rho et al. [69]

<sup>d</sup> Estimated values are obtained from Carson et al. [71]

<sup>e</sup> Estimated values are obtained from Sema et al. [47]

<sup>f</sup> Estimated values are obtained from Shi et al. [74]

<sup>g</sup> Estimated values are obtained from Silva et al. [79]

<sup>h</sup> Estimated values are obtained from Chowdhury et al. [80]

#### 4.5 CO<sub>2</sub> absorption rate in aqueous amine solutions

The CO<sub>2</sub> loading versus time plots at 313 K of 2 M DMAB, HEMAB and HEEAB compared to MDEA and DEAB, are shown in Figure 4.46. Their corresponding absorption rates calculated from the slopes are also summarized in Table 4.23. It was clear that the rate of CO<sub>2</sub> absorption at 313 K was largely affected by the amine structure showing an increase in the order of 0.063, 0.082, 0.088, 0.111 and 0.142 mol CO<sub>2</sub>/min for MDEA, DMAB, DEAB, HEMAB and HEEAB, respectively. By comparing the CO<sub>2</sub> absorption rate within the group of di-alkyl substituted amines, DEAB showed a slightly higher absorption rate than that of DMAB. This was probably due to the influence of a better electron-donating group of DEAB which also dominated over its own steric effect. Even though DMAB showed a slightly less absorption rate, it still absorbed CO<sub>2</sub> moderately faster than the conventional MDEA.

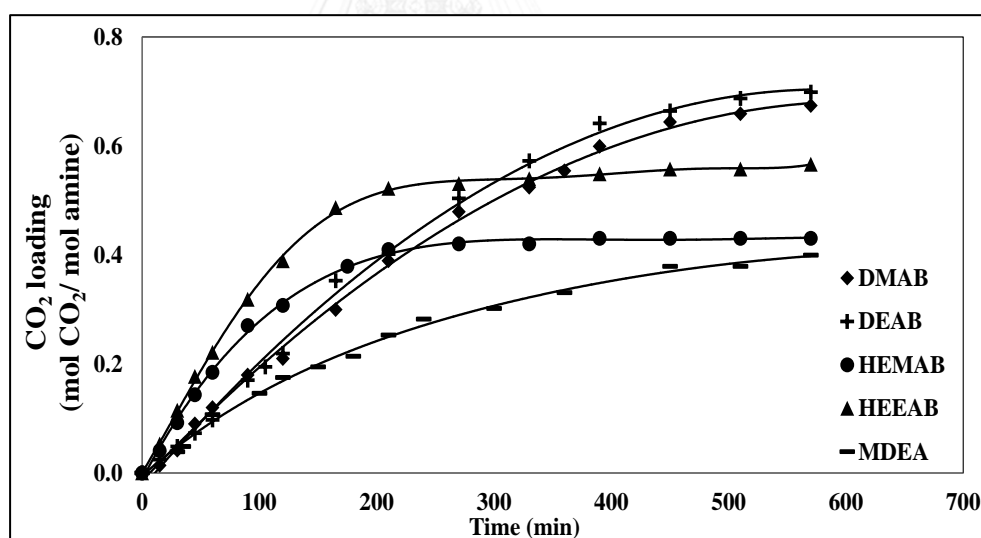
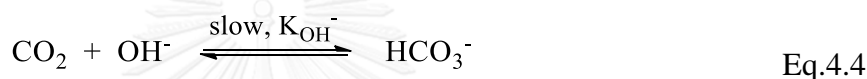
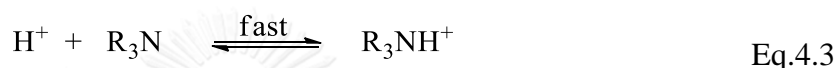
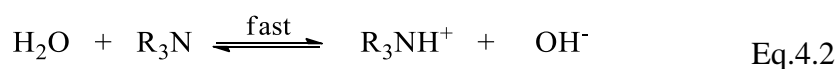
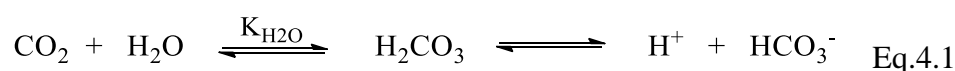


**Figure 4.46** CO<sub>2</sub> loading as a function of time for five amines (DMAB, HEMAB, HEEAB, MDEA and DEAB) at temperature of 313 K.

In the case of the group of hydroxy-alkyl-alkyl substituted amines, HEMAB and HEEAB both showed an excellent enhancement of the absorption with the rates one to two folds higher than that of DMAB, DEAB, and MDEA. In addition to

electron donating ability within this group of amines, having an extra -OH group could have been a factor in boosting up the absorption rate of HEMAB and HEEAB. The presence of more -OH groups likely increased the ability for water to solvate the amine molecule which was essential in CO<sub>2</sub> absorption reactions shown in Equations 4.1-4.4 [52, 74, 81, 82].



Chemical structure containing an extra -OH group *via* hydroxy-alkyl-alkyl substituted amines such as in HEMAB and HEEAB molecules could have allowed these amines to easily come in contact with water, thus enhancing the reaction rates of Equations 4.2 and 4.3. This extra push possibly helped the absorption mechanism to quickly produce OH<sup>-</sup> and R<sub>3</sub>NH<sup>+</sup> necessary for driving the absorption reactions, thus, contributing to a faster overall absorption rate.

Dissociation constant measured as pK<sub>a</sub> values is indicated to be very important for a compound's basicity for the interpretation of the kinetic mechanism of amines such as absorption rate. In this work, the pK<sub>a</sub> values of all amines were experimentally measured at 296.5 K as also shown in Table 4.23. The pK<sub>a</sub> values increased from 8.62 to 9.15, 9.38, 9.81 and 10.16 for MDEA, HEMAB, DMAB, HEEAB and DEAB, respectively. By comparing the pK<sub>a</sub> values within the same amine group, the pK<sub>a</sub> values of HEEAB were higher than that of HEMAB due to a better electron donating ethyl group, helping to increase the electron density to the amine structure. Therefore, the amine was more basic which could contribute to a higher reactivity in the absorption of CO<sub>2</sub>. A similar trend was seen in the group of di-alkyl substituted amines, higher pK<sub>a</sub> DEAB was more alkaline, thus able to react with CO<sub>2</sub> at a slightly faster rate than DMAB.

To compare amines from different groups, the CO<sub>2</sub> absorption rate of HEEAB was the highest. This could be a combination of many factors such as the presence of more hydroxyl (-OH) groups and the type of alkyl group that helped enhance the CO<sub>2</sub> absorption rate. Chowdhury et al. [78] confirmed the effect of extra -OH groups in the amine structures that increased the CO<sub>2</sub> absorption rate. Their work have shown that a tertiary amine having a di-hydroxyl group in the chemical structure such as 3-diethylamino-1,2-propanediol (3DEA-1, 2-PD) could absorb CO<sub>2</sub> at a faster rate than the other tertiary amine with only one hydroxyl group (i.e. 3-diethylamino-2-propanol (DEA-2P)).

The relationship between heat of CO<sub>2</sub> absorption ( $\Delta H_{\text{abs}}$ ) described earlier in Section 4.4 and the CO<sub>2</sub> absorption rate is also shown in Figure 4.47. Based on these two parameters, DEAB, DMAB and HEMAB were among the new amines able to potentially help enhance the capture performance, specifically in the absorber section. Having a lower  $\Delta H_{\text{abs}}$ , especially that of DMAB, could also be beneficial during the regeneration process from the viewpoint of energy efficiency.

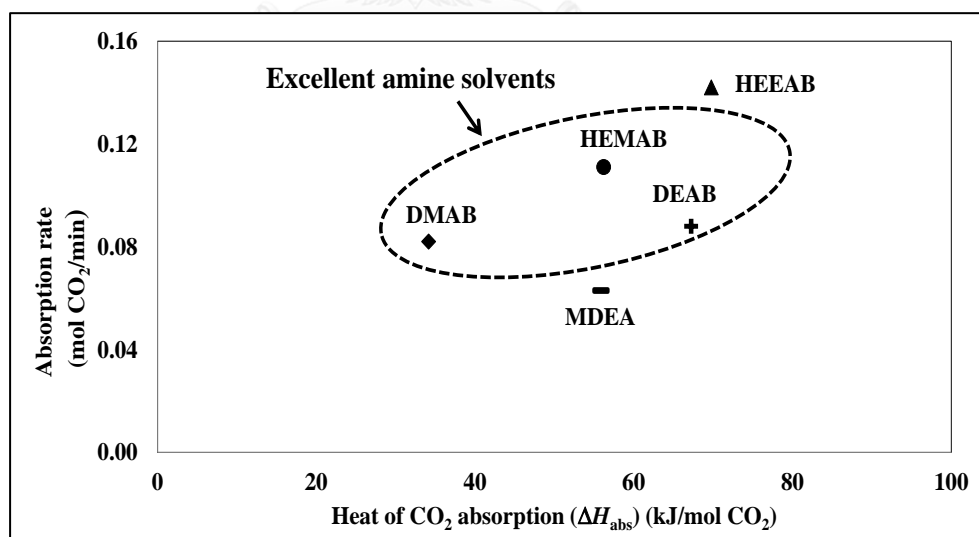


**Figure 4.47** The relationship between heat of CO<sub>2</sub> absorption and CO<sub>2</sub> absorption rate of five amines (DMAB, HEMAB, HEEAB, MDEA and DEAB).



#### 4.6 CO<sub>2</sub> regeneration rate and heat input of CO<sub>2</sub> regeneration in aqueous amine solutions

The CO<sub>2</sub> loading versus time plots at 363 K of 2 M DMAB, HEMAB and HEEAB compared to MDEA and DEAB, were shown in Figure 4.48. Their corresponding regeneration instantaneous rates calculated from the slopes were also summarized in Table 4.23. The CO<sub>2</sub>-amine regeneration rate increased in the order of 0.220, 0.243, 0.295, 0.452 and 0.512 mol CO<sub>2</sub>/min for MDEA, DEAB, HEEAB, HEMAB and DMAB, respectively. This trend of the rate data has shown quite an improvement of all new amines from the heavily used conventional MDEA in terms of easy to regenerate property. Specifically, the CO<sub>2</sub> regeneration ability of DMAB and HEMAB have also improved quite significantly from their starting DEAB.

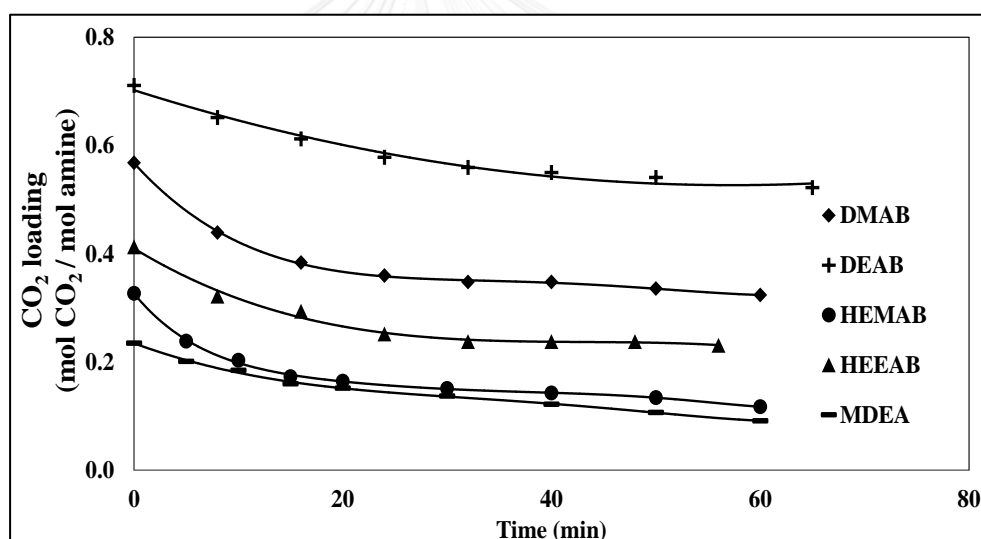


**Figure 4.48** CO<sub>2</sub> loading as a function of time for five amines (DMAB, HEMAB, HEEAB, MDEA and DEAB) at temperature of 363 K.

In terms of heat input for regeneration, DMAB also stands out as seen from only 39.73 kJ/mol heat input required in the CO<sub>2</sub> regeneration test, compared to 72.44, 60.48, 56.59, and 54.37 kJ/mol CO<sub>2</sub> for HEEAB, HEMAB, MDEA, and DEAB respectively. The methyl group in DMAB could be a reason of the amine having such a low heat input due to its least contribution to the amine electron density, thus a

weaker bond with the CO<sub>2</sub> to be broken. The same trend was seen between HEEAB and HEMAB of which, the latter with methyl substituent also required a smaller amount of heat for regeneration. The relationship between heat input and regeneration rate is also shown in Figure 4.49. Considering these two parameters, DMAB and HEMAB showed a greater potential than the rest of amines in reducing the CO<sub>2</sub> capture operational cost, specifically within the regeneration process.

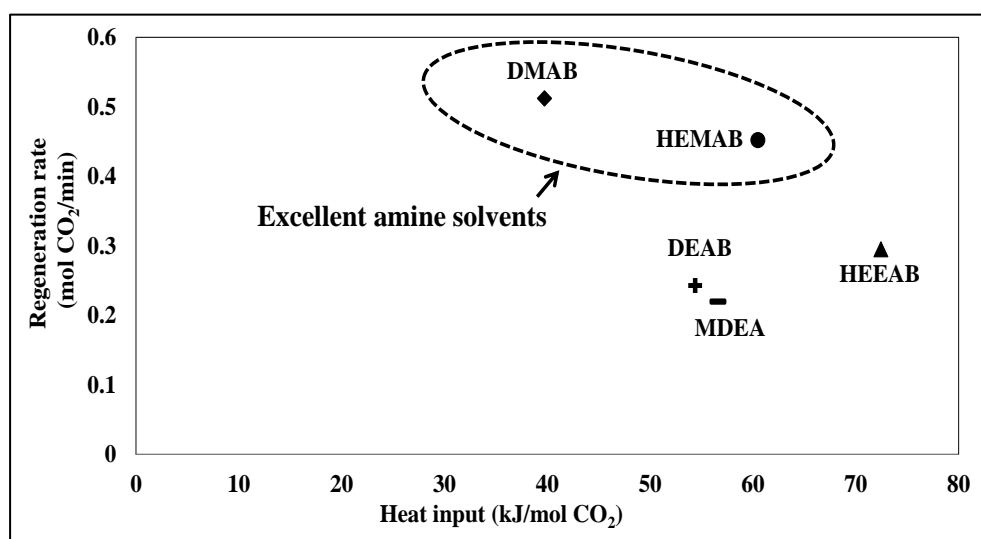


**Figure 4.49** The relationship between heat input and regeneration rate of five amines (DMAB, HEMAB, HEEAB, MDEA and DEAB).

#### 4.7 CO<sub>2</sub> equilibrium solubility and cyclic capacity in blended amine solutions

It is apparently found from section 4.3 that the newly synthesized tertiary amines (i.e. DMAB, HEMAB and HEEAB) are good amines for CO<sub>2</sub> capture, most preferable as blended solvent with a primary amine such as MEA to achieve a more desirable set of absorption capacity and cyclic capacity for use in CO<sub>2</sub> absorption.

The earlier work from Sema et al. [47], blended MEA-DEAB solvent was considered in order to enhance the reaction rate of DEAB and counter the high energy requirement of MEA. The MEA concentration used industrially in the CO<sub>2</sub> treating process is limited to be in a range of 5-7 M, especially 5 M. According to their work, the blended amine solutions of MEA and DEAB at concentration ratio of 5:1.25 M exhibited fastest reaction kinetics of CO<sub>2</sub> absorption in terms of the enhancement factor (*E*) than those over a concentration range of 5:0.25 M to 5:2 M, and single 5 M MEA, respectively. In this study, the MEA concentration in the aqueous solution was kept constant at 5 M. The new tertiary amines (i.e. DMAB, HEMAB and HEEAB), and DEAB and MDEA concentrations were kept constant at 1.25 M. Thus, the total amine concentrations in this work are found to be 6.25 M in water.

The equilibrium loading at 298, 313, and 353 K, and cyclic capacity of blended amine solutions (i.e. MEA-DMAB, MEA-HEMAB, MEA-HEEAB, MEA-DEAB and MEA-MDEA at concentration ratio of 5:1.25 M) compared with single 5 M MEA in water are summarized respectively in Tables 4.24-4.29. The amines' plots of CO<sub>2</sub> partial pressures and the equilibrium loadings at 298, 313, and 353 K corresponding to the data in Tables 4.24-4.29 are also given in Figures 4.50-4.52, respectively.

**Table 4.24** Equilibrium solubility and cyclic capacity of CO<sub>2</sub> in blended amine solutions (MEA-DMAB at ratio 5:1.25 M in water).

CO <sub>2</sub> partial pressure (kPa)	298 K	313 K	353 K	Cyclic capacity 313-353 K
	CO <sub>2</sub> loading [mol CO <sub>2</sub> /mol amine]			
3	0.50	0.46	0.28	0.18
8	0.52	0.48	0.34	0.14
15	0.54	0.50	0.38	0.12
30	0.57	0.52	0.43	0.09
100	0.61	0.56	0.48	0.08

**Table 4.25** Equilibrium solubility and cyclic capacity of CO<sub>2</sub> in blended amine solutions (MEA-HEMAB at ratio 5:1.25 M in water).

CO <sub>2</sub> partial pressure (kPa)	298 K	313 K	353 K	Cyclic capacity 313-353 K
	CO <sub>2</sub> loading [mol CO <sub>2</sub> /mol amine]			
3	0.47	0.44	0.28	0.16
8	0.50	0.47	0.32	0.15
15	0.53	0.48	0.35	0.13
30	0.55	0.50	0.39	0.11
100	0.59	0.55	0.48	0.07

**Table 4.26** Equilibrium solubility and cyclic capacity of CO<sub>2</sub> in blended amine solutions (MEA-HEEAB at ratio 5:1.25 M in water).

CO <sub>2</sub> partial pressure (kPa)	298 K	313 K	353 K	Cyclic capacity 313-353 K
	CO <sub>2</sub> loading [mol CO <sub>2</sub> /mol amine]			
3	0.49	0.45	0.28	0.17
8	0.52	0.48	0.32	0.16
15	0.55	0.50	0.37	0.13
30	0.57	0.52	0.43	0.09
100	0.60	0.56	0.46	0.10

**Table 4.27** Equilibrium solubility and cyclic capacity of CO<sub>2</sub> in blended amine solutions (MEA-DEAB at ratio 5:1.25 M in water).

CO <sub>2</sub> partial pressure (kPa)	298 K	313 K	353 K	Cyclic capacity 313-353 K
	CO <sub>2</sub> loading [mol CO <sub>2</sub> /mol amine]			
3	0.51	0.47	0.29	0.18
8	0.52	0.49	0.36	0.13
15	0.54	0.51	0.39	0.12
30	0.55	0.53	0.42	0.11
100	0.60	0.57	0.47	0.10

**Table 4.28** Equilibrium solubility and cyclic capacity of CO<sub>2</sub> in blended amine solutions (MEA-MDEA at ratio 5:1.25 M in water).

CO <sub>2</sub> partial pressure (kPa)	298 K	313 K	353 K	Cyclic capacity 313-353 K
	CO <sub>2</sub> loading [mol CO <sub>2</sub> /mol amine]			
3	0.48	0.43	0.26	0.17
8	0.50	0.45	0.30	0.15
15	0.51	0.47	0.34	0.13
30	0.55	0.50	0.44	0.06
100	0.60	0.55	0.45	0.10

**Table 4.29** Equilibrium solubility and cyclic capacity of CO<sub>2</sub> in 5 M aqueous MEA solution.

CO <sub>2</sub> partial pressure (kPa)	298 K	313 K	353 K	Cyclic capacity 313-353 K
	CO <sub>2</sub> loading [mol CO <sub>2</sub> /mol amine]			
3	0.49	0.47	0.32	0.15
8	0.51	0.49	0.36	0.13
15	0.53	0.52	0.40	0.12
30	0.56	0.54	0.46	0.08
100	0.61	0.57	0.51	0.06

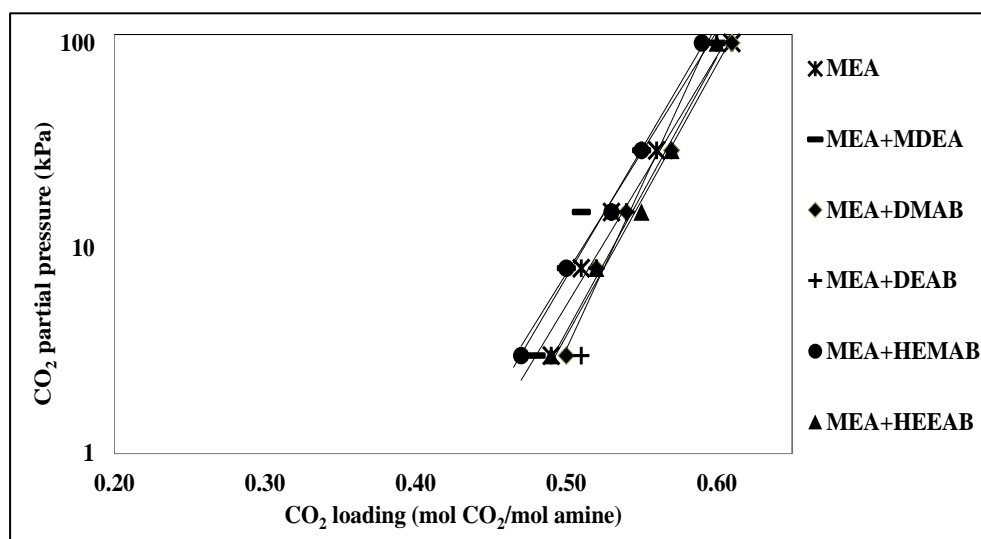


**Figure 4.50** Equilibrium solubility of CO<sub>2</sub> in blended amine solutions (MEA-DMAB, MEA-HEMAB, MEA-HEEAB, MEA-DEAB and MEA-MDEA at ratio 5:1.25 M) compare with 5 M MEA in water at 298 K (solid lines are trend lines).

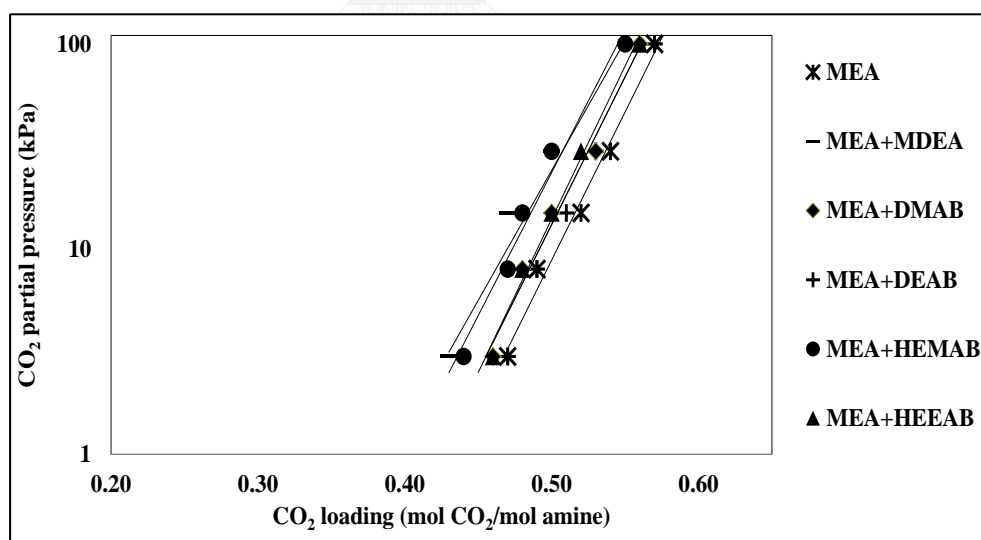


**Figure 4.51** Equilibrium solubility of CO<sub>2</sub> in blended amine solutions (MEA-DMAB, MEA-HEMAB, MEA-HEEAB, MEA-DEAB and MEA-MDEA at ratio 5:1.25 M) compare with 5 M MEA in water at 313 K (solid lines are trend lines).

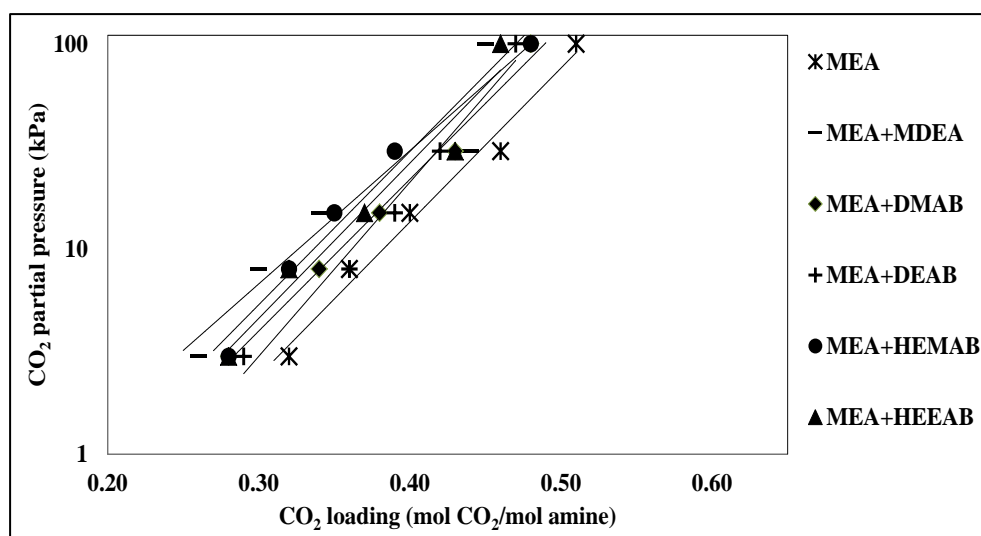


**Figure 4.52** Equilibrium solubility of CO<sub>2</sub> in blended amine solutions (MEA-DMAB, MEA-HEMAB, MEA-HEEAB, MEA-DEAB and MEA-MDEA at ratio 5:1.25 M) compare with 5 M MEA in water at 353 K (solid lines are trend lines).

In Figures 4.50, 4.51 and 4.52, it can be observed that the equilibrium solubility of CO<sub>2</sub> increases as partial pressure increases (from 3 to 100 kPa) due to the higher driving force for CO<sub>2</sub> absorption at higher CO<sub>2</sub> partial pressure. The equilibrium solubility of CO<sub>2</sub> in aqueous solubility of blended amines decreases as temperature increases (from 298 to 353 K) because the solubility of CO<sub>2</sub> declines with increasing temperature.

In Figure 4.50, all blended amine solutions (MEA-DMAB, MEA-HEMAB, MEA-HEEAB, MEA-DEAB and MEA-MDEA) in water shows almost the same range of equilibrium absorption of CO<sub>2</sub>. The amine's loading between 0.47-0.61 mol/mol amine obtained from 3-100 kPa were even comparable to our previously developed MEA-DEAB and MEA-MDEA. The single MEA has similar amine's loading of blended amine solutions.

Similar trends were still observed for all amines when the equilibrium loading was measured at 313 and 353 K as shown in Figures 4.51 and 4.52, respectively. The amine's loading between 0.43-0.57 and 0.26-0.48 mol/mol amine obtained from 3-100 kPa were measured at 313 and 353 K, respectively. Its loading was still



comparable to MEA and the loading capacity of MEA was also within the same range of all blended amines.

In terms of cyclic capacity calculated as a difference between loadings at 353 and 313 K, the results suggested that all blended amines possessed the high cyclic capacity (i.e. 0.12-0.18 mol/mol amine between 3-15 kPa). For MEA, though these amines showed lower amine concentrations, its cyclic capacity was lower and closest to that of blended amines ranging between 0.12-0.15 mol/mol amine.

Therefore, it is clear that the equilibrium solubility of CO<sub>2</sub> in aqueous solution of blended amines (i.e. MEA-DMAB, MEA-HEMAB, MEA-HEEAB, MEA-DEAB and MEA-MDEA) at higher amine concentration (6.25 M) were similar to that of MEA at lower amine concentration (5 M). This could be because of the effect of solution density. At high density, the solutions approach saturation with both of MEA and tertiary amine molecules and less free spaces of the solution for CO<sub>2</sub> to be dissolved in the system. Thus, it prevented the amine molecules from reaching a higher CO<sub>2</sub> loading. Chakrevarty et al. [40] suggested that the blended amine solution resulting in the increase of equilibrium solubility of CO<sub>2</sub> when compared with single amine. There might be a structural interaction between primary and tertiary amine that allows CO<sub>2</sub> to react with amines easily. However, further investigation of an appropriate ratio of primary amine and tertiary amine need to be carried out as to fully benefit from these promising amines.

#### 4.8 CO<sub>2</sub> absorption rate in blended amine solutions

The CO<sub>2</sub> loading versus time plots at 313 K of blended amine solutions (i.e. MEA-DMAB, MEA-HEMAB, MEA-HEEAB, MEA-DEAB and MEA-MDEA at a concentration ratio of 5:1.25 M) compared with single 5 M MEA in water, are shown in Figure 4.53. Their corresponding absorption rates calculated from the slopes are also summarized in Table 4.30. It showed that the rate of CO<sub>2</sub> absorption at 313 K was largely affected by the amine structure showing an increase in the order of 0.088, 0.094, 0.103, 0.108 and 0.129 mol CO<sub>2</sub>/min for MEA-MDEA, MEA-DMAB, MEA-DEAB, MEA-HEMAB, and MEA-HEEAB, respectively. Single MEA showed the rate of CO<sub>2</sub> absorption at 0.117 mol CO<sub>2</sub>/min. By comparing the CO<sub>2</sub> absorption rate within blended amine solutions, MEA-HEEAB showed a slightly higher absorption rate than that of MEA-HEMAB, MEA-DEAB, MEA-DMAB and MEA-MDEA, respectively. This was probably due to the influence of a better electron-donating group and extra –OH groups of HEEAB and HEMAB in the structure could have been a factor in boosting up the absorption rate of these amines, which corresponds well with the results in section 4.5.

The CO<sub>2</sub> absorption rate in aqueous solution of MEA at lower amine concentration (5 M) showed a slightly higher than that of blended amine solutions except MEA-HEEAB. This might be the effect of high density of blended amine solutions, which is limited to amine molecule approach to CO<sub>2</sub> molecule in the solution.

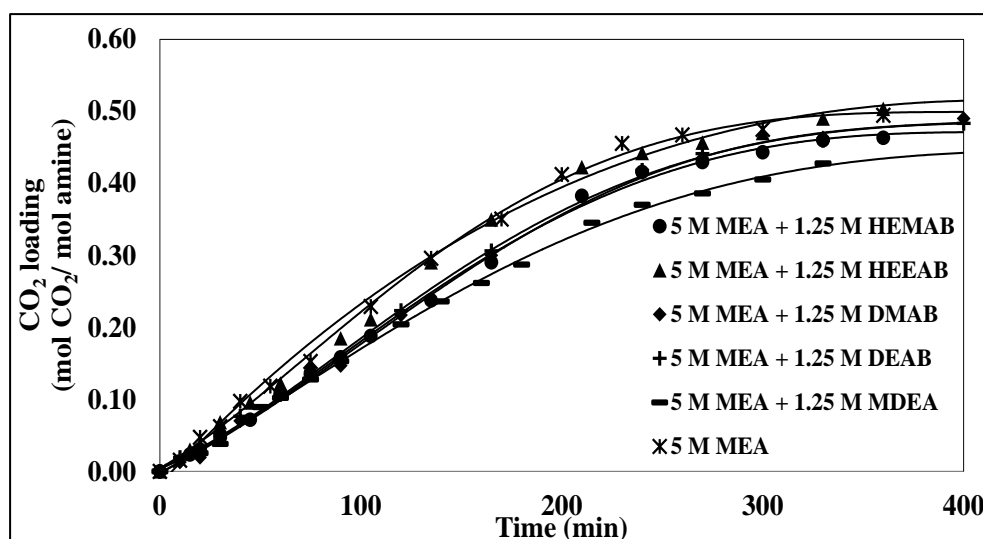


**Figure 4.53** CO<sub>2</sub> loading as a function of time for blended amine solvents (i.e. MEA-DMAB, MEA-HEMAB, MEA-HEEAB, MEA-DEAB and MEA-MDEA at concentration ratio of 5:1.25 M) compare with single 5 M MEA in water at temperature of 313 K.

**Table 4.30** CO<sub>2</sub> absorption rate, CO<sub>2</sub> regeneration rate and heat input for regeneration of blended amine solution (i.e. MEA-DMAB, MEA-HEMAB, MEA-HEEAB, MEA-DEAB and MEA-MDEA at concentration ratio of 5:1.25 M) compare with single 5 M MEA in water

Amine	CO <sub>2</sub> absorption rate at 313 K (mol CO <sub>2</sub> /min)	CO <sub>2</sub> regeneration rate at 363 K (mol CO <sub>2</sub> /min)	Heat input for regeneration (kJ/mol CO <sub>2</sub> )
MEA	0.117	0.077	203.01
MEA-MDEA	0.088	0.061	163.01
MEA-DEAB	0.103	0.069	154.35
MEA-DMAB	0.094	0.070	130.27
MEA-HEMAB	0.108	0.072	171.85
MEA-HEEAB	0.129	0.064	188.78

#### 4.9 CO<sub>2</sub> regeneration rate and heat input of CO<sub>2</sub> regeneration in blended amine solutions

The CO<sub>2</sub> loading versus time plots at 363 K of blended amine solutions (i.e. MEA-DMAB, MEA-HEMAB, MEA-HEEAB, MEA-DEAB and MEA-MDEA at concentration ratio of 5:1.25 M) compare with single 5 M MEA in water, were shown in Figure 4.54. Their corresponding regeneration instantaneous rates calculated from the slopes were also summarized in Table 4.30. The CO<sub>2</sub>-blended amine regeneration rate increased in the order of 0.061, 0.064, 0.069, 0.070 and 0.072 mol CO<sub>2</sub>/min for MEA-MDEA, MEA-HEEAB, MEA-DEAB, MEA-DMAB, and MEA-HEMAB, respectively. This trend of the rate data has shown an improvement of all blended amine solutions from MEA-MDEA in terms of easy to regenerate property.

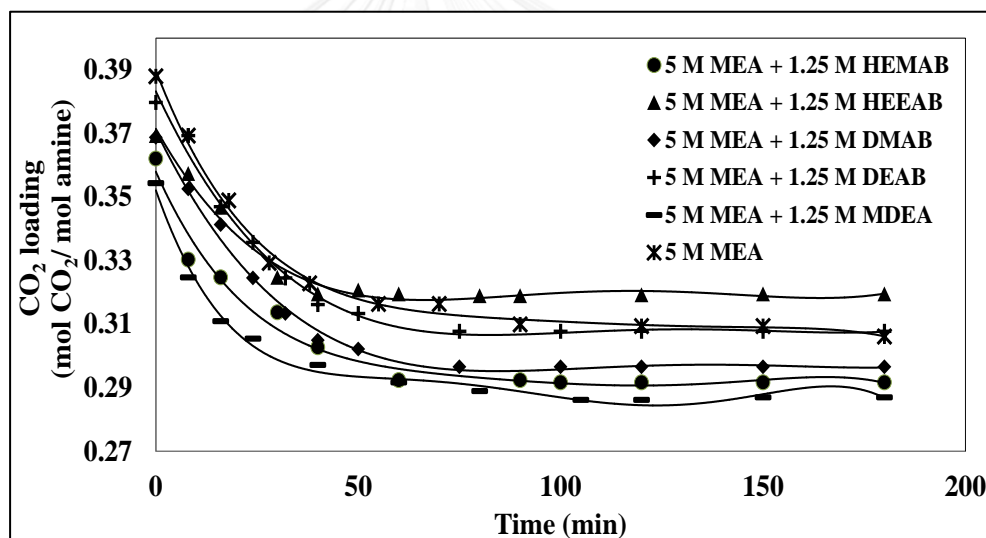


**Figure 4.54** CO<sub>2</sub> loading as a function of time for blended amine solvents (i.e. MEA-DMAB, MEA-HEMAB, MEA-HEEAB, MEA-DEAB and MEA-MDEA at concentration ratio of 5 : 1.25 M) compare with single 5 M MEA in water at temperature of 363 K.

In terms of heat input for regeneration, MEA-DMAB stands out as seen from only 130.27 kJ/mol heat input required in the CO<sub>2</sub> regeneration test, compared to 188.78, 171.85, 163.01 and 154.35 kJ/mol CO<sub>2</sub> for MEA-HEEAB, MEA-HEMAB, MEA-MDEA, and MEA-DEAB respectively. This was probably due to the influence

of the methyl group in DMAB that could be a reason of the amine having such a low heat of regeneration. Single MEA showed the highest of heat input for regeneration at 203.01 kJ/mol CO<sub>2</sub>. This was also consistent with the work of Naami et al. [34] confirming the regeneration energy for the blended MEA-DEAB aqueous solutions is lower than that of single MEA aqueous solutions.

Considering these three parameters such as CO<sub>2</sub> absorption and regeneration rate, heat input for regeneration of blended amine solutions showed a greater potential than single amines solutions in reducing the CO<sub>2</sub> capture operational cost, specifically within the regeneration process.



#### 4.10 CO<sub>2</sub> absorption kinetics of tertiary amines using the stopped-flow apparatus

In earlier publication, Singto et al. [29] developed new tertiary amines, 4-((2-hydroxyethyl)(methyl)amino)-2-butanol (HEMAB), 4-((2-hydroxyethyl)(ethyl)amino)-2-butanol (HEEAB) and 4-(dimethylamino)-2-butanol (DMAB), which were shown quite an improvement from MDEA solvent in terms of high equilibrium solubility, fast absorption and desorption rates, and low heat of absorption and regeneration. However, it is essential to evaluate the reaction kinetics of CO<sub>2</sub> absorption in order to evaluate the potential candidate solvents for CO<sub>2</sub> capture process.

The technique that can be used for study the kinetic of CO<sub>2</sub> absorption into aqueous amine solution is the stopped-flow technique which considered to be a direct method because CO<sub>2</sub> is saturated in the liquid phase which is directly reacted with the amine solvent. This technique that has frequently been used for kinetic study exhibits several intrinsic advantages, such as no limitation of a gas-liquid mass transfer, no effect of the reversibility of reaction, small amount of solvent is consumed ( $\sim 0.1$  mL for every experiment), easy operation, and short experiment run [18, 19].

Before measuring CO<sub>2</sub> absorption kinetics of tertiary amines using the stopped-flow apparatus, the experimental set-up and procedures used in this study were also used to validate the pseudo first-order reaction rate constant ( $k_0$ ) of 0.01-0.1 mol/L for MEA at 298 K by comparing with literature values as shown in Figure 4.55. The results were in good agreement with previously reported data of Ali et al. [20] with an absolute average deviation (% AAD) of 5.11 %. The accuracy of the  $k_0$  shown in terms of the standard deviation (SD) based on at least seven repeated runs was found to be in the range of 0.42-2.67 %.

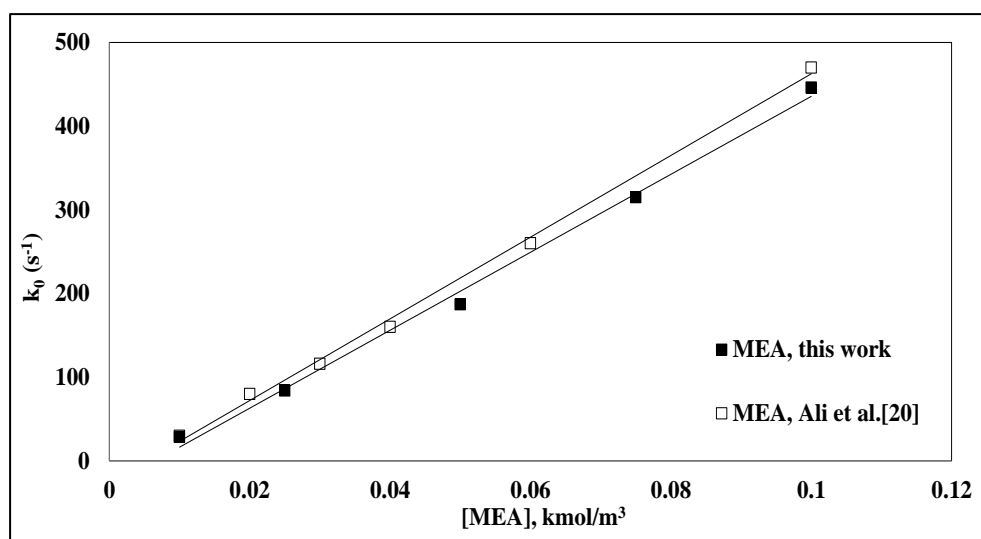


**Figure 4.55** Validation of  $k_0$  values of MEA solution at 298 K by comparing with Ali et al.

The experimental values of the observed pseudo first-order reaction rate constants ( $k_0$ ) obtained from the stopped-flow apparatus at 298, 303, 308 and 313 K of HEMAB, HEEAB, DMAB, DEAB and MDEA are summarized respectively in Tables 4.31-4.35. The amine's plots of the observed pseudo first-order reaction rate constant ( $k_0$ ) and amine concentrations between 0.1-0.5 mol/L for HEMAB and HEEAB, and 0.1-1.0 mol/L for DMAB, DEAB and MDEA at 298, 303, 308 and 313 K corresponding to the data in Figures 4.56-4.60 and are also given in Tables 4.31-4.35, respectively.

**Table 4.31** Experimental kinetics data for HEMAB over ranges of concentration and temperature of 0.1-0.5 M and 293-313 K.

Concentration (M)	Pseudo first-order rate constant ( $k_0$ )			
	298 K	303 K	308 K	313 K
0.10	95.20 ( $\pm 1.9$ )	118.50 ( $\pm 1.7$ )	167.00 ( $\pm 1.8$ )	215.63 ( $\pm 1.2$ )
0.20	250.00 ( $\pm 2$ )	270.00 ( $\pm 2.3$ )	330.00 ( $\pm 2.4$ )	370.00 ( $\pm 2.2$ )
0.30	330.60 ( $\pm 1.6$ )	364.35 ( $\pm 2$ )	467.00 ( $\pm 2.4$ )	539.57 ( $\pm 1.7$ )
0.40	476.00 ( $\pm 2.2$ )	504.00 ( $\pm 1.7$ )	597.00 ( $\pm 1.6$ )	721.00 ( $\pm 1.3$ )
0.50	574.00 ( $\pm 1.6$ )	606.00 ( $\pm 1.3$ )	696.00 ( $\pm 1.7$ )	858.00 ( $\pm 1.3$ )

**Table 4.32** Experimental kinetics data for HEEAB over ranges of concentration and temperature of 0.1-0.5 M and 293-313 K.

Concentration (M)	Pseudo first-order rate constant ( $k_0$ )			
	298 K	303 K	308 K	313 K
0.10	130.40 ( $\pm 1.3$ )	201.58 ( $\pm 1.3$ )	246.73 ( $\pm 1.2$ )	282.00 ( $\pm 1$ )
0.20	284.40 ( $\pm 1.8$ )	367.00 ( $\pm 1.5$ )	390.60 ( $\pm 1.5$ )	439.98 ( $\pm 1.2$ )
0.30	406.00 ( $\pm 1.4$ )	496.00 ( $\pm 1.6$ )	520.00 ( $\pm 1.5$ )	632.90 ( $\pm 2.1$ )
0.40	508.00 ( $\pm 1.6$ )	597.90 ( $\pm 1.6$ )	660.90 ( $\pm 1$ )	771.00 ( $\pm 2$ )
0.50	670.00 ( $\pm 1.7$ )	770.00 ( $\pm 1.5$ )	860.00 ( $\pm 1.7$ )	980.00 ( $\pm 1.8$ )

**Table 4.33** Experimental kinetics data for DMAB over ranges of concentration and temperature of 0.10-1.0 M and 293-313 K.

Concentration (M)	Pseudo first-order rate constant ( $k_0$ )			
	298 K	303 K	308 K	313 K
0.10	2.30 ( $\pm 0.2$ )	3.70 ( $\pm 0.1$ )	4.86 ( $\pm 0.2$ )	6.30 ( $\pm 0.1$ )
0.20	3.88 ( $\pm 0.1$ )	6.59 ( $\pm 0.1$ )	7.49 ( $\pm 0.1$ )	11.04 ( $\pm 0.5$ )
0.40	9.88 ( $\pm 0.3$ )	14.59 ( $\pm 0.5$ )	18.93 ( $\pm 0.4$ )	27.93 ( $\pm 0.4$ )
0.60	11.68 ( $\pm 0.6$ )	18.70 ( $\pm 0.6$ )	25.97 ( $\pm 1$ )	37.64 ( $\pm 1.4$ )
0.80	14.80 ( $\pm 0.7$ )	23.16 ( $\pm 1.3$ )	33.16 ( $\pm 2.1$ )	47.96 ( $\pm 2.7$ )
1.00	19.19 ( $\pm 0.8$ )	26.52 ( $\pm 1.9$ )	38.49 ( $\pm 2$ )	52.57 ( $\pm 1.3$ )



**Table 4.34** Experimental kinetics data for DEAB over ranges of concentration and temperature of 0.10-1.0 M and 293-313 K.

Concentration (M)	Pseudo first-order rate constant ( $k_0$ )			
	298 K	303 K	308 K	313 K
0.10	9.00 ( $\pm 0.6$ )	12.00 ( $\pm 0.9$ )	19.50 ( $\pm 1.04$ )	30.15 ( $\pm 1.2$ )
0.20	12.69 ( $\pm 1.1$ )	18.60 ( $\pm 0.8$ )	28.95 ( $\pm 1.2$ )	40.29 ( $\pm 1.4$ )
0.40	24.91 ( $\pm 1.4$ )	36.80 ( $\pm 1.1$ )	48.00 ( $\pm 1.5$ )	65.26 ( $\pm 1.2$ )
0.60	33.82 ( $\pm 1.6$ )	50.21 ( $\pm 1.3$ )	65.30 ( $\pm 1.3$ )	85.37 ( $\pm 1.3$ )
0.80	41.96 ( $\pm 1.3$ )	62.81 ( $\pm 0.4$ )	78.39 ( $\pm 1.1$ )	105.70 ( $\pm 1.2$ )
1.00	47.25 ( $\pm 1.3$ )	72.00 ( $\pm 1.2$ )	90.63 ( $\pm 1$ )	125.07 ( $\pm 1.5$ )

**Table 4.35** Experimental kinetics data for MDEA over ranges of concentration and temperature of 0.10-1.0 M and 293-313 K.

Concentration (M)	Pseudo first-order rate constant ( $k_0$ )			
	298 K	303 K	308 K	313 K
0.10	0.00	0.00	0.00	0.00
0.20	1.95 ( $\pm 0.1$ )	2.34 ( $\pm 0.2$ )	3.16 ( $\pm 0.1$ )	4.65 ( $\pm 0.2$ )
0.40	3.63 ( $\pm 0.2$ )	4.62 ( $\pm 0.1$ )	6.81 ( $\pm 0.1$ )	9.48 ( $\pm 0.2$ )
0.60	5.64 ( $\pm 0.1$ )	6.68 ( $\pm 0.1$ )	9.07 ( $\pm 0.8$ )	11.53 ( $\pm 1$ )
0.80	9.18 ( $\pm 0.3$ )	11.35 ( $\pm 0.9$ )	14.88 ( $\pm 0.8$ )	19.00 ( $\pm 0.9$ )
1.00	13.43 ( $\pm 0.7$ )	16.17 ( $\pm 0.8$ )	19.61 (0.8)	23.40 ( $\pm 1.4$ )

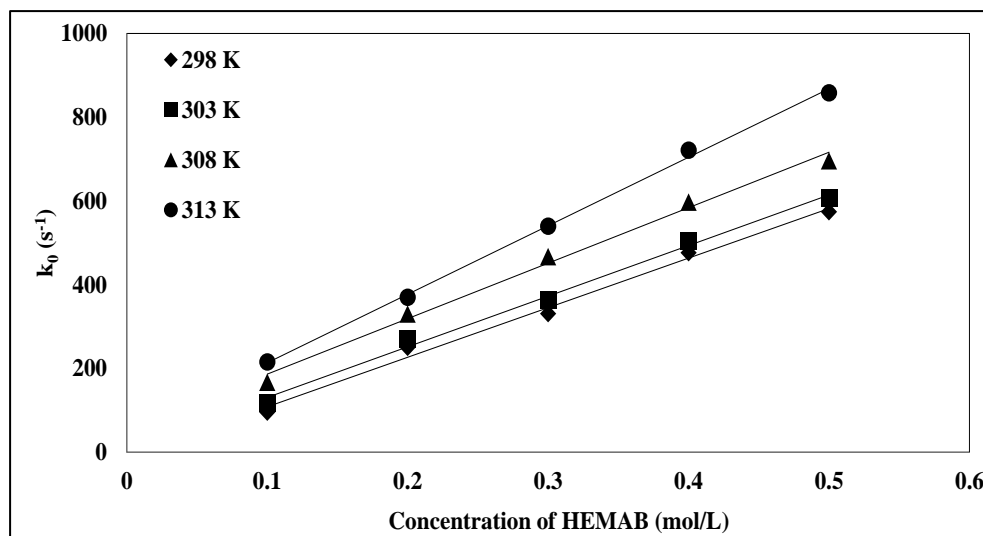


**Figure 4.56** Effect of HEMAB concentration range 0.1-0.5 M and temperature range of 298-313 K on kinetics data in terms of  $k_0$ .

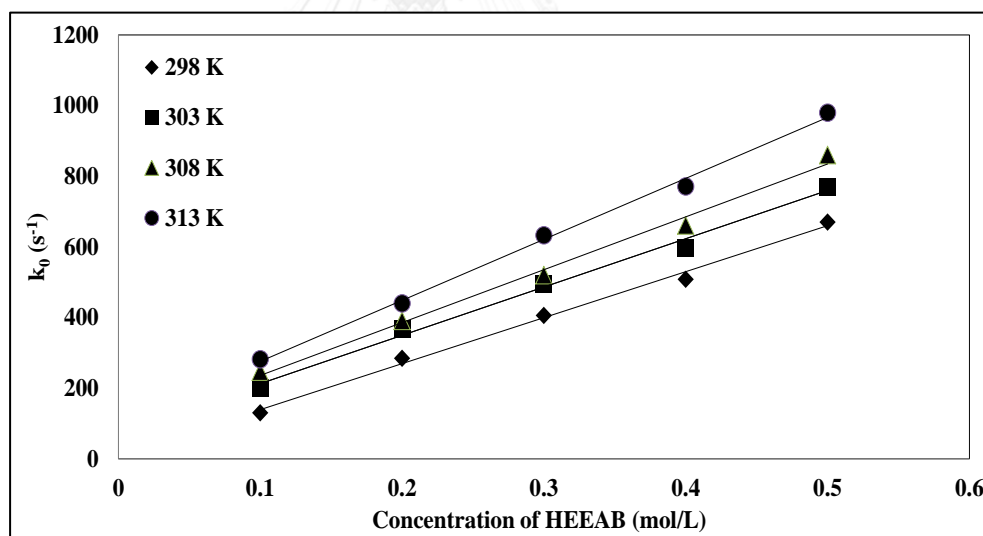


**Figure 4.57** Effect of HEEAB concentration range 0.1-0.5 M and temperature range of 298-313 K on kinetics data in terms of  $k_0$ .

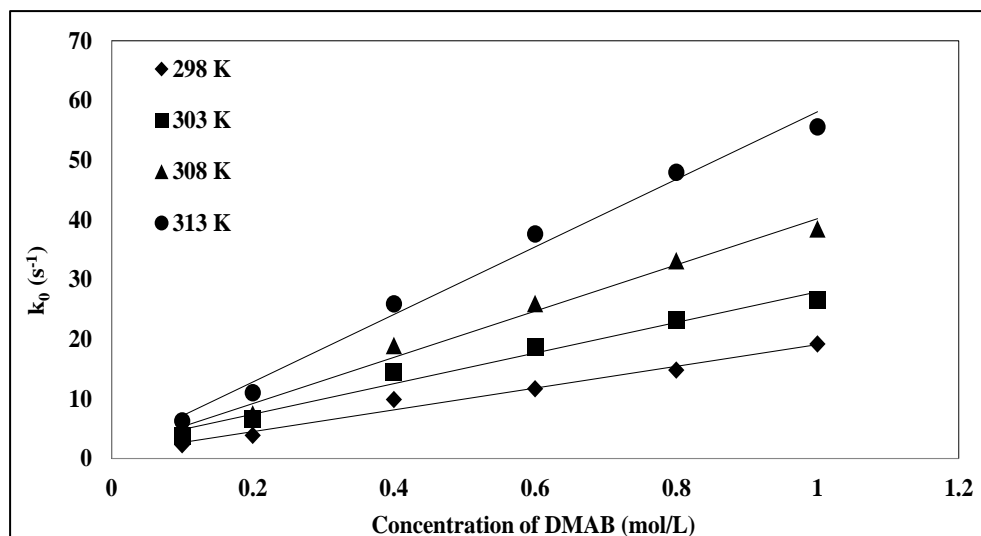


**Figure 4.58** Effect of DMAB concentration range 0.1-1.0 M and temperature range of 298-313 K on kinetics data in terms of  $k_0$ .

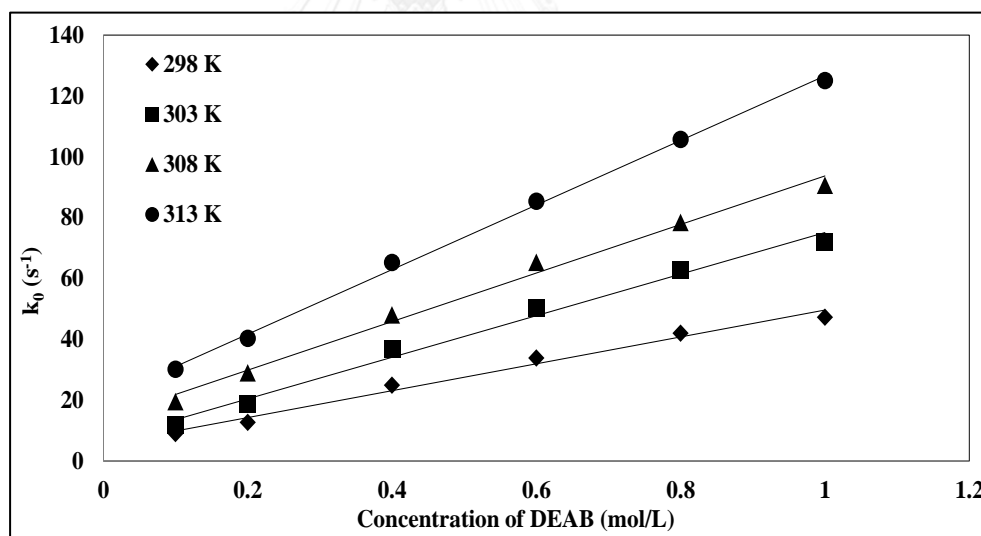


**Figure 4.59** Effect of DEAB concentration range 0.1-1.0 M and temperature range of 298-313 K on kinetics data in terms of  $k_0$ .

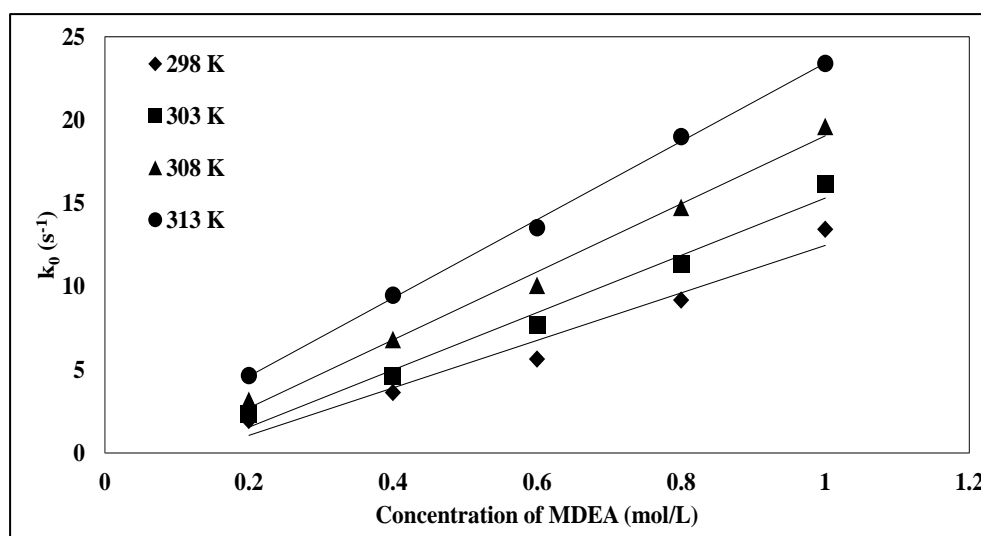


**Figure 4.60** Effect of MDEA concentration range 0.2-1.0 M and temperature range of 298-313 K on kinetics data in terms of  $k_0$ .

The amine concentration was kept at least 10 times higher than the concentration of  $\text{CO}_2$ . The observed pseudo first-order rate constants ( $k_0$ ) for tertiary amine reactions with  $\text{CO}_2$  based on the base-catalyzed hydration mechanism are fitted with the power law equation, as shown in Equations 2.13 and 2.14. It can be seen from Figures 4.56-4.60 that the  $\text{CO}_2$  absorption kinetics of amines increased as both the amine concentration and the temperature increased.

As previously mentioned, the new amine compounds for this work were categorized into two groups consisting of di-alkyl (i.e. DMAB) and hydroxy-alkyl-alkyl-amino-2-butanols (i.e. HEMAB and HEEAB). From the results, the hydroxy-alkyl-alkyl substituted amines (i.e. HEEAB and HEMAB) group showed first and second highest observed  $k_0$  values lying in between 130.40-980.0 and 95.20-858.0  $\text{s}^{-1}$  at 298-313 K as shown in Figures 4.57 and 4.56, and Tables 4.32 and 4.31, respectively. For the group of di-alkyl substituted amines (i.e. DMAB, DEAB), low  $k_0$  values were observed in between 2.3-52.57 and 9.0-125.07  $\text{s}^{-1}$  at 298-313 K as shown in Figures 4.58 and 4.59, and Tables 4.33 and 4.34, respectively. In addition, HEEAB, HEMAB, DMAB and DEAB were all superior to MDEA for the observed  $k_0$  at 1.95-23.40  $\text{s}^{-1}$  as shown in Figure 4.60 and Table 4.35.

By fitting the empirical power law kinetics to the data of the experimentally observed  $k_0$  for  $\text{CO}_2$ , which gave the average reaction order ( $n$ ) of 0.97, 0.83, 0.93, 0.72 and 1.11, with respect to HEMAB, HEEAB, DMAB, DEAB and MDEA at 293-313 K, respectively. However, it should be noted that the order of the reactions was found to be close to unity 1 for all compounds. Thus, the observed  $k_0$  values at various concentrations and temperatures of new tertiary amines were then interpreted by the base-catalyzed hydration mechanism in Equation 3.9 to determine the second-order reaction rate constants ( $k_2$ ).

In order to obtain the second-order rate constant ( $k_2$ ), the values of observed  $k_0$  at various concentrations and temperatures of HEMAB, HEEAB, DMAB, DEAB and MDEA (from Tables 4.31-4.35) were then fitted with Equation 2.14. The  $k_2$  value of all amines can be found in Table 4.36. It is usually accepted that a high value of  $k_2$  leads to fast reaction kinetics. The  $k_2$  values were fitted to an Arrhenius relationship as shown in Equation 4.5.

$$k_2 = A \exp\left(\frac{-E_a}{RT}\right) \quad \text{Eq.4.5}$$

Where,  $A$  is the pre-exponential factor or frequency factor ( $\text{s}^{-1}$ ),  $E_a$  is the activation energy (kJ/mol), and  $R$  is the universal gas constant (0.008315 kJ/mol.K).

The Arrhenius relationship shows the values of  $\ln k_2$  for all amines plotted as a function of the reciprocal of absolute temperature ( $\ln k_2$  vs  $1/T$ ) as shown in Figure 4.61.

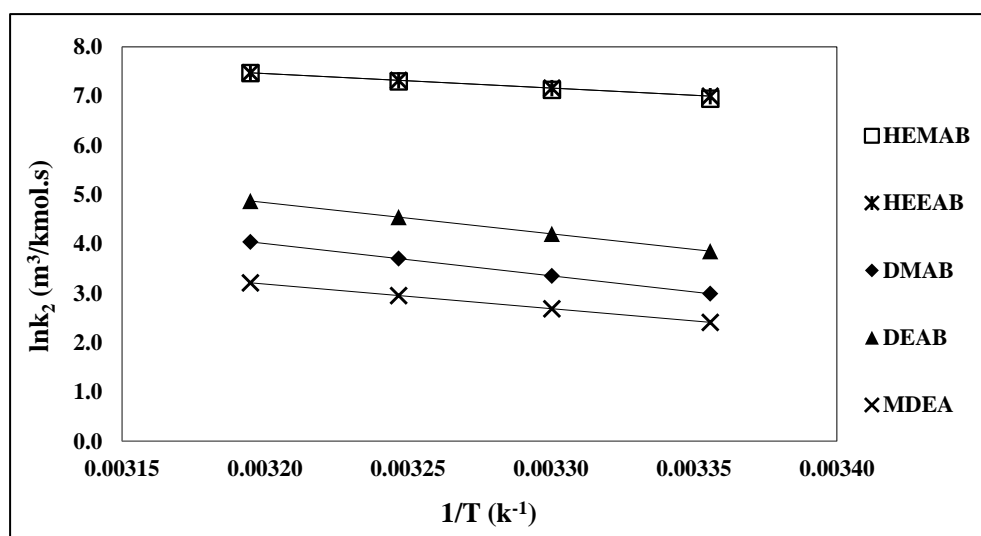
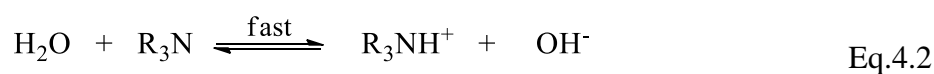


**Figure 4.61** Arrhenius plot of the second-order reaction rate constant ( $k_2$ ) of all amines.

As shown in Figure 4.61,  $\ln k_2$  increased with temperature. It is clear that the  $k_2$  values at 298-313 K are largely affected by the amine structure as shown by the increase from 1096.9, 1043.6, 47.2, 19.9 and 11.2  $\text{m}^3/\text{kmol}\cdot\text{s}$  for HEEAB, HEMAB, DEAB, DMAB and MDEA, respectively. The results suggested that the hydroxy-alkyl-alkyl substituted amines, HEMAB and HEEAB showed excellent enhancement in their reaction rates, which were higher than those of DEAB, DMAB and MDEA.

The higher reaction rate constants for HEMAB and HEEAB are attributed to the presence of more  $-\text{OH}$  groups in their structures as shown in Figure 3.1. The presence of more  $-\text{OH}$  groups, which can potentially increase the ability for water to solvate the amine molecule which was essential in  $\text{CO}_2$  absorption reactions thereby boosting their absorption mechanisms to quickly produce  $\text{OH}^-$  and  $\text{R}_3\text{NH}^+$  necessary for driving the absorption reactions, thus, contributing to a faster overall absorption rate as shown in Equations 4.2 and 4.3 (see in section 4.5).



By comparing the  $k_2$  values within the same amine group, the  $k_2$  values of HEEAB were slightly faster than that of HEMAB due to a stronger electron donating ethyl group, helping to increase the electron density of the amine structure. Therefore, the amine is more basic which could contribute to a higher reactivity in the absorption of CO<sub>2</sub>. A similar trend was seen in the group of di-alkyl substituted amines (i.e. DMAB and DEAB), DEAB contained the longest alkyl chain length thus providing a high electron donating effect and higher basicity, thus able to react with CO<sub>2</sub> at a slightly faster rate than DMAB which contains the shorter alkyl chain length. The comparative kinetics results observed in this work were found to be in accordance with the previous work of CO<sub>2</sub> absorption rate at actual concentrations (see section 4.5), which presents the type and placement of the alkyl and/or hydroxyl functional groups within the amine structure affected the performance of CO<sub>2</sub> absorption rate performances.

In addition, the linear regression equations of the Arrhenius relationship of the second-order rate constant ( $k_2$ ) at different temperatures of HEMAB, HEEAB, DMAB, DEAB and MDEA related to their respective activation energy ( $E_a$ ) are shown in Equations 4.6 to 4.10, respectively.

$$k_2 = (5.17 \times 10^7) \exp\left(-\frac{3221.7}{T}\right) \quad (R^2 = 0.98) \quad \text{Eq.4.6}$$

$$k_2 = (2.12 \times 10^7) \exp\left(-\frac{2941.3}{T}\right) \quad (R^2 = 0.98) \quad \text{Eq.4.7}$$

$$k_2 = (2.15 \times 10^{10}) \exp\left(-\frac{6191.9}{T}\right) \quad (R^2 = 0.99) \quad \text{Eq.4.8}$$

$$k_2 = (8.0 \times 10^{10}) \exp\left(-\frac{6332.5}{T}\right) \quad (R^2 = 0.99) \quad \text{Eq.4.9}$$

$$k_2 = (2.08 \times 10^8) \exp\left(-\frac{4988.6}{T}\right) \quad (R^2 = 0.99) \quad \text{Eq.4.10}$$

The activation energy ( $E_a$ ) values obtained from the linear regression trendlines increased in the order of 24.45, 26.78, 41.47, 52.65 and 54.34 kJ/mol for HEEAB, HEMAB, MDEA, DEAB and DMAB, respectively as shown in Table 4.36. The hydroxy-alkyl-alkyl substituted amines (i.e. HEMAB and HEEAB) showed a lower  $E_a$  than that of the di-alkyl substituted amines (i.e. DEAB and DMAB) due to

the presence of more hydroxyl groups in their amine structures. These hydroxyl groups enhance the solubility of amine in water due to the intermolecular hydrogen bonds between hydroxyl groups and water. The increase in amine solubility in water would facilitate the reaction of the amine-CO<sub>2</sub>-water system. Consequently, lower energy is required for the reaction to occur.

The frequency factor (A) relates to the frequency of collisions (z) and the orientation of a molecule of a favorable collision probability. The frequency factor (A) at 298-313 K is largely affected by the amine structure as shown by the increase in frequency factor (A) from  $8.0 \times 10^{10}$ ,  $2.1 \times 10^{10}$ ,  $2.1 \times 10^8$ ,  $5.2 \times 10^7$  and  $2.1 \times 10^7$  s<sup>-1</sup> for DEAB, DMAB, MDEA, HEMAB, and HEEAB, respectively, as shown in Table 4.36. The di-alkyl substituted amines (i.e. DEAB and DMAB) showed higher frequency factors (A) than those of hydroxy-alkyl-alkyl substituted amines (i.e. HEMAB and HEEAB). The higher frequency factors observed for DEAB and DMAB is likely due to the low molecular weights of these compounds (MW = 145 and 117), causing these small molecules to easily collide with other molecules (i.e. CO<sub>2</sub> and H<sub>2</sub>O). Although these amines showed the high frequency factor (A), the collision might be inefficient or not in the right position to form the products, as evidenced by the high frequency factor (A).

On the other hand, the hydroxy-alkyl-alkyl substituted amines (i.e. HEMAB and HEEAB) have higher molecular weights (MW = 147 and 161) and the large molecules is predominant even though these amines are freely soluble in water. Therefore, these molecules move slightly slower which leads to low frequency factor (A). The collision of these molecules were however more efficient, in other words, the collision probably occurs at the right position to form the products.

For this reason, it is worth mentioning that the frequency factor (A) is affected by both the molecular size and orientation of the molecule. The di-alkyl substituted amines (i.e. DEAB and DMAB) were superior to that of the hydroxy-alkyl-alkyl substituted amines (i.e. HEMAB and HEEAB) and MDEA in terms of higher frequency factor (A).



**Table 4.36** The second-order reaction rate constants ( $k_2$ ) of CO<sub>2</sub> absorption at 298 K, activation energy ( $E_a$ ) and frequency factor (A) at 298-313 K in aqueous solutions of HEEAB, HEMAB and DMAB compared with DEAB and MDEA.

Tertiary Amine	$k_2$ (m <sup>3</sup> /kmol.s)	Activation energy; $E_a$ (kJ/mol)	Frequency factor; A (s <sup>-1</sup> )
HEMAB	1043.62	26.78	$5.2 \times 10^7$
HEEAB	1096.86	24.45	$2.1 \times 10^7$
DMAB	19.94	54.34	$2.1 \times 10^{10}$
DEAB	47.24	52.65	$8.0 \times 10^{10}$
MDEA	11.15	41.48	$2.1 \times 10^8$
DEAB [24]	64.00	58.66	-
MDEA[24]	12.00	41.93	-



#### 4.11 $pK_a$ values of aqueous tertiary amine solutions

The  $pK_a$  value is indicated to be very important for a compound's basicity for the interpretation of the kinetic mechanism of amines such as absorption rate. In this work, the  $pK_a$  values of all amines were experimentally measured at 296.5, 298, 303, 308, 313, 318, 323, 328 and 333 K as shown in Figure 4.62 and Table 4.37.

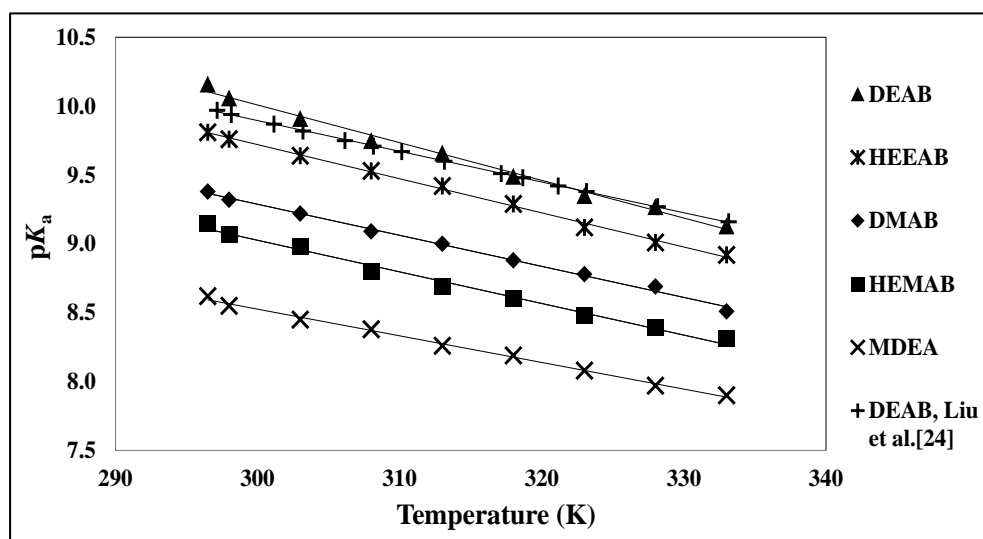


**Figure 4.62**  $pK_a$  values of tertiary amines over a temperature range of 298-313 K.

**Table 4.37**  $pK_a$  values of HEMAB, HEEAB, and DMAB compared with DEAB and MDEA at 296.5-333.0 K.

T(K)	$pK_a$				
	HEMAB	HEEAB	DMAB	DEAB	MDEA
296.5	9.15	9.81	9.38	10.16	8.62
298.0	9.07	9.76	9.32	10.06	8.55
303.0	8.98	9.64	9.22	9.91	8.45
308.0	8.80	9.53	9.09	9.75	8.38
313.0	8.69	9.42	9.00	9.66	8.26
318.0	8.60	9.29	8.88	9.49	8.19
323.0	8.48	9.12	8.78	9.35	8.08
328.0	8.39	9.01	8.69	9.27	7.97
333.0	8.31	8.92	8.51	9.13	7.90

As can be seen in Figure 4.62 by comparing the  $pK_a$  of DEAB obtained in this work to that of Liu et al. [24], it was found that the  $pK_a$  of DEAB obtained from this work is very close to the work of Liu et al. [24] with an absolute average deviation (% ADD) of 1.2 %. The  $pK_a$  values of aqueous tertiary amines solution decrease with respect to an increase in temperature from 8.62-7.90, 9.15-8.31, 9.38-8.51, 9.81-8.92 and 10.16-9.13 for MDEA, HEMAB, DMAB, HEEAB and DEAB, respectively. A predictive correlation of  $pK_a$  can be calculated by plotting the experimental  $pK_a$  values to  $1/T$  as shown in Equations 4.11-4.15.

$$pK_{a,HEMAB} = \frac{2264.4}{T} + 1.48 \quad \text{Eq.4.11}$$

$$pK_{a,HEEAB} = \frac{2435.6}{T} + 1.60 \quad \text{Eq.4.12}$$

$$pK_{a,DMAB} = \frac{2216.1}{T} + 1.90 \quad \text{Eq.4.13}$$

$$pK_{a,DEAB} = \frac{2697}{T} + 1.02 \quad \text{Eq.4.14}$$

$$pK_{a,MDEA} = \frac{1902.1}{T} + 2.19 \quad \text{Eq.4.15}$$

The predicted values of  $pK_a$  of all amines were found to be in very good agreement with experimental results with an absolute average deviation (% ADD) range of 0.01- 0.53 %.

Versteeg and Swaaij [51], proposed the Brønsted relationship to provide a significant contribution to the comprehensive understanding of CO<sub>2</sub> absorption kinetics, the relationship was plotted between the natural logarithm of the second-order reaction rate constant,  $\ln k_2$  and the basicity of the tertiary amine,  $pK_a$ . In this work, the Brønsted relationship of all amines is shown in Figure 4.63, were also generated by using the experimentally measured  $pK_a$  and the  $\ln k_2$  obtained from the stopped-flow reaction over the temperature range of 298-313 K. The developed Brønsted relationship of all amines is shown in Equations 4.16-4.20.

$$\ln(k_{2,HEMAB}) = (-1.29pK_a) + 18.65 \quad \text{Eq.4.16}$$

$$\ln(k_{2,HEEAB}) = (-1.4pK_a) + 20.61 \quad \text{Eq.4.17}$$

$$\ln(k_{2,DMAB}) = (-3.2pK_a) + 32.83 \quad \text{Eq.4.18}$$

$$\ln(k_{2,DEAB}) = (-2.47pK_a) + 28.66 \quad \text{Eq.4.19}$$

$$\ln(k_{2,MDEA}) = (-2.82pK_a) + 26.5 \quad \text{Eq.4.20}$$

The Brønsted relationship can be used to predict the  $k_2$  values of all amines effectively, with an absolute average deviation (% ADD) of 0.01-3.02 %. The results were found to be in good agreement with previously reported data [24] of a % ADD of 8.6 % and 2.8 % for DEAB and MDEA.

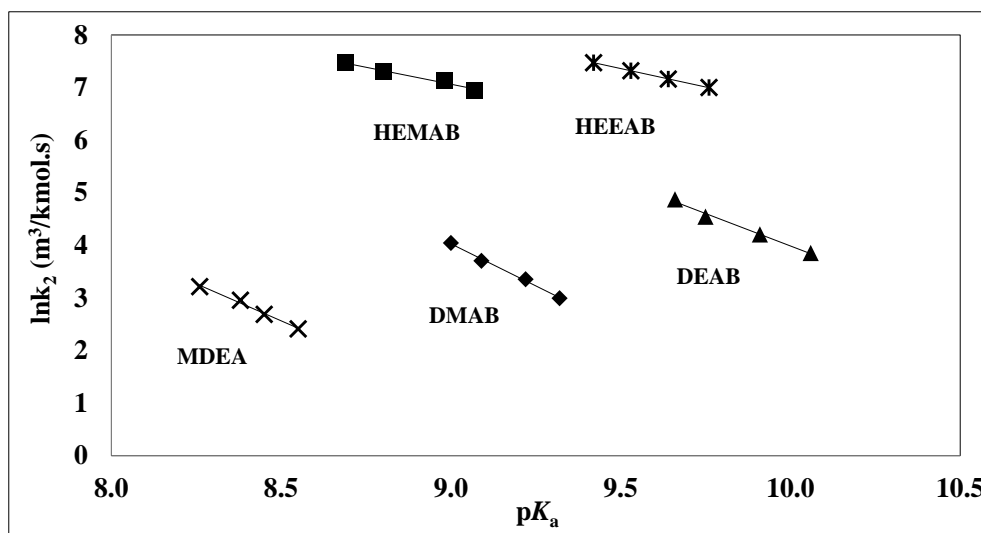


**Figure 4.63** Brønsted plots of HEMAB, HEEAB, DMAB compared with DEAB and MDEA.

From the  $pK_a$  values, the  $pK_a$  of DEAB calculated from Equation 4.16 was greater than that of all amines due to the presence of the stronger electron donating ethyl group, which gives an overall increase in the electron density of the amine structure. Therefore, the more basic amine could contribute to a higher reactivity in the absorption of  $CO_2$ . All other amines (i.e. HEMAB, HEEAB, DMAB, DEAB) showed higher reactivity rates than that of MDEA over the entire temperature range.

Li et al. [25] mentioned that the  $pK_a$  value can only give guidance to preliminary estimation of the reaction kinetics. The reaction kinetics cannot be fully confirmed by the  $pK_a$  value but only by the reaction rate constant ( $k$ ). This is because the reaction kinetics is directly interpreted by the reaction rate constant, which means that the higher the reaction rate constant ( $k$ ), the faster the reaction kinetics. Thus, in order to analyze the  $CO_2$  absorption reaction kinetics comprehensively, both the Arrhenius relationships, which exhibit the temperature dependency of  $\ln k_2$  and Brønsted relationships, which exhibit the relationship between  $\ln k_2$  and  $pK_a$  are also presented in Figure 4.61 and 4.63, respectively. As can be seen in Figure 4.63, the  $pK_a$  values of HEEAB and HEMAB were lower than that of DEAB, but these amines showed a greater potential than the rest of the amines in terms of the second-order

reaction rate constant,  $k_2$  from the stopped-flow measurement. Thus, HEEAB and HEMAB could absorb  $\text{CO}_2$  at a faster rate as can be seen in Figure 4.61 where the trendlines were located at the upper part of the graph. It is worth mentioning that the reaction rate constant ( $k$ ) could be measured of the reaction of  $\text{CO}_2$  absorption.



#### 4.12 The physical properties

Density, viscosity, and refractive index of pure DMAB, DPAB, DBAB, HEMAB, HEEAB, DEAB (purity range of 76-94 %), MDEA (purity  $\geq 98$  %), and water were measured at temperatures from 293 to 333 K as shown in Figures 4.64, 4.65 and 4.66, respectively. The experiments were validated with pure MDEA and DEAB at 293-333 K by comparing with literature values as shown in Figures 4.64-4.66. The results were found to be in good agreement with previously reported data [32] with an absolute average deviation (% AAD) of 0.25 % and 0.97 %, respectively, for MDEA and DEAB. The repeatability in terms of standard deviation based on three repeated runs was found to be less than 2.94 %. Consequently, the equipment and procedure of the density, viscosity and refractive index studies can be used for this measurement.

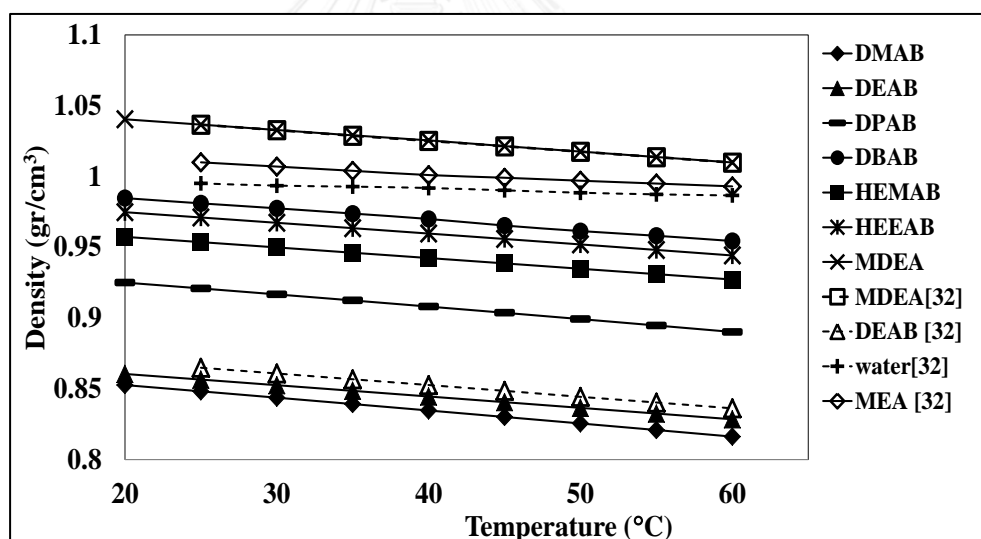


**Figure 4.64** The density changes of pure DMAB, DPAB, DBAB, HEMAB, HEEAB, DEAB, MDEA, MEA, and water at temperatures from 293 to 333 K.

According to Figure 4.64, the density of pure amine solvents decreased as the temperature increased. Specifically, the least sterically hindered amine (DMAB) showed the lowest density values among the new amines synthesized in this study. DEAB, DPAB, HEMAB, HEEAB and DBAB showed the higher density values,

respectively. By comparing the density within the same amine functional group, the density of HEEAB was higher than that of HEMAB, and the density of DBAB was higher than that of DPAB, DEAB and DMAB, due to the higher molecular weights of these compounds. In addition, MDEA were found to be the highest in density over all the other amines.

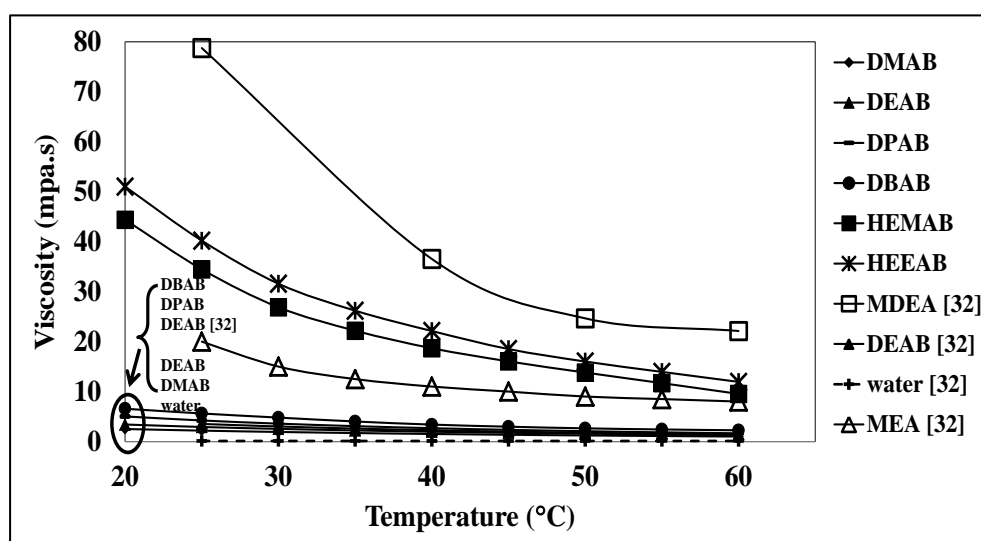


**Figure 4.65** The viscosity of pure DMAB, DPAB, DBAB, HEMAB, HEEAB, DEAB, MDEA, MEA, and water at temperatures from 293 to 333 K.

Similar trends were observed for all pure amines and water when viscosity was measured at 298 to 333 K as shown in Figure 4.65, the viscosity of pure amine solvents decreased with respect to as increase in temperature. The viscosity value of DMAB was still found to be the lowest among the new amines synthesized at all temperatures. DEAB still remained the second least amine in terms of the viscosity followed by DPAB, DBAB, HEMAB and HEEAB. In addition, MDEA showed the highest viscosity among the new amines synthesized in this study. It is shown that the viscosity values of the amines belonging to the hydroxy-alkyl-alkyl-amino-2-butanols group (i.e. HEEAB, HEMAB and MDEA) were higher than those of the amine belonging to the di-alkyl-amino-2-butanols group (i.e. DMAB, DPAB, DBAB and DEAB). This is probably due to the influence of the placement of two hydroxyl (-OH)



group in the amine structure, thereby causing these amines to have a higher degree of hydrogen bonding, making them more viscous.

Both the density and viscosity of solutions play an important role in the efficient design and operation of a gas treating process plant. In addition, density and viscosity are used to determine other properties such as diffusivity and reaction rate constant [32].

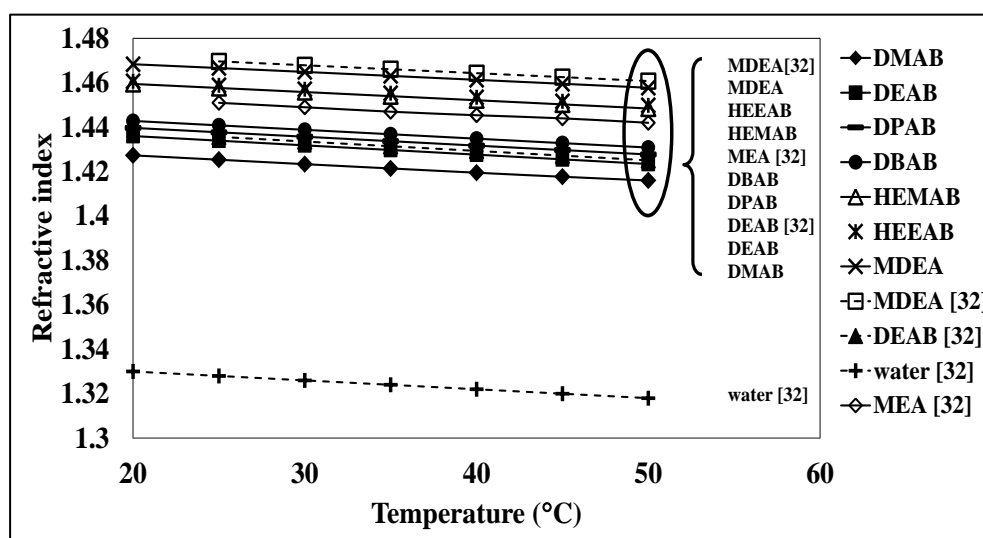


**Figure 4.66** The refractive indices of pure DMAB, DPAB, DBAB, HEMAB, HEEAB, DEAB, MDEA, MEA, and water at temperatures ranging from 293 to 323 K.

According to Figure 4.66, the refractive index of pure amine solvents decreased as the temperature increased. The refractive index of DMAB was still found to be the lowest among the new amines synthesized at all temperatures. DEAB, DPAB, DBAB, HEMAB, and HEEAB showed the higher density values, respectively. MDEA still showed the highest refractive index among the newly synthesized amine solvents in this study.

## CHAPTER V

### CONCLUSION

DMAB, DEAB, DPAB, DBAB, HEMAB and HEEAB have been synthesized using Mannich and Michael addition reactions. The synthesis was based on the concept of enhancing the electron donating ability of the amines using various di-alkyl substituents and placement of hydroxyl (-OH) groups on the alkyl chain for promoting the amines' CO<sub>2</sub> capturing ability. It has been shown that both the type and placement of the mentioned functional groups within the amine structure affected the performances of CO<sub>2</sub> absorption-regeneration and kinetics of the reaction of CO<sub>2</sub> absorption. From the equilibrium solubility of CO<sub>2</sub> in newly synthesized tertiary amines, DMAB, HEEAB and HEMAB all had higher CO<sub>2</sub> absorption capacities and cyclic capacities compared to conventional MDEA. It was also found that the heat of CO<sub>2</sub> absorption ( $\Delta H_{\text{abs}}$ ) of DMAB was the lowest among all amines tested in this study. Hydroxy-alkyl-alkyl substituted amines, HEMAB and HEEAB showed an excellent enhancement of the CO<sub>2</sub> absorption rates which were the highest, due to the presence of more hydroxyl (-OH) groups and higher  $pK_a$  values. DMAB was found to have the fastest rate of regeneration while requiring the lowest heat input for regeneration between all amines. The equilibrium solubility of CO<sub>2</sub> in aqueous solution of blended amine solutions MEA-DMAB, MEA-HEMAB, MEA-HEEAB, MEA-DEAB and MEA-MDEA at a concentration ratio of 5:1.25 M decreases as the temperature and CO<sub>2</sub> partial pressure increases. The CO<sub>2</sub> absorption capacities and cyclic capacities of all blended amine solutions were similar to that of MEA 5 M, due to the effect of high density. MEA-HEEAB showed a slightly higher absorption rate than that of all blended amine solutions. This was probably due to the influence of a stronger electron-donor group and presence of an extra -OH group in the structure. The CO<sub>2</sub> regeneration ability of new blended amine solutions showed slightly faster rates than that of MEA-MDEA. MEA-DMAB stands out for the lowest heat input requirement in the CO<sub>2</sub> regeneration test. Based on the outstanding performance of

DMAB, HEMAB and HEEAB in terms of high equilibrium solubility, fast absorption and desorption rates, and low heats of absorption and regeneration.

The kinetics of the reaction of CO<sub>2</sub> absorption of DMAB, HEMAB and HEEAB compared with DEAB and MDEA were experimentally measured using the stopped-flow apparatus at temperature range of 298-313 K and an amine concentration range of 0.1-1.0 mol/L. The base-catalysed of the CO<sub>2</sub> hydration mechanism could explain and apply to correlation the experimental CO<sub>2</sub> absorption rate constants between CO<sub>2</sub> and the tertiary amine. It was found that the reaction rate of all amines increased as both the amine concentration and temperature increased. The reaction order ( $n$ ) gave approximated to 1 for all amines. This can be hydroxy-alkyl-alkyl substituted amines, HEMAB and HEEAB showed excellent enhancement of reaction kinetics (the second-order reaction rate constants,  $k_2$ ), low activation energy ( $E_a$ ), and low frequency factor ( $A$ ) than those of the di-alkyl substituted amines DMAB, DEAB, and MDEA. This could be beneficial for many factors such as the presence of more hydroxyl (-OH) groups, which can potentially increase the solvation of amine molecules in the aqueous systems and facilitate the reaction of amine-CO<sub>2</sub>-water system. The type of electron donating alkyl group, the longer alkyl chain length could help to increase the electron density of the amine structure, thereby increasing basicity, which helped enhance the CO<sub>2</sub> absorption rate. In addition, the effect of both molecular size and orientation of the molecule are largely affected to the frequency factor ( $A$ ). Lastly, the physical properties of newly synthesized amines were measured at different temperatures. The results have shown that the density, viscosity and refractive indices of these newly synthesized amines were lower than that of MDEA. These properties are significant in the process efficient and economical. Based on these results, DMAB, HEMAB and HEEAB could be considered potential candidate solvents for the CO<sub>2</sub> capture process.

**Recommendations for future work**

The results of this research have demonstrated that these newly synthesized amine solvents (i.e. DMAB, HEMAB and HEEAB) are promising alternative solvents for capturing CO<sub>2</sub> in terms of absorption capacity, cyclic capacity, absorption and regeneration rates, and heats of absorption and regeneration. However, for industrial applications, further investigations to evaluate mass transfer coefficient data for the absorption column need to be determined. Corrosion is one of the main concerns in industry. Therefore, investigating the corrosion characteristics of the new amine solvents, blended amine solvents and potential corrosion inhibitors, need to be studied before using it in an industrial plant. In addition, degradation studies are required in order to determine the solution reclaiming procedures and degradation products.



## REFERENCES

- [1] Paitoon, T. and Raphael, I. Recent Progress and New Developments in Post-Combustion Carbon-Capture Technology with Reactive Solvents. Future Science Book Series. Future Science Ltd, 2013.
- [2] Kosugi, T., et al. Time to realization: Evaluation of CO<sub>2</sub> capture technology R&Ds by GERT (Graphical Evaluation and Review Technique) analyses. Energy 29(9–10) (2004): 1297-1308.
- [3] Rochelle, G.T. Amine Scrubbing for CO<sub>2</sub> Capture. Science 325(5948) (2009): 1652-1654.
- [4] Yang, H., et al. Progress in carbon dioxide separation and capture: A review. Journal of Environmental Sciences 20(1) (2008): 14-27.
- [5] Bernardo, P., Drioli, E., and Golemme, G. Membrane Gas Separation: A Review/State of the Art. Industrial & Engineering Chemistry Research 48(10) (2009): 4638-4663.
- [6] Perry, R.J. and O'Brien, M.J. Amino Disiloxanes for CO<sub>2</sub> Capture. Energy & Fuels 25(4) (2011): 1906-1918.
- [7] Zhou, Q., Chan, C.W., Tontiwachiwuthikul, P., Idem, R., and Gelowitz, D. A statistical analysis of the carbon dioxide capture process. International Journal of Greenhouse Gas Control 3(5) (2009): 535-544.
- [8] Figueroa, J.D., Fout, T., Plasynski, S., McIlvried, H., and Srivastava, R.D. Advances in CO<sub>2</sub> capture technology—The U.S. Department of Energy's Carbon Sequestration Program. International Journal of Greenhouse Gas Control 2(1) (2008): 9-20.

- [9] Rubin, E.S., Mantripragada, H., Marks, A., Versteeg, P., and Kitchin, J. The outlook for improved carbon capture technology. Progress in Energy and Combustion Science 38(5) (2012): 630-671.
- [10] Lee, A.S. and Kitchin, J.R. Chemical and Molecular Descriptors for the Reactivity of Amines with CO<sub>2</sub>. Industrial & Engineering Chemistry Research 51(42) (2012): 13609-13618.
- [11] Rao, A.B. and Rubin, E.S. A Technical, Economic, and Environmental Assessment of Amine-Based CO<sub>2</sub> Capture Technology for Power Plant Greenhouse Gas Control. Environmental Science & Technology 36(20) (2002): 4467-4475.
- [12] Dixon, T., et al. GHGT-11 Proceedings of the 11<sup>th</sup> International Conference on Greenhouse Gas Control Technologies, 18-22 November 2012, Kyoto, Japan Synthesis and characterization of new absorbents for CO<sub>2</sub> capture. Energy Procedia 37 (2013): 265-272.
- [13] Yamada, H., Chowdhury, F.A., Goto, K., and Higashii, T. CO<sub>2</sub> solubility and species distribution in aqueous solutions of 2-(isopropylamino)ethanol and its structural isomers. International Journal of Greenhouse Gas Control 17 (2013): 99-105.
- [14] Rokke, N.A., Hagg, M.-B., Mazzetti, M.J., Bröder, P., and Svendsen, H.F. The 6<sup>th</sup> Trondheim Conference on CO<sub>2</sub> Capture, Transport and Storage Capacity and Kinetics of Solvents for Post-Combustion CO<sub>2</sub> Capture. Energy Procedia 23 (2012): 45-54.

- [15] Puxty, G., et al. Carbon Dioxide Postcombustion Capture: A Novel Screening Study of the Carbon Dioxide Absorption Performance of 76 Amines. Environmental Science & Technology 43(16) (2009): 6427-6433.
- [16] Rayer, A.V., Henni, A., and Li, J. Reaction kinetics of 2-((2-aminoethyl) amino) ethanol in aqueous and non-aqueous solutions using the stopped-flow technique. The Canadian Journal of Chemical Engineering 91(3) (2013): 490-498.
- [17] Henni, A., Li, J., and Tontiwachwuthikul, P. Reaction Kinetics of CO<sub>2</sub> in Aqueous 1-Amino-2-Propanol, 3-Amino-1-Propanol, and Dimethylmonoethanolamine Solutions in the Temperature Range of 298–313 K Using the Stopped-Flow Technique. Industrial & Engineering Chemistry Research 47(7) (2008): 2213-2220.
- [18] Li, J., Henni, A., and Tontiwachwuthikul, P. Reaction Kinetics of CO<sub>2</sub> in Aqueous Ethylenediamine, Ethyl Ethanolamine, and Diethyl Monoethanolamine Solutions in the Temperature Range of 298–313 K, Using the Stopped-Flow Technique. Industrial & Engineering Chemistry Research 46(13) (2007): 4426-4434.
- [19] Couchaux, G., Barth, D., Jacquin, M., Faraj, A., and Grandjean, J. Kinetics of Carbon Dioxide with Amines. I. Stopped-Flow Studies in Aqueous Solutions. A Review. Oil Gas Sci. Technol. – Rev. IFP Energies nouvelles 69(5) (2014): 865-884.
- [20] Ali, S.H. Kinetics of the reaction of carbon dioxide with blends of amines in aqueous media using the stopped-flow technique. International Journal of Chemical Kinetics 37(7) (2005): 391-405.

- [21] Li, J. Kinetic study of CO<sub>2</sub> and alkanolamines both in aqueous and non-aqueous solutions using the stopped flow technique. Master degree thesis, Engineering University of Regina, 2007.
- [22] Kadiwala, S., Rayer, A.V., and Henni, A. Kinetics of carbon dioxide (CO<sub>2</sub>) with ethylenediamine, 3-amino-1-propanol in methanol and ethanol, and with 1-dimethylamino-2-propanol and 3-dimethylamino-1-propanol in water using stopped-flow technique. Chemical Engineering Journal 179 (2012): 262-271.
- [23] Liu, H., et al. Kinetics of CO<sub>2</sub> absorption into a novel 1-diethylamino-2-propanol solvent using stopped-flow technique. AIChE Journal 60(10) (2014): 3502-3510.
- [24] Liu, H., et al. CO<sub>2</sub> absorption kinetics of 4-diethylamine-2-butanol solvent using stopped-flow technique. Separation and Purification Technology 136 (2014): 81-87.
- [25] Li, J., et al. Experimental study of the kinetics of the homogenous reaction of CO<sub>2</sub> into a novel aqueous 3-diethylamino-1,2-propanediol solution using the stopped-flow technique. Chemical Engineering Journal 270 (2015): 485-495.
- [26] Sema, T., Naami, A., Idem, R., and Tontiwachwuthikul, P. Correlations for Equilibrium Solubility of Carbon Dioxide in Aqueous 4-(Diethylamino)-2-butanol Solutions. Industrial & Engineering Chemistry Research 50(24) (2011): 14008-14015.
- [27] Tontiwachwuthikul, P., et al. Method of capturing carbon dioxide from gas streams. 2011, Google Patents.



- [28] Gale, J., et al. Greenhouse Gas Control Technologies 9 Synthesis, solubilities, and cyclic capacities of amino alcohols for CO<sub>2</sub> capture from flue gas streams. Energy Procedia 1(1) (2009): 1327-1334.
- [29] Singto, S., et al. Synthesis of new amines for enhanced carbon dioxide (CO<sub>2</sub>) capture performance: The effect of chemical structure on equilibrium solubility, cyclic capacity, kinetics of absorption and regeneration, and heats of absorption and regeneration. Separation and Purification Technology 167 (2016): 97-107.
- [30] (IEA), T.I.E.A. World Energy Outlook 2015 [Online]. 2015.
- [31] Liang, Z., et al. Recent progress and new developments in post-combustion carbon-capture technology with amine based solvents. International Journal of Greenhouse Gas Control 40 (2015): 26-54.
- [32] Dargah, F.P. Development of On-Line Analytical Technique for Determination of Composition of CO<sub>2</sub>-Loaded Formulated Amine Solvents Based on the Liquid Thermo physical Properties for a Post-Combustion CO<sub>2</sub> Capture Process Ph.D., Industrial Systems Engineering University of Regina, 2015.
- [33] Chow, J.C., et al. Separation and Capture of CO<sub>2</sub> from Large Stationary Sources and Sequestration in Geological Formations. Journal of the Air & Waste Management Association 53(10) (2003): 1172-1182.
- [34] Naami, A. Mass Transfer Studies of Carbon Dioxide Absorption into Aqueous Solutions of 4-(Diethylamine)-2-Butanol, Blended Monoethanolamine with 4-(Diethylamine)-2-Butanol, and Blended Monoethanolamine with

- Methyldiethanolamine Ph.D. , Industrial Systems Engineering University of Regina 2012.
- [35] Brunetti, A., Scura, F., Barbieri, G., and Drioli, E. Membrane technologies for CO<sub>2</sub> separation. Journal of Membrane Science 359(1–2) (2010): 115-125.
- [36] deMontigny, D. Comparing Packed Columns and Membrane Absorbers for CO<sub>2</sub> Capture. Ph.D. thesis, Engineering University of Regina, 2004.
- [37] Bello, A. and Idem, R.O. Pathways for the Formation of Products of the Oxidative Degradation of CO<sub>2</sub>-Loaded Concentrated Aqueous Monoethanolamine Solutions during CO<sub>2</sub> Absorption from Flue Gases. Industrial & Engineering Chemistry Research 44(4) (2005): 945-969.
- [38] Kohl, A.L. and Nielsen, R.B. Chapter 2 - Alkanolamines for Hydrogen Sulfide and Carbon Dioxide Removal. in Gas Purification (Fifth Edition), pp. 40-186. Houston: Gulf Professional Publishing, 1997.
- [39] Sema, T., et al. Part 5b: Solvent chemistry: reaction kinetics of CO<sub>2</sub> absorption into reactive amine solutions. Carbon Management 3(2) (2012): 201-220.
- [40] Chakravarty, T., Phukan, U.K., and Weiland, R.H. Reaction of acid gases with mixtures of amines. Journal Name: Chem. Eng. Prog.: (United States); Journal Volume: 81:4 (1985): Medium: X; Size: Pages: 32-36.
- [41] Rayer, A.V., Sumon, K.Z., Sema, T., Henni, A., Idem, R.O., and Tontiwachwuthikul, P. Part 5c: Solvent chemistry: solubility of CO<sub>2</sub> in reactive solvents for post-combustion CO<sub>2</sub>. Carbon Management 3(5) (2012): 467-484.
- [42] Maneeintr, K. New solvent for acid gas separation. Ph.D. thesis, Industrial Systems Engineering University of Regina, 2009.

- [43] McCullough, J.G., Faucher, J.A., Kubek, D.J., and Barr, K.J. Alkanolamine gas treating composition and process. 1990, Google Patents.
- [44] Pushkar, S. Use of mixed amines for CO<sub>2</sub> removal. Master degree thesis, Chemical and Petroleum Engineering University of Calgary, 1993.
- [45] Li, Y.-G. and Mather, A.E. Correlation and Prediction of the Solubility of Carbon Dioxide in a Mixed Alkanolamine Solution. Industrial & Engineering Chemistry Research 33(8) (1994): 2006-2015.
- [46] Chakravarti, S. and Gupta, A. Carbon dioxide recovery with composite amine blends. 2000, Google Patents.
- [47] Sema, T. Kinetics of Carbon Dioxide Absorption into Aqueous Solutions of 4-(Diethylamino)-2-Butanol and Blended Monoethanolamine and 4-(Diethylamino)-2-Butanol Ph.D. thesis, Industrial System Engineering University of Regina, 2011.
- [48] Silva, E.F.d. Computational Chemistry Study of Solvents for Carbon Dioxide Absorption Ph.D. thesis, Science and Technology Norwegian University of Science and Technology, 2005.
- [49] Gale, J., et al. 10<sup>th</sup> International Conference on Greenhouse Gas Control Technologies Synthesis and selection of hindered new amine absorbents for CO<sub>2</sub> capture. Energy Procedia 4 (2011): 201-208.
- [50] Caplow, M. Kinetics of carbamate formation and breakdown. Journal of the American Chemical Society 90(24) (1968): 6795-6803.
- [51] Versteeg, G.F. and van Swaij, W.P.M. On the kinetics between CO<sub>2</sub> and alkanolamines both in aqueous and non-aqueous solutions—II. Tertiary amines. Chemical Engineering Science 43(3) (1988): 587-591.

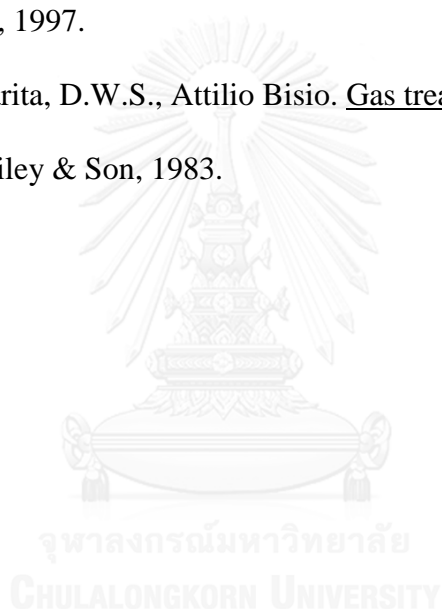
- [52] Donaldson, T.L. and Nguyen, Y.N. Carbon Dioxide Reaction Kinetics and Transport in Aqueous Amine Membranes. Industrial & Engineering Chemistry Fundamentals 19(3) (1980): 260-266.
- [53] Li, M.-H. and Lie, Y.-C. Densities and Viscosities of Solutions of Monoethanolamine + N-methyldiethanolamine + Water and Monoethanolamine + 2-Amino-2-methyl-1-propanol + Water. Journal of Chemical & Engineering Data 39(3) (1994): 444-447.
- [54] Rinker, E.B., Oelschlager, D.W., Colussi, A.T., Henry, K.R., and Sandall, O.C. Viscosity, Density, and Surface Tension of Binary Mixtures of Water and N-Methyldiethanolamine and Water and Diethanolamine and Tertiary Mixtures of These Amines with Water over the Temperature Range 20-100.degree.C. Journal of Chemical & Engineering Data 39(2) (1994): 392-395.
- [55] Mandal, B.P., Kundu, M., and Bandyopadhyay, S.S. Density and Viscosity of Aqueous Solutions of (N-Methyldiethanolamine + Monoethanolamine), (N-Methyldiethanolamine + Diethanolamine), (2-Amino-2-methyl-1-propanol + Monoethanolamine), and (2-Amino-2-methyl-1-propanol + Diethanolamine). Journal of Chemical & Engineering Data 48(3) (2003): 703-707.
- [56] Singh, P., Niederer, J.P.M., and Versteeg, G.F. Structure and activity relationships for amine based CO<sub>2</sub> absorbents—I. International Journal of Greenhouse Gas Control 1(1) (2007): 5-10.
- [57] Singh, P., Niederer, J.P.M., and Versteeg, G.F. Structure and activity relationships for amine-based CO<sub>2</sub> absorbents-II. Chemical Engineering Research and Design 87(2) (2009): 135-144.

- [58] Maneeintr, K., Henni, A., Idem, R.O., Tontiwachwuthikul, P., and Wee, A.G.H. Physical and transport properties of aqueous amino alcohol solutions for CO<sub>2</sub> capture from flue gas streams. Process Safety and Environmental Protection 86(4) (2008): 291-295.
- [59] Aroonwilas, A. and Veawab, A. Characterization and Comparison of the CO<sub>2</sub> Absorption Performance into Single and Blended Alkanolamines in a Packed Column. Industrial & Engineering Chemistry Research 43(9) (2004): 2228-2237.
- [60] Li, J., Mundhwa, M., Tontiwachwuthikul, P., and Henni, A. Volumetric Properties, Viscosities, and Refractive Indices for Aqueous 2-(Methylamino)ethanol Solutions from (298.15 to 343.15) K. Journal of Chemical & Engineering Data 52(2) (2007): 560-565.
- [61] Chowdhury, F.I., Akhtar, S., and Saleh†, M.A. Densities and excess molar volumes of aqueous solutions of some diethanolamines. Physics and Chemistry of Liquids 47(6) (2009): 638-652.
- [62] Horwitz, W. Association of Official Analytical Chemists (AOAC), ed. edition, t. USA: George Banta, 1975.
- [63] Manabe, K. and Kobayashi, S. Mannich-Type Reactions of Aldehydes, Amines, and Ketones in a Colloidal Dispersion System Created by a Brønsted Acid–Surfactant-Combined Catalyst in Water. Organic Letters 1(12) (1999): 1965-1967.
- [64] Pishawikar, S.A. and MORE, H.N. Synthesis of mannish bases of thiosemicarbazide as DNA polymerase inhibitors and novel antibacterial agents. Int. J. Biol. Sci 4 (2013): 549-556.

- [65] Benamor, A. and Aroua, M.K. Modeling of CO<sub>2</sub> solubility and carbamate concentration in DEA, MDEA and their mixtures using the Deshmukh–Mather model. Fluid Phase Equilibria 231(2) (2005): 150-162.
- [66] Baek, J.-I. and Yoon, J.-H. Solubility of Carbon Dioxide in Aqueous Solutions of 2-Amino-2-methyl-1,3-propanediol. Journal of Chemical & Engineering Data 43(4) (1998): 635-637.
- [67] Liang, Y., Liu, H., Rongwong, W., Liang, Z., Idem, R., and Tontiwachwuthikul, P. Solubility, absorption heat and mass transfer studies of CO<sub>2</sub> absorption into aqueous solution of 1-dimethylamino-2-propanol. Fuel 144 (2015): 121-129.
- [68] Kim, I. and Svendsen, H.F. Heat of Absorption of Carbon Dioxide (CO<sub>2</sub>) in Monoethanolamine (MEA) and 2-(Aminoethyl)ethanolamine (AEEA) Solutions. Industrial & Engineering Chemistry Research 46(17) (2007): 5803-5809.
- [69] Rho, S.-W., Yoo, K.-P., Lee, J.S., Nam, S.C., Son, J.E., and Min, B.-M. Solubility of CO<sub>2</sub> in Aqueous Methyldiethanolamine Solutions. Journal of Chemical & Engineering Data 42(6) (1997): 1161-1164.
- [70] Lee, J.I., Otto, F.D., and Mather, A.E. Solubility of carbon dioxide in aqueous diethanolamine solutions at high pressures. Journal of Chemical & Engineering Data 17(4) (1972): 465-468.
- [71] Carson, J.K., Marsh, K.N., and Mather, A.E. Enthalpy of solution of carbon dioxide in (water + monoethanolamine, or diethanolamine, or N-methyldiethanolamine) and (water + monoethanolamine + N-

- methyldiethanolamine) at  $T = 298.15$  K. The Journal of Chemical Thermodynamics 32(9) (2000): 1285-1296.
- [72] Hamborg, E.S. and Versteeg, G.F. Dissociation Constants and Thermodynamic Properties of Amines and Alkanolamines from (293 to 353) K. Journal of Chemical & Engineering Data 54(4) (2009): 1318-1328.
- [73] Crooks, J.E. and Donnellan, J.P. Kinetics of the reaction between carbon dioxide and tertiary amines. The Journal of Organic Chemistry 55(4) (1990): 1372-1374.
- [74] Shi, H., Sema, T., Naami, A., Liang, Z., Idem, R., and Tontiwachwuthikul, P.  $^{13}\text{C}$  NMR Spectroscopy of a Novel Amine Species in the DEAB– $\text{CO}_2$ – $\text{H}_2\text{O}$  system: VLE Model. Industrial & Engineering Chemistry Research 51(25) (2012): 8608-8615.
- [75] Shi, H., Naami, A., Idem, R., and Tontiwachwuthikul, P. Catalytic and non catalytic solvent regeneration during absorption-based  $\text{CO}_2$  capture with single and blended reactive amine solvents. International Journal of Greenhouse Gas Control 26 (2014): 39-50.
- [76] Cengel, Y.A. Heat transfers a practical approach, ed. edition, n.: McGraw-Hill, New York, 2003.
- [77] Knipe, A.C., McLean, D., and Tranter, R.L. A fast response conductivity amplifier for chemical kinetics. Journal of Physics E: Scientific Instruments 7(7) (1974): 586.
- [78] Gale, J., et al. Greenhouse Gas Control Technologies 9Development of novel tertiary amine absorbents for  $\text{CO}_2$  capture. Energy Procedia 1(1) (2009): 1241-1248.

- [79] da Silva, E.F. and Svendsen, H.F. Prediction of the pKa Values of Amines Using ab Initio Methods and Free-Energy Perturbations. Industrial & Engineering Chemistry Research 42(19) (2003): 4414-4421.
- [80] Chowdhury, F.A., Yamada, H., Higashii, T., Goto, K., and Onoda, M. CO<sub>2</sub> Capture by Tertiary Amine Absorbents: A Performance Comparison Study. Industrial & Engineering Chemistry Research 52(24) (2013): 8323-8331.
- [81] Arthur Kohl, R.N. Gas purification. 4<sup>th</sup> edition ed. Houston, TX: Gulf Publishing Co, 1997.
- [82] Giovanni Astarita, D.W.S., Attilio Bisio. Gas treating with chemical solvents. New York: Wiley & Son, 1983.





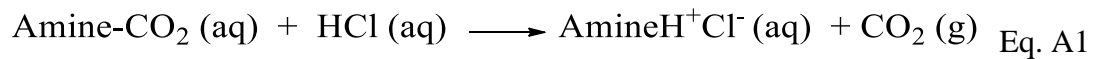
## APPENDIX



จุฬาลงกรณ์มหาวิทยาลัย  
CHULALONGKORN UNIVERSITY

### Appendix A: Determination of CO<sub>2</sub> concentration in amine samples

The total amine was determined by titration with standard 1 N HCl to methyl orange end-point as shown in Equation A1.



The CO<sub>2</sub> loading ( $\alpha$ ) for all amines is defined as the mol of CO<sub>2</sub> divided by mol of amine and calculated by using Equation A2.

$$\text{CO}_2 \text{ loading} = \frac{\frac{V_{\text{CO}_2}}{V_{\text{gas at STP}}}}{C_{\text{amine}} \times V_{\text{amine}}} \quad \text{Eq. A2}$$

Where,  $V_{\text{CO}_2}$  is volume of CO<sub>2</sub> collected in displacement solution (L)

$V_{\text{gas at STP}}$  is volume of gas at 22.41 L/mol

$C_{\text{amine}}$  is concentration of amine (mol/L)

$V_{\text{amine}}$  is volume of amine (L)

## Appendix B: Kinetic reaction from stopped-flow apparatus determination

The observed pseudo first-order rate constant ( $k_0$ ) was automatically generated based on the typical graph of the change of conductivity in solution versus time as shown in Figure B.

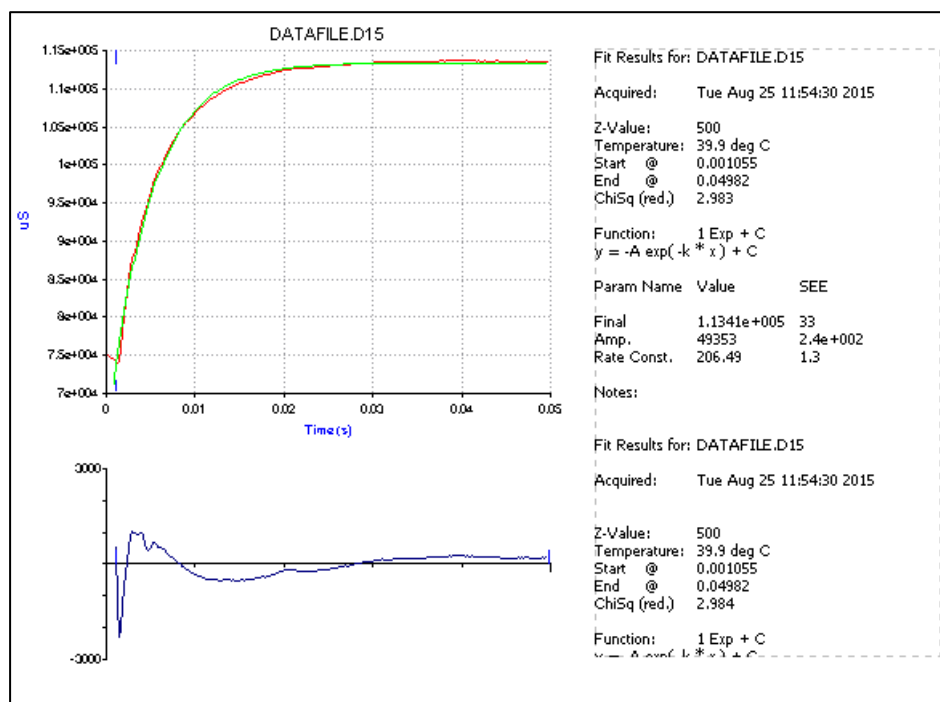


Figure B. The plot of the conductivity against time.

Table B1 Experimental data for the observed pseudo first-order rate constant ( $k_0$ ) into aqueous solution of DMAB

Amine	runs	25 °C		30 °C		35 °C		40 °C	
		$K_0$	Error	$K_0$	Error	$K_0$	Error	$K_0$	Error
DMAB at 0.1 M	1	2.23	0.024	3.70	0.037	4.87	0.052	6.32	0.070
	2	2.45	0.036	3.64	0.048	5.13	0.042	6.26	0.076
	3	2.53	0.019	3.79	0.059	5.04	0.060	6.31	0.070
	4	2.22	0.028	3.75	0.048	4.63	0.053	6.17	0.073
	5	2.19	0.038	3.65	0.045	4.92	0.064	6.29	0.040
	6	2.33	0.034	3.67	0.044	4.69	0.054	6.52	0.082
	7	2.27	0.029	3.66	0.048	4.75	0.061	6.36	0.047
	8	2.55	0.028	3.69	0.040	4.87	0.059	6.25	0.076
	9	2.02	0.032	3.67	0.048	5.02	0.060	6.34	0.071
	10	2.24	0.028	3.75	0.042	4.67	0.040	6.19	0.062
	Average	2.30	0.030	3.70	0.046	4.86	0.055	6.30	0.067

Amine	runs	25 °C		30 °C		35 °C		40 °C	
		$K_0$	Error	$K_0$	Error	$K_0$	Error	$K_0$	Error
DMAB at 0.2 M	1	3.88	0.037	6.65	0.047	7.50	0.062	11.47	0.100
	2	3.85	0.038	6.64	0.048	7.53	0.062	11.31	0.076
	3	3.93	0.009	6.47	0.078	7.61	0.060	10.51	0.070
	4	3.82	0.038	6.68	0.048	7.43	0.056	10.57	0.010
	5	3.89	0.038	6.61	0.049	7.32	0.064	12.01	0.090
	6	3.83	0.038	6.47	0.048	7.39	0.064	10.62	0.062
	7	3.87	0.009	6.62	0.048	7.55	0.061	10.92	0.064
	8	3.85	0.038	6.58	0.048	7.60	0.069	10.91	0.071
	9	3.92	0.038	6.57	0.048	7.48	0.060	10.93	0.071
	10	3.94	0.038	6.65	0.048	7.47	0.070	11.14	0.089
	Average	3.88	0.032	6.59	0.051	7.49	0.063	11.04	0.070

Amine	runs	25 °C		30 °C		35 °C		40 °C	
		$K_0$	Error	$K_0$	Error	$K_0$	Error	$K_0$	Error
DMAB at 0.4 M	1	10.23	0.069	14.53	0.089	18.97	0.120	26.61	0.150
	2	10.25	0.067	14.08	0.091	19.80	0.110	26.11	0.176
	3	10.25	0.067	15.19	0.091	18.67	0.120	25.90	0.170
	4	10.08	0.067	15.25	0.09	19.41	0.110	25.47	0.160
	5	10.01	0.067	14.55	0.091	18.71	0.110	25.98	0.210
	6	9.86	0.069	14.48	0.091	18.58	0.140	25.71	0.017
	7	9.40	0.067	14.03	0.095	18.67	0.170	25.73	0.021
	8	9.54	0.067			18.67	0.160		
	9	9.30	0.070						
	10								
	Average		9.88	0.068	14.59	0.091	18.93	0.130	25.93

Amine	runs	25 °C		30 °C		35 °C		40 °C	
		$K_0$	Error	$K_0$	Error	$K_0$	Error	$K_0$	Error
DMAB at 0.6 M	1	12.63	0.068	19.57	0.095	27.36	0.210	39.78	0.220
	2	12.59	0.064	19.49	0.094	26.36	0.210	39.64	0.220
	3	12.21	0.067	18.67	0.097	26.82	0.210	38.18	0.200
	4	11.73	0.062	18.37	0.100	25.52	0.200	37.11	0.220
	5	11.35	0.064	18.33	0.110	25.36	0.180	37.78	0.240
	6	11.22	0.063	18.29	0.120	25.26	0.170	37.35	0.220
	7	11.23	0.067	18.21	0.110	25.11	0.200	36.78	0.320
	8	11.10	0.070					36.10	0.320
	9	11.03	0.072					36.02	0.330
	10								
	Average		11.68	0.066	18.70	0.104	25.97	0.197	37.64

Amine	runs	25 °C		30 °C		35 °C		40 °C	
		$K_0$	Error	$K_0$	Error	$K_0$	Error	$K_0$	Error
DMAB at 0.8 M	1	16.30	0.080	24.35	0.120	35.96	0.180	50.78	0.315
	2	15.66	0.090	24.13	0.130	35.85	0.170	50.69	0.280
	3	15.10	0.098	24.86	0.135	34.55	0.160	49.98	0.280
	4	14.60	0.112	23.20	0.145	33.16	0.210	48.21	0.274
	5	14.31	0.100	23.11	0.155	32.44	0.170	46.44	0.310
	6	14.62	0.120	22.95	0.165	31.36	0.180	45.64	0.288
	7	14.20	0.111	21.42	0.155	31.62	0.210	44.00	0.430
	8	14.34	0.099	21.27	0.155	30.32	0.200		
	9	14.10	0.100						
	10								
	Average		14.80	0.101	23.16	0.145	33.16	0.185	47.96

Amine	runs	25 °C		30 °C		35 °C		40 °C	
		$K_0$	Error	$K_0$	Error	$K_0$	Error	$K_0$	Error
DMAB at 1.0 M	1	20.17	0.188	28.75	0.195	41.66	0.350	57.44	0.360
	2	19.98	0.110	28.26	0.225	40.10	0.340	56.71	0.506
	3	19.77	0.160	27.71	0.205	39.38	0.333	56.16	0.567
	4	19.76	0.148	27.53	0.185	38.25	0.311	55.78	0.498
	5	19.56	0.190	26.45	0.188	37.15	0.350	54.67	0.660
	6	18.26	0.180	25.58	0.191	36.56	0.410	54.79	0.730
	7	18.30	0.218	24.22	0.192	36.32	0.440	53.47	0.800
	8	18.76	0.228	23.67	0.240				
	9	18.12	0.220						
	10								
	Average		19.19	0.182	26.52	0.203	38.49	0.362	55.57

Table B2 Experimental data for the observed pseudo first-order rate constant ( $k_0$ ) into aqueous solution of DEAB

Amine	runs	25 °C		30 °C		35 °C		40 °C	
		$K_0$	Error	$K_0$	Error	$K_0$	Error	$K_0$	Error
DEAB at 0.1 M	1	9.77	0.051	13.25	0.072	21.37	0.100	32.12	0.160
	2	9.42	0.052	13.33	0.068	20.23	0.110	31.68	0.177
	3	9.27	0.052	12.12	0.071	20.07	0.092	30.55	0.143
	4	9.14	0.050	12.01	0.070	20.17	0.140	30.47	0.160
	5	9.78	0.051	12.16	0.071	19.43	0.130	30.32	0.155
	6	9.03	0.047	12.21	0.068	19.21	0.110	30.42	0.189
	7	9.01	0.050	11.79	0.059	19.79	0.200	29.77	0.188
	8	8.42	0.051	11.74	0.064	18.17	0.150	29.32	0.165
	9	8.16	0.051	10.89	0.071	18.44	0.122	28.62	0.161
	10	8.01	0.053	10.53	0.070	18.11	0.094	28.18	0.168
	Average	9.00	0.051	12.00	0.068	19.50	0.125	30.15	0.167

Amine	runs	25 °C		30 °C		35 °C		40 °C	
		$K_0$	Error	$K_0$	Error	$K_0$	Error	$K_0$	Error
DEAB at 0.2 M	1	13.91	0.011	19.58	0.045	30.36	0.042	41.91	0.080
	2	13.88	0.010	19.32	0.032	30.11	0.034	41.75	0.070
	3	13.72	0.012	18.67	0.040	29.86	0.040	41.68	0.067
	4	13.41	0.013	18.41	0.041	29.49	0.041	40.91	0.058
	5	12.75	0.010	18.31	0.042	28.76	0.040	40.58	0.080
	6	12.22	0.009	18.29	0.048	28.36	0.042	39.75	0.077
	7	12.13	0.010	17.61	0.040	27.40	0.042	38.78	0.056
	8	11.12	0.010	17.35	0.048	27.28	0.043	38.40	0.078
	9	11.03	0.012	17.11	0.039			38.89	0.082
	10								
	Average	12.69	0.011	18.60	0.042	28.95	0.041	40.29	0.072

Amine	runs	25 °C		30 °C		35 °C		40 °C	
		$K_0$	Error	$K_0$	Error	$K_0$	Error	$K_0$	Error
DEAB at 0.4 M	1	26.91	0.018	38.58	0.047	50.33	0.082	67.71	0.180
	2	26.75	0.018	37.32	0.050	49.11	0.085	66.25	0.160
	3	25.93	0.014	36.99	0.064	49.01	0.070	65.18	0.173
	4	25.27	0.019	36.77	0.069	48.37	0.098	65.16	0.189
	5	24.91	0.017	36.95	0.054	47.53	0.078	65.40	0.183
	6	24.55	0.016	35.65	0.044	47.13	0.072	64.23	0.177
	7	23.47	0.013	35.31	0.066	46.31	0.073	64.09	0.177
	8	23.34	0.011			46.17	0.072	64.09	0.189
	9	23.10	0.014						
	10								
	Average		24.91	0.016	36.80	0.056	48.00	0.080	65.26

Amine	runs	25 °C		30 °C		35 °C		40 °C	
		$K_0$	Error	$K_0$	Error	$K_0$	Error	$K_0$	Error
DEAB at 0.6 M	1	36.43	0.088	52.28	0.035	67.33	0.042	87.71	0.280
	2	36.15	0.080	51.54	0.033	66.74	0.065	86.41	0.340
	3	34.43	0.081	50.11	0.054	65.99	0.041	86.02	0.384
	4	34.00	0.082	50.08	0.037	65.33	0.055	85.51	0.364
	5	33.17	0.067	49.18	0.054	64.59	0.054	85.43	0.230
	6	33.01	0.079	49.55	0.044	64.43	0.057	85.13	0.285
	7	32.71	0.067	48.73	0.066	64.05	0.044	84.02	0.430
	8	32.34	0.078	48.54	0.051	63.97	0.040	84.66	0.420
	9	32.10	0.072					83.45	0.359
	10								
	Average		33.82	0.077	50.21	0.047	65.30	0.050	85.37



Amine	runs	25 °C		30 °C		35 °C		40 °C	
		$K_0$	Error	$K_0$	Error	$K_0$	Error	$K_0$	Error
DEAB at 0.8 M	1	43.29	0.080	63.38	0.035	79.83	0.054	107.71	0.358
	2	43.32	0.083	63.13	0.033	79.54	0.045	106.51	0.330
	3	43.19	0.083	63.02	0.054	78.53	0.048	106.33	0.354
	4	42.43	0.084	62.42	0.037	78.43	0.051	105.53	0.364
	5	41.55	0.082	62.58	0.054	78.75	0.053	105.66	0.330
	6	41.25	0.080	62.65	0.044	78.49	0.059	105.55	0.385
	7	40.49	0.081	62.46	0.066	77.03	0.053	104.28	0.330
	8	40.12	0.081	62.02	0.051	76.49	0.047	104.01	0.430
	9								
	10								
	Average		41.96	0.082	62.81	0.047	78.39	0.051	105.70

Amine	runs	25 °C		30 °C		35 °C		40 °C	
		$K_0$	Error	$K_0$	Error	$K_0$	Error	$K_0$	Error
DEAB at 1.0 M	1	48.67	0.080	73.38	0.185	92.38	0.236	127.75	0.458
	2	48.45	0.083	73.13	0.143	91.57	0.245	126.31	0.353
	3	48.49	0.083	72.67	0.153	91.33	0.248	125.41	0.364
	4	48.13	0.084	72.85	0.156	91.17	0.231	125.53	0.364
	5	47.64	0.082	72.58	0.153	90.38	0.243	125.75	0.383
	6	47.35	0.080	71.65	0.163	90.13	0.259	124.31	0.405
	7	46.65	0.081	71.46	0.174	89.50	0.263	123.64	0.345
	8	46.53	0.081	70.21	0.172	89.71	0.245	123.53	0.480
	9	45.46	0.085	70.11	0.170	89.54	0.245	123.40	0.369
	10	45.09	0.082						
	Average		47.25	0.082	72.00	0.163	90.63	0.246	125.07

Table B3 Experimental data for the observed pseudo first-order rate constant ( $k_0$ ) into aqueous solution of HEMAB

Amine	runs	25 °C		30 °C		35 °C		40 °C	
		$K_0$	Error	$K_0$	Error	$K_0$	Error	$K_0$	Error
HEMAB at 0.1 M	1	98.77	0.241	121.25	0.346	169.50	0.784	217.12	1.828
	2	97.33	0.243	120.32	0.374	168.12	0.766	216.45	1.950
	3	96.03	0.244	119.35	0.362	168.66	0.770	216.61	1.715
	4	96.33	0.257	118.75	0.371	168.45	0.787	215.94	1.880
	5	94.66	0.276	118.99	0.358	167.44	0.788	215.62	1.860
	6	94.21	0.256	117.81	0.348	167.25	0.815	214.72	1.770
	7	94.55	0.266	116.94	0.352	166.12	0.876	214.93	1.820
	8	94.47	0.265	116.65	0.345	165.87	0.856	213.63	1.920
	9	93.41	0.271	116.45	0.372	164.43	0.754		
	10	92.27	0.277			164.11	0.816		
	Average		95.20	0.260	118.50	0.359	167.00	0.801	215.63

Amine	runs	25 °C		30 °C		35 °C		40 °C	
		$K_0$	Error	$K_0$	Error	$K_0$	Error	$K_0$	Error
HEMAB at 0.2 M	1	253.44	0.251	273.69	0.472	333.50	0.900	374.12	3.160
	2	252.21	0.276	272.47	0.468	332.53	1.110	372.45	3.177
	3	251.09	0.256	271.71	0.471	331.12	0.920	370.61	3.143
	4	250.69	0.275	271.37	0.470	330.50	1.140	370.64	3.160
	5	250.47	0.266	270.67	0.471	329.18	1.130	369.32	3.155
	6	249.39	0.287	269.17	0.468	328.86	9.110	369.21	3.189
	7	249.54	0.266	268.40	0.459	327.67	1.226	368.21	3.188
	8	248.44	0.265	268.41	0.464	326.62	1.233	367.54	3.133
	9	247.41	0.275	267.11	0.464			367.89	3.138
	10	247.32	0.287	267.00	0.433				
	Average		250.00	0.270	270.00	0.464	330.00	2.096	370.00

Amine	runs	25 °C		30 °C		35 °C		40 °C	
		$K_0$	Error	$K_0$	Error	$K_0$	Error	$K_0$	Error
HEMAB at 0.3 M	1	333.64	0.351	367.78	0.753	470.61	2.521	542.12	4.266
	2	332.13	0.452	366.21	0.780	469.65	2.551	541.64	4.377
	3	331.20	0.500	365.42	0.810	468.56	2.592	540.09	4.431
	4	331.50	0.554	365.21	0.781	467.11	2.284	540.55	4.336
	5	329.14	0.551	364.21	0.830	466.21	2.553	539.29	4.255
	6	329.70	0.567	363.54	0.777	465.11	2.661	539.12	4.323
	7	329.97	0.531	362.52	0.789	464.69	2.721	538.22	4.288
	8	329.62	0.453	362.21	0.814	464.05	2.682	537.65	4.242
	9	328.52	0.561	362.05	0.764			537.41	4.298
	10								
	Average		330.60	0.502	364.35	0.789	467.00	2.571	539.57

Amine	runs	25 °C		30 °C		35 °C		40 °C	
		$K_0$	Error	$K_0$	Error	$K_0$	Error	$K_0$	Error
HEMAB at 0.4 M	1	479.64	0.551	506.22	0.711	599.41	2.100	722.82	4.160
	2	478.01	0.523	506.18	0.764	598.53	2.110	722.32	4.270
	3	477.85	0.521	505.12	0.763	598.11	2.092	722.10	4.243
	4	476.45	0.533	504.54	0.786	597.68	2.140	721.64	4.184
	5	475.66	0.510	503.77	0.713	596.22	2.130	720.58	4.175
	6	475.34	0.470	503.38	0.868	595.49	2.110	720.45	4.122
	7	474.27	0.522	502.35	0.819	595.41	2.200	720.55	4.188
	8	473.64	0.513	502.99	0.824	595.11	2.211	719.92	4.205
	9	473.16	0.534	501.48	0.811			718.59	4.213
	10								
	Average		476.00	0.520	504.00	0.784	597.00	2.137	721.00

Amine	runs	25 °C		30 °C		35 °C		40 °C	
		$K_0$	Error	$K_0$	Error	$K_0$	Error	$K_0$	Error
HEMAB at 0.5 M	1	576.66	1.051	608.22	2.437	699.41	3.300	860.33	5.160
	2	575.53	1.062	607.46	2.680	697.53	3.471	859.12	5.157
	3	575.11	1.068	606.22	2.710	696.11	3.392	859.10	5.143
	4	574.36	1.060	606.54	2.733	695.68	3.400	858.44	5.162
	5	574.22	1.064	605.27	2.724	695.22	3.630	857.18	5.165
	6	574.49	1.067	605.12	2.680	695.62	3.581	857.65	5.174
	7	573.11	1.050	605.35	2.590	694.41	3.672	857.48	5.177
	8	572.19	1.071	605.65	2.644	694.04	3.672	856.51	5.183
	9	572.17	1.069	604.18	2.444			856.22	5.188
	10	572.18	1.073						
	Average		574.00	1.064	606.00	2.627	696.00	3.515	858.00



Table B4 Experimental data for the observed pseudo first-order rate constant ( $k_0$ ) into aqueous solution of HEEAB

Amine	runs	25 °C		30 °C		35 °C		40 °C	
		$K_0$	Error	$K_0$	Error	$K_0$	Error	$K_0$	Error
HEEAB at 0.1 M	1	132.77	0.244	203.25	0.358	249.09	0.815	283.55	1.868
	2	131.44	0.243	203.52	0.348	248.19	0.876	283.45	1.777
	3	131.21	0.276	202.30	0.352	247.32	0.856	282.61	1.829
	4	130.33	0.256	201.93	0.345	247.29	0.754	281.34	1.920
	5	130.56	0.266	201.15	0.360	246.11	0.816	281.62	1.980
	6	130.46	0.256	201.85	0.378	246.54	0.832	281.72	1.880
	7	129.88	0.266	200.52	0.370	246.55	0.886	281.93	1.925
	8	129.48	0.267	199.94	0.375	245.58	0.867	280.81	1.943
	9	129.81	0.273	199.75	0.388	245.32	0.790	280.93	1.941
	10	128.05	0.272			245.32	0.898		
	Average		130.40	0.262	201.58	0.364	246.73	0.839	282.00

Amine	runs	25 °C		30 °C		35 °C		40 °C	
		$K_0$	Error	$K_0$	Error	$K_0$	Error	$K_0$	Error
HEEAB at 0.2 M	1	286.85	0.287	369.82	0.459	393.14	1.130	441.83	3.589
	2	286.53	0.266	368.07	0.464	392.23	9.110	441.68	3.588
	3	285.61	0.265	368.01	0.464	391.72	1.226	440.35	3.633
	4	285.34	0.275	367.12	0.433	390.83	1.233	440.54	3.734
	5	284.87	0.287	366.88	0.475	390.45	1.135	439.57	3.755
	6	284.32	0.291	366.26	0.445	389.79	9.132	439.55	3.865
	7	283.91	0.293	365.53	0.487	389.13	1.243	438.94	3.746
	8	282.13	0.299	365.80	0.443	389.07	1.245	438.76	3.776
	9	282.34	0.296	365.52	0.428	389.00	1.245	438.61	3.951
	10	282.14	0.288	365.20	0.475				
	Average		284.40	0.285	366.82	0.458	390.60	2.967	439.98

Amine	runs	25 °C		30 °C		35 °C		40 °C	
		$K_0$	Error	$K_0$	Error	$K_0$	Error	$K_0$	Error
HEEAB at 0.3 M	1	408.85	0.751	498.82	0.953	523.14	2.832	635.83	4.566
	2	407.51	0.645	498.07	0.980	521.19	2.865	634.58	4.470
	3	406.67	0.620	497.44	0.981	521.12	2.882	634.45	4.511
	4	406.32	0.655	496.12	0.781	520.23	2.840	634.44	4.536
	5	406.11	0.751	495.48	0.830	520.25	2.793	633.23	4.550
	6	405.65	0.847	495.26	1.177	519.14	2.996	632.33	4.433
	7	405.15	0.893	495.53	1.179	519.10	2.982	631.12	4.880
	8	404.88	0.885	494.70	1.814	519.09	2.882	630.07	4.672
	9	404.73	0.786	494.52	1.764	518.63	2.756	630.01	4.980
	10	404.10	0.991	494.04	1.764	518.13	2.953		
	Average		406.00	0.7825	496.00	1.222	520.00	2.878	632.90

Amine	runs	25 °C		30 °C		35 °C		40 °C	
		$K_0$	Error	$K_0$	Error	$K_0$	Error	$K_0$	Error
HEEAB at 0.4 M	1	510.25	1.215	600.82	1.711	662.14	2.353	773.85	4.560
	2	509.15	1.252	599.77	1.764	661.79	2.341	773.58	4.770
	3	509.77	1.252	598.44	1.730	661.62	2.286	772.31	4.543
	4	509.75	1.253	598.12	1.760	661.43	2.467	771.73	4.584
	5	508.34	1.251	597.48	1.734	660.65	2.640	770.49	4.575
	6	507.12	1.347	597.26	1.880	660.34	2.560	770.33	4.622
	7	507.17	1.352	596.53	1.890	659.66	2.325	769.76	4.388
	8	506.25	1.251	596.21	1.844	659.60	2.233	768.64	4.305
	9	506.11	1.334	596.45	1.840			768.27	4.521
	10	506.04	1.313						
	Average		508.00	1.279	597.90	1.795	660.90	2.401	771.00

Amine	runs	25 °C		30 °C		35 °C		40 °C	
		$K_0$	Error	$K_0$	Error	$K_0$	Error	$K_0$	Error
HEEAB at 0.5 M	1	672.25	1.785	772.52	2.680	862.84	3.630	982.75	5.757
	2	672.21	1.690	771.57	2.590	861.32	3.581	981.72	5.766
	3	671.06	1.689	771.34	2.644	861.62	3.672	981.23	5.773
	4	671.55	1.654	770.12	2.444	860.13	3.651	980.15	5.843
	5	670.34	1.641	769.38	2.752	860.05	3.730	980.44	0.975
	6	669.55	1.670	769.26	2.668	859.34	3.643	980.53	6.017
	7	668.22	1.549	769.43	2.556	858.36	3.975	979.86	6.177
	8	668.28	1.710	768.21	2.643	858.22	3.852	978.74	6.183
	9	668.26	1.645	768.15	2.664	858.10	3.821	977.42	6.188
	10	668.23	1.734					977.15	6.022
	Average		670.00	1.677	770.00	2.627	860.00	3.717	980.00



Table B5 Experimental data for the observed pseudo first-order rate constant ( $k_0$ ) into aqueous solution of MDEA

Amine	runs	25 °C		30 °C		35 °C		40 °C	
		$K_0$	Error	$K_0$	Error	$K_0$	Error	$K_0$	Error
MDEA at 0.2 M	1	2.11	0.004	2.60	0.003	3.30	0.072	4.87	0.089
	2	2.03	0.003	2.61	0.002	3.14	0.070	4.29	0.080
	3	2.01	0.004	2.34	0.003	3.09	0.083	4.74	0.070
	4	1.98	0.003	2.57	0.002	3.15	0.081	4.83	0.083
	5	1.97	0.005	2.21	0.004	3.04	0.060	4.62	0.070
	6	1.89	0.003	2.02	0.002	3.27	0.065	4.59	0.073
	7	1.89	0.004	2.05	0.003	3.26	0.070	4.75	0.085
	8	1.88	0.002	2.14	0.003	3.19	0.071	4.37	0.088
	9	1.85	0.003	2.45	0.002	3.04	0.070	4.72	0.071
	10	1.84	0.005	2.41	0.003	3.15	0.077	4.67	0.081
	Average	1.95	0.004	2.34	0.003	3.16	0.072	4.65	0.079

Amine	runs	25 °C		30 °C		35 °C		40 °C	
		$K_0$	Error	$K_0$	Error	$K_0$	Error	$K_0$	Error
MDEA at 0.4 M	1	3.30	0.003	4.71	0.002	6.80	0.052	9.67	0.056
	2	3.64	0.004	4.49	0.002	6.98	0.030	9.64	0.066
	3	3.79	0.004	4.54	0.001	6.74	0.053	9.65	0.070
	4	3.65	0.003	4.63	0.002	6.81	0.042	9.51	0.077
	5	3.84	0.002	4.72	0.002	6.79	0.053	9.49	0.064
	6	3.97	0.003	4.49	0.002	6.95	0.035	9.47	0.075
	7	3.36	0.003	4.79	0.003	6.56	0.470	9.40	0.085
	8	3.49	0.002	4.54	0.001	6.91	0.048	9.31	0.073
	9	3.84	0.004	4.42	0.002	6.79	0.065	9.14	0.069
	10	3.45	0.004	4.87	0.002				
	Average	3.63	0.003	4.62	0.002	6.81	0.094	9.48	0.071



Amine	runs	25 °C		30 °C		35 °C		40 °C	
		$K_0$	Error	$K_0$	Error	$K_0$	Error	$K_0$	Error
MDEA at 0.6 M	1	5.78	0.033	7.59	0.002	11.67	0.012	14.78	0.046
	2	5.55	0.035	7.68	0.002	10.55	0.011	14.57	0.056
	3	5.54	0.032	7.84	0.001	10.47	0.010	14.51	0.039
	4	5.75	0.034	7.71	0.002	10.05	0.012	13.33	0.039
	5	5.42	0.031	7.79	0.002	9.81	0.010	13.27	0.040
	6	5.57	0.033	7.65	0.002	9.58	0.012	13.09	0.039
	7	5.69	0.032	7.56	0.003	9.26	0.011	12.43	0.044
	8	5.70	0.031	7.51	0.001	9.17	0.012	12.27	0.042
	9	5.72	0.034	7.79	0.002				
	10								
	Average		5.64	0.033	7.68	0.002	10.07	0.011	13.53

Amine	runs	25 °C		30 °C		35 °C		40 °C	
		$K_0$	Error	$K_0$	Error	$K_0$	Error	$K_0$	Error
MDEA at 0.8 M	1	9.66	0.052	12.67	0.076	15.57	0.046	19.98	0.042
	2	9.34	0.045	11.99	0.056	15.48	0.054	19.77	0.053
	3	9.25	0.053	11.87	0.059	15.71	0.043	19.94	0.035
	4	9.21	0.042	11.75	0.037	14.55	0.055	19.78	0.042
	5	9.19	0.053	10.87	0.045	14.60	0.043	18.53	0.053
	6	9.17	0.055	10.78	0.059	14.65	0.052	18.09	0.035
	7	9.13	0.047	10.96	0.044	13.78	0.034	18.03	0.470
	8	8.91	0.048	9.89	0.047	13.64	0.042	17.87	0.048
	9	8.74	0.055						
	10								
	Average		9.18	0.050	11.35	0.053	14.75	0.046	19.00

Amine	runs	25 °C		30 °C		35 °C		40 °C	
		$K_0$	Error	$K_0$	Error	$K_0$	Error	$K_0$	Error
MDEA at 1.0 M	1	14.45	0.052	17.38	0.043	20.64	0.035	24.98	0.142
	2	14.50	0.045	17.13	0.055	20.55	0.042	24.77	0.159
	3	14.25	0.053	16.44	0.043	19.73	0.053	24.84	0.144
	4	13.58	0.042	16.38	0.052	19.85	0.035	24.36	0.153
	5	13.24	0.053	16.35	0.046	19.82	0.042	22.23	0.162
	6	13.35	0.055	15.89	0.054	19.77	0.053	22.09	0.155
	7	13.37	0.047	15.73	0.043	18.94	0.035	22.03	0.164
	8	13.32	0.048	15.24	0.055	18.78	0.470	21.87	0.165
	9	12.17	0.055	15.02	0.055	18.38	0.048		
	10	12.03	0.051						
	Average		13.43	0.050	16.17	0.050	19.61	0.090	23.40



### Appendix C: The pH and $pK_a$ values of tertiary amines

Table C1 The pH and  $pK_a$  values of HEMAB solution at different temperatures.

Temperature (K)	HCl amount (mL)	Experiment 1		Experiment 2	
		pH	$pK_a$	pH	$pK_a$
296.5	0	11.12		11.10	
	0.5	10.37	9.42	10.15	9.20
	1.0	9.97	9.37	9.69	9.09
	1.5	9.67	9.30	9.43	9.06
	2.0	9.44	9.26	9.21	9.03
	2.5	9.23	9.23	8.99	8.99
	3.0	9.02	9.20	8.75	8.93
	4.0	8.56	9.16	8.47	9.07
	4.5	8.19	9.14	8.06	9.01
	5.0	7.51		7.24	
	5.5	2.40		2.40	
Average $pK_a = 9.15$					
298.0	0	10.99		11.07	
	0.5	10.24	9.29	10.12	9.17
	1.0	9.84	9.24	9.66	9.06
	1.5	9.54	9.17	9.40	9.03
	2.0	9.31	9.13	9.18	9.00
	2.5	9.10	9.10	8.96	8.96
	3.0	8.89	9.07	8.72	8.90
	4.0	8.43	9.03	8.44	9.04
	4.5	8.06	9.01	8.03	8.98
	5.0	7.38		7.21	
	5.5	2.27		2.37	
Average $pK_a = 9.07$					
303.0	0	10.89		11.00	
	0.5	10.14	9.19	10.05	9.10
	1.0	9.74	9.14	9.59	8.99
	1.5	9.44	9.07	9.33	8.96
	2.0	9.21	9.03	9.11	8.93
	2.5	9.00	9.00	8.89	8.89
	3.0	8.79	8.97	8.65	8.83
	4.0	8.33	8.93	8.37	8.97
	4.5	7.96	8.91	7.96	8.91
	5.0	7.28		7.14	
	5.5	2.17		2.30	
Average $pK_a = 8.98$					

Temperature (K)	HCl amount (mL)	Experiment 1		Experiment 2		
		pH	pK <sub>a</sub>	pH	pK <sub>a</sub>	
308.0	0	10.72		10.80		
	0.5	9.97	9.02	9.85	8.90	
	1.0	9.57	8.97	9.39	8.79	
	1.5	9.27	8.90	9.13	8.76	
	2.0	9.04	8.86	8.91	8.73	
	2.5	8.83	8.83	8.69	8.69	
	3.0	8.62	8.80	8.45	8.63	
	4.0	8.16	8.76	8.17	8.77	
	4.5	7.79	8.74	7.76	8.71	
	5.0	7.11		6.94		
	5.5	2.27		2.10		
	0	10.72		10.80		
	Average pK <sub>a</sub> = 8.80					
313.0	0	10.72		10.77		
	0.5	9.77	8.82	9.82	8.87	
	1.0	9.31	8.71	9.36	8.76	
	1.5	9.05	8.68	9.1	8.73	
	2.0	8.83	8.65	8.88	8.70	
	2.5	8.61	8.61	8.66	8.66	
	3.0	8.37	8.55	8.42	8.60	
	4.0	8.09	8.69	8.14	8.74	
	4.5	7.68	8.63	7.73	8.68	
	5.0	6.86		6.91		
	5.5	2.02		2.07		
	Average pK <sub>a</sub> = 8.69					
	318.0	0	10.45		10.48	
0.5		9.70	8.75	9.73	8.78	
1.0		9.30	8.70	9.33	8.73	
1.5		9.00	8.63	9.03	8.66	
2.0		8.77	8.59	8.80	8.62	
2.5		8.56	8.56	8.59	8.59	
3.0		8.35	8.53	8.38	8.56	
4.0		7.89	8.49	7.92	8.52	
4.5		7.52	8.47	7.55	8.50	
5.0		6.84		6.87		
5.5		1.73		1.76		
Average pK <sub>a</sub> = 8.60						

Temperature (K)	HCl amount (mL)	Experiment 1		Experiment 2	
		pH	$pK_a$	pH	$pK_a$
323.0	0	10.41		10.48	
	0.5	9.66	8.71	9.53	8.58
	1.0	9.26	8.66	9.07	8.47
	1.5	8.96	8.59	8.81	8.44
	2.0	8.73	8.55	8.59	8.41
	2.5	8.52	8.52	8.37	8.37
	3.0	8.31	8.49	8.13	8.31
	4.0	7.85	8.45	7.85	8.45
	4.5	7.48	8.43	7.44	8.39
	5.0	6.80		6.62	
	5.5	1.69		1.78	
Average $pK_a = 8.48$					
328.0	0	10.28		10.25	
	0.5	9.53	8.58	9.50	8.55
	1.0	9.13	8.53	9.10	8.50
	1.5	8.83	8.46	8.80	8.43
	2.0	8.60	8.42	8.57	8.39
	2.5	8.39	8.39	8.36	8.36
	3.0	8.18	8.36	8.15	8.33
	4.0	7.72	8.32	7.69	8.29
	4.5	7.35	8.30	7.32	8.27
	5.0	6.67		6.64	
	5.5	1.56		1.53	
Average $pK_a = 8.40$					
333.0	0	10.16		10.19	
	0.5	9.41	8.46	9.44	8.49
	1.0	9.01	8.41	9.04	8.44
	1.5	8.71	8.34	8.74	8.37
	2.0	8.48	8.30	8.51	8.33
	2.5	8.27	8.27	8.3	8.30
	3.0	8.06	8.24	8.09	8.27
	4.0	7.6	8.20	7.63	8.23
	4.5	7.23	8.18	7.26	8.21
	5.0	6.55		6.58	
	5.5	1.44		1.47	
Average $pK_a = 8.31$					

Table C2 The pH and  $pK_a$  values of HEEAB solution at different temperatures.

Temperature (K)	HCl amount (mL)	Experiment 1		Experiment 2	
		pH	$pK_a$	pH	$pK_a$
296.5	0	11.35		11.41	
	0.5	10.77	9.82	10.86	9.91
	1.0	10.43	9.83	10.51	9.91
	1.5	10.17	9.80	10.23	9.86
	2.0	9.95	9.77	10.02	9.84
	2.5	9.75	9.75	9.79	9.79
	3.0	9.57	9.75	9.61	9.79
	3.5	9.38	9.75	9.42	9.79
	4.0	9.13	9.73	9.21	9.81
	4.5	8.91	9.86	8.97	9.92
	5.0	8.58		8.67	
	5.5	7.81		8.02	
	6.0	2.41		2.55	
	Average $pK_a = 9.81$				
298.0	0	11.32		11.34	
	0.5	10.74	9.79	10.79	9.84
	1.0	10.4	9.80	10.44	9.84
	1.5	10.14	9.77	10.16	9.79
	2.0	9.92	9.74	9.95	9.77
	2.5	9.72	9.72	9.72	9.72
	3.0	9.54	9.72	9.54	9.72
	3.5	9.35	9.72	9.35	9.72
	4.0	9.1	9.70	9.14	9.74
	4.5	8.88	9.83	8.9	9.85
	5.0	8.55		8.6	
	5.5	7.78		7.95	
	6.0	2.38		2.48	
	Average $pK_a = 9.76$				

Temperature (K)	HCl amount (mL)	Experiment 1		Experiment 2	
		pH	$pK_a$	pH	$pK_a$
303.0	0	11.19		11.22	
	0.5	10.61	9.66	10.67	9.72
	1.0	10.27	9.67	10.32	9.72
	1.5	10.01	9.64	10.04	9.67
	2.0	9.79	9.61	9.83	9.65
	2.5	9.59	9.59	9.6	9.60
	3.0	9.41	9.59	9.42	9.60
	3.5	9.22	9.59	9.23	9.60
	4.0	8.97	9.57	9.02	9.62
	4.5	8.75	9.70	8.78	9.73
	5.0	8.42		8.48	
	5.5	7.65		7.83	
	6.0	2.25		2.36	
Average $pK_a = 9.64$					
308.0	0	11.07		11.12	
	0.5	10.49	9.54	10.57	9.62
	1.0	10.15	9.55	10.22	9.62
	1.5	9.89	9.52	9.94	9.57
	2.0	9.67	9.49	9.73	9.55
	2.5	9.47	9.47	9.5	9.50
	3.0	9.29	9.47	9.32	9.50
	3.5	9.1	9.47	9.13	9.50
	4.0	8.85	9.45	8.92	9.52
	4.5	8.63	9.58	8.68	9.63
	5.0	8.3		8.38	
	5.5	7.53		7.73	
	6.0	2.13		2.26	
Average $pK_a = 9.53$					

Temperature (K)	HCl amount (mL)	Experiment 1		Experiment 2	
		pH	$pK_a$	pH	$pK_a$
313.0	0	10.96		11.01	
	0.5	10.38	9.43	10.46	9.51
	1.0	10.04	9.44	10.11	9.51
	1.5	9.78	9.41	9.83	9.46
	2.0	9.56	9.38	9.62	9.44
	2.5	9.36	9.36	9.39	9.39
	3.0	9.18	9.36	9.21	9.39
	3.5	8.99	9.36	9.02	9.39
	4.0	8.74	9.34	8.81	9.41
	4.5	8.52	9.47	8.57	9.52
	5.0	8.19		8.27	
	5.5	7.42		7.62	
	6.0	2.02		2.15	
	Average $pK_a = 9.42$				
318.0	0	10.83		10.89	
	0.5	10.25	9.30	10.34	9.39
	1.0	9.91	9.31	9.99	9.39
	1.5	9.65	9.28	9.71	9.34
	2.0	9.43	9.25	9.5	9.32
	2.5	9.23	9.23	9.27	9.27
	3.0	9.05	9.23	9.09	9.27
	3.5	8.86	9.23	8.9	9.27
	4.0	8.61	9.21	8.69	9.29
	4.5	8.39	9.34	8.45	9.40
	5.0	8.06		8.15	
	5.5	7.29		7.5	
	6.0	1.89		2.03	
	Average $pK_a = 9.29$				



Temperature (K)	HCl amount (mL)	Experiment 1		Experiment 2	
		pH	$pK_a$	pH	$pK_a$
323.0	0	10.71		10.66	
	0.5	10.13	9.18	10.11	9.16
	1.0	9.79	9.19	9.76	9.16
	1.5	9.53	9.16	9.48	9.11
	2.0	9.31	9.13	9.27	9.09
	2.5	9.11	9.11	9.04	9.04
	3.0	8.93	9.11	8.86	9.04
	3.5	8.74	9.11	8.67	9.04
	4.0	8.49	9.09	8.46	9.06
	4.5	8.27	9.22	8.22	9.17
	5.0	7.94		7.92	
	5.5	7.17		7.27	
	6.0	1.77		1.8	
	Average $pK_a = 9.12$				
328.0	0	10.54		10.61	
	0.5	9.96	9.01	10.06	9.11
	1.0	9.62	9.02	9.71	9.11
	1.5	9.36	8.99	9.43	9.06
	2.0	9.14	8.96	9.22	9.04
	2.5	8.94	8.94	8.99	8.99
	3.0	8.76	8.94	8.81	8.99
	3.5	8.57	8.94	8.62	8.99
	4.0	8.32	8.92	8.41	9.01
	4.5	8.10	9.05	8.17	9.12
	5.0	7.77		7.87	
	5.5	7.00		7.22	
	6.0	1.60		1.75	
	Average $pK_a = 9.01$				
333.0	0	10.45		10.53	
	0.5	9.87	8.92	9.98	9.03
	1.0	9.53	8.93	9.63	9.03
	1.5	9.27	8.90	9.35	8.98
	2.0	9.05	8.87	9.14	8.96
	2.5	8.85	8.85	8.91	8.91
	3.0	8.67	8.85	8.73	8.91
	3.5	8.48	8.85	8.54	8.91
	4.0	8.23	8.83	8.33	8.93
	4.5	8.01	8.96	8.09	9.04
	5.0	7.68		7.79	
	5.5	6.91		7.14	
	6.0	1.51		1.67	
	Average $pK_a = 8.92$				

Table C3 The pH and  $pK_a$  values of DMAB solution at different temperatures.

Temperature (K)	HCl amount (mL)	Experiment 1		Experiment 2	
		pH	$pK_a$	pH	$pK_a$
296.5	0	11.09		11.1	
	0.5	10.49	9.54	10.43	9.48
	1.0	10.11	9.51	10.06	9.46
	1.5	9.82	9.45	9.79	9.42
	2.0	9.59	9.41	9.55	9.37
	2.5	9.31	9.31	9.26	9.26
	3.0	8.98	9.16	8.92	
	3.5	8.42		8.26	
	4.0	3.08		2.83	
Average $pK_a = 9.38$					
298.0	0	11.18		11.13	
	0.5	10.46	9.51	10.5	9.55
	1.0	10.04	9.44	10.12	9.52
	1.5	9.71	9.34	9.87	9.50
	2.0	9.4	9.22	9.62	9.44
	2.5	8.94	8.94	9.32	9.32
	3.0	7.69		8.99	9.17
	3.2	3.06		8.77	
	3.4	2.64		8.50	
	4.0	2.24		2.83	
Average $pK_a = 9.32$					
303.0	0.0	10.98		10.99	
	0.5	10.35	9.40	10.36	9.41
	1.0	9.97	9.37	9.98	9.38
	1.5	9.72	9.35	9.73	9.36
	2.0	9.47	9.29	9.48	9.30
	2.5	9.17	9.17	9.18	9.18
	3.0	8.84	9.02	8.85	9.03
	3.2	8.62	8.87	8.63	
	3.4	8.35		8.36	
	3.6	7.74		7.75	
	3.8	3.56		3.57	
4.0	2.68		2.69		
Average $pK_a = 9.22$					
308.0	0	10.84		10.89	
	0.5	10.21	9.26	10.17	9.22
	1.0	9.83	9.23	9.75	9.15
	1.5	9.58	9.21	9.42	9.05
	2.0	9.33	9.15	9.11	8.93
	2.5	9.03	9.03	8.65	
	3.0	8.70		7.40	
	3.2	3.42		2.77	
	4.0	2.54		1.95	
Average $pK_a = 9.13$					

Temperature (K)	HCl amount (mL)	Experiment 1		Experiment 2	
		pH	$pK_a$	pH	$pK_a$
313.0	0	10.74		10.69	
	0.5	10.14	9.19	10.02	9.07
	1.0	9.76	9.16	9.65	9.05
	1.5	9.47	9.10	9.38	9.01
	2.0	9.24	9.06	9.14	8.96
	2.5	8.96	8.96	8.85	8.85
	3.0	8.63	8.81	8.51	
	3.5	8.07		7.85	
	4.0	2.73		2.42	
	Average $pK_a = 9.00$				
318.0	0	10.57		10.61	
	0.5	9.97	9.02	9.94	8.99
	1.0	9.59	8.99	9.57	8.97
	1.5	9.30	8.93	9.30	8.93
	2.0	9.07	8.89	9.06	8.88
	2.5	8.79	8.79	8.77	8.77
	3.0	8.46	8.64	8.43	
	3.5	7.90		7.77	
	4.0	2.56		2.34	
	Average $pK_a = 8.88$				
323.0	0	10.50		10.48	
	0.5	9.90	8.95	9.81	8.86
	1.0	9.52	8.92	9.44	8.84
	1.5	9.23	8.86	9.17	8.80
	2.0	9.00	8.82	8.93	8.75
	2.5	8.72	8.72	8.64	8.64
	3.0	8.39	8.57	8.30	
	3.5	7.83		7.64	
	4.0	2.49		2.21	
	Average $pK_a = 8.78$				
328.0	0	10.39		10.41	
	0.5	9.72	8.77	9.81	8.86
	1.0	9.35	8.75	9.43	8.83
	1.5	9.08	8.71	9.14	8.77
	2.0	8.84	8.66	8.91	8.73
	2.5	8.55	8.55	8.63	8.63
	3.0	8.21		8.30	8.48
	3.5	7.55		7.74	
	4.0	2.12		2.40	
	Average $pK_a = 8.69$				

Temperature (K)	HCl amount (mL)	Experiment 1		Experiment 2	
		pH	$pK_a$	pH	$pK_a$
333.0	0	10.30		10.21	
	0.5	9.58	8.63	9.58	8.63
	1.0	9.16	8.56	9.20	8.60
	1.5	8.83	8.46	8.95	8.58
	2.0	8.52	8.34	8.70	8.52
	2.5	8.06		8.40	8.40
	3.0	6.81		7.58	
	3.2	2.18		2.79	
	4.0	1.36		1.91	
	Average $pK_a = 8.51$				



Table C4 The pH and  $pK_a$  values of DEAB solution at different temperatures.

Temperature (K)	HCl amount (mL)	Experiment 1		Experiment 2	
		pH	$pK_a$	pH	$pK_a$
296.5	0	11.43		11.52	
	0.5	11.03	10.08	11.14	10.19
	1.0	10.70	10.10	10.8	10.20
	1.5	10.45	10.08	10.57	10.21
	2.0	10.25	10.07	10.37	10.20
	2.5	10.07	10.07	10.16	10.17
	3.0	9.82	10.00	9.94	10.13
	3.5	9.54	9.91	9.66	10.04
	4.0	8.91		9.17	
	4.5	2.47		2.95	
	5.0	2.12		2.52	
Average $pK_a = 10.10$					
298.0	0	11.4		11.44	
	0.5	11	10.05	11.06	10.11
	1.0	10.67	10.07	10.72	10.12
	1.5	10.42	10.05	10.49	10.13
	2.0	10.22	10.04	10.29	10.12
	2.5	10.04	10.04	10.08	10.09
	3.0	9.79	9.97	9.86	10.05
	3.5	9.51	9.88	9.58	9.96
	4.0	8.88		9.09	
	4.5	2.44		2.87	
	5.0	2.09		2.14	
Average $pK_a = 10.06$					
303.0	0	11.29		11.25	
	0.5	10.89	9.94	10.87	9.92
	1.0	10.56	9.96	10.53	9.93
	1.5	10.31	9.94	10.3	9.94
	2.0	10.11	9.93	10.1	9.93
	2.5	9.93	9.93	9.89	9.90
	3.0	9.68	9.86	9.67	9.86
	3.5	9.40	9.77	9.39	9.77
	4.0	8.77		8.90	
	4.5	2.33		2.68	
	5.0	1.98		2.34	
Average $pK_a = 9.91$					

Temperature (K)	HCl amount (mL)	Experiment 1		Experiment 2	
		pH	$pK_a$	pH	$pK_a$
308.0	0	11.11		11.12	
	0.5	10.71	9.76	10.74	9.79
	1.0	10.38	9.78	10.40	9.80
	1.5	10.13	9.76	10.17	9.81
	2.0	9.93	9.75	9.97	9.80
	2.5	9.75	9.75	9.76	9.77
	3.0	9.50	9.68	9.54	9.73
	3.5	9.22	9.59	9.26	9.64
	4.0	8.59		8.77	
	4.5	2.15		2.55	
	5.0	1.80		1.43	
Average $pK_a = 9.75$					
313.0	0	11.03		11.01	
	0.5	10.63	9.68	10.63	9.68
	1.0	10.30	9.70	10.29	9.69
	1.5	10.05	9.68	10.06	9.70
	2.0	9.85	9.67	9.86	9.69
	2.5	9.67	9.67	9.65	9.66
	3.0	9.42	9.60	9.43	9.62
	3.5	9.14	9.51	9.15	9.53
	4.0	8.51		8.66	
	4.5	2.07		2.44	
	5.0	1.72		1.87	
Average $pK_a = 9.66$					
318.0	0	10.87		10.83	
	0.5	10.47	9.52	10.45	9.50
	1.0	10.14	9.54	10.11	9.51
	1.5	9.89	9.52	9.88	9.52
	2.0	9.69	9.51	9.68	9.51
	2.5	9.51	9.51	9.47	9.48
	3.0	9.26	9.44	9.25	9.44
	3.5	8.98	9.35	8.97	9.35
	4.0	8.35		8.48	
	4.5	1.91		2.26	
	5.0	1.56		2.14	
Average $pK_a = 9.49$					

Temperature (K)	HCl amount (mL)	Experiment 1		Experiment 2	
		pH	pK <sub>a</sub>	pH	pK <sub>a</sub>
323.0	0	10.73		10.7	
	0.5	10.33	9.38	10.32	9.37
	1.0	10.00	9.40	9.98	9.38
	1.5	9.75	9.38	9.75	9.39
	2.0	9.55	9.37	9.55	9.38
	2.5	9.37	9.37	9.34	9.35
	3.0	9.12	9.30	9.12	9.31
	3.5	8.84	9.21	8.84	9.22
	4.0	8.21		8.35	
	4.5	1.77		2.13	
	5.0	1.42		1.86	
Average pK <sub>a</sub> = 9.35					
328.0	0	10.64		10.63	
	0.5	10.24	9.29	10.25	9.30
	1.0	9.91	9.31	9.91	9.31
	1.5	9.66	9.29	9.68	9.32
	2.0	9.46	9.28	9.48	9.31
	2.5	9.28	9.28	9.27	9.28
	3.0	9.03	9.21	9.05	9.24
	3.5	8.75	9.12	8.77	9.15
	4.0	8.12		8.28	
	4.5	1.68		2.06	
	5.0	1.33		1.65	
Average pK <sub>a</sub> = 9.27					
333.0	0	10.53		10.5	
	0.5	10.13	9.18	10.12	9.17
	1.0	9.8	9.20	9.78	9.18
	1.5	9.55	9.18	9.55	9.19
	2.0	9.35	9.17	9.35	9.18
	2.5	9.17	9.17	9.14	9.15
	3.0	8.92	9.10	8.92	9.11
	3.5	8.64	9.01	8.64	9.02
	4.0	8.01		8.15	
	4.5	1.57		1.93	
	5	1.22		1.64	
Average pK <sub>a</sub> = 9.15					

Table C5 The pH and  $pK_a$  values of MDEA solution at different temperatures.

Temperature (K)	HCl amount (mL)	Experiment 1		Experiment 2	
		pH	$pK_a$	pH	$pK_a$
296.5	0	10.65		10.56	
	0.5	9.56	8.61	9.72	8.53
	1.0	9.25	8.65	9.37	8.50
	1.5	9.00	8.63	9.10	8.44
	2.0	8.81	8.63	8.95	8.45
	2.5	8.63	8.63	8.79	8.42
	3.0	8.46	8.64	8.61	8.43
	3.5	8.26	8.63	8.40	8.40
	4.0	8.01	8.61	8.15	8.33
	4.5	7.61	8.56	7.86	8.23
	5.0	3.02		3.12	
Average $pK_a = 8.62$					
298.0	0	10.65		10.6	
	0.5	9.53	8.58	9.51	8.56
	1.0	9.16	8.56	9.2	8.60
	1.5	8.93	8.56	8.95	8.58
	2.0	8.71	8.53	8.76	8.58
	2.5	8.54	8.54	8.58	8.58
	3.0	8.34	8.52	8.41	8.59
	3.5	8.13	8.50	8.21	8.58
	4.0	7.84	8.44	7.96	8.56
	4.5	7.39		7.56	8.51
	5.0	2.70		2.97	
Average $pK_a = 8.55$					
303.0	0	10.56		10.59	
	0.3	9.72	8.53	9.75	8.56
	0.6	9.37	8.50	9.4	8.53
	0.9	9.1	8.44	9.13	8.47
	1.2	8.95	8.45	8.98	8.48
	1.5	8.79	8.42	8.82	8.45
	2	8.61	8.43	8.64	8.46
	2.5	8.4	8.40	8.43	8.43
	3	8.15	8.33	8.18	8.36
	4	7.31		7.34	
	Average $pK_a = 8.45$				



Temperature (K)	HCl amount (mL)	Experiment 1		Experiment 2	
		pH	$pK_a$	pH	$pK_a$
308.0	0	10.51		10.41	
	0.5	9.39	8.44	9.32	8.37
	1.0	9.02	8.42	9.01	8.41
	1.5	8.79	8.42	8.76	8.39
	2.0	8.57	8.39	8.57	8.39
	2.5	8.4	8.40	8.39	8.39
	3.0	8.2	8.38	8.22	8.40
	3.5	7.99	8.36	8.02	8.39
	4.0	7.7	8.30	7.77	8.37
	4.5	7.25		7.37	8.32
	5.0	2.56		2.78	
Average $pK_a = 8.38$					
313.0	0	10.36		10.42	
	0.3	9.52	8.33	9.58	8.39
	0.6	9.17	8.30	9.23	8.36
	0.9	8.90	8.24	8.96	8.30
	1.2	8.75	8.25	8.81	8.31
	1.5	8.59	8.22	8.65	8.28
	2.0	8.41	8.23	8.47	8.29
	2.5	8.20	8.20	8.26	8.26
	3.0	7.95	8.13	8.01	8.19
	3.5	7.66		7.72	
	4.0	7.11		7.17	
	Average $pK_a = 8.26$				

Temperature (K)	HCl amount (mL)	Experiment 1		Experiment 2	
		pH	$pK_a$	pH	$pK_a$
318.0	0	10.27		10.27	
	0.5	9.18	8.23	9.15	8.20
	1.0	8.87	8.27	8.78	8.18
	1.5	8.62	8.25	8.55	8.18
	2.0	8.43	8.25	8.33	8.15
	2.5	8.25	8.25	8.16	8.16
	3.0	8.08	8.26	7.96	8.14
	3.5	7.88	8.25	7.75	8.12
	4.0	7.63	8.23	7.46	8.06
	4.5	7.23	8.18	7.01	
	5.0	2.64		2.32	
Average $pK_a = 8.19$					
323.0	0	10.13		10.18	
	0.5	9.04	8.09	9.06	8.11
	1.0	8.73	8.13	8.69	8.09
	1.5	8.48	8.11	8.46	8.09
	2.0	8.29	8.11	8.24	8.06
	2.5	8.11	8.11	8.07	8.07
	3.0	7.94	8.12	7.87	8.05
	3.5	7.74	8.11	7.66	8.03
	4.0	7.49	8.09	7.37	7.97
	4.5	7.09	8.04	6.92	
	5.0	2.50		2.23	
Average $pK_a = 8.08$					

Temperature (K)	HCl amount (mL)	Experiment 1		Experiment 2	
		pH	$pK_a$	pH	$pK_a$
328.0	0	10.08		10.12	
	0.3	9.24	8.05	9.28	8.09
	0.6	8.89	8.02	8.93	8.06
	0.9	8.62	7.96	8.66	8.00
	1.2	8.47	7.97	8.51	8.01
	1.5	8.31	7.94	8.35	7.98
	2.0	8.13	7.95	8.17	7.99
	2.5	7.92	7.92	7.96	7.96
	3.0	7.67	7.85	7.71	7.89
	3.5	7.38		7.42	
	4.0	6.83		6.87	
Average $pK_a = 7.97$					
333.0	0	9.99		9.97	
	0.5	8.87	7.92	8.88	7.93
	1.0	8.5	7.90	8.57	7.97
	1.5	8.27	7.90	8.32	7.95
	2.0	8.05	7.87	8.13	7.95
	2.5	7.88	7.88	7.95	7.95
	3.0	7.68	7.86	7.78	7.96
	3.5	7.47	7.84	7.58	7.95
	4.0	7.18	7.78	7.33	7.93
	4.5	6.73		6.93	7.88
	5.0	2.04		2.34	
Average $pK_a = 7.90$					

### Appendix D: Density, viscosity and refractive index

Table D1 The density of amine solutions at different temperatures.

Amine	Temperature (°C)				
	20	25	30	35	40
DMAB	0.8526	0.8482	0.8437	0.8392	0.8347
DEAB	0.8605	0.8565	0.8525	0.8485	0.8445
DPAB	0.9250	0.9209	0.9167	0.9124	0.9081
DBAB	0.9847	0.9810	0.9775	0.9738	0.9700
HEMAB	0.9573	0.9536	0.9499	0.9461	0.9424
HEEAB	0.9748	0.9710	0.9673	0.9635	0.9597
MDEA	1.0404	1.0366	1.0329	1.0291	1.0255

Amine	Temperature (°C)			
	45	50	55	60
DMAB	0.8301	0.8255	0.8209	0.8162
DEAB	0.8405	0.8365	0.8325	0.8285
DPAB	0.9037	0.8992	0.8947	0.8902
DBAB	0.9653	0.9614	0.9581	0.9544
HEMAB	0.9386	0.9348	0.9310	0.9272
HEEAB	0.9559	0.9520	0.9481	0.9442
MDEA	1.0214	1.0176	1.0138	1.0099

Table D2 The viscosity of amine solutions at different temperatures.

Amine	Temperature (°C)				
	20	25	30	35	40
DMAB	2.506	2.182	1.918	1.698	1.511
DEAB	3.409	2.912	2.533	2.221	1.964
DPAB	5.025	4.213	3.584	3.08	2.671
DBAB	6.564	5.613	4.791	4.0134	3.389
HEMAB	44.395	34.477	26.874	22.186	18.671
HEEAB	51.025	40.213	31.584	26.192	22.121

Amine	Temperature (°C)			
	45	50	55	60
DMAB	1.353	1.217	1.1	0.999
DEAB	1.749	1.567	1.413	1.281
DPAB	2.342	2.069	1.841	1.648
DBAB	2.97	2.641	2.416	2.248
HEMAB	16.042	13.807	11.69	9.533
HEEAB	18.512	16.011	13.941	11.94

Table D3 The refractive index of amine solutions at different temperatures.

Amine	Temperature (°C)						
	20	25	30	35	40	45	50
DMAB	1.4595	1.4577	1.4558	1.4540	1.4522	1.4503	1.4484
DEAB	1.4684	1.4667	1.4649	1.4631	1.4613	1.4596	1.4578
DPAB	1.4397	1.4377	1.4357	1.4337	1.4317	1.4297	1.4277
DBAB	1.4397	1.4377	1.4357	1.4337	1.4317	1.4297	1.4277
HEEAB	1.4378	1.4357	1.4336	1.4314	1.4293	1.4272	1.4251
HEMAB	1.4360	1.4339	1.4318	1.4298	1.4277	1.4255	1.4234
MDEA	1.4428	1.4408	1.4388	1.4368	1.4348	1.4328	1.4308



## VITA

Name: Ms. Sudkanueng Singto

Date of Birth: September 24, 1981

Residence: 245 Moo 11 Kokkruat, Amphoe Mueng Nakornratchasima 30280

Education:

In 2008 M.Sc. in Program of Petrochemistry and Polymer Science

Chulalongkorn University, Bangkok, Thailand.

In 2005 B.Sc. in Chemistry

Chulalongkorn University, Bangkok, Thailand.

Publication:

In 2016 Sudkanueng Singto, Teeradet Supap, Raphael Idem, Paitoon Tontiwachwuthikul, Supawan Tantayanon, Mohammed J. Al-Marri, Abdelbaki Benamor, "Synthesis of new amines for enhanced carbon dioxide (CO<sub>2</sub>) capture performance: The effect of chemical structure on equilibrium solubility, cyclic capacity, kinetics of absorption and regeneration, and heat of absorption and regeneration" Separation and Purification Technology 167 (2016) 97-107, doi.org/10.1016/j.seppur. 2016.05.002

Oral Presentation:

In 2015

- Sudkanueng Singto, Teeradet Supap, Raphael Idem, Paitoon Tontiwachwuthikul, Supawan Tantayanon, "Development of New Amines for Post Combustion Capture of Carbon dioxide (CO<sub>2</sub>) absorption" in Post Combustion Capture Conference and SaskPower CCS Symposium (PCCC3), Regina, Saskatchewan, Canada on 8th -11th September 2015.

- Sudkanueng Singto, Teeradet Supap, Raphael Idem, Paitoon Tontiwachwuthikul, Supawan Tantayanon, "Effect of Chemical Structure of New Tertiary Amines used for the Post Combustion Capture Process on Carbon Dioxide (CO<sub>2</sub>) Kinetic Absorption Rate" in 65th Canadian Chemical Engineering Conference, Calgary, Alberta, Canada on 4th -7th October 2015.

Award:

In 2011 Certificate of "Bangkok Bank Yong Chemist Winners" in the 14rd Asian Chemical Congress, Bangkok Thailand.